

Copyright
By
Lee Michael Blaney
2011

**The Dissertation Committee for Lee Michael Blaney certifies that this is the
approved version of the following dissertation:**

**OXIDATION OF PHARMACEUTICALS: IMPACTS OF NATURAL ORGANIC MATTER AND
ELIMINATION OF RESIDUAL PHARMACOLOGICAL ACTIVITY**

Committee:

Lynn E. Katz, Co-Supervisor

Desmond F. Lawler, Co-Supervisor

Mary Jo Kirisits

Howard M. Liljestrand

John H. Richburg

Gerald E. Speitel Jr.

**OXIDATION OF PHARMACEUTICALS: IMPACTS OF NATURAL ORGANIC MATTER AND
ELIMINATION OF RESIDUAL PHARMACOLOGICAL ACTIVITY**

by

Lee Michael Blaney, B.S., M.S.

Dissertation

Presented to the Faculty of the Graduate School of
The University of Texas at Austin
in Partial Fulfillment
of the Requirements
for the Degree of

Doctor of Philosophy

The University of Texas
August 2011

Dedication

In loving memory of my grandfather, Leon Kosmalski.

ACKNOWLEDGEMENTS

My most sincere thanks go to my two wonderful advisors, Dr. Lynn E. Katz and Dr. Desmond F. Lawler. Since day one, Drs. Katz and Lawler have encouraged me to push myself towards success. Their continued faith in my abilities has allowed me to pursue new and exciting aspects of environmental engineering research, and I greatly appreciate the wisdom and support that they provided along the way. They have served as role models and mentors to me for the past four years and I greatly appreciate their role in transforming me into an Assistant Professor. Thank you for an amazing Ph.D. experience!

Special thanks go to my Ph.D. committee members: Mary Jo Kirisits, Howard Liljestrand, John Richburg, and Gerald Speitel. Their experience and profound knowledge of the subjects involved with my research inspired me in the laboratory. Their constructive criticism and comments have helped to strengthen not only my dissertation, but also my critical thinking abilities. As I transition into my new position, I will continually reflect on the direction they brought to my dissertation project.

So many thanks are due to the many wonderful individuals in the Environmental and Water Resources Engineering (EWRE) program. First, I thank Corin Marron, Ling Huang, Stephanie Tong, Hersy Enriquez, and Raul Tenorio for their involvement (and enthusiasm!) with this research. Special thanks go out to my officemates (and office neighbors): Ram, Amanda, Ellison, Shane, Hector, Younggy, Lily, and Jerry. I also thank the many members of the Lawler and Katz research groups that I have interacted with over the past four years, including Mark, Ijung, Nate, Celina, Jinyong, Lauren, Chia-Chen, Pat, Yamuna, Katie, Catherine, Fernando, Shannon, Ashlynn, Scott, Michael, Changmin, Allison, Mara, Yeonjeong, Aurore, Matt, Dave, Jonny, Elena, Anne, and Luwei. You have all impacted me in so many ways, and you have made this journey extremely entertaining and rewarding. Finally, I would like to acknowledge the many

people who work behind the scenes to make our research possible, especially Rebecca Christian, Marcy Betak, Sharon Bernard, Kathy Rose, and the people that handle the Inter Library Loan program at UT – thanks for putting up with me!

In Austin, I found a new family of friends, and I am so thankful for their continual support. In particular, I would like to thank Grace for understanding my relationship with the ozone. Special thanks go to Jake, Taylor, Wade, Ashley, Amelia, Ken, Dave, and all of the kids at the House of Commons for making my time in Austin a fun experience. I would also like to acknowledge the Board of Directors at Wheatsville Co-op for the privilege of serving with them for these past two years and for providing constant motivation to make the world a better place.

Finally, I would like to thank my family for understanding my being so far from home for these past four years. Your constant love and support has helped me keep on track, and I am looking forward to being closer to you next year.

**OXIDATION OF PHARMACEUTICALS: IMPACTS OF NATURAL ORGANIC MATTER AND
ELIMINATION OF RESIDUAL PHARMACOLOGICAL ACTIVITY**

Lee Michael Blaney, Ph.D.
The University of Texas at Austin, 2011

Supervisors: Lynn E. Katz and Desmond F. Lawler

Anthropogenically-derived substances, including pharmaceuticals and personal care products, endocrine-disrupting chemicals, and pesticides, are increasingly being detected in drinking water supplies and wastewater effluents. Concerns over the presence of these compounds in water supplies include their ability to impart toxicological activity, their capacity to spread antibiotic resistance, and their potential to affect cell-signaling processes. For these reasons, water treatment processes geared towards removal of these trace organic contaminants are vital.

In this work, ozone was used to treat four pharmaceutical contaminants: ciprofloxacin, cyclophosphamide, erythromycin, and ifosfamide. Ciprofloxacin and erythromycin are antibiotic/antimicrobial compounds, and cyclophosphamide and ifosfamide are chemotherapy agents. Ozone effectively transformed all four pharmaceuticals, even in the presence of background natural organic matter, which exerts a considerable ozone demand. The apparent rate constants for the reaction of the pharmaceuticals with ozone at pH 7 were determined: $3.03 \text{ M}^{-1}\text{s}^{-1}$ for cyclophosphamide; $7.38 \text{ M}^{-1}\text{s}^{-1}$ for ifosfamide; $1.57 \times 10^4 \text{ M}^{-1}\text{s}^{-1}$ for ciprofloxacin; and $7.18 \times 10^4 \text{ M}^{-1}\text{s}^{-1}$ for erythromycin. Cyclophosphamide and ifosfamide, which do not react quickly with ozone, exhibited high rate constants ($2.7 \times 10^9 \text{ M}^{-1}\text{s}^{-1}$) for transformation by hydroxyl radicals, which are formed through ozone decomposition. Nevertheless, complete

removal of cyclophosphamide and ifosfamide was achievable using a novel continuous aqueous ozone addition reactor and an ozone-based advanced oxidation process (peroxone).

In ozone-based processes, pharmaceuticals are systematically transformed via complex oxidative pathways towards CO_2 , H_2O , and the oxidized forms of other elements. Intermediate oxidation products containing oxygen atoms or hydroxyl groups substituted into the chemical structure of the parent pharmaceutical were identified using liquid chromatography-mass spectrometry (LC-MS). Given the structural similarity of intermediate oxidation products to the parent pharmaceuticals, an antimicrobial activity assay was employed to monitor the removal of pharmacological activity associated with ciprofloxacin, erythromycin, and their respective intermediate oxidation products throughout treatment. For solutions containing ciprofloxacin or erythromycin, ozone was able to completely eliminate the corresponding antimicrobial activity. Ciprofloxacin intermediate oxidation products were pharmacologically active; however, erythromycin's intermediate products did not contribute to the residual antimicrobial activity. These results suggest that the design of conventional and advanced ozone-based processes must incorporate ozone demand from background organic matter and account for destruction of pharmacologically active intermediates.

TABLE OF CONTENTS

List of Tables.....	xiii
List of Figures.....	xv
 Chapter 1: Introduction.....	 1
Problem Statement.....	2
Objectives.....	3
Approach.....	4
Significance.....	6
 Chapter 2: Literature Review.....	 8
Pharmaceuticals in the Environment.....	8
Avenues for Pharmaceutical Introduction into the Environment.....	11
Legislation of Pharmaceutical Contaminants.....	13
Pharmaceuticals of Concern in this Study.....	16
Ciprofloxacin.....	16
Erythromycin.....	18
Cyclophosphamide and Ifosfamide.....	19
Environmental Presence of Compounds of Concern.....	19
Human and Environmental Health Threat from PhAC Presence in Drinking Water Supplies.....	23
Water and Wastewater Treatment of Trace Organic Contaminants.....	26
Ozone and Peroxone Chemistry.....	29
Ozone Reactor Schemes.....	34
Gaseous Ozonation.....	34
Aqueous Ozone Addition.....	37
Measuring Ozone and Hydroxyl Radical Kinetics.....	40
Isolating Ozone Kinetics.....	40

Determining Hydroxyl Radical Kinetics.....	41
Oxidation and Advanced Oxidation Processes (AOPs).....	43
Impact of Natural Organic Matter on Oxidation Processes.....	45
Intermediate Oxidation Products.....	47
Residual Pharmacological Activity.....	49
Chapter 3: Materials and Methods.....	50
Chemicals.....	51
Pharmacologically Active Compounds.....	52
Natural Organic Matter.....	52
Analytical Methods.....	55
Ozone Analysis.....	55
Ciprofloxacin Analysis.....	59
Cyclophosphamide Analysis.....	60
Erythromycin Analysis.....	62
Ifosfamide Analysis.....	64
<i>para</i> -Chlorobenzoic Acid (<i>p</i> CBA) Analysis.....	66
NOM Analysis.....	67
Hydrogen Peroxide Titration.....	68
pH.....	69
Ozone Reactors.....	70
Determination of PhAC Transformation in Batch Reactors with Aqueous	
Ozone.....	71
Continuous Aqueous Ozone Addition Reactor.....	72
Continuous Peroxone Addition Reactor.....	76
Measurement of Ozone and Hydroxyl Radical Kinetics.....	79
Isolating Ozone Kinetics.....	80
Determination of Hydroxyl Radical Kinetics.....	82
Anti-Microbial Susceptibility Assay.....	89

Chapter 4: Ozonation of Cyclophosphamide and Ifosfamide: Determination of Rate Constants, Impact of Organic Matter, and Identification of Major Intermediate Products.....	95
Abstract.....	95
Introduction.....	96
Materials and Methods.....	99
Results.....	105
Kinetics.....	105
Percent Transformation.....	113
Intermediate Product Identification.....	117
 Chapter 5: Effects of Natural Organic Matter on Ozonation of Ciprofloxacin and Removal of Antimicrobial Activity.....	126
Abstract.....	126
Introduction.....	127
Materials and Methods.....	132
Results and Discussion.....	139
 Chapter 6: Ozonation of Erythromycin: Determination of Rate Constants, Identification of Major Intermediate Products, and Removal of Antimicrobial Activity.....	155
Abstract.....	155
Introduction.....	156
Materials and Methods.....	160
Results.....	165
Chemical Structure of Erythromycin and Erythromycin Degradation Products.....	165
Erythromycin Kinetics with Ozone.....	167

Inhibition Profile of Erythromycin.....	174
Antimicrobial Activity of Erythromycin Intermediate Oxidation Products.....	178
Conclusions.....	184
Chapter 7: Conclusions.....	186
Significance.....	190
Recommendations for Future Work.....	192
Appendix A: Dish Washing and Autoclave Protocols.....	196
Appendix B: Fluorescence EEM Data for NOM isolates.....	197
Appendix C: Antimicrobial Activity Assay Data Analysis.....	200
Appendix D: Cytotoxicity Assay.....	211
Appendix E: Comparison of the Variable Volume, Constant Volume, and Modified Constant Volume Models for Pharmaceutical Transformation in the Continuous Ozone Addition Reactor.....	216
References.....	226
Vita.....	243

LIST OF TABLES

Table 2-1.	State bills relating to regulation of unused pharmaceuticals.	14
Table 2-2.	Salient information for the chemicals of concern.	17
Table 2-3.	Mode of action for PhACs of concern.	18
Table 2-4.	Detection of the four pharmaceuticals of concern.	21
Table 2-5.	Ozone decomposition models.	31
Table 2-6.	Properties of <i>t</i> -BuOH and <i>p</i> CBA.	41
Table 3-1.	Summary of organic matter recovery during NOM extractions.	53
Table 3-2.	Raw water quality of Claremore Lake and Lake Austin water sources.	54
Table 4-1.	Properties of ifosfamide and cyclophosphamide.	97
Table 4-2.	Rate constants for cyclophosphamide and ifosfamide with ozone and hydroxyl radicals.	110
Table 4-3.	Proposed intermediate products formed via ozonation of cyclophosphamide and ifosfamide.	121
Table 5-1.	Salient properties of ciprofloxacin and depiction of structure-activity relationship for quinolones.	127
Table 5-2.	Source water and NOM characteristics.	133
Table 5-3.	Applied ozone dose (mg/L) necessary for 50% removal of ciprofloxacin and antimicrobial activity for a variety of NOM matrices.	151
Table 6-1.	Salient information for erythromycin.	156
Table 6-2.	Apparent second order rate constants ($k''_{O_3,app,EA}$) for the transformation of erythromycin A by ozone at pH 5.35-6.81.	168

Table B-1.	Fluorescence index for organic matter isolates.....	199
Table C-1.	Summary of inhibition data for antimicrobial activity assay with ciprofloxacin.	202
Table C-2.	Summary of inhibition data for antimicrobial activity assay with erythromycin run using the potency equivalents protocol.....	207

LIST OF FIGURES

Figure 2-1. SciFinder returns for keywords relating to pharmaceutical presence in the environment and water treatment processes aimed at treating pharmaceuticals.	10
Figure 2-2. Peroxone chemistry (adapted from Acero and von Gunten, 2001).	33
Figure 2-3. (a) Vosmaer sterilizer in Philadelphia circa 1905 (Vosmaer, 1916); (b) Schematic of Vosmaer sterilizer (Vosmaer, 1916).	35
Figure 2-4. (a) Schematic of a gaseous ozone reactor. (b) The ozone mass flow rate is a function of the oxygen gas flow rate and the ozone generator settings.	36
Figure 2-5. Representation of the interfacial film for a pseudo-first order kinetic regime with respect to ozone consumption (Dodd <i>et al.</i> , 2008).	37
Figure 2-6. Aqueous ozone experimental setup for batch experimentation.	39
Figure 2-7. Impact of SUVA on NOM reactivity with ozone (Westerhoff <i>et al.</i> , 1999a).	47
Figure 2-8. Structure-activity relationship for quinolone antibiotics (Lemke and Williams, 2008).	48
Figure 3-1. Examples of direct ozone measurement at 258 nm and the corresponding ozone concentrations found using Eq. 3-1.	56
Figure 3-2. Ozone reaction with indigotrisulfonate, and the resulting ozonation products (adapted from Bader and Hoigné, 1981).	57
Figure 3-3. Example of indirect ozone measurement using indigotrisulfonate, which absorbs light at 600 nm.	58
Figure 3-4. Representative chromatogram of ciprofloxacin analysis using HPLC with FLD.	59
Figure 3-5. Cyclophosphamide (100 µg/L) peak using LC-MS/MS.	60

Figure 3-6. Typical peaks for cyclophosphamide and intermediate oxidation products generated by ozone and hydroxyl radical reaction with cyclophosphamide.	61
Figure 3-7. A representative erythromycin peak using the LC-MS/MS analytical method described above.....	62
Figure 3-8. Examples of erythromycin and erythromycin intermediate oxidation products generated by erythromycin reaction with aqueous ozone.	63
Figure 3-9. A typical ifosfamide peak using the LC-MS/MS method described above.....	64
Figure 3-10. Example of combined method allowing concomitant analysis of cyclophosphamide and ifosfamide for the same injection volume.	65
Figure 3-11. Ifosfamide and ifosfamide intermediate peaks detected using LC-MS. Ifosfamide and ifosfamide intermediate oxidation products were detected by their distinctive <i>m/z</i> values and separated from the total ion current.	66
Figure 3-12. A representative <i>p</i> CBA peak (10 μ M) using the HPLC with PDA.	67
Figure 3-13. Schematic of the ozone reactor showing gaseous generation of ozone and the ozone stock solution container.	70
Figure 3-14. Schematic of experimental setup for batch transformation studies.	72
Figure 3-15. Schematic of the experimental setup for continuous ozone addition experiments.	73
Figure 3-16. Typical ozone concentration and ozone exposure profiles during experimentation.	75
Figure 3-17. Demonstration of the impact that dosing 1 mg/L DOC from Lake Austin HPOA on the aqueous ozone concentration in continuous ozone reactor.	76
Figure 3-18. Schematic of the continuous peroxone addition reactor.	78
Figure 3-19. (a) Ozone concentration and hydroxyl radical exposure history throughout a typical continuous peroxone addition experiment; (b) Hydroxyl radical exposure as a function of applied ozone exposure.	78
Figure 3-20. Determination of the second-order rate constant for ozone reaction with ifosfamide.	82

Figure 3-21. Determination of R_{ct} using the relationship described in Eq. 3-11.....	84
Figure 3-22. Ozone and hydroxyl radical exposure throughout an experiment employing 10 μ M <i>p</i> CBA.	85
Figure 3-23. Determination of the second-order rate constant for hydroxyl radical reaction with ifosfamide.	86
Figure 3-24. Ifosfamide transformation in the peroxone system as described by Eq. 3-17.....	88
Figure 3-25. Representative data and model fits (solid lines) collected from (a) the inhibition profile protocol (with ciprofloxacin) and (b) the potency equivalents protocol (with erythromycin) for running the antimicrobial activity assay.	93
Figure 4-1. (a) Schematic of the continuous liquid ozone addition reactor; (b) Behavior of ozone concentrations and ozone exposure throughout a continuous ozone addition experiment.	101
Figure 4-2. Determination of second order rate constant for hydroxyl radical reaction with cyclophosphamide (a) and ifosfamide (b) using the continuous addition peroxone reactor.	107
Figure 4-3. Determination of cyclophosphamide and ifosfamide second-order rate constants with ozone.	109
Figure 4-4. (a) Determination of R_{ct} and (b) plots of ozone and hydroxyl radical exposure corresponding to ozonation of a solution containing 1.71×10^{-3} M NaCl, 2.38×10^{-3} M NaHCO ₃ , 10^{-5} M <i>p</i> CBA, 3.83×10^{-7} M cyclophosphamide, and 3.83×10^{-7} μ g/L ifosfamide at pH 8.3.....	111
Figure 4-5. Transformation of cyclophosphamide and ifosfamide in a system that demonstrates ozone and hydroxyl radical exposure.	113
Figure 4-6. The impact of three different concentrations (0, 0.28, and 27.6 mg/L DOC) of organic matter (Lake Austin HPOA) on (a) Cyclophosphamide and (b) Ifosfamide removal as a function of the applied ozone dose (mol/L).	116
Figure 4-7. Cyclophosphamide transformation and production of intermediate products as a function of the molar ratio of applied ozone to the initial cyclophosphamide concentration (mol O ₃ / mol CYP) at a.) pH	

2.5 and b.) pH 9.6. Ifosfamide transformation and production of intermediate products as a function of the molar ratio of applied ozone to the initial ifosfamide concentration (mol O ₃ / mol IFO) at c.) pH 2.5 and d.) pH 9.6.....	118
Figure 4-8. Formation and transformation of m/z = 221.0, which corresponds to phosphoramidate mustard (cyclophosphamide) and isophosphoramidate mustard (ifosfamide) as a percentage of the initial cyclophosphamide/ ifosfamide response.	123
Figure 4-9. Typical LC-MS peaks for (a) cyclophosphamide and phosphoramidate mustard and (b) ifosfamide and isophosphamide mustard.	125
Figure 5-1. The impact of NOM source (no organic matter, Lake Austin HPOA, and Claremore Lake HPOA) and concentration (0, 2, and 4 mg/L DOC) on ciprofloxacin oxidation.	140
Figure 5-2. Kinetics of ciprofloxacin reaction with ozone and hydroxyl radical at pH 7 with 1mM NaHCO ₃ . in two solutions, one without organic matter and one with 0.5 mg/L DOC from Claremore Lake HPOA.....	143
Figure 5-3. The impact of NOM composition (hydrophobic organic acids and transphilic organic acids fractions) and pH (8.4 and 6.5) of Claremore Lake organic matter on ciprofloxacin oxidation.	145
Figure 5-4. <i>E.coli</i> inhibition profiles with ciprofloxacin for standards (“without oxidation”) and ozonated samples (“with oxidation”).....	147
Figure 5-5. Simultaneous removal of ciprofloxacin (heavy curves; corresponding to the model fits from Figure 5-1) and antimicrobial activity (hollow symbols) in the synthetic (0 mg/L DOC) and Lake Austin HPOA (2 and 4 mg/L DOC) solutions.....	149
Figure 5-6. Elimination of antimicrobial activity in the synthetic (0 mg/L DOC), Lake Austin HPOA (4 mg/L DOC), and Claremore Lake HPOA and TPIA (4 mg/L DOC) water matrices.	150
Figure 6-1. (a) Ozone reactor setup; (b) aqueous ozone concentration with time.....	161

Figure 6-2.	(a) Erythromycin transformation at different pH values; (b) determination of specific second order rate constant for erythromycin with ozone.	169
Figure 6-3.	Changes in erythromycin and anhydroerythromycin concentrations as a function of the mass ratio of applied ozone to DOC concentration.	171
Figure 6-4.	Verification of erythromycin rate constants through comparison of ozone exposure calculated from changes in erythromycin A and anhydroerythromycin A concentrations.	174
Figure 6-5.	Inhibition profile for erythromycin A against <i>E. coli</i> at pH 8.3.	176
Figure 6-6.	Difference between solutions containing erythromycin A and anhydroerythromycin A as the dominant species in solution on the <i>E. coli</i> -based antimicrobial activity assay.	177
Figure 6-7.	Antimicrobial activity data for experimental samples overlaid on the inhibition profile of erythromycin.	179
Figure 6-8.	Peaks for intermediate oxidation products generated by ozonation of erythromycin and anhydroerythromycin.	181
Figure B-1.	Description of the major regimes of a Fluorescence EEM map.	197
Figure B-2.	Fluorescence maps of (a) Claremore Lake HPOA, b.) Claremore Lake TPIA, c.) Lake Austin raw water, and d.) Lake Austin HPOA.	198
Figure C-1.	GraphPad Prism input/output for analysis of the ciprofloxacin and percent inhibition data presented above in Table C-1.	203
Figure C-2.	The inhibition profile of ciprofloxacin against <i>E. coli</i>	204
Figure C-3.	Percent inhibition plotted against LOG(C/C_0) for the ten data sets described in Table C-2.	209
Figure C-4.	Potency equivalents plotted against normalized erythromycin concentration.	210

Figure D-1.	a.) A microphotograph of a portion of the hemacytometer grid; each of the small boxes shown is 0.0625-mm × 0.0625-mm. b.) An illustration of the grid pattern on the hemacytometer and presentation of what areas (A-D) are used for cell counting.	212
Figure D-2.	Photograph of the solution coloring throughout the cell-response calibration experiment using HEK-293 cells and the MTS/PMS reagent solution.	213
Figure D-3.	Calibration curve of initial number of HEK-293 cells added to the microplate wells with the response determined using the difference in absorbance at 490 nm and 650 nm.	214
Figure D-4.	Results from an attempt to standardize the response of the MTS cytotoxicity assay to standard solutions of cyclophosphamide.	215
Figure E-1.	Comparison of the constant volume, variable volume, and modified constant volume models for ifosfamide transformation.	222
Figure E-2.	Comparison of the constant volume, variable volume, and modified constant volume models for cyclophosphamide transformation.	223
Figure E- 3.	Comparison of the constant volume, variable volume, and modified constant volume models for ifosfamide transformation.	224
Figure E-4.	Comparison of the constant volume, variable volume, and modified constant volume models for cyclophosphamide transformation.	225

CHAPTER 1: INTRODUCTION

This is an especially interesting time in the field of environmental engineering. In the past, water and wastewater treatment for specific compounds were reactionary measures aimed at resolving issues surrounding the contamination of water supplies. In fact, the birth of the modern environmental movement can be considered a reaction to Rachel Carson's landmark book, *Silent Spring* (Carson, 1962). With the rapid advances in environmental engineering since the 1970s, we are now in a unique position to engineer treatment processes aimed at removing emerging contaminants from water sources. The focus of this dissertation is on the removal of pharmacologically active compounds (PhACs) from water.

The sheer number of chemical compounds that the human population produces and employs is intimidating. PhACs represent only a small portion of these compounds. While it is difficult to estimate the total number of PhACs used in the world, 7,929 approved drugs are listed in the National Institutes of Health (NIH) Chemical Genomics Center (NCGC) pharmaceutical collection (NPC) browser (Huang *et al.*, 2011). From 2004 to 2008, global pharmaceutical sales grew from \$578 billion to over \$735 billion (IMS Health, 2007).

Documentation of the presence of such compounds in water is widespread, with PhACs being detected in surface waters on every continent (Ternes, 1998; Stumpf *et al.*, 1999; Schulz and Peall, 2000; Kolpin *et al.*, 2002; Falconer *et al.*, 2006; Kim *et al.*, 2007; Hale *et al.*, 2008). The concentrations of PhACs in the environment tend to range from less than 1 ng/L to several µg/L (Ternes, 1998; Kolpin *et al.*, 2002; Kim *et al.*, 2007). However, exceptions exist; most notably, Larsson *et al.* (2007) reported ciprofloxacin

concentrations up to 31 mg/L in the wastewater effluent of a treatment plant serving ninety bulk drug manufacturers.

A considerable amount of research has concentrated on assessing the impact of pharmaceuticals and personal care products (PPCPs), endocrine-disrupting chemicals (EDCs), and pesticides/insecticides, among other chemicals, on aquatic life. Aquatic life is especially susceptible to hydrophobic contaminants, including many of the EDCs and PhACs, because of the potential for bioaccumulation in low trophic levels and biomagnification of these compounds in the marine food chain (Tyler *et al.*, 1998; Vos *et al.*, 2000). The impact of PhACs on human health is not yet fully understood; however, progress has been made in three major areas of study: direct impacts on human cells (Pomati *et al.*, 2006), spread of antibiotic resistance (Schwartz *et al.*, 2003; Duong *et al.*, 2008; Szczepanowski *et al.*, 2009), and indirect impacts on cell signaling processes (Linares *et al.*, 2006; Fajardo and Martínez, 2008). To lessen the threat from PhAC contamination, several states (Maine, 2005; California, 2007; Iowa, 2007; Oregon, 2007; Wisconsin, 2007; Pennsylvania, 2008) have enacted legislation to encourage proper disposal of unused and expired medication. On the federal level, concern over the presence of PhACs in the environment has prompted Congress to propose adding hazardous pharmaceutical wastes to The Universal Waste Rule (EPA, 2008).

PROBLEM STATEMENT

Research efforts aimed at identifying the capabilities of water treatment plants to remove pharmaceuticals in various background water quality matrices are ongoing (Steger-Hartmann *et al.*, 1997; Ternes, 1998; Stumpf *et al.*, 1999; Adams *et al.*, 2002; Westerhoff *et al.*, 2005). Several research studies have focused on oxidation and advanced oxidation processes (AOPs) for removal of PhACs due to process flexibility, ease of installation, and competitive economics (Huber *et al.*, 2003; Snyder *et al.*, 2006). Ozone-based processes have great potential, as reflected in their increasingly frequent use in water reuse scenarios (Halliday, 2006; APTwater, 2011; Windhoek, 2011). The work

of von Gunten has demonstrated the use of aqueous ozone stock solutions for various purposes, including the determination of ozone–PhAC reaction kinetics (Dodd *et al.*, 2006), PhAC transformation for specific ozone doses (Suarez *et al.*, 2007), and measurement of hydroxyl radical exposure (Elovitz and von Gunten, 1999; Elovitz *et al.*, 2000). This body of literature builds on earlier work by Hoigné, Stachelin, and Bader (Hoigné and Bader, 1976; Stachelin and Hoigné, 1982) in understanding ozone decomposition in water and reaction chemistry with chemical contaminants.

Oxidative treatment is a transformative process. DeWitte *et al.* (2008) identified some of the operative ciprofloxacin transformations during ozonation; the chemical structures of the twelve intermediate oxidation products that were suggested are markedly similar to the structure of ciprofloxacin. Since pharmacological activity is a strong function of chemical structure (Lemke and Williams, 2008), one key hypothesis associated with this research is that some oxidative intermediate products may exert pharmacological or toxicological activity. In the past few years, several researchers (Suarez *et al.*, 2007; Baeza, 2008; Dodd *et al.*, 2009; Paul *et al.*, 2010) have used an antimicrobial susceptibility assay (NCCLS, 2004) to describe treatment efficiency in terms of pharmacological activity. The ability to monitor residual antimicrobial activity allows for pragmatic treatment goals (*i.e.*, treatment goals based upon removal of the biological response exerted by the contaminants rather than individual targets for each PhAC).

OBJECTIVES

The overall goal of this research was to develop an approach for considering water treatment of PhACs in terms of not only parent compound removal but also elimination of residual pharmacological activity. In this research, four pharmaceuticals (*i.e.*, ciprofloxacin, cyclophosphamide, erythromycin, and ifosfamide) were employed to build a comprehensive story about how transformation of parent compounds by ozonation and advanced oxidation processes relates to the elimination of pharmacological

activity in a water treatment context. To elucidate this relationship, the following objectives were undertaken:

1. To investigate the transformation of the four compounds of concern in the ozone and peroxone systems;
2. To describe the kinetics of degradation of the four compounds of concern with aqueous ozone and hydroxyl radicals;
3. To identify the early intermediate oxidation products for the compounds of concern;
4. To measure the antimicrobial activity of water sources containing ciprofloxacin and erythromycin throughout the treatment process; and,
5. To characterize the impact of natural organic matter (NOM) on the transformation of the four compounds of concern and on the elimination of residual antimicrobial activity.

APPROACH

The findings from Objective 1 were employed to determine the suitability of ozone-based processes to treat PhACs. In Objective 2, the rate constants for the PhACs of concern with ozone and hydroxyl radicals were found to enable prediction of PhAC transformation in treatment processes where ozone exposure and hydroxyl radical exposure can be controlled. The intermediate oxidation products formed through PhAC reaction with ozone and hydroxyl radicals were identified in Objective 3. The cumulative findings from Objectives 1-2 illustrate the amount and rate of PhAC transformation expected in ozone-based processes; furthermore, the structures of the resulting intermediate oxidation products were characterized in Objective 3. For the four PhACs of concern, the structures of intermediate products suggested their relative ability to exert a specific biological response. For ciprofloxacin and erythromycin, the ability of intermediate oxidation products to maintain residual antimicrobial activity was tested in Objective 4; however, for cyclophosphamide and ifosfamide, the discussion was limited

to the theoretical potential for intermediate oxidation products to manifest pharmacological activity. Finally, the impacts of NOM (Objective 5) on pharmaceutical oxidation in ozone-based systems were investigated in terms of parent compound transformation, intermediate product formation, and elimination of residual pharmacological activity.

The chapters of this dissertation are organized as follows. Chapter 2 contains an extensive literature review of pharmaceutical presence in water sources, the chemistry of the four compounds studied in this research, ozone chemistry, ozone application strategies (gaseous vs. aqueous ozone addition), and the impact of NOM on ozone processes. Chapter 3 describes the materials and methods employed in the research with a particular emphasis on the analytical methods used to measure pharmaceuticals, the experimental designs employed for ozone experiments, and the antimicrobial activity protocols utilized to measure residual antimicrobial activity. Chapter 4 discusses ozone and peroxone treatment of the two chemotherapy agents (cyclophosphamide and ifosfamide), including identification of rate constants using the novel continuous aqueous ozone addition reactor, demonstration of the impact of DOC on transformation, and characterization of intermediate oxidation products. Chapter 5 presents results showing ciprofloxacin oxidation in a continuous aqueous ozone addition reactor and how the presence and composition of NOM can impact not only ciprofloxacin transformation, but also antimicrobial activity elimination. Chapter 6 examines the transformation kinetics of erythromycin and a major erythromycin metabolic product, anhydroerythromycin A, with ozone, the intermediate oxidation products formed via ozonation, and the antimicrobial activity of erythromycin, anhydroerythromycin A, and their intermediate oxidation products. Chapters 4 through 6 were written as drafts of papers to be submitted for publication in refereed journals and therefore repeat, in abbreviated form, some of the background and methods from Chapters 2 and 3. Chapter 7 draws conclusions about the results presented in Chapters 4-6 and describes plans for future work.

SIGNIFICANCE

The significance of this research lies in the extension of the results to water and wastewater treatment applications. Of particular interest is the application for water reuse scenarios. One of the most contentious aspects of water reuse and wastewater reclamation is the ability for trace organic contaminants to pass through treatment processes and enter drinking water supplies. Many water reuse facilities employ tertiary treatment processes aimed at disinfection and treatment of trace organic contaminants (Halliday, 2006; APTwater, 2011; Windhoek, 2011). As ozonation is a typical unit process employed in water reuse scenarios, understanding the ability of the ozone process to remove trace organic contaminants, including pharmacologically active compounds, from the water source is crucial.

As the length of the pathway between wastewater and drinking water is reduced, the efficacy of ozonation processes needs to be better understood and changes to traditional ozonation processes need to be developed. This dissertation introduces the employment of two novel ozone processes to determine the kinetics of PhAC transformation by ozone and hydroxyl radicals: the continuous aqueous ozone addition reactor and the continuous peroxone addition reactor. In the first scenario, a highly concentrated ozone solution is continuously pumped into a reactor containing the water of interest; in the second scenario, hydrogen peroxide and the highly concentrated ozone solution are concurrently pumped into a reactor containing the water of interest.

Finally, this research takes important strides beyond many previous ozone-based research efforts. Traditionally, researchers have investigated individual aspects of ozone treatment processes relevant to water treatment scenarios. In this body of work, I demonstrate not only the ability of ozone-based treatment processes to transform pharmaceuticals, but also the impact of NOM on the removal efficiency of pharmaceuticals; furthermore, I characterize intermediate oxidation products. Perhaps the most important aspect of this research is the measurement of residual antimicrobial

activity throughout treatment processes for ciprofloxacin and erythromycin. As treatment goals should be based upon the ability of the water to exert a biological response, demonstrating the means to measure the residual pharmacological activity is extremely important.

CHAPTER 2: LITERATURE REVIEW

In *Pharma-ecology: The Occurrence and Fate of Pharmaceuticals and Personal Care Products in the Environment*, Jjemba (2008) states, “The human impulse for a cure runs quite deep, and our first instinct whenever we feel sick or heading toward sickness is to medicate.” This impulse has contributed to the rapid rise of the pharmaceutical industry, and our increased consumption of various medications. As with many other anthropogenically-derived substances, increased consumption inevitably leads to environmental contamination.

PHARMACEUTICALS IN THE ENVIRONMENT

The presence of trace organic compounds, and pharmacologically active compounds (PhACs) in particular, in global water supplies has been widely documented during the last decade (Halling-Sorensen *et al.*, 1998; Daughton and Ternes, 1999; Kolpin *et al.*, 2002). Halling-Sorensen *et al.*’s (1998) review article discussed the presence of pharmaceutical substances in groundwater, river water, sediments, ocean dumping sites, and soils; the paper goes on to describe studies investigating the biodegradability, sorption, and toxicity of pharmaceutical substances in a variety of media. In the conclusion of the article, Halling-Sorensen *et al.* note that “further research in this hitherto little explored field would be necessary to assess the environmental risk involved in exposing medical substances to the environment.” In 1999, Daughton and Ternes asked whether pharmaceuticals and personal care products are “agents of subtle change.” In this landmark review, Daughton and Ternes (1999) aimed “to catalyze a discussion in the environmental science community to determine the significance of PPCPs in the environment.” A few years later, Kolpin *et al.* (2002) documented the results of a nationwide reconnaissance conducted by the United States Geological Survey

(USGS) to assess the presence of trace organic contaminants, including pharmaceuticals, personal care products, hormones, pesticides, and plasticizers, among other wastewater-derived contaminants, in U.S. surface water. That study sampled from 139 streams across 30 U.S. states; the analytical methods developed for the study were able to test for 95 different trace organic contaminants (TrOCs) found in municipal wastewater. Of the 95 compounds investigated, 82 compounds were detected at least once in the study; furthermore, 80% of the 139 streams investigated contained at least one compound. Kolpin *et al.* (2002) interpreted these results as evidence that TrOCs pass through wastewater treatment and persist in the environment.

In 2008, this issue was brought to the public's attention through an Associated Press news report by Donn *et al.* (2008). The journalists contacted water utilities around the country and inquired as to whether pharmaceuticals had been detected in drinking water supplies or finished drinking water. This report was distributed in major newspapers around the country with headlines such as *AP Probe Finds Drugs in Drinking Water* (Donn *et al.*, 2008). The original article opens with the following statement: "A vast array of pharmaceuticals – including antibiotics, anti-convulsants, mood stabilizers and sex hormones – have been found in the drinking water supplies of at least 41 million Americans..." Other findings from this report include the following:

"Officials in Philadelphia said testing there discovered 56 pharmaceuticals or byproducts in treated drinking water, including medicines for pain, infection, high cholesterol, asthma, epilepsy, mental illness and heart problems. Sixty-three pharmaceuticals or byproducts were found in the city's watersheds.

Anti-epileptic and anti-anxiety medications were detected in a portion of the treated drinking water for 18.5 million people in Southern California.

A sex hormone was detected in San Francisco's drinking water." (Donn *et al.*, 2008)

Needless to say, this article generated a media frenzy regarding the presence of pharmaceuticals in drinking water; that frenzy has resulted in increased research activity with respect to treatment processes aimed at removing trace organic contaminants in

water and wastewater treatment plants. As mentioned above, the first major articles addressing the issue of pharmaceutical presence in the environment came in the late 1990s. Figure 2-1 shows the number of SciFinder returns for two separate searches: (1) “pharmaceutical” & “environment” & “contamination” and (2) “pharmaceutical” & “water treatment.” In the mid-late 1990s, the slope of the curve steepens. Recall that this period coincides with publication of the first major articles (Halling-Sorensen *et al.*, 1998; Daughton and Ternes, 1999) calling attention to this topic. The dates for release of the Kolpin *et al.* (2002) and Donn *et al.* (2008) studies are also superimposed on the plot. Clearly, release of these reports coincided with increased research activity in this field.

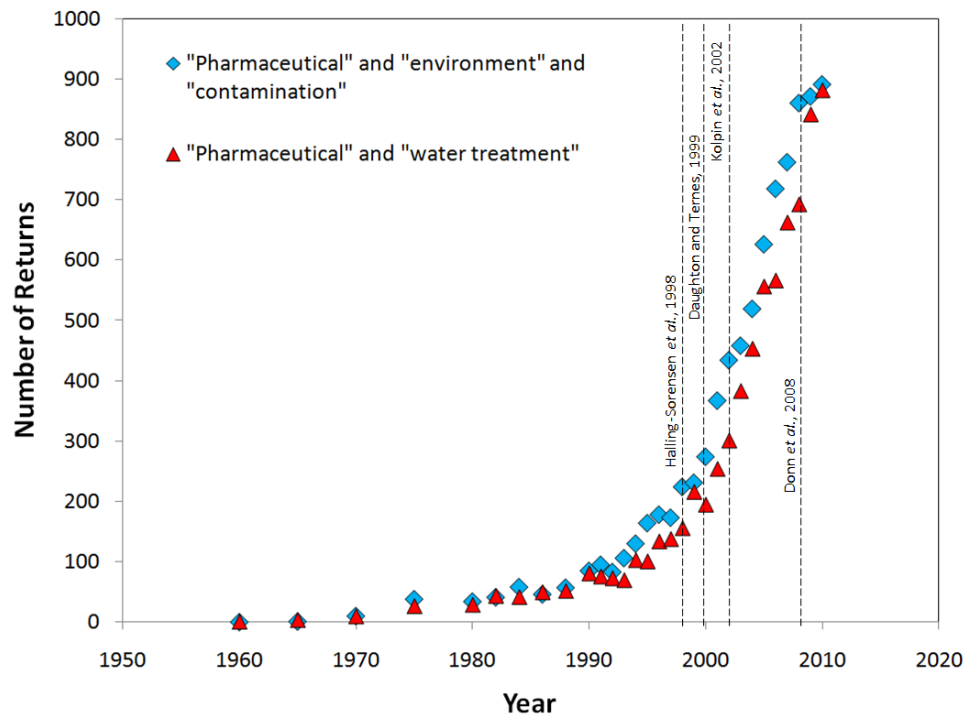


Figure 2-1. SciFinder returns for keywords relating to pharmaceutical presence in the environment and water treatment processes aimed at treating pharmaceuticals.

Avenues for Pharmaceutical Introduction into the Environment

Daughton (2007) recently published a figure documenting the avenues for pharmaceutical contamination of the environment, including usage by individuals and pets, release of treated/untreated hospital wastes to domestic sewage systems, release to private septic/leach fields, applications of biosolids to agricultural land, direct release to open waters via washing, bathing, and swimming, discharge of regulated/controlled industrial manufacturing waste streams, disposal to landfills, release to open waters from aquaculture, and release of drugs that serve as pest control agents, among others. In this dissertation, the focus rests on wastewater treatment plants (WWTPs). In WWTPs, the two major avenues for pharmaceutical contamination are excretion of unmetabolized pharmaceuticals from the human body and improper disposal of medication.

Excretion of pharmaceuticals and active metabolites from the human body (Lienert *et al.*, 2007) is a direct function of drug uptake into plasma, metabolism of the drug, and the urinary excretion rate (Lemke and Williams, 2008). The excretion rate of pharmaceuticals depends on the chemical structure and properties of individual compounds and is expressed as

$$F_{ex} (\%) = \frac{M_{PhAC,urine}}{M_{PhAC,dose}} \times 100\% \quad \text{Eq. 2-1}$$

In Eq. 2-1, F_{ex} is the urinary excretion factor, $M_{PhAC,urine}$ is the mass of the parent pharmaceuticals excreted in the urine, and $M_{PhAC,dose}$ is the mass of parent pharmaceutical dosed to the patient. Additionally, the administered dose can also affect the excretion factor. For example, ifosfamide administered at low doses (1.5 g/m² oral dose) demonstrates an excretion factor of 12-18%; however, at high doses (5 g/m² IV dose and 1.5 g/m² oral dose) shows a much higher excretion factor, 53.1±9.6% (Brunton *et al.*, 2006). Here, the m² refers to body surface area, which is calculated as a function of height and weight. Other compounds demonstrate a wide range of urinary excretion

factors; for instance, heparin, an anticoagulant, exhibits negligible urinary excretion, and metformin, one of the most widely prescribed antidiabetic drugs, has a urinary excretion factor of 99.9% (Brunton *et al.*, 2006). While other factors are involved, higher excretion factors correlate to higher PhAC concentrations in raw wastewater.

Disposal of unused or expired medication has been a topic of recent investigations (Bound *et al.*, 2006; Braund *et al.*, 2009; Glassmeyer *et al.*, 2009). Glassmeyer *et al.* (2009) found that only 2% of respondents from the United States used all of their medication, while 7.2% of respondents did not dispose of unused medications, 1.4% returned the unused medication to the pharmacy, 35.4% disposed of unused medication down the sink or toilet, and 54% disposed of unused medication in the garbage. Disposal of medication down the sink or toilet constitutes improper disposal due to the potential for pharmacologically active compounds to enter the aquatic environment and drinking water supplies. Bound *et al.* (2006) found that the disposal method for unused medications by people in the United Kingdom varied by pharmaceutical class. For example, 75.3% of respondents said that they dispose of antihistamines into the trash, 9.1% into the toilet/sink, and 14.3% are returned to the pharmacy; however, 66.7% of respondents said that dispose of antidepressants in the trash, and the other 33.3% return unused antidepressants to the pharmacy. Later, Braund *et al.* (2009) found that the disposal method for unused medications in New Zealand varies depending on the medication formulation (*i.e.*, liquid, tablet/capsule, or ointment/cream). Liquid medications are more likely to be disposed of into the sink/toilet, whereas tablets/capsules and ointments/creams are more likely to be disposed of into the garbage (Braund *et al.*, 2009). Recently, legislative action in the United States has aimed to decrease the amount of PhACs entering wastewater streams through improper disposal of unused and/or expired medication.

LEGISLATION OF PHARMACEUTICAL CONTAMINANTS

The Office of National Drug Control Policy published a document titled “Proper Disposal of Prescription Drugs” in October, 2009 (ONDCP, 2009). In that document, citizens are advised to only flush drugs approved for flushing by the Federal Drug Administration (FDA, 2010); the FDA list contains 27 drugs. If the drugs are not recommended for flushing, citizens are told to use community drug take-back programs or household hazardous waste collection events. If drug collection programs are not available, citizens are told to mix the drugs with cat litter or coffee grounds, seal the mixture in a disposable container or sealable bag, and to dispose of the container in the trash.

In 2005, Maine became the first state to legislate the disposal of unused pharmaceuticals. Title 22 §2700 of the Maine Revised Statutes (Maine, 2005) established the Unused Pharmaceutical Disposal Program, the purpose of which is “to ensure the safe, effective, and proper disposal of unused pharmaceuticals.” The legislation calls for the creation of a system that provides for the return of unused pharmaceuticals through the use of prepaid mailing envelopes (Maine, 2005). Since that time, a number of other states have enacted similar bills; short descriptions of those bills (California, 2007; Iowa, 2007; Oregon, 2007; Wisconsin, 2007; Pennsylvania, 2008; Virginia, 2008) are provided in Table 2-1.

Table 2-1. State bills relating to regulation of unused pharmaceuticals.

State	Year	Bill	Description
Maine	2005	Revised Statutes Title 22 § 2700	Unused Pharmaceutical Disposal Program collects unused pharmaceuticals and ensures safe, effective, and proper disposal.
California	2007	Public Resources Code § 47120-47126	The new sections of the code tasked state agencies with developing a model for the safe take-back of drugs and the diversion of drug waste for use or sale.
Iowa	2007	Senate File 579	This act appropriated \$225,000 for a pharmaceutical collection and disposal pilot project.
Oregon	2007	Senate Bill 737	The bill relates to bettering water quality. One of the measures listed is the institution of pharmaceutical take-back programs.
Wisconsin	2007	Senate Bill 40	The bill makes amendments to household hazardous waste laws.
Pennsylvania	2008	House Bill 2073	The Pharmaceutical Drug Disposal Act requires pharmaceutical retailers to establish means for collecting pharmaceutical drugs for proper disposal.
Virginia	2008	House Bill 86	The bill created the Unused Pharmaceutical Disposal Program, which establishes a system for returning unused pharmaceuticals to a single collection location.

Concern over the presence of PhACs in the environment has prompted Congress to propose adding hazardous pharmaceutical wastes to The Universal Waste Rule (EPA, 2008). The proposed regulation would essentially mandate pharmaceutical waste collection guidelines to minimize the amount of pharmaceuticals being introduced into the environment; however, the rule relies on pharmacies, hospitals, physicians' offices, dentists' offices, outpatient care centers, ambulatory health care services, residential care facilities, veterinary clinics, and other facilities that generate hazardous pharmaceutical wastes to act as collection centers for expired and unused medications. Although this legislation was proposed in 2008, these changes to the Universal Waste Rule have not yet been finalized.

While states are starting to adopt legislation requiring proper handling and disposal of unused and expired medication, treatment of pharmaceuticals in wastewater streams or drinking water sources has not yet been included in legislation. Given the media buzz generated by the 2008 Associated Press article (Donn *et al.*, 2008), future legislation on the discharge of pharmacologically active compounds from wastewater treatment plants is expected. In fact, the EPA's Candidate Contaminant List 3 (CCL3) lists several PPCPs and EDCs including 1,4-dioxane, 17 α -ethinylestradiol, 2-methoxyethanol, 2-propen-1-ol, benzyl chloride, cobalt, equilenin, equilin, erythromycin, 17 β -estradiol, estriol, estrone, mestranol, nitrobenzene, nitroglycerin, 19-norethisterone, σ -toluidine, quinoline, tellurium, and, triethylamine (EPA, 2009). Selection of a contaminant to the EPA CCL3 means that these chemicals are currently being considered for regulation under the Safe Drinking Water Act; therefore, it seems likely that future contaminant candidate lists will also include pharmaceuticals. For that reason, study of the ability of water treatment processes to treat PhACs is merited. In this research, ozone-based water treatment processes are employed to treat four model pharmaceuticals.

PHARMACEUTICALS OF CONCERN IN THIS STUDY

This study focused on four pharmacologically active compounds (PhACs): ciprofloxacin, cyclophosphamide, ifosfamide, and erythromycin. Salient information for the four compounds of concern is provided in Table 2-2. These compounds represent two pharmaceutical classes, namely, antibiotic (ciprofloxacin and erythromycin) and chemotherapy agents (cyclophosphamide and ifosfamide). Clearly, these compounds are distinctly different in their degree of aromaticity, molecular weight, and speciation; however, they also demonstrate chemical similarities, especially the two chemotherapy agents, cyclophosphamide and ifosfamide, which are structural isomers. In this case, cyclophosphamide and ifosfamide were both studied to determine how the placement of the two chloroethyl functional groups affects transformation kinetics with ozone and hydroxyl radicals, as well as the structures of the resultant intermediate oxidation products.

Ciprofloxacin

Ciprofloxacin is a second generation fluoroquinolonic antibiotic. Shortly after the introduction of fluoroquinolonic antibiotics in the late 1980s, ciprofloxacin became the most widely used antibiotic in the world (Norrby and Lietman, 1993). In 2006, ciprofloxacin ranked 139th in pharmaceutical sales with \$755 million in sales (Humphreys, 2007). As of 2006, ciprofloxacin had generated a lifetime sales profit of \$19 billion (Finch and Hunter, 2006); and in 2009, fluoroquinolones were the third most profitable class of antibiotics with sales of \$7.1 billion (Hamad, 2010). Ciprofloxacin is widely prescribed for urinary tract infections, cystitis, diarrhea, Typhoid fever, sinusitis, and gonorrhea, among others (FDA, 2004). Most notably, ciprofloxacin was prescribed for anthrax infections (Meyerhoff *et al.*, 2004). Given the extremely active research into newer fluoroquinolones (De Souza, 2005), ciprofloxacin use is beginning to decline; however, it is still a widely prescribed pharmaceutical (Prescription, 2011). The mode of

action for ciprofloxacin, as well as the other three pharmaceuticals of concern, is provided in Table 2-3.

Table 2-2. Salient information for the chemicals of concern.

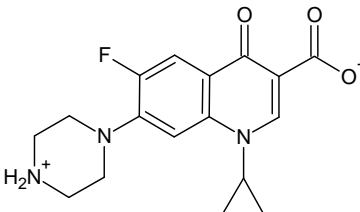
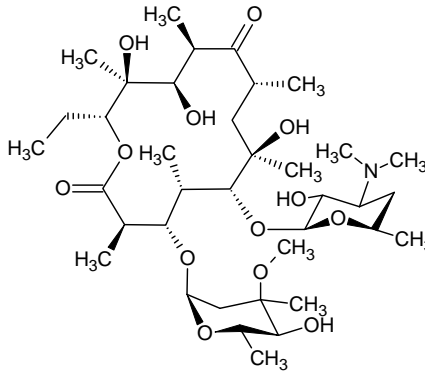
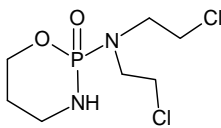
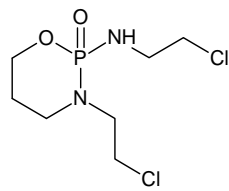
NAME	CIPROFLOXACIN	ERYTHROMYCIN
Chemical Formula	$C_{17}H_{18}FN_3O_3$	$C_{37}H_{67}NO_{13}$
Molecular Weight (g/mol)	331.3	733.9
Structure		
Class	Antibiotic	Antibiotic
CAS Number	85721-33-1	114-07-8
pK _a	6.2, 8.8	8.8
F _{ex} (%)	50 ± 5	12 ± 7
Name	CYCLOPHOSPHAMIDE	IFOSFAMIDE
Chemical Formula	$C_7H_{15}Cl_2N_2O_2P$	$C_7H_{15}Cl_2N_2O_2P$
Molecular Weight (g/mol)	260.9	260.9
Structure		
Class	Chemotherapy Agent	Chemotherapy Agent
CAS Number	50-18-0	3778-73-2
pK _a	2.84 - 6.5	1.45 - 4.0
F _{ex} (%)	6.5 ± 4.3	12-18 (low dose), 53.1 ± 9.6 (high dose)

Table 2-3. Mode of action for PhACs of concern.

Pharmaceutical	Mode of Action
Ciprofloxacin	Inhibits DNA gyrase and topoisomerase IV, which relieve stress during DNA unwinding. Inhibition of these enzymes disallows bacterial DNA separation, thereby inhibiting cell division.
Erythromycin	Binds to the 50S subunit of the bacterial 70S rRNA complex. Erythromycin interferes with aminoacyl translocation, preventing the transfer of the tRNA bound at the A site of the rRNA complex to the P site of the rRNA complex. Without this translocation, the A site remains occupied, which interferes with the production of functionally useful proteins.
Cyclophosphamide	Cyclophosphamide is metabolized by cytochrome P450 to 4-hydroxycyclophosphamide, which is then metabolized to phosphoramidate mustard. Phosphoramidate mustard forms DNA crosslinks between and within DNA strands at guanine N-7 positions.
Ifosfamide	Ifosfamide is metabolized by cytochrome P450 to 4-hydroxyifosfamide, which is then metabolized to isophosphoramidate mustard. Isophosphoramidate mustard forms DNA crosslinks between and within DNA strands at guanine N-7.

Erythromycin

Erythromycin was discovered in 1952 when it was isolated from the metabolic products of a strain of *Streptomyces erythreus* (McGuire *et al.*, 1952). Erythromycin is a broad-spectrum antibiotic in the macrolide family, and it is prescribed for bacterial infections like bronchitis, diphtheria, Legionnaires' disease, pertussis, pneumonia, and ear, urinary tract, and skin infections, among others (Wishart *et al.*, 2008). Since the discovery of erythromycin, a number of other macrolide compounds have been developed, including clarithromycin (1970s), azithromycin (1980), roxithromycin (1987), and telithromycin (1998); regardless, erythromycin remains one of the most successful drugs of all time (Omura, 2002; Pal, 2006). In 2009, macrolides were the fourth most popular class of antibiotics with total sales of \$4.8 billion (Hamad, 2010).

Cyclophosphamide and Ifosfamide

Cyclophosphamide and ifosfamide are structural isomers. These compounds are prodrugs, meaning that cyclophosphamide and ifosfamide, themselves, are pharmacologically inactive; the compounds are converted into their active forms during metabolism. First, the two compounds are converted to 4-hydroxycyclophosphamide and 4-hydroxyifosfamide, respectively, which are also prodrugs (Low *et al.*, 1983). The 4-hydroxy derivatives are further metabolized to the reactive mustards, phosphoramidate mustard (cyclophosphamide) and isophosphoramidate mustard (ifosfamide), respectively (Low *et al.*, 1983). The reactive mustards are cytotoxic and work by alkylating DNA, prohibiting separation of DNA strands during replication (Fleming, 1997). In addition to being cytotoxic, cyclophosphamide and ifosfamide are teratogenic, mutagenic, and carcinogenic (Bus *et al.*, 1973; Murthy *et al.*, 1973; Mohn and Ellenberger, 1976). The concentrations associated with cyclophosphamide and ifosfamide toxicity are organism dependent.

Environmental Presence of Compounds of Concern

As discussed in a previous section, many avenues exist for pharmacologically active compounds to enter the environment; however, for the compounds studied in this research, the major source is wastewater treatment plants (WWTPs). The excretion factors for the four pharmaceuticals of concern range from 6.5% to 50%, indicating that a relatively large fraction of the consumed pharmaceuticals is excreted and sent to WWTPs. As a result, all four of these compounds have been detected in hospital wastewater, wastewater treatment plant influent, wastewater treatment plant effluent, and surface water (Table 2-4). While the measured concentrations vary by compound, PhAC concentrations in hospital wastewater can be relatively high (1-150 µg/L). Due to dilution and some removal in wastewater treatment plants, surface water concentrations were low for all four compounds, typically on the order of tens of ng/L or less. Two notable exceptions to this trend are the following: Larsson *et al.* (2007) reported concentrations of 28-31 mg/L ciprofloxacin in effluent from a WWTP serving about 90

bulk drug manufacturers and Kolpin *et al.* (2002) detected surface water erythromycin concentrations of up to 1.7 µg/L. The presence of the four chemicals of concern in surface waters suggests the potential for occurrence in drinking water but no literature has reported their presence to date.

Table 2-4. Detection of the four pharmaceuticals of concern.

Drug	Source	Concentration (ng/L)	Concentration Type	Reference
Ciprofloxacin	Groundwater	nd *	range	Barnes <i>et al.</i> , 2008
	Hospital WW	140,000	max	Vasconcelos <i>et al.</i> , 2009
	Hospital WW	nd – 54,049	range	Thomas <i>et al.</i> , 2007
	Hospital WW	1,100 – 25,800	range	Duong <i>et al.</i> , 2008
	Hospital WW (treated)	3,700	average	Duong <i>et al.</i> , 2008
	Surface water	nd - 26.15	range	Calamari <i>et al.</i> , 2003
	Surface water	26	average	Castiglioni <i>et al.</i> , 2004
	Surface water	nd-18	range	Golet <i>et al.</i> , 2002
	Surface water	nd	range	Tamtam <i>et al.</i> , 2008
	Surface water	nd – 36	range	Vieno <i>et al.</i> , 2007
	Surface water	nd - 30	range	Kolpin <i>et al.</i> , 2002
	WW effluent	62-106	range	Golet <i>et al.</i> , 2002
	WW effluent	nd – 400	range	Miao <i>et al.</i> , 2004
	WW effluent	251	median	Zuccato <i>et al.</i> , 2005
	WW effluent	nd – 2,700	range	Bhandari <i>et al.</i> , 2008
	WW effluent	nd - 742	range	Thomas <i>et al.</i> , 2007
	WW effluent	45 - 405	range	Golet <i>et al.</i> , 2001
	WW effluent	28,000,000 – 31,000,000	range	Larsson <i>et al.</i> , 2007
	WW influent	313-568	range	Golet <i>et al.</i> , 2002
	WW influent	nd - 4600	range	Bhandari <i>et al.</i> , 2008
	WW influent	nd - 5876	range	Thomas <i>et al.</i> , 2007
Cyclophosphamide	Hospital WW	nd - 21	range	Thomas <i>et al.</i> , 2007
	Surface water	nd	range	Calamari <i>et al.</i> , 2003
	Surface water	0.05 - 0.17	range	Buerge <i>et al.</i> , 2006
	WW effluent	0.6	median	Zuccato <i>et al.</i> , 2005

Drug	Source	Concentration (ng/L)	Concentration Type	Reference
Cyclophosphamide	WW effluent	nd	range	Thomas <i>et al.</i> , 2007
	WW effluent	2 - 10	range	Buerge <i>et al.</i> , 2006
	WW effluent	nd - 17	range	Steger-Hartmann <i>et al.</i> , 1997
	WW effluent	6	average	Kim <i>et al.</i> , 2009
	WW influent	nd	range	Thomas <i>et al.</i> , 2007
	WW influent	2 - 11	range	Buerge <i>et al.</i> , 2006
	WW influent	nd - 143	range	Steger-Hartmann <i>et al.</i> , 1997
Ifosfamide	Hospital WW	nd - 338	range	Thomas <i>et al.</i> , 2007
	Surface water	nd - 0.14	range	Buerge <i>et al.</i> , 2006
	WW effluent	nd - 71	range	Thomas <i>et al.</i> , 2007
	WW effluent	nd - 6	range	Buerge <i>et al.</i> , 2006
	WW influent	nd	range	Thomas <i>et al.</i> , 2007
	WW influent	nd - 5	range	Buerge <i>et al.</i> , 2006
Erythromycin	Groundwater	nd	range	Barnes <i>et al.</i> , 2008
	Reclaimed WW	154 - 611	range	Kinney <i>et al.</i> , 2006
	Surface water	1.40-15.90	range	Calamari <i>et al.</i> , 2003
	Surface water	5	average	Castiglioni <i>et al.</i> , 2004
	Surface water	nd - 6.9	range	Hao <i>et al.</i> , 2006
	Surface water	nd – 1,700	range	Kolpin <i>et al.</i> , 2002
	WW effluent	838	maximum	Miao <i>et al.</i> , 2004
	WW effluent	47.4	median	Zuccato <i>et al.</i> , 2005
	WW effluent	nd	range	Ternes <i>et al.</i> , 2003
	WW effluent	110	average	Kim <i>et al.</i> , 2009
	WW effluent	6,000	maximum	Hirsch <i>et al.</i> , 1999
	WW influent	620	average	Ternes <i>et al.</i> , 2003

* nd = non-detect

HUMAN AND ENVIRONMENTAL HEALTH THREAT FROM PHAC PRESENCE IN DRINKING WATER SUPPLIES

Based upon their pharmaceutical class, the four compounds listed above are of concern due to documented and perceived threats to human and environmental health. Pomati and coworkers (2006; 2007; 2008) have undertaken several studies to investigate the effects of 13 pharmaceuticals on *Escherichia coli*, zebrafish liver, human embryonic kidney, and human ovarian carcinoma cells. They have found that trace levels of pharmaceuticals can inhibit the growth of human embryonic kidney cells by up to 30% (Pomati *et al.*, 2006), and that the pharmacological activity of drug mixtures can vary from that of individual compounds (Pomati *et al.*, 2008). These findings are of great importance because they include the first toxicological investigation into the effects of trace levels of (non-endocrine disrupting) PhAC mixtures on human cells. In addition to effects of trace organic contaminants on proliferation of select bacterial and mammalian cell lines, other human health and environmental concerns include the spread of antibiotic resistance, toxicity, and interruption of cell signaling processes.

As mentioned in a previous section, several authors have detected antibiotic resistance genes in and downstream from wastewater treatment plants (Schwartz *et al.*, 2003; Volkmann *et al.*, 2004; Mispagel and Gray, 2005; Baquero *et al.*, 2008; Duong *et al.*, 2008; Szczepanowski *et al.*, 2009). While hundreds of antibiotic resistance genes have been detected in wastewater treatment plants and in wastewater treatment plant effluent, consider the Szczepanowski *et al.* (2009) paper that identified the following ciprofloxacin resistance genes: *qnrB1*, *qnrB2*, *qnrB5*, *qnr*, and *qnrS2*, as well as general quinolone resistance genes such as *qnrB4*; all of these genes were found in the activated sludge tank and the final WWTP effluent. Erythromycin resistance genes were also detected: *ereA2*, *ereA*, *ereB*, *mph(B)*, *mph(A)*, *mph*, *ermA*, *ermB*, *mef(A)*, *mefE*, *mefI*, *mel*, *msrA*, and *mexD*, as well as general macrolide resistance genes like *mphBM* (Szczepanowski *et al.*, 2009). All of these genes were detected in the activated sludge

tank; however, only *ereA2*, *ereA*, *mph(B)*, *mph(A)*, *mph*, *ermB*, *mel*, and *mexD*, were found within the viable microorganism population in the final WWTP effluent. Clearly, antibiotic resistance is widespread in wastewater treatment plants and wastewater treatment plant effluent. Previous research has described wastewater effluent as the third tier of the transfer of antibiotic resistance, with the first tier composed of antibiotic use in animals and humans and the second tier composed of hospitals, long-term care facilities, and farms (Baquero *et al.*, 2008).

Documented evidence describes the decreasing susceptibility of microorganisms in patients to fluoroquinolones, including ciprofloxacin (Ridley and Threlfall, 1998; Karlowsky *et al.*, 2002; Bhavnani *et al.*, 2003). In the Bhavnani *et al.* (2003) paper, the authors compiled data from 174 hospitals and reported that the median susceptibility of *Pseudomonas aeruginosa* to ciprofloxacin fell from 84% in 1993 to 71% in 1999. Similar concerns exist for erythromycin (Seppala *et al.*, 1992; Descheemaeker *et al.*, 2000) and other macrolides. In Finland, erythromycin resistance in Group A streptococci rose from 4% in 1988 to 24% in 1990 (Seppala *et al.*, 1992). To combat antibiotic resistance, several countries have actually lowered consumption of antibiotic medications; in fact, between 2000 and 2009, France and Japan decreased antibiotic usage by 21% and 15%, respectively (Hamad, 2010).

Several authors (Kummerer *et al.*, 1997; Steger-Hartmann *et al.*, 1997; Buerge *et al.*, 2006; Johnson *et al.*, 2007; Chen *et al.*, 2008) have indicated concern for the presence of chemotherapy agents in the environment. The basis for this concern often stems from the fact that chemotherapy agents tend to exhibit carcinogenicity, mutagenicity, teratogenicity, and embryotoxicity, among other toxic effects. The mechanism of action for cyclophosphamide and ifosfamide was described above in Table 2-3; recall that these compounds are metabolized into products that alkylate DNA (Low *et al.*, 1983; Fleming, 1997). No research efforts have investigated whether environmental degradation of

chemotherapy agents can lead to formation of the active compounds; furthermore, the excretion of metabolic products is not typically reported.

Recently, an increasing amount of attention has been given to characterization of the sub-lethal effects caused by PhACs, and antibiotics in particular. In 2006, Linares *et al.* (2006) reported on the ability of antibiotics to act as intermicrobial signaling agents rather than “weapons.” In that study, the authors reported that ciprofloxacin induced expression of 1.4% and repressed expression of 3.8% of a specific subset of 555 genes. In conclusion, the authors state that “subinhibitory concentrations of antibiotics can produce specific changes in the behavior of susceptible bacteria.” Fajardo and Martinez (2008) also reported that low concentrations of antibiotics can trigger specific transcriptional responses; the authors reference the inhibition of the quorum sensing response by macrolides as an example of how antibiotics can affect cell signaling processes. Quorum sensing is the regulation of gene expression in response to changes in cell density. Davies *et al.* (2006) assembled a table showing a snapshot of the functional groups of genes affected by subinhibitory concentrations of antibiotics. In that work, the authors describe several effects caused by fluoroquinolones and macrolides, including the ability of fluoroquinolones to reduce hemolytic activity and induce colicin synthesis in *E. coli*. They also documented the ability of macrolides to decrease biofilm formation in *Mycobacterium fortuitum* and to inhibit quorum sensing in *Pseudomonas aeruginosa* (Davies *et al.*, 2006). Most of these subinhibitory effects are organism dependent, but regardless of the specific effect, more research into the implications for ecological systems is required.

WATER AND WASTEWATER TREATMENT OF TRACE ORGANIC CONTAMINANTS

Shortly after publication of the initial review articles (Halling-Sorensen *et al.*, 1998; Daughton and Ternes, 1999) documenting the presence of pharmaceuticals in the environment, a number of research investigations targeting water and wastewater treatment of pharmaceuticals and other TrOCs were undertaken. Several authors have documented the transport of PPCPs and EDCs through wastewater treatment processes (Ternes, 1998; Stumpf *et al.*, 1999; Thomas *et al.*, 2007; Okuda *et al.*, 2008). Similar studies have been conducted at drinking water treatment plants (Ternes *et al.*, 2002; Stackelberg *et al.*, 2004; Vieno *et al.*, 2007). This review focuses on drinking water treatment processes employed to remove PhACs from various water sources.

Adams *et al.* (2002) treated Missouri River water spiked with seven antibiotics at concentrations of 50 µg/L using conventional water treatment processes, including the following: coagulation/flocculation/sedimentation with alum and iron salts, excess lime / soda ash softening, ultraviolet irradiation (at disinfection dosages), ion exchange, sorption onto powdered activated carbon (PAC), reverse osmosis, chlorination, and ozonation. Their results showed that coagulation, softening, UV disinfection, and ion exchange did not demonstrate high removal efficiencies for the seven antibiotics of concern. The other processes (PAC, reverse osmosis, chlorination, and ozonation) all demonstrated high potential to treat the seven antibiotics employed in this study. Ultimately, this work established which unit processes could successfully treat pharmaceuticals in water matrices. Other efforts focused on testing the treatment efficacy of many unit processes have yielded similar results. For example, Westerhoff *et al.* (2005) investigated removal of 62 different PPCPs and EDCs at concentrations ranging from 10-250 ng/L using alum (0-72% removal) and iron (0 - ~80%) coagulation, softening (0 - ~80%) , PAC (14-98%), hypochlorite oxidation (0-99%), and ozonation (2-99%). Removal efficiencies varied widely depending on the chemical structure and

properties of each individual PPCP or EDC; regardless, the highest individual removal efficiencies were observed for the ozone-based oxidation process.

Other authors have investigated cumulative removal throughout an entire drinking water treatment process train. Stackelburg *et al.* (2004) followed the concentrations of eleven PPCPs throughout a conventional drinking water treatment plant with coagulation, sedimentation, filtration (granular activated carbon; GAC), and disinfection (hypochlorite). The concentrations of the eleven PPCPs in the raw water ranged from 6-860 ng/L. Of the eleven PPCPs followed through this drinking water treatment plant, only one compound, caffeine, showed significant removal. Vieno *et al.* (2007) conducted a similar investigation, in which the authors documented changes in the concentrations of eleven pharmaceuticals (6-55 ng/L) through a pilot-scale drinking water treatment plant. The post-sedimentation and post-sand filtration concentrations were not statistically different from raw water concentrations. The water was then ozonated, and the concentrations of all eleven pharmaceuticals were significantly reduced (16-99%). The final units of the process train consisted of two granular activated carbon beds and UV-disinfection. Only three compounds were present above the detection limit after ozonation; two of those compounds, ibuprofen and naproxen, were removed below the detection limit after the first GAC bed. The third compound, ciprofloxacin, did not demonstrate statistically significant removal after UV disinfection.

Other researchers (Xu *et al.*, 2005; Kim *et al.*, 2007; Snyder *et al.*, 2007; Wang *et al.*, 2009) have investigated the ability of membrane-based processes to remove pharmacologically active compounds from water and wastewater sources. Xu *et al.* (2005) looked into the ability for reverse osmosis (RO) and nanofiltration (NF) membranes to remove seven pharmaceuticals at concentrations of 300 ng/L. In that study, RO successfully removed over 90% of all seven compounds, but NF removal efficiencies varied from 10% to 70%. Snyder *et al.* (2007) demonstrated the ability of ultrafiltration, membrane bioreactor (MBR), and RO processes to treat a cocktail of 36

pharmaceuticals. In the ultrafiltration study, three compounds showed negative removal efficiencies; the other compounds demonstrated a wide range of removal (2.63 to greater than 98.85%). Removal efficiencies in the MBR process ranged from 0% to greater than 96.4%. In the RO system, all compounds except caffeine (84.9% removal) and pentoxifylline (90.4% removal) were removed to below detection limits. While reverse osmosis can effectively remove pharmaceuticals from water sources, the energy cost of using RO for low ionic strength water sources can be relatively high; for example, Lee *et al.* (2010) determined that the energy consumption of reverse osmosis was 1.1-1.5 kWh/1000 gallons compared to 0.061-0.12 kWh/1000 gallons for ozone treatment.

While the removal efficiencies for various PPCPs and EDCs in the drinking water treatment processes outlined in these studies (Adams *et al.*, 2002; Stackelberg *et al.*, 2004; Westerhoff *et al.*, 2005; Vieno *et al.*, 2007) vary widely, the studies utilizing ozone processes always demonstrated the highest removal efficiencies with the possible exception of RO processes, which tend to be cost- and energy-intensive for water sources with low salt concentrations. As a result, ozone-based treatment processes have emerged as the leading technology for removing trace concentrations of pharmacologically active compounds. In this work, ozone and the peroxone process were employed in treating the four pharmaceuticals of concern.

OZONE AND PEROXONE CHEMISTRY

Ozone can effectively oxidize trace concentrations of organic contaminants, including pharmaceuticals. While all four of the selected compounds react with ozone to some degree, hydroxyl radicals, the principal ozone decomposition product, also contribute some oxidative capacity. Peroxone, *i.e.*, the combination of ozone and hydrogen peroxide, is an advanced oxidation process (AOP) that provides rapid generation of hydroxyl radicals by initiating ozone decomposition by hydrogen peroxide. For these reasons, it is important to consider ozone decomposition chemistry in the absence and presence of hydrogen peroxide. Ozone decomposition reactions are presented below (Table 2-5). These reactions essentially describe the rate of ozone decomposition in solution in pure water (Hoigné and Bader, 1976; Staehelin and Hoigné, 1982; Buehler *et al.*, 1984; Staehelin *et al.*, 1984) and in water at alkaline conditions (Tomiyasu *et al.*, 1985). The reactions are split into three categories: initiation, propagation, and termination reactions. As the names suggest, initiation reactions trigger ozone decomposition, propagation reactions continue the ozone decomposition chain, and termination reactions end that chain of reactions. In both scenarios, ozone decomposes into two radical species, which then undergo a complex set of propagation reactions to form hydroxyl radicals ($\text{HO}\cdot$) and other reactive oxygen species (ROS), including the superoxide radical ($\text{O}_2^{\cdot-}$) and the peroxy radical ($\text{HO}_2\cdot$).

Below, two initiation reactions (Reactions 2-1, 2-2; Tomiyasu *et al.*, 1985) and two propagation reactions (Reactions 2-3 (Westerhoff *et al.*, 1997), 2-4 (Tomiyasu *et al.*, 1985)) are shown for pure water at alkaline conditions. The major oxidizing agents formed via ozone decomposition include hydroxyl radicals ($\text{HO}\cdot$) and superoxide radicals ($\text{O}_2^{\cdot-}$). Both of these radicals are highly reactive and will attack almost all molecules present in solution. In Reaction 2-5, a generic reaction for ROS attack on a pharmaceutical compound is shown. Ozone, itself, will also attack organic molecules (Reaction 2-6).

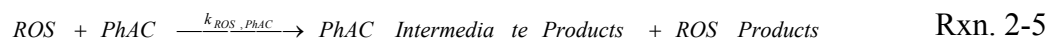
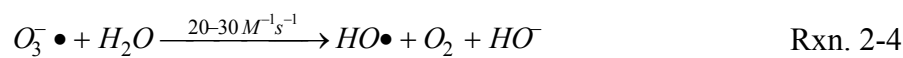
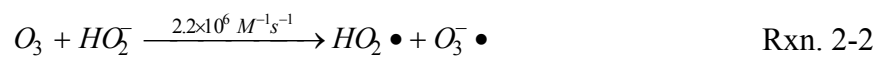
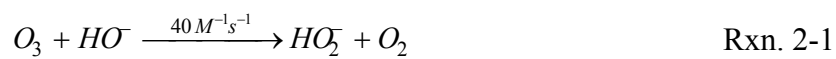


Table 2-5. Ozone decomposition models.

Ozone Decomposition in Pure Water (Buehler <i>et al.</i> , 1984; Stachelin <i>et al.</i> , 1984; Westerhoff <i>et al.</i> , 1997)		Ozone Decomposition in Pure Water at Alkaline Conditions (Tomiyasu <i>et al.</i> , 1985; Westerhoff <i>et al.</i> , 1997)	
Initiation Reaction		Initiation Reaction	
$O_3 + HO^- \longrightarrow HO_2 \bullet + O_2^- \bullet$	$70 \text{ M}^{-1} \text{ s}^{-1}$	$O_3 + HO^- \longrightarrow HO_2^- + O_2$	$40 \text{ M}^{-1} \text{ s}^{-1} *$
		$O_3 + HO_2^- \longrightarrow HO_2 \bullet + O_3^- \bullet$	$2.2 \times 10^6 \text{ M}^{-1} \text{ s}^{-1}$
Propagation Reactions		Propagation Reactions	
$HO_2 \bullet \longrightarrow O_2^- \bullet + H^+$	$7.9 \times 10^5 \text{ s}^{-1}$	$HO_2 \bullet \longrightarrow O_2^- \bullet + H^+$	$7.9 \times 10^5 \text{ s}^{-1}$
$O_2^- \bullet + H^+ \longrightarrow HO_2 \bullet$	$5 \times 10^{10} \text{ M}^{-1} \text{ s}^{-1}$	$O_2^- \bullet + H^+ \longrightarrow HO_2 \bullet$	$5 \times 10^{10} \text{ M}^{-1} \text{ s}^{-1}$
$O_3 + O_2^- \bullet \longrightarrow O_3^- \bullet + O_2$	$1.6 \times 10^9 \text{ M}^{-1} \text{ s}^{-1}$	$O_3 + O_2^- \bullet \longrightarrow O_3^- \bullet + O_2$	$1.6 \times 10^9 \text{ M}^{-1} \text{ s}^{-1}$
$O_3^- \bullet + H^+ \longrightarrow HO_3 \bullet$	$5.2 \times 10^{10} \text{ M}^{-1} \text{ s}^{-1}$	$O_3^- \bullet + H_2O \longrightarrow HO \bullet + O_2 + HO^-$	$20 - 30 \text{ M}^{-1} \text{ s}^{-1}$
$HO_3 \bullet \longrightarrow O_3^- \bullet + H^+$	$3.3 \times 10^2 \text{ s}^{-1}$	$O_3^- \bullet + HO \bullet \longrightarrow HO_2 \bullet + O_2^- \bullet$	$6 \times 10^9 \text{ M}^{-1} \text{ s}^{-1}$
$HO_3 \bullet \longrightarrow HO \bullet + O_2$	$1.1 \times 10^5 \text{ s}^{-1}$	$O_3 + HO \bullet \longrightarrow HO_2 \bullet + O_2$	$3 \times 10^9 \text{ M}^{-1} \text{ s}^{-1}$
$O_3 + HO \bullet \longrightarrow HO_4 \bullet$	$2 \times 10^9 \text{ M}^{-1} \text{ s}^{-1}$	$HO_2^- + H^+ \longrightarrow H_2O_2$	$5 \times 10^{10} \text{ M}^{-1} \text{ s}^{-1}$
$HO_4 \bullet \longrightarrow HO_2 \bullet + O_2$	$2.8 \times 10^4 \text{ s}^{-1}$	$H_2O_2 \longrightarrow HO_2^- + H^+$	0.25 s^{-1}
Termination Reactions		Termination Reactions	
$HO_4 \bullet + HO_4 \bullet \longrightarrow H_2O_2 \bullet + 2 O_3$	$5 \times 10^9 \text{ M}^{-1} \text{ s}^{-1}$	$O_3 + HO \bullet \longrightarrow O_3 + HO^-$	$2.5 \times 10^9 \text{ M}^{-1} \text{ s}^{-1}$
$HO_4 \bullet + HO_3 \bullet \longrightarrow H_2O_2 \bullet + O_2 + O_3$	$5 \times 10^9 \text{ M}^{-1} \text{ s}^{-1}$	$HO \bullet + CO_3^{2-} \longrightarrow HO^- + CO_3^- \bullet$	$4.2 \times 10^8 \text{ M}^{-1} \text{ s}^{-1}$
		$CO_3^- \bullet + O_3 \longrightarrow O_2 + CO_2 + O_2^- \bullet$	no data given

* A value of $70 \text{ M}^{-1} \text{ s}^{-1}$ is more widely employed for the ozone decomposition initiation reaction.

Reactions 2-2 to 2-5 also apply to the peroxone system as ozone is rapidly decomposed into a number of radical compounds that ultimately form ROS, including hydroxyl radicals and superoxide radicals, that are capable of transforming organic molecules. Dissociation of hydrogen peroxide (Rxn. 2-7) leads to formation of peroxide (HO_2^-), which can react with ozone as described above (Rxns. 2-2, 2-4). The general reaction can be written as shown in Reaction 2-8 (Glaze and Kang, 1989; Alsheyab and Muñoz, 2006). Ultimately, this reaction shows that, in the peroxone system, every mole of ozone is transformed into one mole of hydroxyl radicals; furthermore, the ideal molar ratio of hydrogen peroxide to ozone is 0.5 mol H_2O_2 / mol O_3 . If the ratio is lower than 0.5 mol H_2O_2 / mol O_3 , some ozone will not react, and lower hydroxyl radical exposures ($\int[\text{HO}\cdot]dt$) will be attained. On the other hand, if the molar ratio of H_2O_2 to ozone is greater than 0.5 mol/mol, the excess H_2O_2 will react with hydroxyl radicals (Rxns. 2-9, 2-10; Beltran, 2003), effectively scavenging them and preventing their reaction with PhACs.

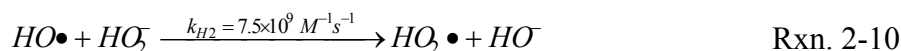
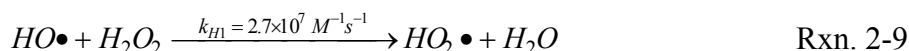
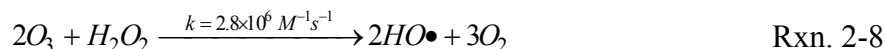


Figure 2-2 illustrates the complexity of hydroxyl radical reactions, which are formed during ozonation and can be scavenged by carbonate (HCO_3^- , CO_3^{2-}), NOM, or *t*-butanol (*t*-BuOH), among other compounds. Hydroxyl radicals can also interact with NOM, methanol (MeOH), or formaldehyde, among other compounds, to generate the superoxide anion (O_2^-), which promotes ozone decomposition. Ozone decomposition to hydroxyl radicals is also facilitated by interaction with the hydroxide ion (HO^-); therefore, ozone can be considered an AOP at high pH.

The left side of Figure 2-2 shows ozone decomposition in the peroxone system. In this scheme, carbonate actually promotes ozone decomposition through formation of superoxide. As discussed in Reactions 2-2 and 2-8, hydrogen peroxide and peroxide also react with ozone to form hydroxyl radicals. This reaction is extremely fast, *i.e.*, the rate constant for ozone reaction with peroxide is $2.2 \times 10^6 \text{ M}^{-1} \text{ s}^{-1}$ (Tomiyasu *et al.*, 1985).

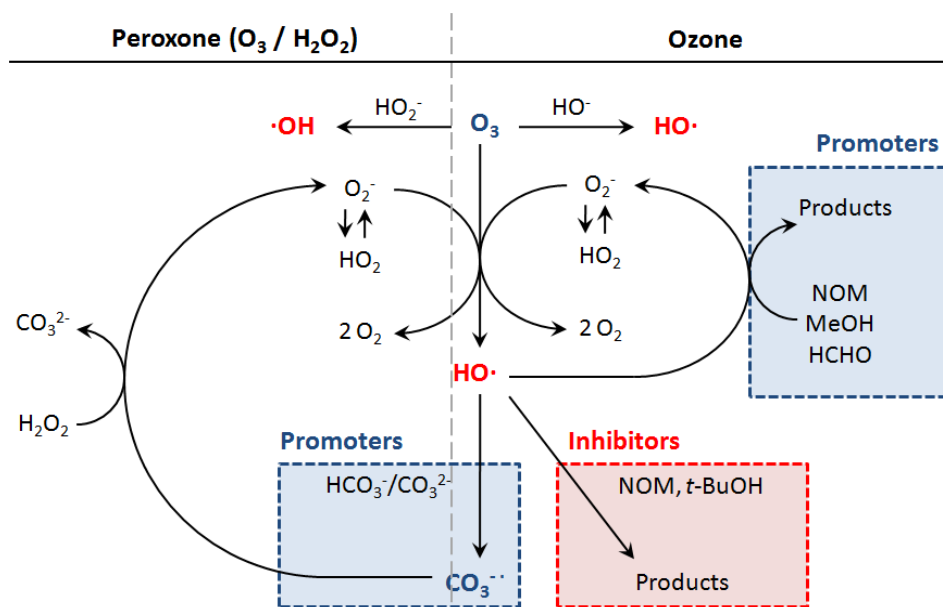


Figure 2-2. Peroxone chemistry (adapted from Acero and von Gunten, 2001).

OZONE REACTOR SCHEMES

Throughout the history of ozone in water treatment, a number of ozonation schemes have been utilized. Some researchers have used gaseous ozonation (Andreozzi *et al.*, 2003; Andreozzi *et al.*, 2005; Snyder *et al.*, 2006; DeWitte *et al.*, 2008; Dodd *et al.*, 2008; DeWitte *et al.*, 2009), while others have employed aqueous ozone (Acero *et al.*, 2000; Huber *et al.*, 2003; McDowell *et al.*, 2005; Dodd *et al.*, 2006; Suarez *et al.*, 2007; Dodd *et al.*, 2009).

Gaseous Ozonation

Gaseous ozonation was the original ozone application method employed for water disinfection in the early 20th century. In 1905, the experimental ozonation plant in Philadelphia (Vosmaer, 1916), employed a Vosmaer sterilizer (Figure 2-3). Essentially, a gaseous stream containing some fraction of ozone, which was produced via electrolysis of water, was bubbled through the raw water. The gaseous stream ran counter to the raw water stream to maximize contact time.

While the technology has changed substantially over the last 100 years, the basic methodology of gaseous ozonation remains the same. An ozone generator is employed to convert some fraction of an inlet oxygen gas stream into ozone (typically 8-12% O₃ v/v); that ozone/oxygen gaseous stream is bubbled into a reactor containing the water of interest. Typically, the amount of ozone adsorbed into solution is determined via mass balance (Eq. 2-2); this value represents the applied ozone dose.

$$[O_3]_{aq,absorbed} = [O_3]_{aq,applied\ dose} = \frac{\int_0^t ([O_3]_{g,inlet} - [O_3]_{g,outlet}) dt}{t} \quad \text{Eq. 2-2}$$

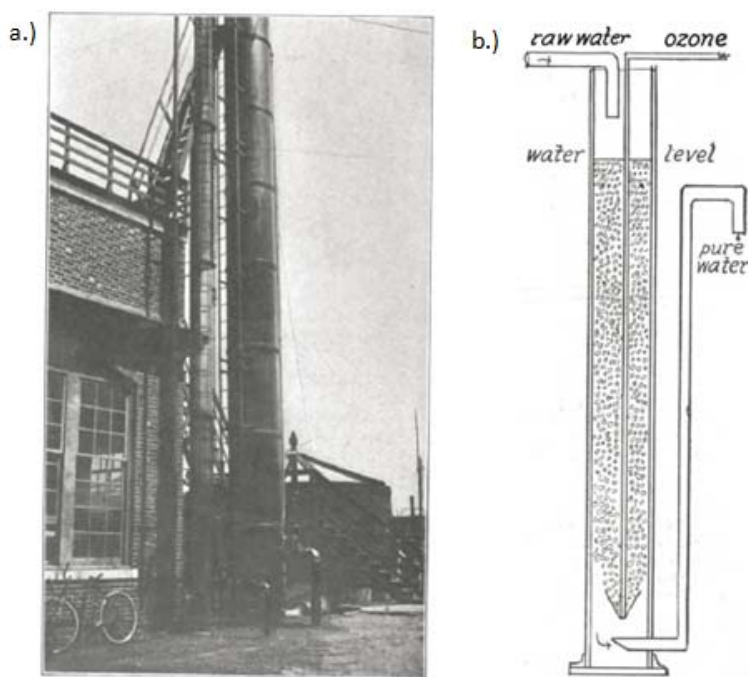


Figure 2-3. (a) Vosmaer sterilizer in Philadelphia circa 1905 (Vosmaer, 1916); (b) Schematic of Vosmaer sterilizer (Vosmaer, 1916).

A multitude of research efforts have focused on application of gaseous ozone to remove organic contaminants of interest, from natural organic matter (Olson and Barbier, 1994; Siddiqui *et al.*, 1997; Volk *et al.*, 1997; Westerhoff *et al.*, 1999a) to trace organic compounds such as PPCPs and EDCs (Huber *et al.*, 2003; Ternes *et al.*, 2003; Westerhoff *et al.*, 2005; Dodd *et al.*, 2006; Hua *et al.*, 2006; Snyder *et al.*, 2006). For laboratory studies, most of these endeavors have employed a gas-washing bottle containing the sample of interest; this scenario is represented schematically in Figure 2-4a. Pilot- and full-scale studies employ ozone contactor tanks that are typically operated in a counter-flow fashion (Huber *et al.*, 2005; Snyder *et al.*, 2006; Hollender *et al.*, 2009). For experimental studies, an ozone/oxygen gas is bubbled into the gas-washing bottle starting at time, $t = 0$. Hence, at time, $t = 0$, the ozone and hydroxyl radical concentrations are both 0 M. As the experiment progresses, ozone dissolves into solution, interacts with other dissolved compounds, and decomposes to form ROS, including hydroxyl radicals

(Table 2-5). The ozone mass flow rate is dependent upon the oxygen gas flow rate and the ozone generator settings (Figure 2-4b).

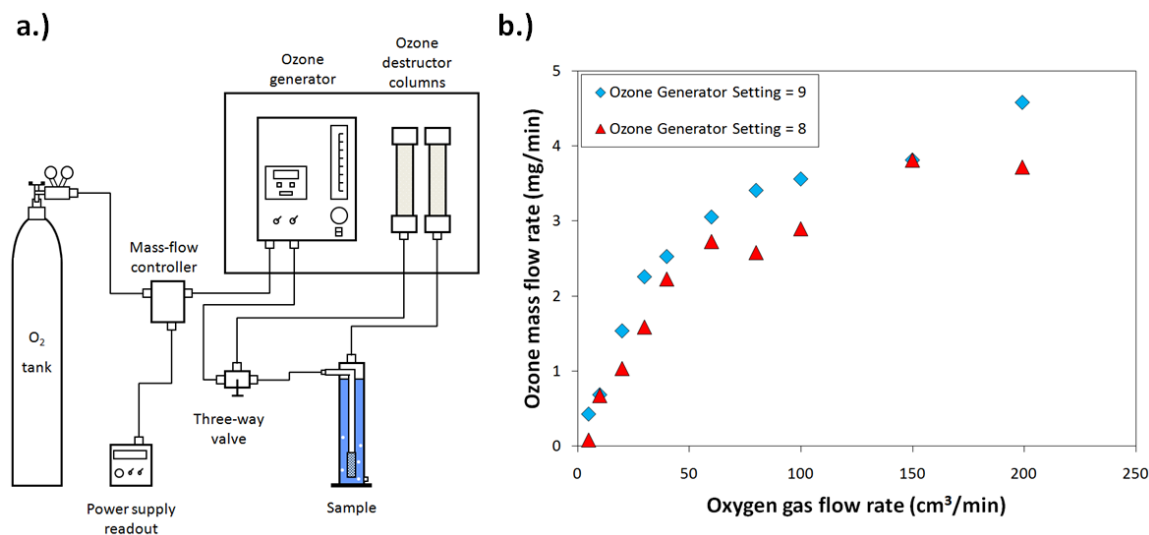


Figure 2-4. (a) Schematic of a gaseous ozone reactor. (b) The ozone mass flow rate is a function of the oxygen gas flow rate and the ozone generator settings. (The sample is placed into the gas washing bottle and ozone is introduced to the sample in the gaseous phase. The gaseous ozone concentration is measured in the inlet/outlet lines to determine the amount of ozone dissolved in solution.)

For the most part, researchers employing gaseous ozonation tend to use pseudo-first order kinetics to describe the transformation of organic compounds via ozonation (Huber *et al.*, 2003; DeWitte *et al.*, 2008; DeWitte *et al.*, 2009). By analyzing PhAC concentrations throughout the batch experiment, and assuming that the ozone concentration is constant throughout experimentation, the pseudo-first order rate constant ($k'_{pseudo, O_3, PhAC}$) can be found (Eq. 2-3). It should be noted that since $[O_3]$ and $[HO\cdot]$ are both 0 M at time, $t = 0$, pseudo-first order kinetics do not apply at early times. Regardless, this kinetic model is employed, and typically provides a nice fit to experimental data.

$$r_{PhAC} = \frac{d[PhAC]}{dt} = -k'_{O_3, pseud o PhAC} \times [PhAC]$$

Eq. 2-3

The mass transfer involved with gaseous ozonation is quite complicated. Dodd *et al.* (2008) investigated gaseous ozonation of EDCs in urine. In that paper, the authors present a kinetic snapshot (Figure 2-5) of what occurs in a gaseous ozonation scenario. Accounting for all of the different terms in Figure 2-5 is a complex undertaking and complicates experimentation; therefore, many researchers have moved to using concentrated aqueous ozone stock solutions (Acero *et al.*, 2000; Huber *et al.*, 2003; McDowell *et al.*, 2005; Dodd *et al.*, 2006; Suarez *et al.*, 2007; Dodd *et al.*, 2009).

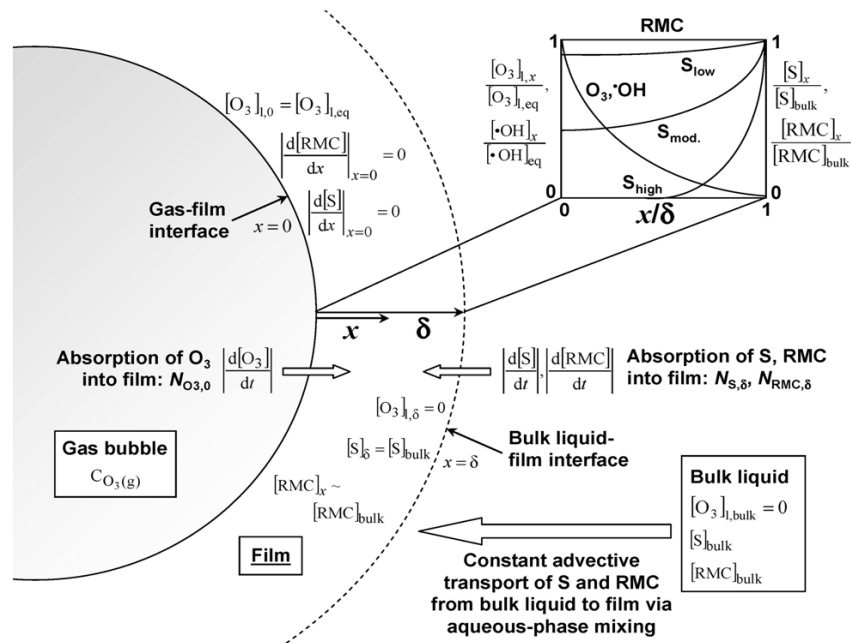


Figure 2-5. Representation of the interfacial film for a pseudo-first order kinetic regime with respect to ozone consumption (Dodd *et al.*, 2008).

Aqueous Ozone Addition

The use of concentrated ozone stock solutions dates back to the early work of Hoigné and Bader (Hoigné and Bader, 1975; 1976; Bader and Hoigné, 1981). That work employed aqueous ozone stocks to measure ozone decomposition kinetics; regardless, the

bulk of water treatment applications and studies employed gaseous ozone. Recently, several researchers have returned to aqueous ozone for treatment of trace organic contaminants (Elovitz and von Gunten, 1999; Acero *et al.*, 2000; Huber *et al.*, 2003; McDowell *et al.*, 2005; Dodd *et al.*, 2006; Suarez *et al.*, 2007) especially in experimental scenarios. Given the complicated mass transfer picture associated with gaseous ozonation (Figure 2-5), the use of aqueous ozone presents a unique advantage to studying transformation reactions between ozone (and other ROS, including hydroxyl radicals) and PhACs.

This ozonation scenario involves generating a concentrated ozone stock solution by bubbling gaseous ozone into deionized water (DI) for several hours. Figure 2-6 shows a schematic representation of this setup. The solution is placed in an ice bath to increase the ozone saturation concentration; some researchers also acidify the stock solution to increase ozone stability in solution (recall, HO^\cdot initiates O_3 decomposition; Table 2-5). After 5-6 hours of ozonation, the ozone concentration of a stock solution at 0.5°C and near neutral pH can reach 60-70 mg O_3/L ; however, this concentration is dependent on the ozone generator, the gas diffuser, and the ozone solution vessel.

The ozone stock solution can then be dosed into other reaction vessels at the desired concentration. It is important to note that, at time $t = 0$, the ozone concentration is the applied dose (Eq. 2-4).

$$[\text{O}_3]_{\text{applied dose}} = \frac{[\text{O}_3]_{\text{stock}} \times V_{\text{stock}}}{V_{\text{reactor}}} \quad \text{Eq. 2-4}$$

As ozone decomposition products, including hydroxyl radicals, are present in the stock solution, some concentration of those decomposition products are introduced into the reaction vessel. For this reason, the initial conditions are different with liquid ozone addition than with the gaseous addition counterpart; recall that for gaseous ozonation, $[\text{O}_3]$ and $[\text{HO}^\cdot]$ were both zero at time, $t = 0$. More importantly, since differences may

exist between ozone generators, warm-up time, diffuser size, and the temperature and pH of the stock solution, the $\text{HO}\cdot$ concentration in the stock solution may not be uniform among laboratories.

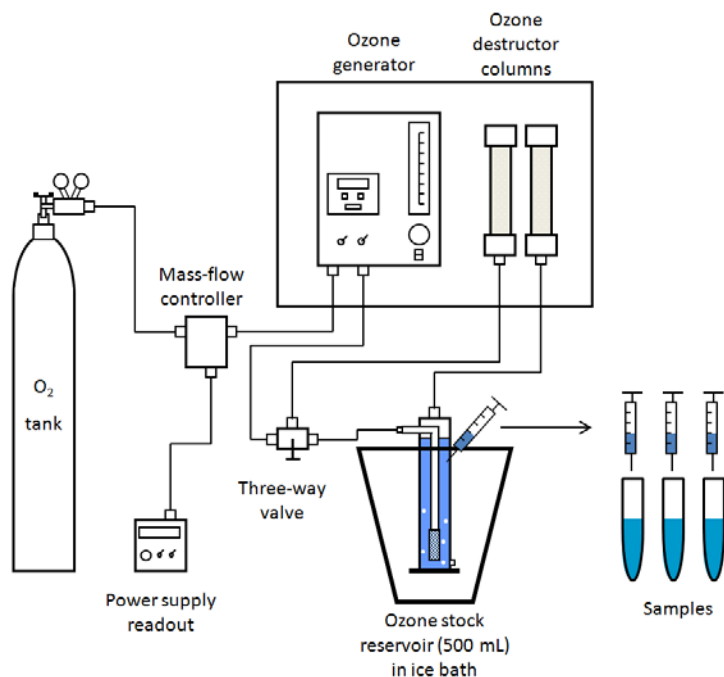


Figure 2-6. Aqueous ozone experimental setup for batch experimentation.

At time, $t = 0$, a volume of ozone stock solution, corresponding to a specific ozone dose, is added to a water sample containing the PhAC and background matrix of interest. The concentrations of ozone and PhAC are followed throughout the duration of the experiment. As the experiment progresses, the ozone concentration goes to zero because of reaction with organic compounds, interaction with the background matrix, and decomposition. Therefore, at some point, ozone is no longer present. More information on the ozone reactor is provided in Chapter 3.

Measuring Ozone and Hydroxyl Radical Kinetics

As discussed above, two dominant oxidants are present in ozonation applications: ozone (O_3) and hydroxyl radicals ($HO\cdot$). Typically, second order kinetics are used to describe the transformation of organic compounds with aqueous ozone and hydroxyl radicals (Yao and Haag, 1991; Dodd *et al.*, 2006). The transformation of a PhAC by ozone and hydroxyl radicals in a batch experiment is described by Eq. 2-5. By running two batch experiments (described below), the second order rate constants for PhAC transformation by ozone ($k''_{O_3,app,PhAC}$) and hydroxyl radicals ($k''_{HO\cdot,app,PhAC}$) can be determined.

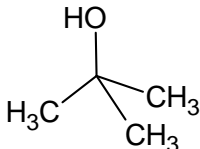
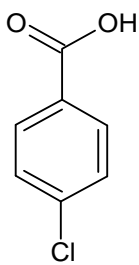
$$r_{PhAC} = \frac{d[PhAC]}{dt} = -k''_{O_3,app,PhAC} \times [O_3] \times [PhAC] - k''_{HO\cdot,app,PhAC} \times [HO\cdot] \times [PhAC]$$

Eq. 2-5

Isolating Ozone Kinetics

To isolate the contribution of ozone to the transformation of a PhAC, hydroxyl radicals need to be scavenged. Ideally, hydroxyl radical scavengers should react minimally with ozone and rapidly with hydroxyl radicals. Most researchers use *t*-BuOH for this purpose; however, a number of other compounds, including 2-propanol (Ho and Ho, 1976), octanol (von Gunten and Hoigne, 1994), and others, have been employed. In this study we employed *t*-BuOH. The second order rate constants for *t*-BuOH transformation by ozone and hydroxyl radicals are provided in Table 2-6. Clearly, *t*-BuOH does not significantly react with O_3 .

Table 2-6. Properties of *t*-BuOH and *p*CBA.

Property	<i>t</i> -BuOH	<i>p</i> CBA
Chemical formula	C ₄ H ₁₀ O	C ₇ H ₅ ClO ₂
Molecular weight (g/mol)	74.1	156.6
Structure		
$k''_{O_3,app}$ (M ⁻¹ s ⁻¹)	0.003 (Hoigné and Bader, 1983a)	0.15 (Yao and Haag, 1991)
$k''_{HO\cdot,app}$ (M ⁻¹ s ⁻¹)	6×10^8 (Buxton <i>et al.</i> , 1988)	5.9×10^9 (Neta and Dorfman, 1968)

Assuming that *t*-BuOH scavenges the hydroxyl radicals in solution, the change in [PhAC] caused by hydroxyl radicals (the last term in Eq. 2-5) goes to zero. Therefore, by plotting the change in PhAC concentration vs. ozone exposure ($\int [O_3] dt$), the second order rate constant for PhAC transformation by ozone can be deduced. Several authors have employed this protocol to determine the rate constants for transformation of various organic contaminants with ozone (McDowell *et al.*, 2005; Dodd *et al.*, 2006; Suarez *et al.*, 2007). More information regarding experimental conditions and the mathematics of solving for the second order rate constant are provided in Chapter 3.

Determining Hydroxyl Radical Kinetics

A number of hydroxyl radical probe compounds have been used to determine hydroxyl radical exposure; however, the most frequently employed compound is para-chlorobenzoic acid (*p*CBA; Table 2-6). The second order rate constants for *p*CBA reaction with O₃ and HO· are listed in Table 2-6. Like *t*-BuOH, *p*CBA reacts negligibly with ozone; hence, any change in *p*CBA concentration is mainly due to reaction with hydroxyl radicals. Given that relationship, the change in *p*CBA concentration can be used to solve for the hydroxyl radical exposure. The second order rate constant for the

reaction between hydroxyl radicals and pharmaceuticals can be found once the second order rate constant for PhAC transformation by ozone, measured values of ozone exposure, measured values of pharmaceutical concentration, and the hydroxyl radical exposure are known. Again, the experimental conditions and mathematics of these calculations are provided in Chapter 3. Ultimately, determination of the rate constants for PhAC transformation by ozone and hydroxyl radicals allows for calculation of the ozone and/or hydroxyl radical exposure required to meet treatment requirements.

OXIDATION AND ADVANCED OXIDATION PROCESSES (AOPs)

Ternes and coworkers (2002; 2003) investigated the abilities of ozone processes to treat 22 PPCPs and EDCs. In the earlier work, Ternes *et al.* (2002) demonstrated removals of approximately 80% for carbamazepine, diclofenac, bezafibrate, and primidone at an applied ozone dose of 3 mg/L; however, clofibric acid (a metabolic product of the cholesterol-lowering drug, clofibrate) only achieved ~40% removal for the same applied ozone dose. In the later paper, Ternes *et al.* (2003) investigated the ability of two different applied ozone doses to successfully transform 22 different PPCPs and EDCs (with concentrations ranging from 15-2100 ng/L) in municipal wastewater. At an applied ozone dose of 5 mg/L, fourteen compounds were treated to below the limit of quantification (LOQ). With an applied ozone dose of 10 mg/L, all compounds were successfully treated below their LOQs; these removals corresponded to greater than 50% to greater than 98% for individual compounds.

Huber *et al.* (2003) studied the removal of five pharmaceuticals in lake water from Finland ([DOC] = 3.7 mg/L, alkalinity = 0.7 mM) and bank filtrate from the River Seine ([DOC] = 1.3 mg/L, alkalinity = 4.1 mM) at pH 8. Overall, higher removal efficiencies were found in the bank filtrate matrix, presumably due to the lower DOC concentration, which acts as the primary ozone scavenger in water treatment processes. Subsequently, Huber *et al.* (2004) investigated ozonation of 17 α -ethinylestradiol, removal of estrogenic activity, and identification of the intermediate oxidation products. The reaction kinetics of eleven PPCPs and EDCs were determined by Huber *et al.* (2005); at pH 7, the apparent second order rate constants for PhAC transformation by ozone varied from 0.75 M⁻¹s⁻¹ (diazepam) to 3 \times 10⁶ M⁻¹s⁻¹ (17 α -ethinylestradiol) and the second order rate constants for PhAC transformation with hydroxyl radicals varied in the narrow range of 3.3 \times 10⁹ M⁻¹s⁻¹ (iopromide) to 9.8 \times 10⁹ M⁻¹s⁻¹ (17 α -ethinylestradiol). In batch transformation studies, most compounds demonstrated high transformation (>95%) for an applied ozone dose of 3.5 mg/L; iopromide, the compound exhibiting the lowest

second order rate constant, did not achieve high removal efficiencies even at applied ozone doses up to 5 mg/L.

Other researchers have identified the reaction kinetics of various PPCPs and EDCs with ozone and hydroxyl radicals (Andreozzi *et al.*, 2003; Lopez *et al.*, 2003; Andreozzi *et al.*, 2005; McDowell *et al.*, 2005; Dodd *et al.*, 2006; Suarez *et al.*, 2007; Rosal *et al.*, 2008; An *et al.*, 2010; Garcia-Ac *et al.*, 2010). Based on the work of these investigators, as well as that of earlier authors, especially Hoigné and coworkers (Hoigné and Bader, 1983a; b; Hoigné *et al.*, 1985) and Yao and Haag (Yao and Haag, 1991; Haag and Yao, 1992), kinetic regimes for ozone and hydroxyl radicals have been established. For this work, we define the fast and slow regimes of transformation by ozone as greater than and less than $10^3 \text{ M}^{-1}\text{s}^{-1}$, respectively. The rate constant is a function of the molecular structure of the target compound. Ozone preferentially oxidizes electron-rich molecules like alkenes and aromatic alcohols (Hoigné and Bader, 1983a; b); therefore, compounds with double bonds, free amines, and other electron-rich areas will demonstrate high reactivity with ozone. Most organic molecules interact with hydroxyl radicals on the order of $10^8\text{--}10^{10} \text{ M}^{-1}\text{s}^{-1}$; given the magnitude of these rate constants, the “slowness” or “fastness” of the reaction is dependent upon hydroxyl radical exposure. Furthermore, as a result of the high reactivity and instability of hydroxyl radicals in solution, hydroxyl radicals essentially react randomly with adjacent molecules; the relatively narrow range of rate constants observed for hydroxyl radical reaction with PhACs corroborates this statement.

From the results described above, it is clear that ozone-based water treatment processes offer a great deal of potential for effectively treating trace organic contaminants. This potential is based on the reactivity of PPCPs with not only ozone, but also with ozone decomposition products, particularly hydroxyl radicals. Some investigators have encouraged the implementation of advanced oxidation processes (AOPs) to treat PhACs. Recall that AOPs are oxidation processes that are engineered to

rapidly produce hydroxyl radicals. Many authors have reported on the peroxone process (Acero and von Gunten, 2001; Venta *et al.*, 2005; Rosal *et al.*, 2008; DeWitte *et al.*, 2009; Lin *et al.*, 2009; Vasconcelos *et al.*, 2009), which uses the reaction between ozone and hydrogen peroxide to generate hydroxyl radicals. Depending on the specific contaminants present in a water source, the user can determine whether ozone or peroxone processes would be ideal. This decision would be based on two pieces of information: the rate constants for the specific PhACs of concern and the background water quality matrix, which controls the ratio of hydroxyl radical exposure to ozone exposure.

Impact of Natural Organic Matter on Oxidation Processes

Huber *et al.* (2003) investigated the ability of ozone (O_3) and peroxone (O_3/H_2O_2) to treat nine pharmaceuticals in four different water matrices; the results indicated that pharmaceutical structure and the alkalinity and dissolved organic carbon (DOC) concentration of the water source are the most important variables in determining treatment efficiency. In that research, the peroxone process demonstrated better overall performance than ozone treatment. Other researchers have documented the impacts of DOC on O_3 and O_3/H_2O_2 processes (Westerhoff *et al.*, 1999a) and UV/ H_2O_2 processes (Baeza, 2008). Ultimately, these impacts are likely to govern the oxidant dose required to treat a given water containing PhACs. Furthermore, it is likely that the organic matter composition, particularly the relative amounts of terrestrially-, microbially-, and anthropogenically-derived organic matter, will exert an impact on treatment efficiency, mainly through the different rate constants for different DOC sources with ozone and hydroxyl radicals.

Throughout the past few decades, water treatment engineers have discovered that organic matter affects virtually every treatment process. Since composition of the organic matter matrix differs from location to location, we can expect the organic matter impact on PhAC treatment to be source dependent. Traditionally, the term natural

organic matter (NOM) was used to refer to organic matter present in surface waters; however, the increased use of indirect and direct potable water reuse has changed the organic matter matrix. For this reason, the composition of organic matter in surface waters consists of both NOM and wastewater effluent-derived organic matter, or EfOM. Ma *et al.* (2001) compiled an extensive summary of the organic matter differences between several NOM-dominated waters and a wastewater effluent. Sirivedhin and Gray (2005a; 2005b) showed the differences between the organic matter present in WWTP effluent (EfOM) and NOM; the authors went on to demonstrate that these structural differences impact the formation of disinfection byproducts. For that reason, it seems plausible that the compositional differences should also affect the behavior of organic matter in oxidation and advanced oxidation processes.

For advanced oxidation, organic matter affects treatment via the following means: direct oxidant consumption, initiator for oxidant consumption, promoter of oxidant consumption, or inhibitor of oxidant consumption (Westerhoff *et al.*, 1999a). The most important mechanism is direct oxidant consumption, which essentially causes organic matter to compete with PhACs for the oxidant. Westerhoff *et al.* (1999a) showed that ozone consumption by organic matter varied with $SUVA_{254}$ and organic matter structure (Figure 2-7); that paper also showed that hydroxyl radical consumption varies with $SUVA_{254}$ (Figure 2-7). In a second paper, Westerhoff *et al.* (1999b) described the changes in NOM structure caused by reaction with ozone. Ozone specifically reacted with aromatic carbon and this reaction resulted in the insertion of an oxygen atom at the carbon-carbon double bond; furthermore, the authors postulated that increased oxygen functionality may affect NOM reactions, including chlorination and disinfection by-product formation.

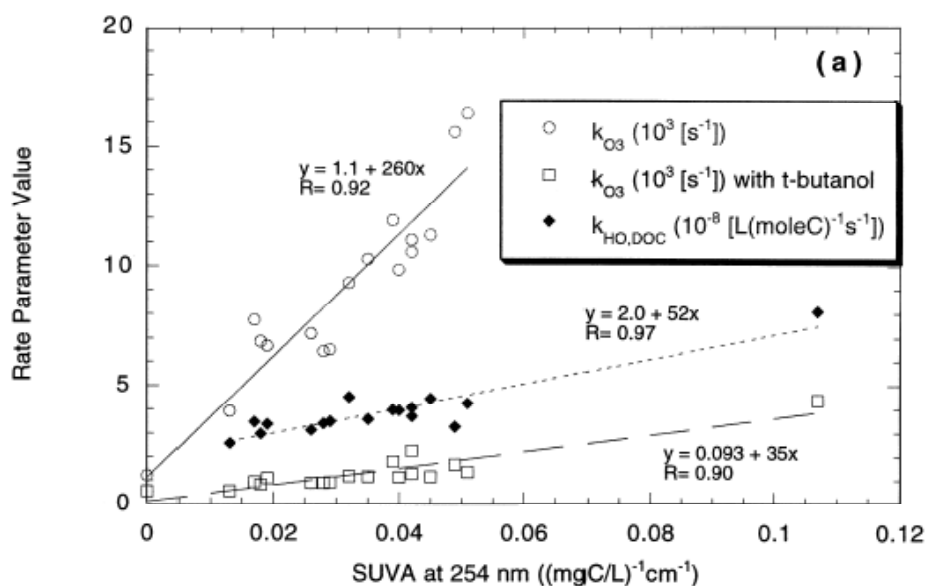


Figure 2-7. Impact of SUVA on NOM reactivity with ozone (Westerhoff *et al.*, 1999a).

Intermediate Oxidation Products

Oxidative treatment, unlike ion exchange, PAC, or RO, is a transformative process. Parent compounds (*i.e.*, pharmaceuticals) are attacked by the oxidant and a complex oxidative transformation pathway follows. Several researchers (Acero *et al.*, 2000; Huber *et al.*, 2004; Andreozzi *et al.*, 2005; McDowell *et al.*, 2005; DeWitte *et al.*, 2008) have characterized the oxidation products formed through ozone reaction with PPCPs and EDCs. These investigators identified transformation products of 17 α -ethinylestradiol, amoxicillin, atrazine, carbamazepine, and ciprofloxacin after exposure to ozone and hydroxyl radicals. McDowell *et al.* (2005) proposed a classical ozone attack on the double bond present in carbamazepine's central ring, resulting in the addition of oxygen atoms to the chemical structure. The ozonation products of 17 α -ethinylestradiol were investigated by Huber *et al.* (2004); the initial transformation mechanism occurs at aromatic rings and effectively open the ring forming carboxylic acid functional groups. These results are consistent with Westerhoff *et al.*'s (1999b) findings regarding the structural changes induced in NOM via ozonation.

Recent work by DeWitte *et al.* (2008) suggested twelve structures for intermediate oxidation products formed during gaseous ozonation of ciprofloxacin. These compounds are structurally similar to ciprofloxacin. Lemke and Williams (2008) delineated the structure-activity relationship for quinolonic compounds, as seen in Figure 2-8. The pharmacophore is the core structure required for the compound to exert pharmacological activity; furthermore, three functional groups determine the pharmacological capabilities of the compound. The R₆ group contributes to the ability of the compound to penetrate cell walls; fluoroquinolones, such as ciprofloxacin, have a fluoro group at R₆. The R₇ group relates to the compound's spectrum of activity, *i.e.*, this functional group establishes what microorganisms will be affected by the compound. The R group determines the relative potency of the compound. Of the twelve intermediate oxidation products determined by DeWitte *et al.* (2008), all twelve structures retained the fluoro group on R₆, all twelve compounds retained the same potency group as ciprofloxacin, and six intermediate oxidation products retained the pharmacophore. The majority of oxidative transformations target the piperazinyl group (R₇; DeWitte *et al.*, 2008), which may change the spectrum of microorganisms affected by the compound but does not necessarily remove pharmacological activity. Therefore, the potential for oxidative intermediate products to exhibit residual pharmacological activity is high.

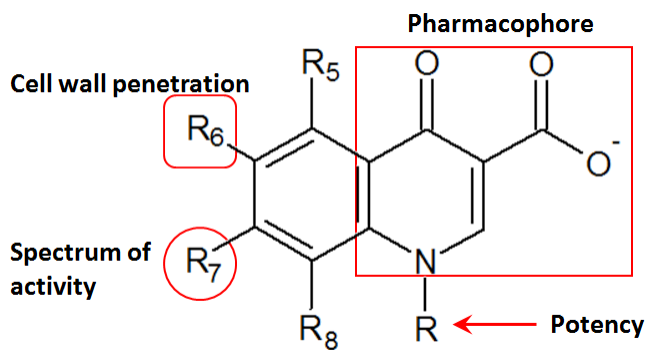


Figure 2-8. Structure-activity relationship for quinolone antibiotics (Lemke and Williams, 2008).

Residual Pharmacological Activity

In the past few years, a few researchers (Suarez *et al.*, 2007; Baeza, 2008; Dodd *et al.*, 2009; Paul *et al.*, 2010) have used an antimicrobial susceptibility assay (NCCLS, 2004) to describe treatment efficacy in terms of pharmacological activity. Suarez *et al.* (2007) treated triclosan with aqueous ozone and showed that antibacterial activity closely followed triclosan concentration. Baeza (2008) used this assay in combination with UV photolysis and photochemical UV/H₂O₂ treatment of four antimicrobials to demonstrate that the impact of the background water matrix varied depending on the treatment conditions. Dodd *et al.* (2009) employed an antimicrobial susceptibility assay to track the pharmacological activity of 14 antimicrobial compounds from various pharmaceutical classes, including macrolides, fluoroquinolones, and β -lactams, among others. The findings from the Dodd *et al.* (2009) study suggest that intermediate oxidation products generated through ozonation of roxithromycin, penicillin G, and cephalexin retain some residual antibacterial activity; furthermore, no apparent contribution of ciprofloxacin's intermediate oxidation products to the residual antimicrobial activity was detected. A recent paper by Paul *et al.* (2010) indicates that ciprofloxacin degradation products from photolytic (UV) and photocatalytic (UV-TiO₂) processes exert some antimicrobial activity. In summary, many questions remain unresolved regarding the pharmacological activity of intermediate oxidation products resulting from transformations of pharmaceuticals in natural and engineered systems.

CHAPTER 3: MATERIALS AND METHODS

The research approach used in this work was employed to meet the primary research objectives discussed in Chapter 1. These objectives include investigating the transformation of four model PhACs in ozone-based treatment processes, characterizing the impact of NOM on PhAC removal efficiency, and description of the residual antimicrobial activity of water sources containing antimicrobial PhACs. In this chapter, the properties of the chemicals, pharmaceuticals of concern, and natural organic matter (NOM) isolates are presented. Furthermore, the analytical methods employed to measure ozone, the pharmaceuticals of concern, intermediate oxidation products, *para*-chlorobenzoic acid, NOM, hydrogen peroxide, and pH are described.

Several different ozone reactors were employed to meet the research objectives. In particular, batch ozonation experiments were conducted to demonstrate the impact of NOM on the transformation of cyclophosphamide, erythromycin, and ifosfamide, to characterize the intermediate oxidation products formed via ozonation and peroxonation of cyclophosphamide, erythromycin, and ifosfamide, and to monitor the residual antimicrobial activity of ozone-treated solutions containing erythromycin. Continuous aqueous ozone addition experiments were employed to demonstrate the impact of NOM on ciprofloxacin transformation and elimination of ciprofloxacin-associated antimicrobial activity and to determine the transformation kinetics of cyclophosphamide and ifosfamide with ozone and hydroxyl radicals. The continuous peroxone addition reactor was used to verify the rate constants for the reaction of cyclophosphamide and ifosfamide with hydroxyl radicals. These reactor setups are described in detail below; furthermore, the data analysis procedures for the different types of experiments are also explained. The antimicrobial activity assay, which is used to measure the residual antimicrobial activity

of samples, is also presented in this chapter; analysis of data resulting from the antimicrobial activity assay is demonstrated in Appendix C.

CHEMICALS

All chemicals were purchased through VWR. The pharmaceuticals employed in this work are discussed in the following section. Certain chemicals (*p*CBA (99%), *t*-BuOH, and indigotrisulfonate) were employed for various reasons as documented throughout this Chapter. Hydrogen peroxide was purchased as 30% H₂O₂; stock solutions of 0.105 M were created and stored in amber bottles in a dark, 4°C environment; the stock solution was stable for at least 6 months. Several inorganic salts, including NaCl, NaHCO₃, NaH₂PO₄, Na₂HPO₄, and BaCl were employed in experimentation; these chemicals were ACS grade. Hydrochloric (trace metal grade), sulfuric (trace metal grade), and phosphoric acids (ACS grade) were employed for various uses. Sodium hydroxide (10 N) was diluted to 1N and 0.1N solutions that were employed for pH adjustment purposes. A 0.1 N potassium permanganate solution (ACS grade) was employed for H₂O₂ titrations. ACS grade pH buffers (4.01, 7.01, and 10.01) were employed for calibration of pH probes.

Several different solutions were employed in the analytical methods relevant to this research. HPLC analysis of ciprofloxacin employed HPLC grade acetonitrile and a 25 mM phosphate buffer, which was made by adding H₃PO₄ to deionized water (DI). LC-MS grade methanol and LC-MS grade water were employed in measurement of cyclophosphamide and ifosfamide via LC-MS and LC-MS/MS. LC-MS grade acetonitrile was employed for measurement of erythromycin using LC-MS and LC-MS/MS methods. The erythromycin LC-MS and LC-MS/MS methods also employed a 0.1% formic acid eluent, which was generated by adding ACS grade formic acid (88%) to DI. LC-MS grade methanol and the 25 mM phosphate buffer, discussed above for ciprofloxacin analysis, were employed for HPLC analysis of *para*-chlorobenzoic acid (*p*CBA).

All glassware was meticulously washed using the washing procedure described in Appendix A, which also contains information regarding autoclave protocols.

Pharmacologically Active Compounds

The four pharmacologically active compounds (ciprofloxacin, cyclophosphamide, erythromycin, and ifosfamide) employed in these studies were purchased from VWR. Ciprofloxacin, cyclophosphamide monohydrate, and ifosfamide were all purchased in the powder form, while erythromycin was purchased as a 50 mg/mL solution in ethanol.

Working stock solutions of ciprofloxacin (10 mg/L), cyclophosphamide (1000 mg/L), and ifosfamide (1000 mg/L) were created by dissolving the appropriate mass of the compounds into DI water. A working stock solution of erythromycin (1000 mg/L) was produced by diluting the purchased solution (50 mg/mL) with DI. Working solutions were kept in amber bottles, and these solutions were stored in a dark, 4°C environment. New stock solutions were made every three months; ciprofloxacin and erythromycin concentrations were periodically confirmed using the antimicrobial activity assay described below. Detailed description of these compounds and their presence in environmental waters is provided in Chapter 2 and is not repeated here.

Natural Organic Matter

Organic matter was extracted from two sources: Lake Austin (LA; Austin, TX) and Claremore Lake (CL; Claremore, OK). The extractions followed the method developed by Thurman and Malcolm (1981) and later refined by Aiken *et al.* (1992). The details of these extraction materials and methods are presented in Marron (2010) and are not described in extensive detail here. After isolation, the concentrated NOM solutions were freeze-dried at the USGS to yield a solid product.

Claremore Lake water was collected near the Ranger Station on D4168 Road (Latitude = +36.329864°, Longitude = -95.581356°) in Claremore, OK. Approximately

200 L of raw Claremore Lake water was collected. Extractions of Claremore Lake hydrophobic organic acids (HPOA) and transphilic organic acids (TPIA) were conducted at the USGS (Boulder, CO) under the direction of George Aiken and Kenna Butler. Knowing the volume of water passed through the XAD-8 and XAD-4 resins, as well as the dissolved organic carbon (DOC) concentration of the raw water, the percent recovery of DOC for the HPOA and TPIA isolates could be calculated (Table 3-1). Approximately 95% and 89% DOC recovery was experienced for the Claremore Lake HPOA and TPIA, respectively.

Approximately 400 L of Lake Austin water was collected from the raw water pump station on Forest View Drive at the Ullrich Drinking Water Treatment Plant (Austin, TX). The HPOA fraction of the Lake Austin NOM was isolated at the University of Texas. Approximately 89% of the HPOA present in the raw Lake Austin water was recovered during the organic matter extraction.

Table 3-1. Summary of organic matter recovery during NOM extractions.

Parameter	Claremore Lake TPIA	Claremore Lake HPOA	Lake Austin HPOA
Volume of sample loaded onto columns (L)	201.6	201.6	423.3
Expected mass recovery (mg)	490	1161	1037
Mass recovered (mg)	436	1100	923
Percent recovered	89%	95%	89%

The raw water quality of the Claremore Lake and Lake Austin sources is presented in Table 3-2. While pH, alkalinity, and turbidity are important water quality parameters for ozone-based processes, these characteristics are for the whole waters, not the NOM isolates. In most of the experimentation discussed in this dissertation, organic matter was added to solution in extract form; furthermore, pH and alkalinity were controllable parameters. While the turbidity of experimental samples was not tested, no significant turbidity should have been present in any experimental samples. On the contrary, the UV_{254 nm}, DOC concentration, specific ultraviolet absorbance at 254 nm

(SUVA_{254 nm}), percent of HPOA, and percent of TPIA are important raw water characteristics because these parameters describe the makeup of the HPOA and TPIA isolates, which impact the reactivity of these fractions with ozone and hydroxyl radicals. The distinction between the absorbance at 254 nm for the Claremore Lake (UV_{254 nm,CL} = 0.185 cm⁻¹) and Lake Austin (UV_{254 nm,LA} = 0.059 cm⁻¹) waters indicates that the Claremore Lake water contains more aromatic substances, which are highly reactive with ozone as discussed in Chapter 2. That difference is somewhat due to the higher DOC concentration of the Claremore Lake ([DOC] = 6.4 mg/L) water as compared to the Lake Austin water ([DOC] = 3.5 mg/L). Since the organic matter isolates are available in extract form, we can control the [DOC] of experimental solutions. The SUVA_{254 nm} value, which is an inherent characteristic of individual organic matter isolates, provides one way to compare the impact of these three organic matter isolates on ozone-based processes for treatment of pharmacologically active compounds. In this case, the higher SUVA_{254 nm} of the Claremore Lake raw water (SUVA_{254 nm,CL} = 2.9 L/mg-m) as compared to the Lake Austin raw water (SUVA_{254 nm,LA} = 1.7 L/mg-m) suggests that the Claremore Lake organic matter matrix is more reactive with ozone and hydroxyl radicals (Westerhoff *et al.*, 1999a).

Table 3-2. Raw water quality of Claremore Lake and Lake Austin water sources.

Parameter	Claremore Lake	Lake Austin
Collection Date	6/18/09	7/22/09
pH	7.5	8.0
Alkalinity (mg CaCO ₃ /L)	57	164.5
UV _{254 nm} (cm ⁻¹)	0.185	0.059
[DOC] (mg/L)	6.4	3.5
Turbidity (NTU)	8.5	4.5
SUVA _{254 nm} (L/mg-m)	2.9	1.7
HPOA (%)	45	35
TPIA (%)	19	20

ANALYTICAL METHODS

Ozone Analysis

Dissolved ozone concentrations of stock solutions were measured directly at 258 nm on a UV-VIS spectrophotometer (Agilent). This method was only used for stock ozone solutions with aqueous ozone concentrations greater than 10 mg/L. Typically, 0.5 mL of the ozone stock solution was mixed into 3.5 mL of 5 mM phosphate buffer in a 1 cm quartz cuvette with Teflon cap. These samples were measured immediately after addition of the ozone stock solution. Using the absorbance at 258 nm and the molar absorptivity of ozone, the concentration of aqueous ozone can be calculated using Eq. 3-1,

$$[O_3] \left(\frac{mg}{L} \right) = \frac{UV_{258-nm} \left(\frac{1}{cm} \right) \times MW \left(\frac{mg}{mmol} \right) \times dil \times 1000 \left(\frac{mmol}{mol} \right)}{\epsilon_{O_3} \left(\frac{1}{M-cm} \right)} \quad \text{Eq. 3-1}$$

where, $UV_{258\text{ nm}}$ is the absorbance at 258 nm, MW is the molecular weight of ozone (48 mg/mmol), dil is the dilution factor (typically, 8), and ϵ_{O_3} is the molar absorptivity of ozone ($3000\text{ M}^{-1}\text{cm}^{-1}$; Acero and von Gunten, 2000). Typical absorbance scans are shown in Figure 3-1; the corresponding aqueous ozone concentration is listed next to each peak.

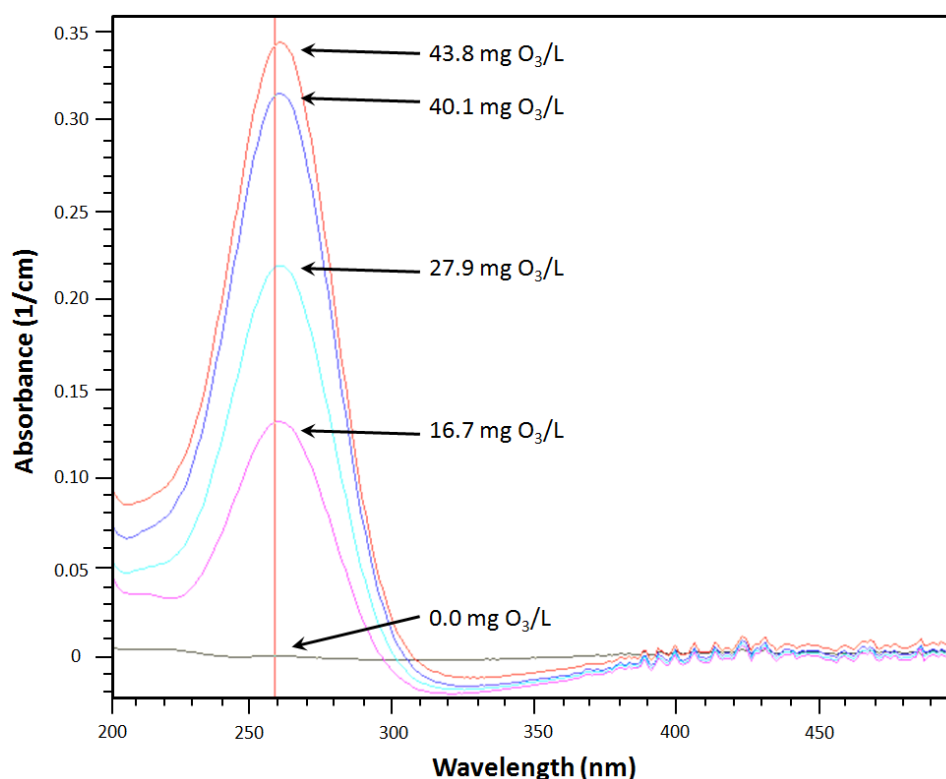


Figure 3-1. Examples of direct ozone measurement at 258 nm and the corresponding ozone concentrations found using Eq. 3-1.

Aqueous ozone concentrations in the 2-L continuous aqueous ozone addition reactor were measured using the indigo blue method (Bader and Hoigné, 1981). In this method, indigotrisulfonate (Figure 3-2) is cleaved by ozone at the double bond in the center of the molecule to form the products shown. Indigotrisulfonate has a significant molar absorptivity at 600 nm, whereas the products do not demonstrate any absorbance at 600 nm; this difference allows the use of indigotrisulfonate for quantification of aqueous ozone concentrations. Indigotrisulfonate reacts very quickly with ozone ($k''_{\text{O}_3, \text{indigotrisulfonate}} = 9.4 \times 10^7 \text{ M}^{-1} \text{ s}^{-1}$; Munoz and von Sonntag, 2000). Hence, addition of indigotrisulfonate allows measurement of the aqueous ozone concentration while also quenching aqueous ozone concentrations, thereby stopping both the generation of hydroxyl radicals and the oxidation of any organic compounds of interest.

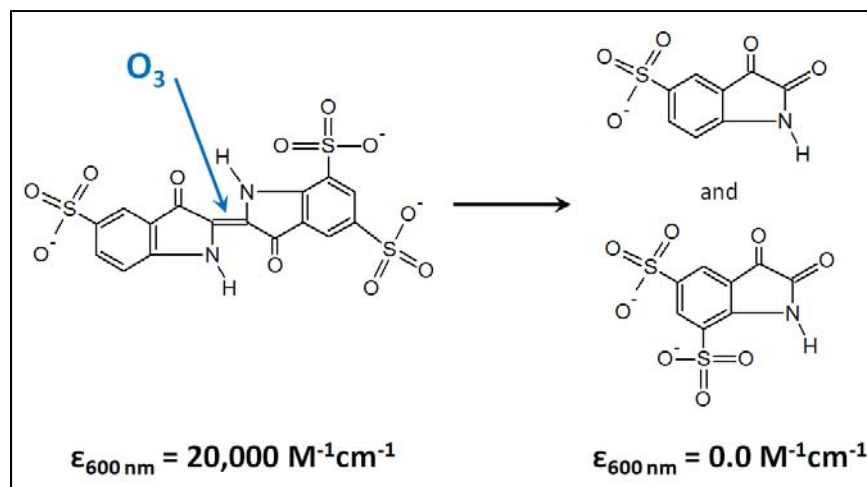


Figure 3-2. Ozone reaction with indigotrisulfonate, and the resulting ozonation products (adapted from Bader and Hoigné, 1981).

Indigo Reagent I and Indigo Reagent II solutions (Standard Method 4500-O₃ B. Indigo Colorimetric Method; APHA *et al.*, 2006) were employed in this research. Indigo stock solution was created by dissolving 770 mg of indigotrisulfonic acid (C₁₆H₁₀N₂O₁₁S₃), 1 mL phosphoric acid, and 12 mg Na₂HPO₄ in 100 mL of DI. Indigo reagent I was made by adding 1000 mg of Na₂HPO₄, 0.7 mL of phosphoric acid, and 2 mL of indigo stock solution to 100 mL of DI; indigo reagent II was made in the same manner, albeit with 10 mL of indigo stock solution. Indigo Reagent I was employed for lower aqueous ozone concentrations (6×10⁻⁸ – 2×10⁻⁶ M with a 4-cm quartz cuvette); however, Indigo Reagent II offered a larger range of ozone measurement (6×10⁻⁸ – 10×10⁻⁶ M with a 4-cm quartz cuvette), and so was used more often than Indigo Reagent I. In select cases, a 10-cm quartz cuvette was employed to provide higher sensitivity and lower aqueous ozone detection (2.5×10⁻⁸ – 10×10⁻⁶ M). It should be noted that samples were often diluted to ensure incomplete indigo transformation, which is required for calculation of aqueous ozone calculations. For example, as the aqueous ozone concentration increases during continuous ozonation experimentation, samples were diluted 1:1 or 1:3 with DI. Indigo was measured at 600 nm on the UV-VIS spectrophotometer (Figure 3-3). Aqueous ozone concentrations were calculated using Eq. 3-2:

$$[O_3] \left(\frac{mg}{L} \right) = \frac{\left[ABS_{600-nm, initial} \left(\frac{1}{cm} \right) - ABS_{600-nm, sample} \left(\frac{1}{cm} \right) \right] \times V_T \text{ (mL)}}{f \left(\frac{L-cm}{mg} \right) \times l \times V_{sample} \text{ (mL)}} \quad \text{Eq. 3-2}$$

where $[O_3]$ is the aqueous ozone concentration, $ABS_{600\text{ nm}, initial}$ is the absorbance at 600 nm of the initial solution (pre-ozonation), $ABS_{600\text{ nm}, sample}$ is the absorbance at 600 nm of the sample, V_T is the total volume of the solution (indigo reagent, sample, and DI) being measured, f is a constant based on the molar absorptivity of indigo ($20,000\text{ M}^{-1}\text{cm}^{-1}$; Bader and Hoigné, 1981) and is equal to 0.42 L-cm/mg , l is the path length (in cm , the units are incorporated into the $ABS_{600\text{ nm}}$ values), and V_{sample} is the volume of the sample added to the total solution.

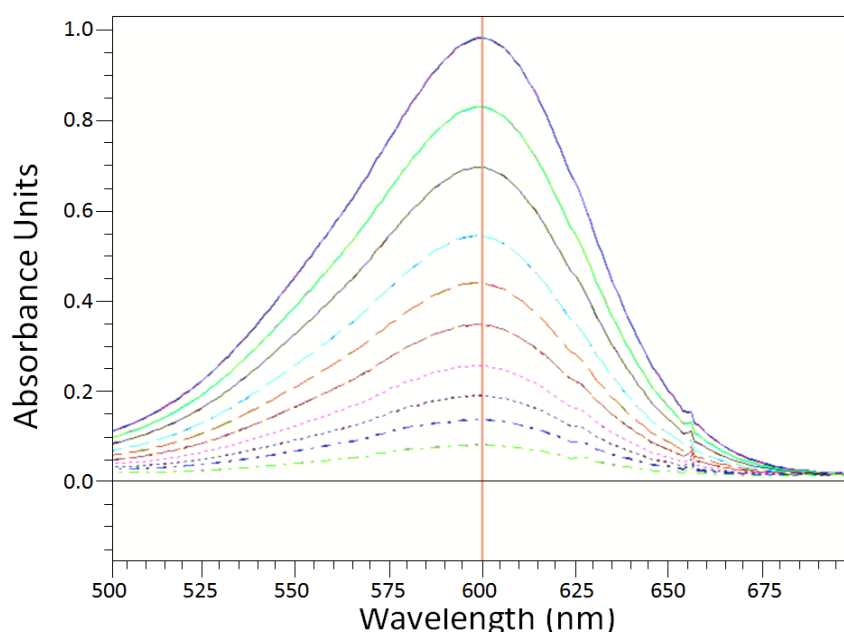


Figure 3-3. Example of indirect ozone measurement using indigotrisulfonate, which absorbs light at 600 nm. (The different spectra correspond to different aqueous ozone concentrations. As the UV_{600} decreases, less indigotrisulfonate is remaining in solution; therefore, more aqueous ozone was introduced to the sample.)

Ciprofloxacin Analysis

Ciprofloxacin was measured by high performance liquid chromatography (HPLC; Waters 2795, Waters Corporation, Milford, MA) equipped with a fluorescence detector (FLD); a Phenomenex (Torrence, CA) Luna 5u C₁₈(2) (250×4.6mm, 5μm) column was utilized for analyte separation. Fifty microliter aliquots were directly injected into the HPLC. The analytical method is based on the procedure developed by Golet *et al.* (2001) but several changes were made to optimize the response on the instrument. The eluent gradient was 7% acetonitrile (ACN), 93% 25-mM H₃PO₄ for 2 min; 3 min ramp to 12% ACN, 88% 25-mM H₃PO₄; 2 min ramp to 15% ACN, 85% 25-mM H₃PO₄; 3 min ramp to 20% ACN, 80% 25-mM H₃PO₄; 10 min isocratic. The flow rate was 0.70 mL/min, and the column temperature was set at 40°C. Excitation and emission wavelengths were set at 278 nm and 445 nm, respectively. Ciprofloxacin was eluted at 8.3 minutes (Figure 3-4).

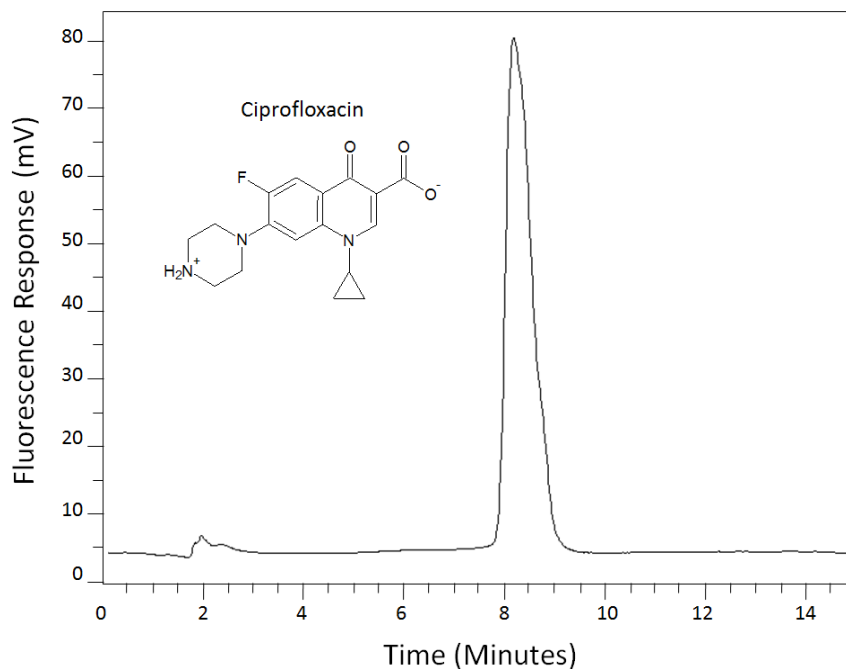


Figure 3-4. Representative chromatogram of ciprofloxacin analysis using HPLC with FLD. (The concentration of ciprofloxacin in this sample was 100 μg/L.)

Cyclophosphamide Analysis

Cyclophosphamide was measured with LC-MS/MS (TSQ Quantum, Thermo Finnigan, Waltham, MA). The injection volume was 10 μ L and the flow rate was 700 μ L/min. HPLC separation was achieved with a C₁₈ (Shimadzu 150 \times 4.6 mm; particle size, 5 μ m) column; the eluent gradient was 5% MeOH, 95% H₂O (0-3 min); ramp to 80% MeOH, 20% H₂O (3-10 min); 80% MeOH, 20% H₂O (10-12 min); ramp to 100% MeOH, 0% H₂O (12-12.1 min); 100% MeOH, 0% H₂O (12.1-16 min); ramp to 5% MeOH, 95% H₂O (16-16.1 min); 5% MeOH, 95% H₂O (16.1-18 min). The electrospray ionization tandem mass spectrometer was operated in positive ion mode. Method parameters include the following: parent mass, 261.0 mg; product mass, 139.8 mg; collision gas pressure, 1.5 mTorr; collision energy, 20 V; spray voltage, 4000 V; vaporizer temperature, 400 °C; sheath gas pressure, 50 psi; and auxiliary gas pressure, 30 psi. Cyclophosphamide was eluted at 12.0 minutes as shown in Figure 3-5.

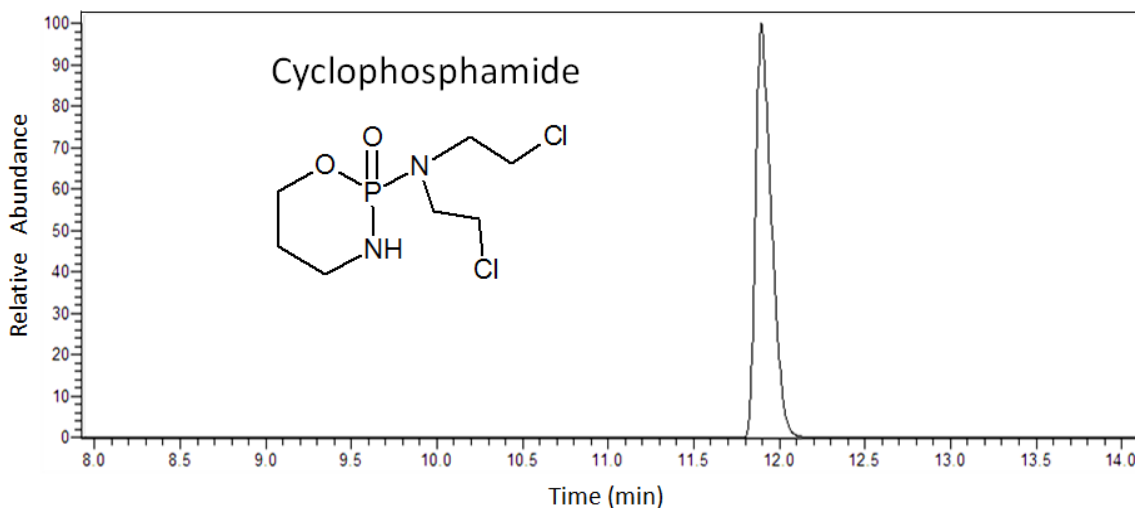


Figure 3-5. Cyclophosphamide (100 μ g/L) peak using LC-MS/MS.

Cyclophosphamide intermediate products were analyzed using LC-MS; the measured m/z range was 30–1500. The injection volume was 20 μ L and the flow rate was 350 μ L/min. The eluent gradient was 5% MeOH, 95% H₂O (0-15 min); ramp to

80% MeOH, 20% H₂O (15-22 min); 80% MeOH, 20% H₂O (22-29 min); ramp to 100% MeOH, 0% H₂O (29-29.1 min); 100% MeOH, 0% H₂O (29.1-33 min); ramp to 5% MeOH, 95% H₂O (33-33.1 min); 5% MeOH, 95% H₂O (33.1-35 min). The electrospray ionization tandem mass spectrometer was operated in positive ion mode. Method parameters include the following: parent mass, 261.0 mg; collision gas pressure, 1.5 mTorr; collision energy, 20 V; spray voltage, 4000 V; vaporizer temperature, 400 °C; sheath gas pressure, 25 psi; and auxiliary gas pressure, 15 psi. Example LC-MS peaks for cyclophosphamide and cyclophosphamide intermediate oxidation products are shown in Figure 3-6. These compounds were eluted in the 26-29 minutes range.

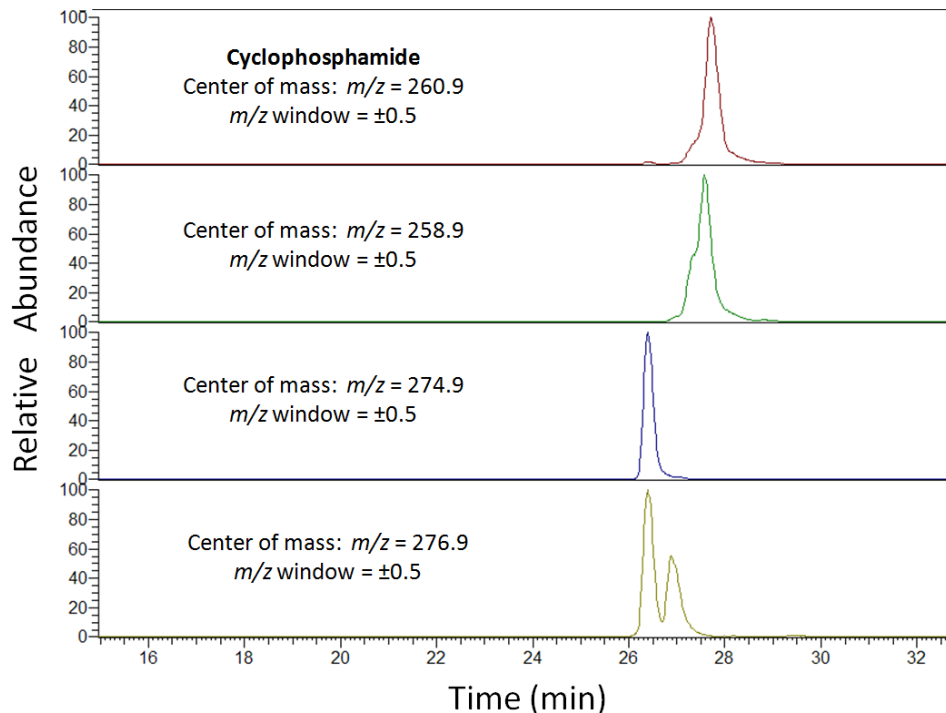


Figure 3-6. Typical peaks for cyclophosphamide and intermediate oxidation products generated by ozone and hydroxyl radical reaction with cyclophosphamide. (Intermediate oxidation products were detected by peak presence in the total ion current; those peaks were then extracted and plotted individually. In this case, the m/z window was ± 0.5 m/z units to either side of the central m/z value.)

Erythromycin Analysis

Erythromycin was analyzed using LC-MS/MS (Thermo Finnigan, TSQ Quantum). The injection volume was 10 μ L and the flow rate was 700 μ L/min. LC separation was achieved with a C₁₈ column (Shimadzu Premier C18 5 μ 150 \times 4.6-mm); the eluent gradient was 100% 0.1% Formic acid (FA), 0% Acetonitrile (ACN) (0-3 min); ramp to 88% 0.1% FA, 12% ACN (3-10 min); 75% 0.1% FA, 25% ACN (10-12 min); ramp to 50% 0.1% FA, 50% ACN (12-12.1 min); 50% 0.1% FA, 50% ACN (12.1-16 min); ramp to 50% 0.1% FA, 50% ACN (16-16.1 min); 88% 0.1% FA, 12% ACN (16.1-18 min). The electrospray ionization tandem mass spectrometer was operated in positive ion mode. Method parameters include the following: parent mass, 734.4 mg; product mass, 576.2 mg; collision gas pressure, 1.5 mTorr; collision energy, 24 V; spray voltage, 4000 V; vaporizer temperature, 400 $^{\circ}$ C; sheath gas pressure, 25 psi; and auxiliary gas pressure, 20 psi. Erythromycin was eluted at 15.2 minutes (Figure 3-7). A similar method was employed by Huang (2011) to measure anhydroerythromycin A, an erythromycin degradation product.

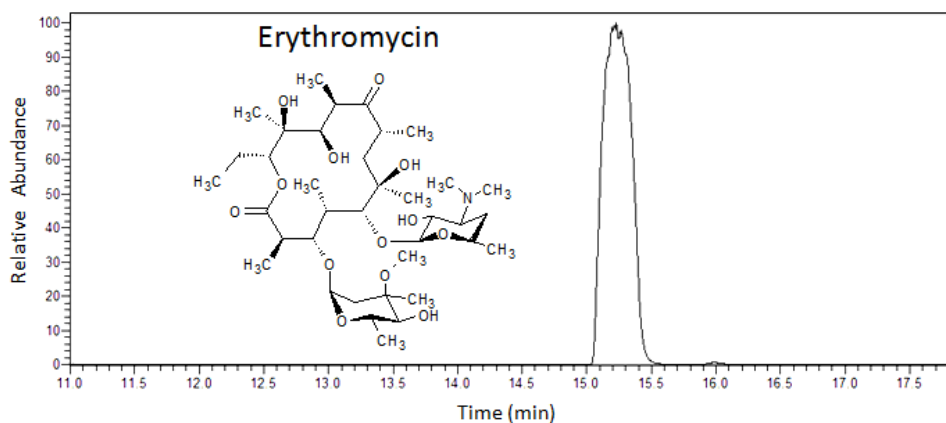


Figure 3-7. A representative erythromycin peak using the LC-MS/MS analytical method described above. (The erythromycin concentration of this sample was 100 mg/L.)

Samples were also analyzed using LC-MS to detect erythromycin's intermediate oxidation products; the measured m/z range was 150–1500. The injection volume was 20

μL and the flow rate was $350\ \mu\text{L}/\text{min}$. The eluent gradient was 100% 0.1% FA, 0% ACN (0-2 min); ramp to 88% 0.1% FA, 12% ACN (2-12 min); 75% 0.1% FA, 25% ACN (12-16 min); ramp to 50% 0.1% FA, 50% ACN (16-21 min); 50% 0.1% FA, 50% ACN (21-28 min); ramp to 50% 0.1% FA, 50% ACN (28-30 min); 88% 0.1% FA, 12% ACN (30-35). The electrospray ionization tandem mass spectrometer was operated in positive ion mode. Method parameters include the following: parent mass, 734.4 mg; collision gas pressure, 1.5 mTorr; collision energy, 24 V; spray voltage, 4000 V; vaporizer temperature, $400\ ^\circ\text{C}$; sheath gas pressure, 25 psi; and auxiliary gas pressure, 20 psi. Example LC-MS peaks for erythromycin and erythromycin intermediate oxidation products are shown in Figure 3-8. These compounds were eluted in the 26-28 minutes range.

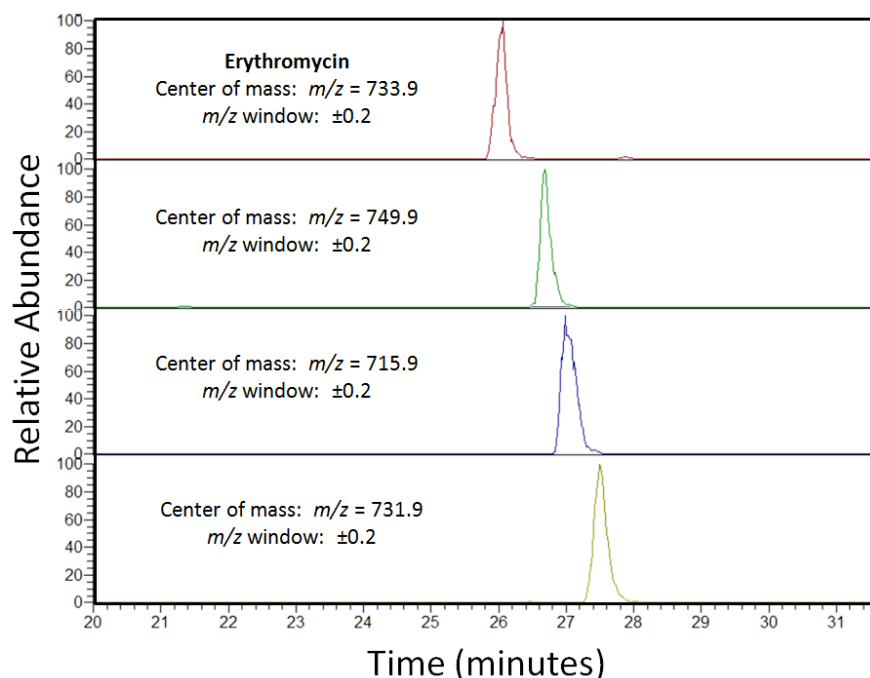


Figure 3-8. Examples of erythromycin and erythromycin intermediate oxidation products generated by erythromycin reaction with aqueous ozone. (In this case, erythromycin and erythromycin intermediate oxidation products were detected from the total ion current of the sample. The individual peaks were separated and are plotted according to the major m/z values found in the total ion current. For erythromycin, m/z windows of ± 0.2 m/z units were employed.)

Ifosfamide Analysis

Ifosfamide was measured with LC-MS/MS (Thermo Finnigan, TSQ Quantum). The injection volume was 10 μ L and the flow rate was 700 μ L/min. HPLC separation was achieved with a C₁₈ (Shimadzu 150 \times 4.6 mm; particle size, 5 μ m) column; the eluent gradient was the same as that employed in the LC-MS/MS method used for cyclophosphamide analysis. The electrospray ionization tandem mass spectrometer was operated in positive ion mode. Method parameters include the following: parent mass, 261.0 mg; product mass, 153.9; collision gas pressure, 1.5 mTorr; collision energy, 20 V; spray voltage, 4000 V; vaporizer temperature, 400 $^{\circ}$ C; sheath gas pressure, 30 psi; and auxiliary gas pressure, 10 psi. Ifosfamide was eluted at 11.7 minutes (Figure 3-9).

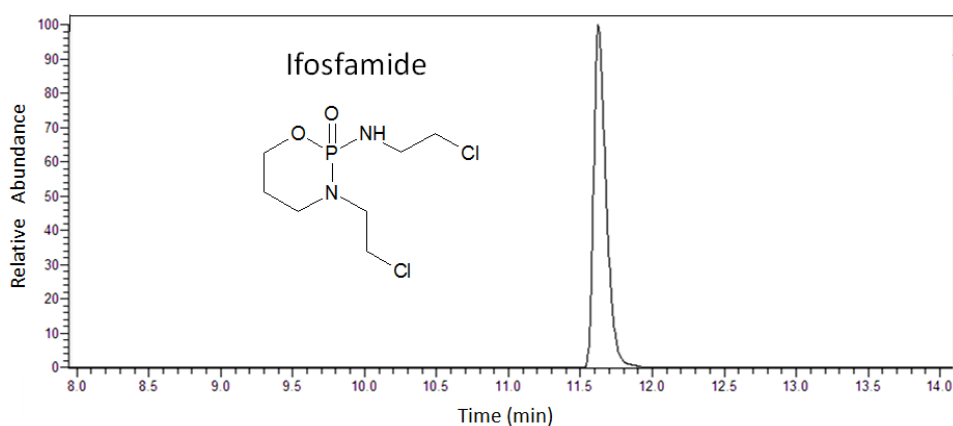


Figure 3-9. A typical ifosfamide peak using the LC-MS/MS method described above. (In this sample, the ifosfamide concentration was 100 μ g/L.)

In kinetics experiments, cyclophosphamide and ifosfamide were typically both present in solution. For that reason, these two compounds were often both analyzed in LC-MS/MS mode using a combined method. That method essentially combined the ifosfamide method described above from minutes 0 to 11.85, and then the detection method was switched to the cyclophosphamide LC-MS/MS method described earlier. An example of the chromatogram observed using this method is shown in Figure 3-10.

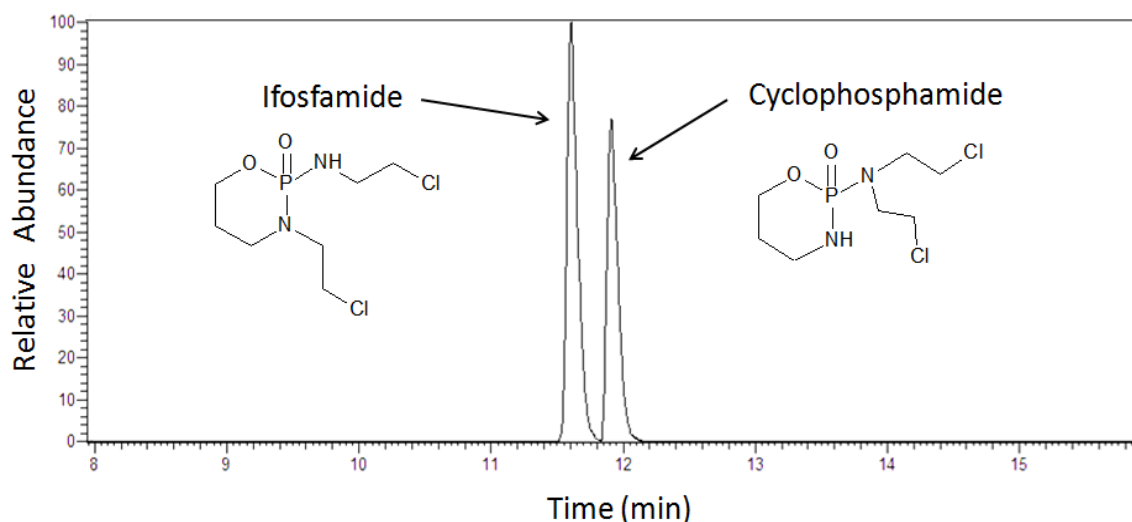


Figure 3-10. Example of combined method allowing concomitant analysis of cyclophosphamide and ifosfamide for the same injection volume. (For this sample, the concentration of both PhACs was 100 µg/L.)

Ifosfamide intermediate products were analyzed using LC-MS; the measured m/z range was 30–1500. The injection volume was 20 µL and the flow rate was 350 µL/min. The eluent gradient was the same employed in LC-MS analysis of cyclophosphamide and cyclophosphamide intermediate oxidation products. The electrospray ionization tandem mass spectrometer was operated in positive ion mode. Method parameters include the following: parent mass, 261.0 mg; collision gas pressure, 1.5 mTorr; collision energy, 20 V; spray voltage, 4000 V; vaporizer temperature, 400 °C; sheath gas pressure, 15 psi; and auxiliary gas pressure, 5 psi. Example LC-MS peaks for ifosfamide and ifosfamide intermediate oxidation products are shown in Figure 3-11. These peaks are eluted in the 24 to 29 minute range.

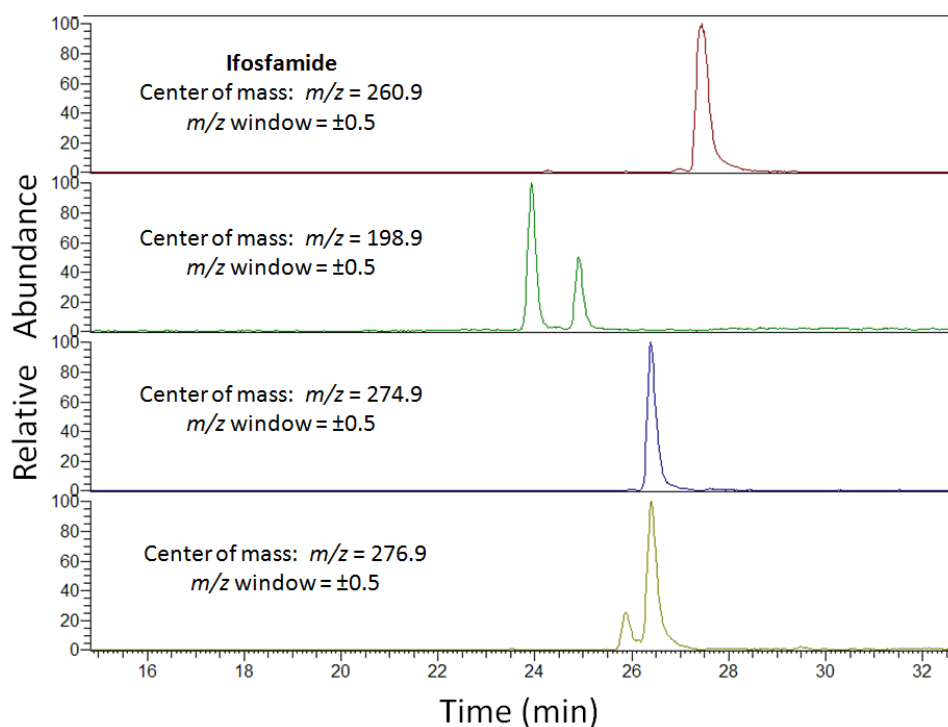


Figure 3-11. Ifosfamide and ifosfamide intermediate peaks detected using LC-MS. Ifosfamide and ifosfamide intermediate oxidation products were detected by their distinctive m/z values and separated from the total ion current. (In the figure, all compounds are plotted across a window of m/z values (central $m/z \pm 0.5$) as described above.)

***para*-Chlorobenzoic Acid (*p*CBA) Analysis**

The hydroxyl radical probe compound, *p*CBA, was measured at 234 nm using an HPLC (Waters Corporation) with PDA. HPLC separation was achieved with a C₁₈ column (Sonoma C18(2), 3 μ 100 Å). The eluent, 60% MeOH, 40% 25 mM H₃PO₄, was pumped at a constant flow rate (0.5 mL/min). *p*CBA was eluted after 5.35 minutes as shown in Figure 3-12.

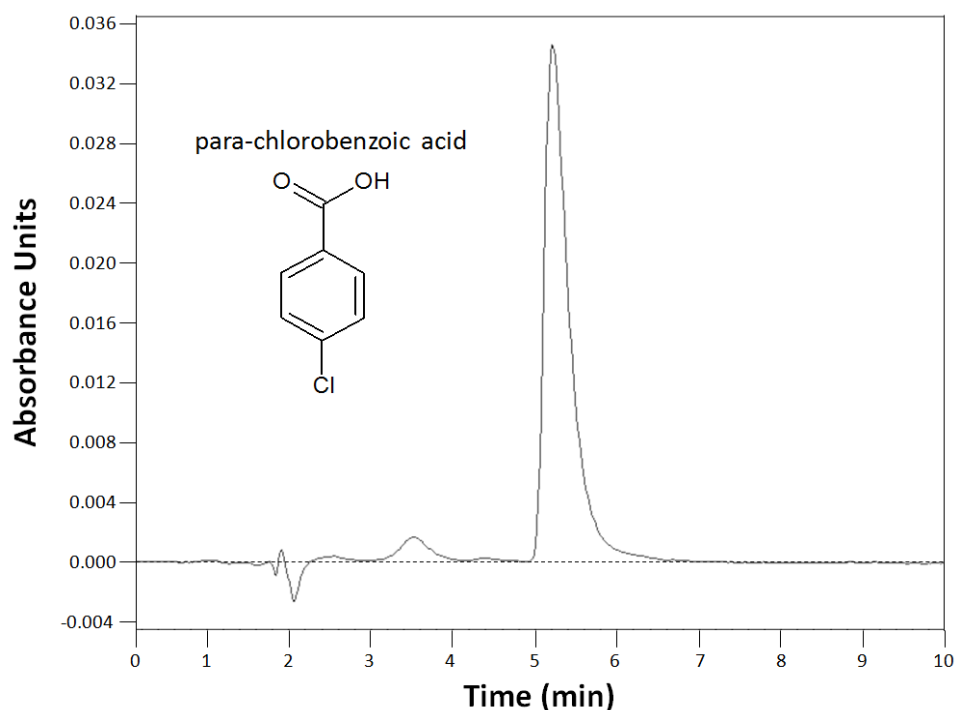


Figure 3-12. A representative *p*CBA peak (10 μ M) using the HPLC with PDA.

NOM Analysis

Preliminary analysis of the NOM source waters and the NOM isolates was conducted at the USGS laboratories in Boulder, CO (Marron, 2010). As discussed in Marron's thesis (2010), the NOM isolates were freeze-dried to provide a solid NOM powder. NOM working solutions were prepared by dissolving 100 mg of the dried NOM extract in 100 mL of DI; the pH of the NOM solutions was dropped to pH \sim 1.9 through the addition of concentrated phosphoric acid. After dissolution of the NOM extract in the acidified working solution, several water quality parameters, namely, pH, total organic carbon (TOC), and the absorbance at 254 nm (UV_{254}), were measured to characterize the strength of the NOM working solution. The pH was measured using a Thermo Electron Corporation pH meter (Orion 720 A+) as described below.

The TOC of working solutions was measured using a TOC Analyzer (O.I. Corporation, College Station, TX). Standard organic carbon solutions were prepared using potassium hydrogen phthalate according to Standard Methods (5310 B. Combustion-Infrared Method; APHA *et al.*, 2006). Due to the high concentration of the working solutions (1 g NOM / L), these solutions were diluted 100× before analysis on the TOC Analyzer. While the TOC concentration of the different NOM working solutions varied, the TOC was typically 380-420 mg C / L; therefore, the percentage of organic carbon in the NOM isolates was approximately 38-42%.

The UV_{254} was measured using a UV-VIS spectrophotometer (Agilent Technologies). Approximately 12 mL of the 100× dilution used for TOC analysis was placed into a 10-cm quartz cuvette, and the absorbance was measured at 254 nm. The resultant absorbance at 254 nm and the TOC concentration can be used to calculate the $SUVA_{254\text{ nm}}$ of the NOM working solutions, according to Eq. 3-3.

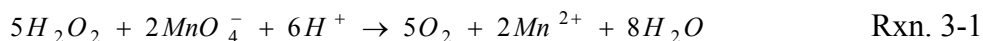
$$SUVA_{254\text{ nm}} \left(\frac{L}{mg - cm} \right) = \frac{UV_{254} \left(\frac{1}{10\text{ cm}} \right)}{TOC \left(\frac{mg}{L} \right)} \quad \text{Eq. 3-3}$$

The NOM isolates were also analyzed using Excitation-Emission Matrix (EEM) fluorescence spectroscopy. As the results of that analysis are not discussed in the body of this document, the fluorescence EEM characterization of all three organic matter isolates as well as the Lake Austin whole water used in the NOM extractions are provided in Appendix B.

Hydrogen Peroxide Titration

For peroxone experiments, a hydrogen peroxide solution was employed. A hydrogen peroxide stock solution (30% H_2O_2) was purchased from VWR. A hydrogen peroxide working solution (0.105 M) was made by diluting the stock solution (30%

H₂O₂) with DI. The working solution was kept in an amber bottle at 4°C in a dark environment to prevent hydrogen peroxide decomposition. Hydrogen peroxide concentrations were measured via titration with permanganate according to Reaction 3-1.



For experimental titrations, 1 mL of the H₂O₂ working solution, 0.4 mL of H₂SO₄, and 8.6 mL of DI were mixed together to constitute the sample. The titrant was 0.1 N KMnO₄ (0.02 M MnO₄⁻). The titration endpoint was reached when the sample solution changed color from clear to pink. The hydrogen peroxide concentration (Eq. 3-4) was calculated using the volume of titrant ($V_{titrant}$), the volume of the sample ($V_{sample} = 1$ mL), and the stoichiometry of Rxn. 3-1.

$$[H_2O_2] \left(\frac{mol}{L} \right) = \frac{5 mol H_2O_2}{2 mol MnO_4^-} \times \frac{0.02 mol MnO_4^-}{L} \times \frac{V_{titrant} (mL)}{V_{sample} (mL)} \quad \text{Eq. 3-4}$$

Over the course of six months, the hydrogen peroxide concentration of the working solution (0.105 M) did not change; regardless, new working solutions were prepared every six months.

pH

The pH was measured and recorded during continuous ozone and peroxone addition experiments, as well as in other solutions throughout this research. A Thermo Electron Corporation pH meter (Orion 720 A+) was employed for these purposes; the probe was a Thermo Fisher Scientific Orion ROSS Sure-Flow pH electrode. The pH meter was calibrated before every use using standard buffer solutions (pH 4.01, 7.01, and 10.01).

OZONE REACTORS

A schematic of the ozone supply system and reactor is shown in Figure 3-13. Oxygen gas flowed into the ozone generator at 30 cm³/min; a fraction of that oxygen was converted to ozone. This combined gas stream was directed into a gas-washing bottle, which served as a stock ozone solution. The ozone stock solution was kept on ice (T_{solution} ~ 0.5°C) to increase the solubility of ozone (Sotelo *et al.*, 1989). After 4-6 hours, the ozone concentration in the stock solution reached a plateau at 50-60 mg O₃/L. These concentrations are comparable to ozone concentrations in stock solutions used by other researchers (Buffle *et al.*, 2004; Buffle *et al.*, 2006; Suarez *et al.*, 2007). For all experiments discussed in this dissertation, the aqueous ozone stock solution was employed as the primary supply of ozone.

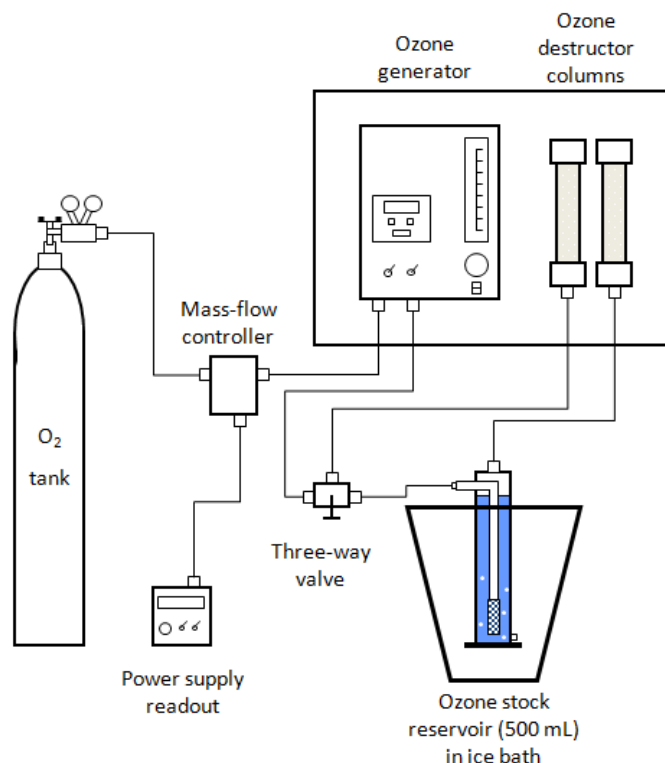


Figure 3-13. Schematic of the ozone reactor showing gaseous generation of ozone and the ozone stock solution container.

Determination of PhAC Transformation in Batch Reactors with Aqueous Ozone

Small aliquots of the ozone stock solution were added to culture tubes containing the solution of interest (Figure 3-14) for a variety of reasons, including the following: to demonstrate the impact of NOM on the transformation of cyclophosphamide, erythromycin, and ifosfamide; to characterize the intermediate oxidation products formed via ozonation and peroxonation of cyclophosphamide, erythromycin, and ifosfamide; and to monitor the residual antimicrobial activity of ozone-treated solutions containing erythromycin. The water quality matrix varied depending on the type of experiment; for instance, lower PhAC concentrations were employed in experiments documenting the transformation of the parent pharmaceutical, but higher PhAC concentrations were employed for experiments aimed at characterization of intermediate oxidation products. The background water quality matrix (*e.g.*, pH, NOM, [DOC], *t*-BuOH, *p*CBA, and alkalinity, among others) also changed between experiments. For batch experiments, all solutions were immediately capped, shaken, and placed into a dark environment (at room temperature) for at least 24 hours before analysis; before analysis, samples were quenched using indigotrisulfonate. Details on specific ozone doses added to samples containing the PhACs of interest are provided in Chapters 4 and 6.

An essentially identical protocol was employed for batch peroxone experiments. Hydrogen peroxide was added to the individual batch solutions in concentrations that were calculated to yield specific H₂O₂ to O₃ molar ratios after application of aqueous ozone. Besides inclusion of hydrogen peroxide in the water quality matrix, no differences between batch ozone experiments and batch peroxone experiments existed.

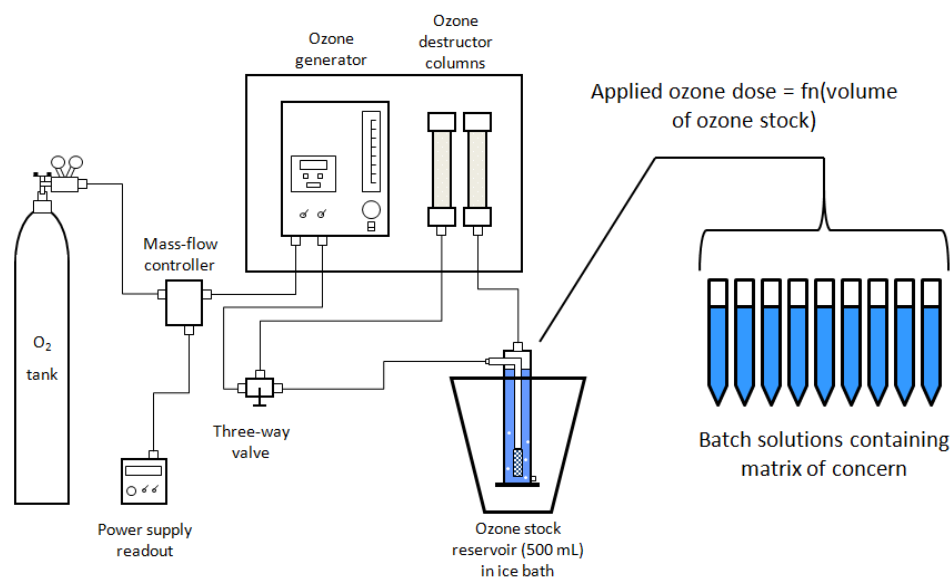


Figure 3-14. Schematic of experimental setup for batch transformation studies.

Continuous Aqueous Ozone Addition Reactor

The continuous aqueous ozone addition reactor (Figure 3-15) is a novel method for investigating the transformation of organic compounds. Teflon tubing and stainless steel connections were employed to reduce ozone loss from the stock reservoir and into the 2-L reactor. Prior to all experiments, the ozone stock solution was continuously cycled through the tubing; hence any ozone demand from the tubing would have been sated. In addition, quality control experiments were run to ascertain whether any significant ozone loss occurred between the stock reservoir and the reactor; the results show that for a stock ozone solution containing $36.96 (\pm 0.41)$ mg/L O₃, the ozone concentration measured at the effluent of the tubing (*i.e.*, the influent line to the reactor) was $36.89 (\pm 0.44)$ mg/L O₃. Given these results, no appreciable changes in ozone concentration from the stock reservoir to the reactor were encountered.

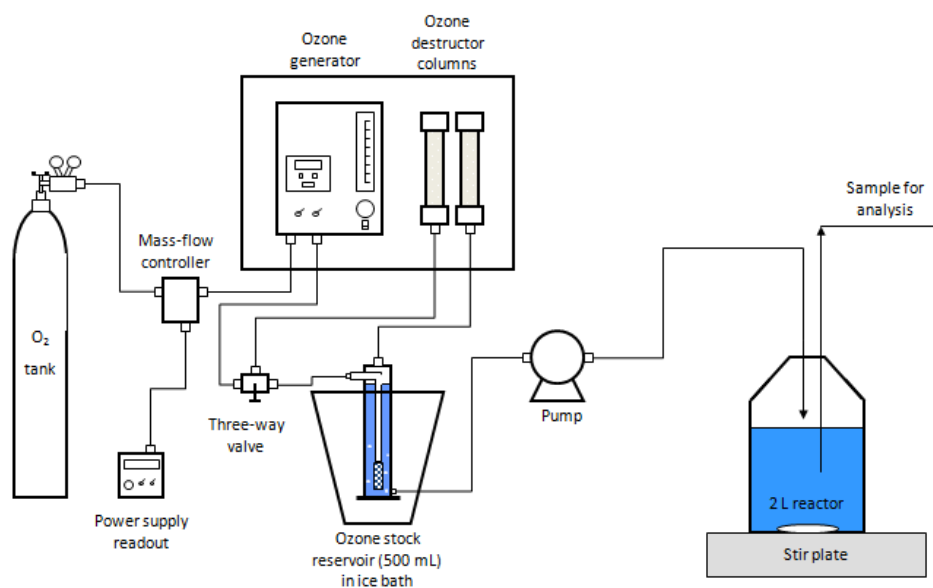


Figure 3-15. Schematic of the experimental setup for continuous ozone addition experiments.

In this research, the continuous ozone reactor was employed to demonstrate the impact of NOM on ciprofloxacin transformation and elimination of ciprofloxacin-associated antimicrobial activity and to determine the transformation kinetics of cyclophosphamide and ifosfamide with ozone and hydroxyl radicals. Two experimental protocols were utilized. In the first scenario (Method 1), concentrated ozone stock solution was continuously pumped into the separate 2-L reactor, which contained the water matrix of interest, to determine the impact of NOM on transformation of ciprofloxacin and elimination of the associated antimicrobial activity. Samples were taken at set time intervals. This reactor setup is discussed in more detail in Chapter 5, which shows how this process is utilized for removal of ciprofloxacin, and its associated antimicrobial activity, from various water sources. The second operational scenario (Method 2) was utilized to elucidate the reaction kinetics of cyclophosphamide and ifosfamide reaction with aqueous ozone and hydroxyl radicals. In this method, the ozone stock solution was pumped into the 2-L reactor for a set period of time (typically, 30 minutes) before dosing in the organic compounds of interest. During this period, the aqueous ozone concentration in the reactor builds up to a controllable concentration.

This concentration is a function of several variables, including the ozone stock solution concentration, the pumping rate, and the composition of the background matrix, specifically the carbonate species and other compounds that affect ozone decomposition. As ozone is being continually introduced into the reactor, the ozone concentration can be controlled throughout experimentation; therefore, at time, $t = 0$, defined as the time at which the pharmaceuticals and the background water matrix are dosed into the reactor, an excess of ozone and hydroxyl radicals are present in solution. This process is explained in more detail in Chapter 4, which details the investigation of cyclophosphamide and ifosfamide kinetics with ozone and hydroxyl radicals.

The ozone profile for a continuous ozone addition experiment with pre-ozonation (Method 2) is shown in Figure 3-16. The initial solution contained 100 mg/L NaCl, 200 mg/L NaHCO₃, and 10 mM *t*-BuOH at a pH of 8.3. At time, $t = 0$, 100 µg/L of cyclophosphamide and 100 µg/L of ifosfamide was dosed into the reactor. Figure 3-16 also shows the ozone exposure (integration of [O₃] with respect to time) for the duration of the experiment. Clearly, the ozone exposure in the continuous liquid addition reactor increases in a linear fashion throughout experimentation due to the relatively steady aqueous ozone concentrations; in contrast, for a batch ozonation experiment, the ozone exposure approaches an asymptote as the aqueous ozone concentration decreases to zero. As the ozone exposure is controllable (through maintenance of a desired ozone concentration), the continuous ozone reactor provides a unique advantage over more traditional methods for determining the kinetics of compounds that react slowly with ozone. It should be noted that this process is novel, that is, this research is the first time that a continuous liquid ozone addition reactor was employed for determination of the reaction kinetics of compounds with ozone and hydroxyl radicals. In Chapter 4, the rate constants for cyclophosphamide reaction with ozone and hydroxyl radicals are determined using Method 2, and those values compare well to previously published data.

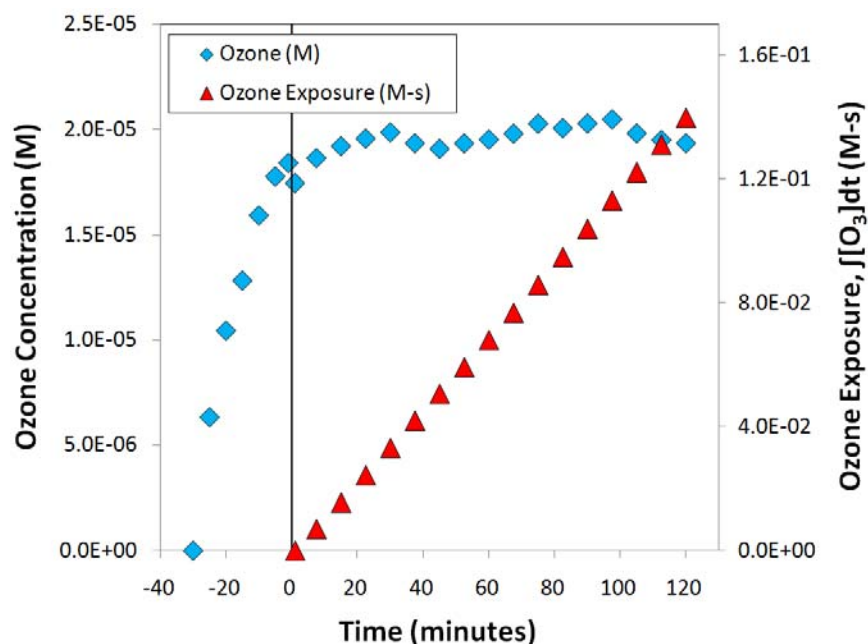


Figure 3-16. Typical ozone concentration and ozone exposure profiles during experimentation. (100 mg/L NaCl, 200 mg/L NaHCO₃, and 10 mm *t*-BuOH at pH 8.3. At time, *t* = 0 minutes, 100 µg/L cyclophosphamide and 100 µg/L ifosfamide were introduced to the reactor.)

Upon dosing of organic compounds, an immediate loss in ozone and hydroxyl radical concentration occurs due to “instantaneous” reaction with the organic matrix. In this case, the loss in ozone concentration is minimal because of the low reactivity of cyclophosphamide/ifosfamide with ozone (see Chapter 4). For this experiment, hydroxyl radicals were scavenged using *t*-BuOH; therefore, no effect of ifosfamide addition on hydroxyl radical exposure is expected. More details about the use of *t*-BuOH are presented below. For other cases, the initial drop in pharmaceutical and ozone concentrations is more drastic (Marron, 2010). One example of a more drastic initial drop in ozone concentration upon dosing of the chemicals of interest is illustrated in Figure 3-17. In this experiment, a 2-L reactor containing 100 mg/L NaCl and 200 mg/L NaHCO₃ at pH 8.3; at time, *t* = 0, 1 mg/L DOC from Lake Austin HPOA was applied to the reactor. As Figure 3-17 demonstrates, the aqueous ozone concentration in the reactor quickly drops and then begins to recover as the more reactive fractions of the NOM are exhausted. The recovery of ozone in this scenario demonstrates that the continuous

aqueous ozone addition reactor can maintain ozone exposure even in the presence of background NOM; therefore, PhACS can be effectively treated even in the presence of relatively high concentrations of NOM.

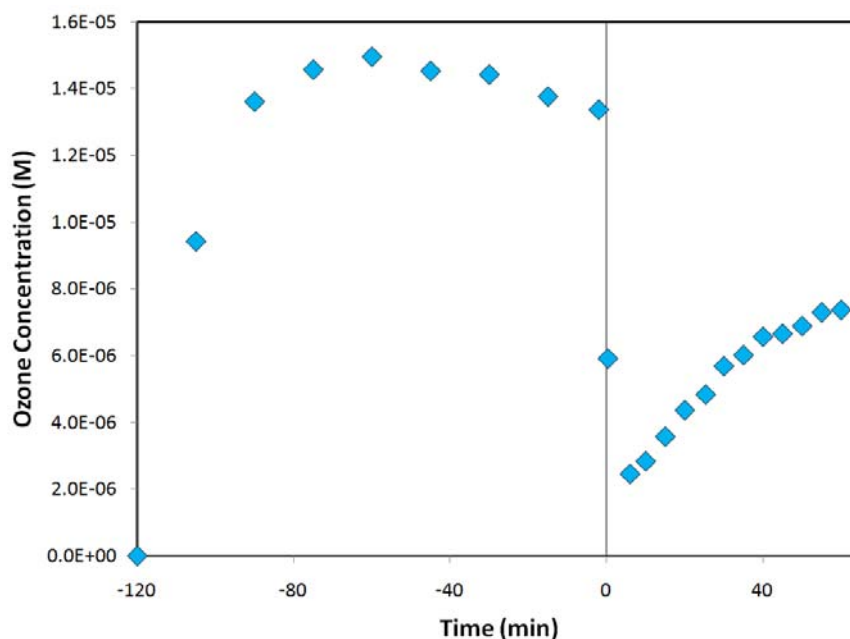


Figure 3-17. Demonstration of the impact that dosing 1 mg/L DOC from Lake Austin HPOA on the aqueous ozone concentration in continuous ozone reactor.

Continuous Peroxone Addition Reactor

Continuous peroxone addition was achieved by concomitantly pumping the ozone stock solution and a hydrogen peroxide stock solution into a separate 2-L reactor (Figure 3-18). This reactor was used to verify the rate constants for the reaction of cyclophosphamide and ifosfamide with hydroxyl radicals. The 2-L reactor contained the water composition of interest, which included PhACs, 100 mg/L NaCl, 200 mg/L NaHCO_3 , and 10 μM *p*CBA at a particular pH. At time, $t = 0$, both pumps (the one connected to the ozone stock solution and the one connected to the hydrogen peroxide working solution) were switched on. The ozone and hydrogen peroxide concentrations (of the ozone stock solution and the hydrogen peroxide working solution) were used to

determine what ozone and hydrogen peroxide pumping rates were required to achieve the desired H_2O_2 to O_3 molar ratio.

As discussed in Chapters 2 and 4, hydrogen peroxide reacts quickly with ozone to promote ozone decomposition and, ultimately, to form hydroxyl radicals. Therefore, in this reactor setup, very low concentrations of aqueous ozone are expected; furthermore, hydroxyl radical exposure should continually increase. Figure 3-19a shows the measured ozone concentrations (via the indigo method) and the hydroxyl radical exposure (determined by the change in [*p*CBA]). These data were obtained from an experiment in which ozone (9.77×10^{-4} M) and hydrogen peroxide (1.05×10^{-3} M) were continuously pumped into a 2-L reactor containing 200 mg/L NaHCO_3 , 100 mg/L NaCl, 100 $\mu\text{g/L}$ ifosfamide, and 10 μM *p*CBA at pH 8.3. The pumping rate of the ozone and hydrogen peroxide solutions were 3.1 mL/min and 2.53 mL/min, respectively. Therefore, the molar ratio of hydrogen peroxide to ozone was 0.88 mol/mol. This ratio is higher than the ideal molar ratio of 0.5 mol H_2O_2 / mol O_3 , indicating that the excess hydrogen peroxide may have scavenged some of the hydroxyl radicals, which would lower the achievable hydroxyl radical exposure. In Figure 3-19b, the hydroxyl radical exposure is plotted as a function of the applied ozone exposure, that is, the integration of the cumulative ozone dose with respect to time. Clearly, the attainable hydroxyl radical exposure is a function of the applied ozone exposure; this relationship makes sense as hydroxyl radicals are a product of ozone decomposition. These relationships were typical of all of the continuous peroxone addition experiments. The hydroxyl radical exposure was used in combination with changes in PhAC concentration throughout treatment to determine the second order rate constant for PhAC transformation with hydroxyl radicals.

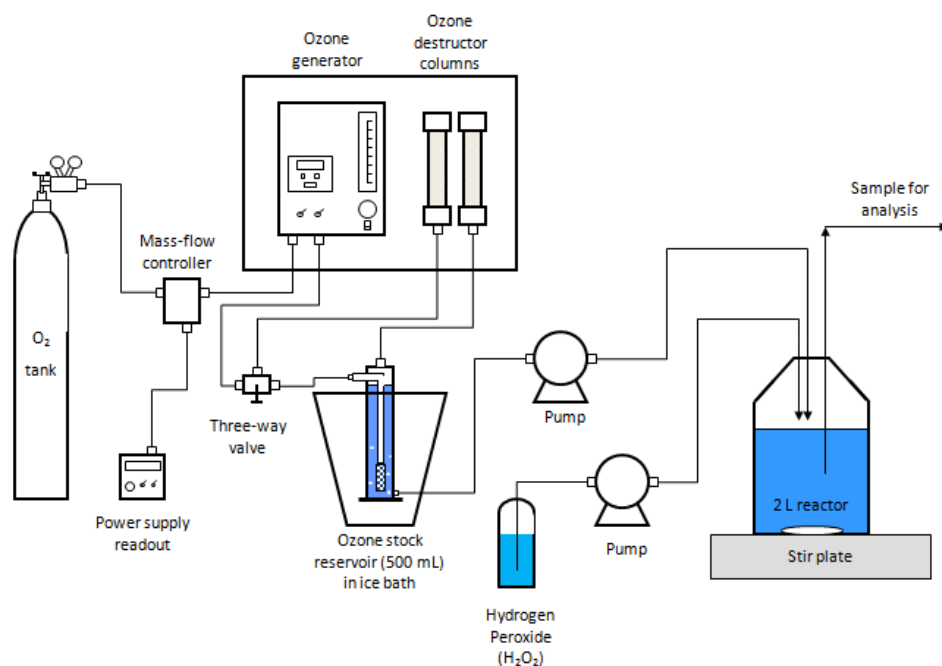


Figure 3-18. Schematic of the continuous peroxone addition reactor.

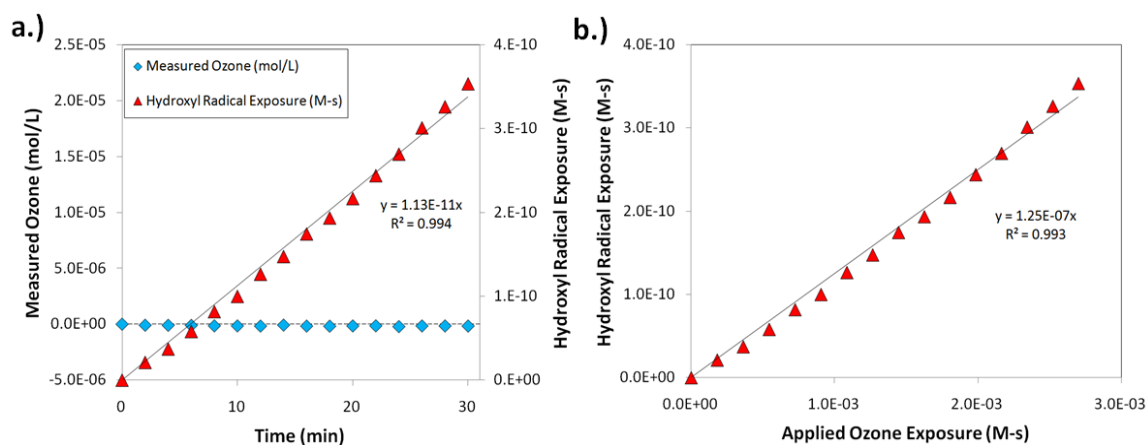


Figure 3-19. (a) Ozone concentration and hydroxyl radical exposure history throughout a typical continuous peroxone addition experiment; (b) Hydroxyl radical exposure as a function of applied ozone exposure.

MEASUREMENT OF OZONE AND HYDROXYL RADICAL KINETICS

As discussed in Chapter 2, in ozone-based oxidation processes, organic molecules interact not only with ozone but also with hydroxyl radicals (Eq. 3-5).

$$r_{PhAC} = \frac{d[PhAC]}{dt} = -k_{O_3,app,PhAC} [O_3][PhAC] - k_{HO\cdot,app,PhAC} [HO\cdot][PhAC] \quad \text{Eq. 3-5}$$

where $[PhAC]$ is the concentration of the pharmacologically active compound at time t in a batch reactor, $k_{O_3,app,PhAC}$ is the apparent rate constant for the reaction between ozone and the PhAC, $[O_3]$ is the ozone concentration at time t , $[HO\cdot]$ is the hydroxyl radical concentration at time t , and $k_{HO\cdot,app,PhAC}$ is the rate constant for the reaction between ozone and the PhAC. In this work, the rate constants for PhAC transformation by ozone and hydroxyl radicals were determined using three different means. Cyclophosphamide and ifosfamide kinetics with ozone and hydroxyl radicals were determined using the continuous addition ozone reactor. The rate constants for ciprofloxacin and erythromycin transformation by ozone were found using a conventional batch ozone reactor; however, these tasks were primarily completed by Marron (2010) for ciprofloxacin and Huang (2011) for erythromycin and so are not described in detail here. The rate constant for erythromycin was used in batch tests to calculate the rate constant for anhydroerythromycin transformation by ozone. This section focuses on the use of the continuous aqueous ozone addition reactor to determine rate constants for cyclophosphamide and ifosfamide transformation by ozone and hydroxyl radicals.

After continuous ozonation for 6-8 hours, a highly concentrated ozone stock solution (50-60 mg/L O_3) was generated. That solution was continuously pumped into a 2-L reactor containing the background matrix of interest for at least 30 minutes. During the course of these 30 minutes, an excess of aqueous ozone was built up in the reactor as shown in Figure 3-16a. Note that the pre-ozonation time is listed as negative time in Figure 3-16a. At time, $t = 0$ min, a small volume of cyclophosphamide and/or ifosfamide stock solution was added to the reactor to achieve an initial concentration of

approximately 100 µg/L. These details were the same for all experiments; however, two separate background matrices were employed to determine the rate constants for the PhACs with ozone and hydroxyl radicals. The two experiments were run with the following background matrices: (1) 10 mM *t*-BuOH was added to scavenge hydroxyl radicals and (2) 1-10 µM *p*CBA was included as a hydroxyl radical probe compound. The strategy for using the results of experiments with these chemicals to elucidate the rate constants for PhAC transformation by ozone and hydroxyl radicals is presented below.

Isolating Ozone Kinetics

As discussed above and earlier in Chapter 2, *t*-BuOH is an excellent hydroxyl radical scavenger. Recall, *t*-BuOH reacts slowly with ozone ($k''_{app,O_3,t-BuOH} = 0.003 \text{ M}^{-1}\text{s}^{-1}$; Hoigné and Bader, 1983a) but quickly with hydroxyl radicals ($k''_{app,HO\cdot,t-BuOH} = 6 \times 10^8 \text{ M}^{-1}\text{s}^{-1}$; Buxton *et al.*, 1988). For this reason, *t*-BuOH is not expected to significantly affect aqueous ozone concentrations, and therefore, should not greatly impact the aqueous ozone exposure. However, due to the relatively high concentration of *t*-BuOH in solution and the high rate constant for *t*-BuOH transformation with hydroxyl radicals, *t*-BuOH will scavenge virtually all of the hydroxyl radicals in solution; therefore, any changes in PhAC concentration can be attributed to reaction with ozone (Eq. 3-6).

$$\frac{d[PhAC]}{dt} = -k''_{app,O_3,PhAC} [O_3][PhAC] \quad \text{Eq. 3-6}$$

It should be noted that the reactor volume varies with time in these experiments due to the continuous flow of ozone stock solution into the reactor and sample withdrawal. Here, a modified constant volume equation was employed; in this case, the effects of dilution on PhAC concentrations were accounted for in the data analysis by multiplying the pharmaceutical concentration by the ratio of the initial reactor volume to the reactor volume at time, *t*. Appendix E demonstrates that this assumption has a

negligible impact on calculation of the rate constant for pharmaceutical transformation by ozone; therefore, the modified constant volume model was used here.

At a concentration of 10mM *t*-BuOH, the molar ratio of *t*-BuOH to ifosfamide (100 µg/L or 0.38 µM) is over 26,000. Assuming that hydroxyl radicals react with *t*-BuOH at the same rate as ifosfamide, then *t*-BuOH will scavenge 99.996% of the hydroxyl radicals in solution. During experimentation, *t*-BuOH is transformed through reaction with hydroxyl radicals. In these experiments, the maximum hydroxyl radical exposure observed is approximately 10⁻⁹ M-s, which would transform 45% of the *t*-BuOH in solution; even then, the residual *t*-BuOH would still scavenge 99.993% of the hydroxyl radicals formed.

The rearrangement and integration of Eq. 3-6 yields Eq. 3-7.

$$\int_0^t \frac{d[PhAC]}{[PhAC]} = \int_0^t -k''_{app,O_3,PhAC} [O_3] dt \quad \text{Eq. 3-7}$$

By carrying out the integrations shown in Eq. 3-7, a direct relationship between changes in PhAC concentration and ozone exposure can be determined (Eq. 3-8).

$$\ln \frac{[PhAC]}{[PhAC]_o} = -k''_{app,O_3,PhAC} \int_0^t [O_3] dt \quad \text{Eq. 3-8}$$

By plotting $\ln [PhAC]/[PhAC]_o$ vs. the ozone exposure ($\int [O_3] dt$), the second order rate constant for PhAC transformation with ozone ($k''_{app,O_3,PhAC}$) can be measured. Figure 3-20 demonstrates such a plot; in this case, the rate constant for ifosfamide reaction with ozone was determined to be $k''_{app,O_3,IFO} = 6.07 \text{ M}^{-1}\text{s}^{-1}$. This model (Eq. 8) has been extensively employed by previous authors (McDowell *et al.*, 2005; Dodd *et al.*, 2006; Suarez *et al.*, 2007) to determine the second order rate constant for ozone with various

trace organic contaminants. It should be noted that, if a significant fraction of the *t*-BuOH added into solution is transformed, the data in this plot would exhibit a steepening slope due to PhAC transformation through reaction with hydroxyl radicals. This issue was never observed; therefore, it can be concluded that the original *t*-BuOH concentration was sufficient to allow effective scavenging of hydroxyl radicals throughout experimentation. More details on these experiments and the meaning of the results are presented in Chapter 4.

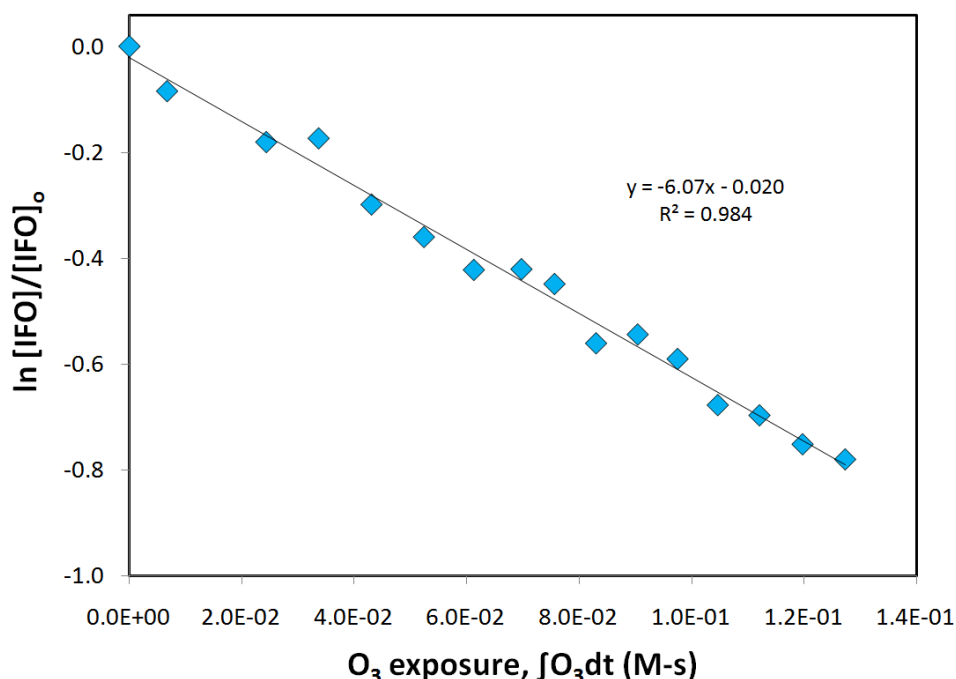


Figure 3-20. Determination of the second-order rate constant for ozone reaction with ifosfamide. (The slope of the curve represents $k_{app,O_3,IFO}$. The data in this figure correspond to a background solution containing 100 mg/L NaCl, 200 mg/L NaHCO₃, 10 mM *t*-BuOH, 100 µg/L cyclophosphamide, and 100 µg/L ifosfamide at pH 8.3.)

Determination of Hydroxyl Radical Kinetics

The second type of experiment involved using a hydroxyl radical probe compound. In this work, *para*-chlorobenzoic acid (*p*CBA) was employed. The second-

order rate constants for *p*CBA with ozone and hydroxyl radical are known from the literature: $k''_{app,O_3,pCBA} = 0.15 \text{ M}^{-1}\text{s}^{-1}$ (Yao and Haag, 1991) and $k''_{app,HO\cdot,pCBA} = 5.2 \times 10^9 \text{ M}^{-1}\text{s}^{-1}$ (Buxton *et al.*, 1988). Because of the low reactivity with ozone, we can consider changes in *p*CBA concentration in a batch reactor to be due solely to reaction with hydroxyl radicals (Eq. 3-9).

$$\frac{d[pCBA]}{dt} = k''_{app,HO\cdot,pCBA} [HO\cdot][pCBA] \quad \text{Eq. 3-9}$$

Integration of Eq. 3-9 with respect to time yields Eq. 3-10.

$$\ln \frac{[pCBA]}{[pCBA]_o} = -k''_{app,HO\cdot,pCBA} \int_0^t [HO\cdot] dt \quad \text{Eq. 3-10}$$

By plotting $\ln [pCBA]/[pCBA]_o$ versus ozone exposure (Eq. 3-11), we can solve for Elovitz and von Gunten's (1999) R_{ct} term (Eq. 3-12) as shown in Figure 3-21. R_{ct} is the ratio of hydroxyl radical exposure to ozone exposure. In this case, the value of R_{ct} was $2.16 \times 10^{-8} \text{ mol HO}\cdot / \text{mol O}_3$.

$$\ln \frac{[pCBA]}{[pCBA]_o} = -k''_{app,HO\cdot,pCBA} \times R_{ct} \times \int_0^t [O_3] dt \quad \text{Eq. 3-11}$$

$$R_{ct} = \frac{\int_0^t [HO\cdot] dt}{\int_0^t [O_3] dt} \quad \text{Eq. 3-12}$$

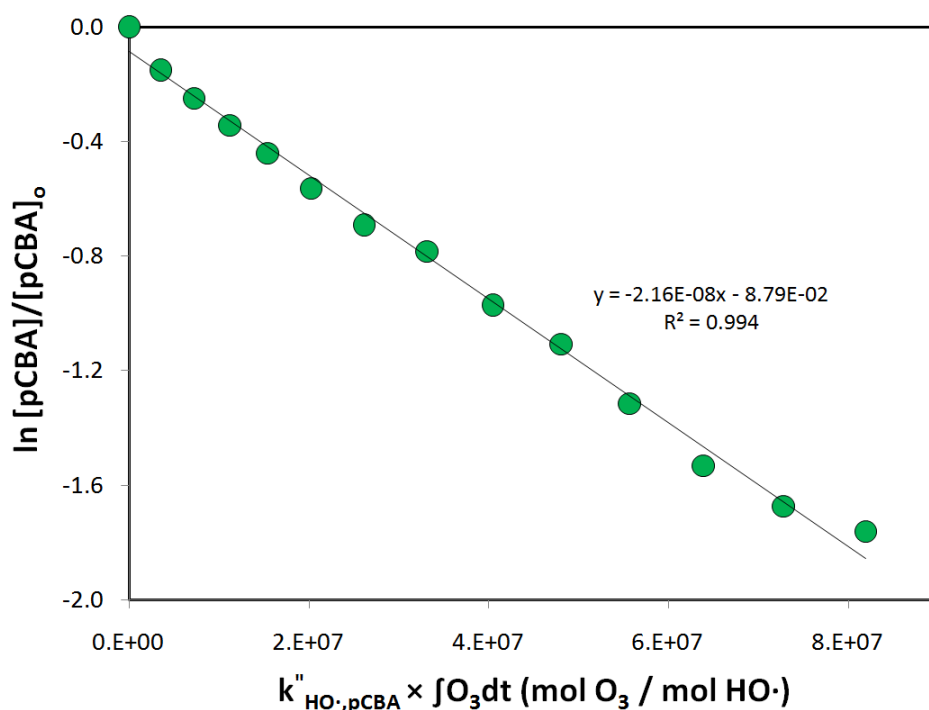


Figure 3-21. Determination of R_{ct} using the relationship described in Eq. 3-11. (The slope of the data corresponds to the R_{ct} for this particular experiment. The data in this figure correspond to a solution containing 100 mg/L NaCl, 200 mg/L $NaHCO_3$, 10 μM *p*CBA, 100 $\mu g/L$ cyclophosphamide, and 100 $\mu g/L$ ifosfamide at pH 8.3.)

In batch ozonation tests (*i.e.*, experiments with one dose of ozone stock solution at time, $t = 0$), most real waters demonstrate an R_{ct} in the range of 4.9×10^{-7} to 7.0×10^{-10} mol $HO\cdot$ / mol O_3 (Elovitz *et al.*, 2000). In synthetic matrices containing acetate, *t*-BuOH, carbonate, and phosphate buffer (pH 8.0), Elovitz and von Gunten (Elovitz and von Gunten, 1999) found R_{ct} values on the order of 1.4×10^{-10} mol $HO\cdot$ / mol O_3 . While the value found in Figure 3-21 is on the higher end of the range observed by Elovitz *et al.* (2000), the water matrix is relatively clean, which means that fewer hydroxyl radical scavengers are present in solution. With fewer hydroxyl radical scavengers in solution, hydroxyl radical exposure and R_{ct} will both be higher. Thus, it appears that continuous aqueous ozone addition scenarios yield R_{ct} values that are consistent with those observed in batch ozone experiments.

The ozone and hydroxyl radical exposures for this scenario are shown in Figure 3-22. Unlike the *t*-BuOH experiments (Figure 3-20) where hydroxyl radicals are scavenged, the *p*CBA experiment does exhibit hydroxyl radical exposure (Figure 3-22). Furthermore, the *p*CBA experiment also demonstrates significant ozone exposure (Figure 3-22). For that reason, it is clear that PhACs can interact with both ozone and hydroxyl radicals (Eq. 3-5), and both terms must be incorporated into the rate expression. Integration of the overall rate expression for PhAC degradation (Eq. 3-5) with respect to time, and substitution of Eq. 3-12 yields Eq. 3-13.

$$\ln \frac{[PhAC]}{[PhAC]_o} = - \left(k_{app,O_3,PhAC}'' + k_{app,HO\cdot,PhAC}'' \times R_{ct} \right) \int_0^t [O_3] dt \quad \text{Eq. 3-13}$$

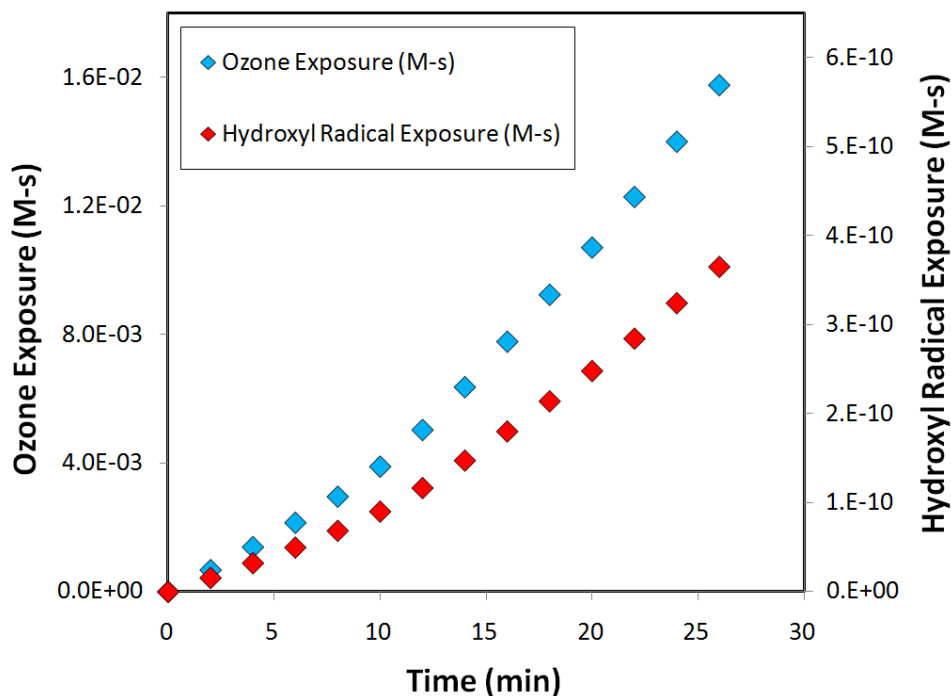


Figure 3-22. Ozone and hydroxyl radical exposure throughout an experiment employing 10 μ M *p*CBA. (The magnitudes of ozone and hydroxyl radical exposure are sufficient for transformation of ifosfamide according to both mechanisms. The data in this figure correspond to the same experiment described by Figure 3-21.)

The slope of a plot of $\ln [\text{PhAC}]/[\text{PhAC}]_0$ vs. ozone exposure is represented by Eq. 3-14.

$$\text{slope} = -\left(k_{app,O_3,PhAC}'' + k_{app,HO\cdot,PhAC}'' \times R_{ct}\right) \quad \text{Eq. 3-14}$$

The second-order rate constant for PhAC transformation with ozone was determined using Eq. 3-8 and R_{ct} was calculated from Eq. 3-11; therefore, Eq. 3-14 can be solved for the second-order rate constant for the PhAC with hydroxyl radicals. Example plots of Eq. 3-13 for cyclophosphamide and ifosfamide are shown in Figure 3-23. In this case, the slope (Eq. 3-14) is equal to $121 \text{ M}^{-1}\text{s}^{-1}$.

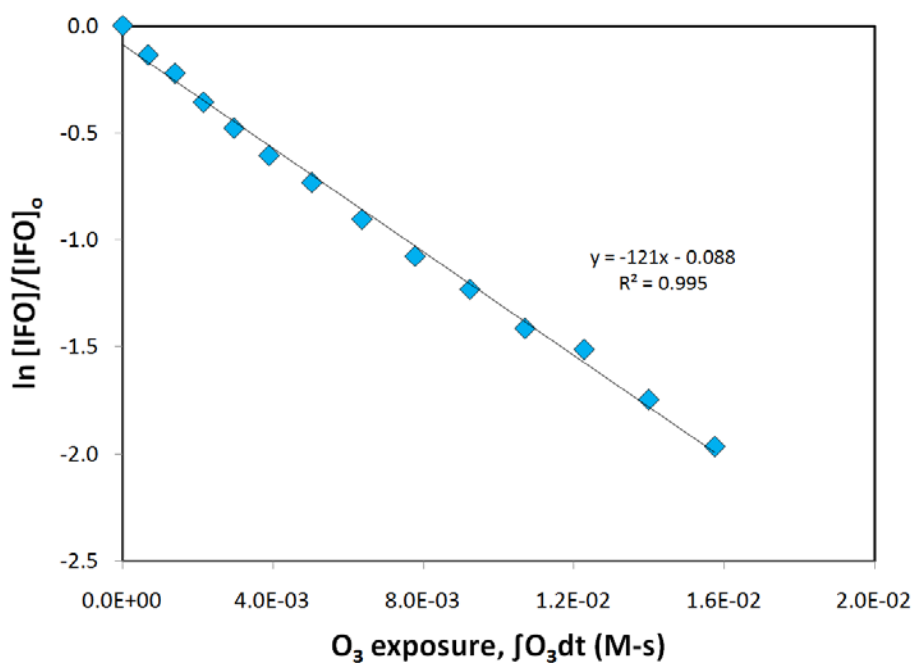


Figure 3-23. Determination of the second-order rate constant for hydroxyl radical reaction with ifosfamide. (The slope was used to solve for the second-order rate constant of ifosfamide PhAC with hydroxyl radicals (Eq. 3-14). The data in this figure correspond to the same experimental conditions described in Figure 3-21 and Figure 3-22.)

In the continuous peroxone reactor, the rate constant for PhAC transformation by hydroxyl radicals was determined using only the experiment with *p*CBA because

hydroxyl radicals are the dominant oxidant present in the system. Indeed, as shown in Figure 3-19a, the aqueous ozone concentration in continuous peroxone experiments was negligible; therefore, the ozone component of Eq. 3-5 goes to zero. Then, transformation of PhACs can be described by Eq. 3-15.

$$\frac{d[PhAC]}{dt} = k_{app,HO\cdot,PhAC}'' [HO\cdot][PhAC] \quad \text{Eq. 3-15}$$

Integration of Eq. 3-15 with respect to time yields Eq. 3-16.

$$\ln \frac{[PhAC]}{[PhAC]_0} = -k_{app,HO\cdot,PhAC}'' \int_0^t [HO\cdot] dt \quad \text{Eq. 3-16}$$

The change in *p*CBA concentration can be used to obtain the hydroxyl radical exposure; therefore, the change in *p*CBA concentration and the rate constant for *p*CBA reaction with hydroxyl radicals can be substituted into Eq. 3-16 to yield Eq. 3-17.

$$\ln \frac{[PhAC]}{[PhAC]_0} = \frac{k_{app,HO\cdot,PhAC}''}{k_{app,HO\cdot,pCBA}''} \times \ln \frac{[pCBA]}{[pCBA]_0} \quad \text{Eq. 3-17}$$

Eq. 3-17 is a competition kinetics model that relates the hydroxyl radical exposure found through manipulation of the $[pCBA]$ data with the hydroxyl radical exposure determined from the $[PhAC]$ data. An example of the use of Eq. 3-17 to determine the second order rate constant for ifosfamide reaction with hydroxyl radicals is shown in Figure 3-24. In this case, the second-order rate constant for ifosfamide transformation by hydroxyl radicals (with 95% confidence intervals) is $2.73(\pm 0.16) \times 10^9 \text{ M}^{-1} \text{ s}^{-1}$.

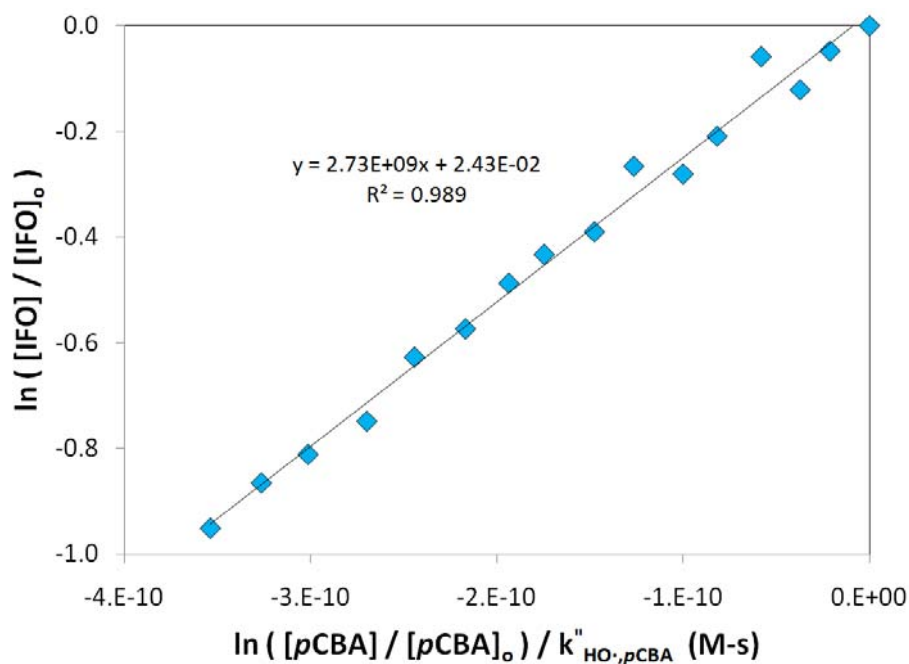


Figure 3-24. Ifosfamide transformation in the peroxone system as described by Eq. 3-17. (The slope of the plot represents the second order rate constant for ifosfamide reaction with hydroxyl radicals. The data correspond to an experiment run at a molar ratio of 0.88 mol H_2O_2 / mol O_3 ; the reactor solution contained 100 mg/L NaCl, 200 mg/L $NaHCO_3$, 100 μ g/L ifosfamide, and 10 μ M pCBA at pH 8.3.)

As shown in Chapter 6, a competition kinetics model (Dodd *et al.*, 2006) is used to determine the kinetics of an erythromycin degradation product, anhydroerythromycin A, with ozone. In that situation, the hydroxyl radical exposure is negligible; therefore, the known rate constant for erythromycin transformation by ozone, the ozone exposure calculated from erythromycin data, and the ozone exposure from anhydroerythromycin data were used to calculate the rate constant for anhydroerythromycin reaction with ozone. This relationship (Eq. 3-18) is similar to that shown in Eq. 3-17. In Eq. 3-18, a general form of this equation is shown.

$$\ln \frac{[PhAC_{unknown}]}{[PhAC_{unknown}]_o} = \frac{k''_{app, O3, PhAC_{unknown}}}{k''_{app, O3, PhAC_{known}}} \times \ln \frac{[PhAC_{known}]}{[PhAC_{known}]_o} \quad \text{Eq. 3-18}$$

ANTI-MICROBIAL SUSCEPTIBILITY ASSAY

To determine the antimicrobial activity of the pharmaceuticals of concern and the residual antimicrobial activity throughout treatment, the Clinical Laboratory Standards Institute (CLSI) standard, *Methods for Dilution Antimicrobial Susceptibility Tests for Bacteria That Grow Aerobically* (NCCLS, 2004), was employed. This assay was developed to test the ability of antimicrobial pharmaceuticals (*i.e.*, ciprofloxacin and erythromycin, in this case) to inhibit the growth of various microorganisms. A standard microorganism, *Escherichia coli* (ATCC #25922), was employed to describe the inhibition profile of individual pharmaceuticals and to determine how ozone treatment affects the residual antimicrobial activity of a water containing the PhACs of concern, PhAC intermediate oxidation products, and other compounds, including background electrolytes and NOM, among others. The protocol for using the antimicrobial activity assay is described below, and more detail on the data analysis is presented in Appendix C. All glassware, disposables, and solutions employed in antimicrobial activity studies were sterilized using the autoclave protocol available in Appendix A.

E. coli was purchased from the American Type Culture Collection (ATCC). Upon arrival, a small aliquot of the *E. coli* stock was scraped into 10-mL of Mueller-Hinton Broth (MHB). The suspension was incubated in an ambient air environment at 37°C for 48 hours. After the incubation time, the *E. coli* suspension was quite dense. Using a sterile inoculation loop, a streak plate was made on Trypticase Soy Agar. One distinct colony forming unit was selected and mixed into a solution of 10-mL MHB. That suspension was incubated for three days at 37°C in ambient air. The resulting *E. coli* suspension was mixed 1:1 with a 50% glycerol solution; aliquots of 1-mL were placed into 5 separate sterile cryotubes. These *E. coli* stock suspensions were then placed into a dark, -80°C freezer for storage.

Every month, an *E. coli* working solution was generated by scraping a small amount of frozen (-80°C) *E. coli* suspension into 10-mL of Mueller-Hinton broth (MHB)

and incubating the mixture in ambient air at 37°C overnight (12-18 hours). Throughout the month, the *E. coli* working solution was split 1:10 at least every three days. The purity of the *E. coli* working solutions were confirmed throughout the month by comparing the inhibition profiles of ciprofloxacin/erythromycin standards.

The inoculum for antimicrobial activity assays was prepared by diluting the *E. coli* working solution with sterile MHB to obtain the same absorbance at 625 nm as a BaSO₄ turbidity standard equivalent to a 0.5 McFarland standard. The BaSO₄ standard was produced by mixing 0.5-mL of a 0.048 M BaCl solution with 99.5-mL of 0.36 N H₂SO₄ (NCCLS, 2004). The antimicrobial susceptibility assays were run in 96-well microplates. Assays were run according to two different protocols, as described below.

Inhibition Profile Protocol. Wells were partially filled with 100 µL of either a standard containing a known concentration of an antimicrobial PhAC in the background matrix of choice or a sample from experimentation; then, 100 µL of the *E. coli* inoculum was added to the well. Positive growth controls consisted of 100 µL of the background matrix without the drug and 100 µL of inoculum; negative growth controls were made up of 100 µL of the background matrix and 100 µL of MHB. Triplicate analyses were run for all standards, samples, and controls.

Potency Equivalent Protocol. In the first row (“A”) of the microplate, the wells (A2-A11) are filled with 250 µL of either a standard containing a known concentration of an antimicrobial PhAC in the background matrix of choice or a sample from experimentation. All other wells (*i.e.*, rows “B” through “H”) are filled with 100 µL of sterile DI water. Each sample/standard from row “A” is serially diluted into the subsequent rows. In most cases, a dilution factor of 0.6 was used, *i.e.*, the concentration in row “B” was 60% of the concentration in row “A.” Therefore, 150 µL of the sample/standard in row “A” was added to the 100 µL in row “B.” Next, 150 µL of the solution now in row “B” was added to the 100 µL in row “C,” and so on. After all

samples/standards are serially diluted, 100 μ L of the *E. coli* inoculum is added to each well. The resultant wells contain 100 μ L of the sample/standard and 100 μ L of the *E. coli* inoculum. Columns 1 and 12 contained positive and negative growth controls, respectively.

After each plate was prepared, microplates were covered in Parafilm to prevent evaporative water loss and incubated in ambient air at 37°C for 20 hours. After the 20 hour incubation period, plates were read on a microplate reader (BioTek) at 600 nm. No condensation was observable on the Parafilm covers. This wavelength is routinely used to correlate absorbance with microbial growth (or optical density). Therefore, low absorbance values correspond to high inhibition, whereas high absorbance values indicate *E. coli* growth and, therefore, low inhibition. The percent inhibition can be calculated from the absorbance at 600 nm ($ABS_{600\text{ nm}}$) according to Equation 3-19.

$$\% \text{ Inhibition} = \left(1 - \frac{ABS_{600\text{-nm},\text{sample}} - ABS_{600\text{-nm},\text{negative}}}{ABS_{600\text{-nm},\text{positive}} - ABS_{600\text{-nm},\text{negative}}} \right) \times 100\% \quad \text{Eq. 3-19}$$

After calculation of the percent inhibition, GraphPad Prism (GraphPad Software, Inc.) was used to fit the data to the Hill curve. This software was used to determine the half maximal inhibitory concentration (IC_{50}) and the Hill slope, H , and also to calculate 95% confidence intervals on the resultant Hill curve. When the inhibition profile protocol was employed, all data were modeled together in GraphPad Prism, that is, one curve was fit to each set of samples or standards. With the potency equivalents method, “inhibition profiles” were generated for each set of serial dilutions by plotting the percent inhibition against $\text{LOG}(C_{\text{PhAC},i}/C_{\text{PhAC},o})$, where $C_{\text{PhAC},i}$ and $C_{\text{PhAC},o}$ are the PhAC concentration in the “i”th dilution and the PhAC concentration in the original sample/standard. The equivalent of IC_{50} (*i.e.*, the value of $\text{LOG}(C_{\text{PhAC},i}/C_{\text{PhAC},o})$ that corresponds to 50% inhibition) for these curves was calculated by GraphPad Prism.

Using those values, the potency equivalents (PEQ) were calculated according to Equation 3-20 (Suarez *et al.*, 2007; Dodd *et al.*, 2009; Paul *et al.*, 2010).

$$PEQ = \frac{\left(\frac{C_i}{C_o} \right)_{50,o}}{\left(\frac{C_i}{C_o} \right)_{50,x}} \quad \text{Eq. 3-20}$$

In Eq. 3-20, the numerator refers to the antilog of the value of $\text{LOG}(C_{\text{PhAC},i}/C_{\text{PhAC},o})$ that corresponds to 50% inhibition for the serial diluted data derived from the initial (highest concentration) sample; the term in the denominator corresponds to the same value for treated samples or standards at concentrations lower than the initial sample.

Potency equivalents are a tool designed to provide quantitative measurement of antimicrobial activity at drug concentrations that demonstrate high inhibition. With solutions containing only standards, every step down in concentration results in an equivalent drop in potency equivalents. While more details are presented in Appendix C, a graphical description of these different data analysis mechanisms is shown in Figure 3-25. Figure 3-25a presents the inhibition profile of ciprofloxacin against *E. coli* ATCC 25922. In Figure 3-25b, the “inhibition profile”s of ten individual samples (containing erythromycin) introduced to the potency equivalent protocol for measurement of antimicrobial activity are shown.

These tools allow for effective description of the residual antimicrobial activity throughout water treatment; by plotting percent inhibition and parent compound concentration against treatment dose or time, the relationship between parent compound concentration and antimicrobial activity can be determined. Furthermore, the impact of intermediate oxidation products and/or advanced oxidation byproducts can be assessed by comparing the standard inhibition profile with that of the treated samples. The potency equivalents protocol allows for greater elucidation of the impact of early (*i.e.*, the first

products formed by ozone/hydroxyl radical attack on the parent compound) intermediate oxidation products on residual antimicrobial activity.

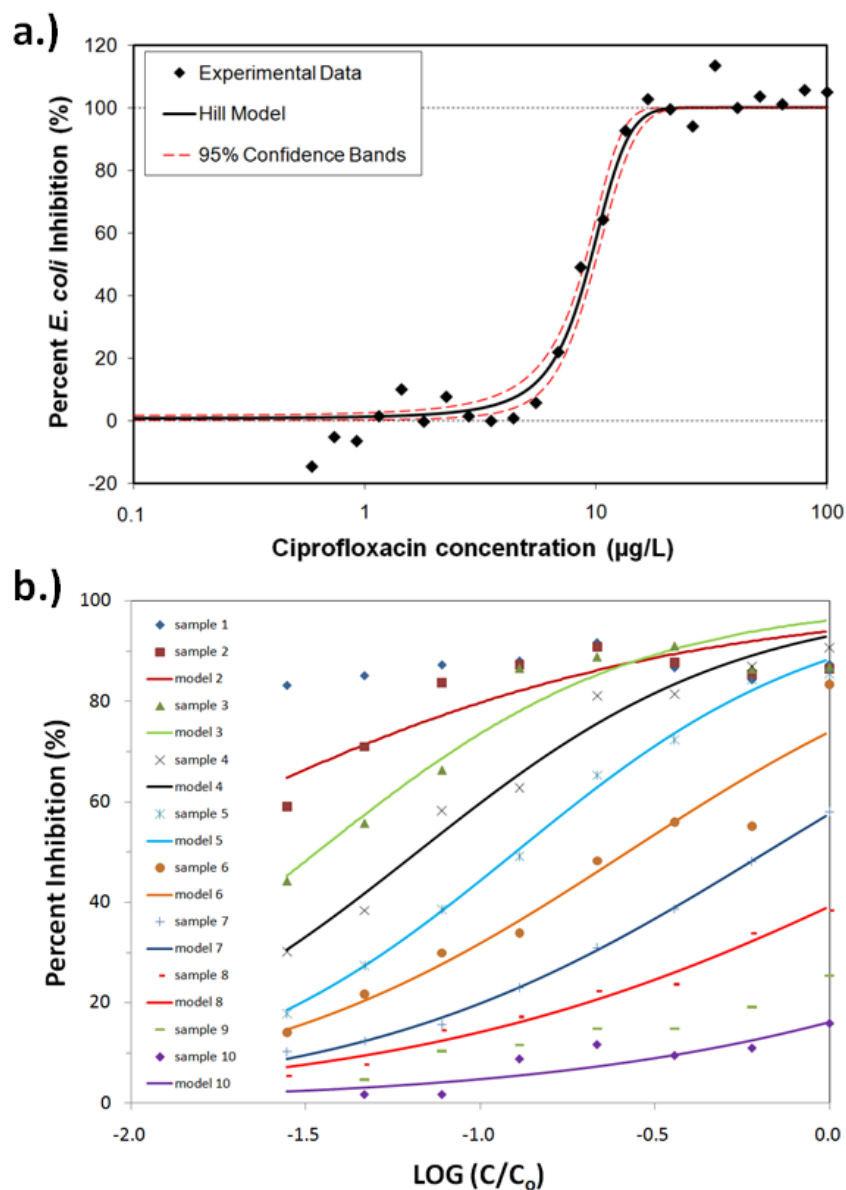


Figure 3-25. Representative data and model fits (solid lines) collected from (a) the inhibition profile protocol (with ciprofloxacin) and (b) the potency equivalents protocol (with erythromycin) for running the antimicrobial activity assay.

Both protocols have advantages. In the inhibition profile protocol, the change in antimicrobial activity throughout treatment can be easily conveyed; as treatment occurs, the PhAC concentration decreases and the residual antimicrobial activity is eliminated. Furthermore, by plotting the antimicrobial activity of treated samples, the contributions of intermediate oxidation products to the residual antimicrobial activity can be identified. In the serial dilution protocol, deviations from the 1:1 relationship of potency equivalents with the normalized PhAC concentration suggest positive or negative contributions of intermediate products with respect to residual pharmacological activity. This protocol is especially relevant at high PhAC concentrations (*e.g.*, ones that demonstrate >90% inhibition) because it allows quantitative analysis of the residual antimicrobial activity. Regardless, for some compounds, the antimicrobial activity stemming from the presence of intermediate oxidation products may be masked in the serial dilution scheme. Substantial discussion regarding the employment of these two techniques for measurement of antimicrobial activity is provided in Chapters 5-6 within the context of ciprofloxacin and erythromycin treatment.

CHAPTER 4: OZONATION OF CYCLOPHOSPHAMIDE AND IFOSFAMIDE: DETERMINATION OF RATE CONSTANTS, IMPACT OF ORGANIC MATTER, AND IDENTIFICATION OF MAJOR INTERMEDIATE PRODUCTS

ABSTRACT

A novel continuous aqueous ozone addition reactor was employed to determine the rate constants for the transformation of two environmentally-relevant chemotherapy agents, cyclophosphamide and ifosfamide, by ozone and hydroxyl radicals. The rate constants for cyclophosphamide and ifosfamide transformation with ozone were determined to be $3.23(\pm 0.71) \text{ M}^{-1}\text{s}^{-1}$ and $6.84 (\pm 0.37) \text{ M}^{-1}\text{s}^{-1}$, respectively. The second-order rate constants for cyclophosphamide and ifosfamide transformation by hydroxyl radicals were found to be $2.69(\pm 0.17) \times 10^9 \text{ M}^{-1}\text{s}^{-1}$ and $2.73(\pm 0.16) \times 10^9 \text{ M}^{-1}\text{s}^{-1}$, respectively; these rate constants were verified using a continuous peroxone addition reactor. Batch ozone experiments demonstrated that NOM can significantly decrease hydroxyl radical exposure, and thereby, decrease transformation of cyclophosphamide and ifosfamide. Overlap in m/z values of intermediate oxidation products was observed for the two chemotherapy agents, which are structural isomers. The 4-keto-, 4-hydroxy-, and imino- derivatives of the parent compounds were the most dominant intermediate oxidation products in the applied ozone dose range employed in this research. Furthermore, the active metabolites of cyclophosphamide and ifosfamide (phosphoramidate mustard and isophosphoramidate mustard, respectively) were also detected in treated samples. The presence of the active metabolites suggests that treated solutions could retain some residual pharmacological activity.

Key words: cyclophosphamide, ifosfamide, ozone, pharmacologically active compounds, reaction kinetics, intermediate oxidation products

Manuscript to be submitted to *Water Research*

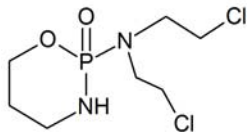
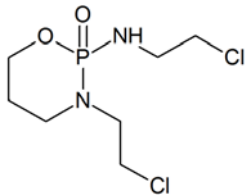
INTRODUCTION

Recently, several authors have reported a wide range of pharmacologically active compounds (PhACs) in wastewater streams, surface waters, and treated drinking water (Ternes, 1998; Kolpin *et al.*, 2002; Kim *et al.*, 2007). The list of PhACs detected in these water supplies includes compounds from many different pharmaceutical classes, including antibiotics, anti-microbials, anti-inflammatories, chemotherapy agents, and anti-depressants, among others. Several authors (Kummerer *et al.*, 1997; Steger-Hartmann *et al.*, 1997; Buerge *et al.*, 2006; Johnson *et al.*, 2007; Chen *et al.*, 2008) have indicated concern for chemotherapy agent presence in the environment because of the tendency for such chemicals to exhibit toxic effects. This paper concentrates on ozone-based treatment processes for removing two chemotherapy agents, cyclophosphamide and ifosfamide, from water.

Cyclophosphamide and ifosfamide are structural isomers as shown in Table 4-1. These compounds are prodrugs, meaning that cyclophosphamide and ifosfamide, themselves, are inactive; the compounds are converted into their active forms during metabolism. First, the two compounds are converted to 4-hydroxycyclophosphamide and 4-hydroxyifosfamide, respectively, which are also prodrugs (Low *et al.*, 1983). The 4-hydroxy derivatives are further metabolized to the reactive mustards, phosphoramidate mustard (cyclophosphamide) and isophosphoramidate mustard (ifosfamide), respectively, and acrolein (Low *et al.*, 1983). The reactive mustards are cytotoxic and work by alkylating DNA, prohibiting separation of DNA strands during replication (Fleming, 1997). No research into whether treatment processes or environmental degradation pathways lead to the active compounds formed through metabolism has yet been performed; furthermore, the excretion of metabolic products is not typically reported. As the parent compounds are not pharmacologically active, characterization of intermediate oxidation products and comparison of those compounds to metabolic products warrants study.

In addition to being cytotoxic, cyclophosphamide and ifosfamide are teratogenic, mutagenic, and carcinogenic (Bus *et al.*, 1973; Murthy *et al.*, 1973; Mohn and Ellenberger, 1976). The concentrations associated with cyclophosphamide and ifosfamide toxicity are organism-dependent. Currently, the contribution of trace concentrations of cyclophosphamide and ifosfamide to the ultimate ecotoxicological activity of a water are unknown; however, some researchers (Pomati *et al.*, 2006; Pomati *et al.*, 2007; Pomati *et al.*, 2008) have investigated the impact of environmentally-relevant concentrations of a suite of 11 pharmaceuticals, including cyclophosphamide, on inhibition of *E. coli*, ovarian cancer cells (OVCAR3), human embryonic kidney cells (HEK-293), and zebrafish liver cells. Pomati *et al.* (2006) found that HEK-293 proliferation can be inhibited by up to 30% in the presence of trace concentrations of pharmaceuticals. Nevertheless, the ecotoxicological impact of trace concentrations of cyclophosphamide and ifosfamide is not yet fully understood.

Table 4-1. Properties of ifosfamide and cyclophosphamide.

Property	Cyclophosphamide	Ifosfamide
Molecular Formula	C ₇ H ₁₅ Cl ₂ N ₂ O ₂ P	C ₇ H ₁₅ Cl ₂ N ₂ O ₂ P
Molecular Weight (g/mol)	261.1	261.1
Molecular Structure		
log K _{ow}	0.63	0.86
pK _a	2.84-6.5 *	1.45-4.0 **
CAS number	50-18-0	3778-73-2

* Mahoney *et al.*, 2003; Sottani *et al.*, 2008; Wang *et al.*, 2009

** Mahoney *et al.*, 2003; Sottani *et al.*, 2008

The log K_{ow} for cyclophosphamide and ifosfamide are 0.63 and 0.86 (Hansch *et al.*, 1995), respectively; hence, these compounds can be expected to pass through traditional wastewater treatment processes without being adsorbed onto particles or

microorganisms. Steger-Hartmann *et al.* (1997) found that cyclophosphamide is poorly removed in sewage treatment plants (STPs); additionally, Kiffmeyer *et al.* (1998) concluded that cyclophosphamide is not biodegradable. Unsurprisingly, cyclophosphamide and ifosfamide have been detected in various water sources over the past 15 years. Ifosfamide (5-338 ng/L) and cyclophosphamide (2-21 ng/L) have been detected in hospital wastewater (Steger-Hartmann *et al.*, 1997; Thomas *et al.*, 2007). Cyclophosphamide and ifosfamide have also been detected at concentrations of 1-143 ng/L in STPs (Steger-Hartmann *et al.*, 1997; Metcalfe *et al.*, 2003; Zuccato *et al.*, 2005; Buerge *et al.*, 2006; Thomas *et al.*, 2007). Significant concentrations of these two compounds have been detected in landfill leachate: 97-192 ng/L for cyclophosphamide and 32-42 ng/L for ifosfamide (Jjemba, 2008).

Ozonation has proven an effective treatment process for removal of PhACs (Huber *et al.*, 2003; Ternes *et al.*, 2003; von Gunten, 2003; Westerhoff *et al.*, 2005). Several authors have investigated ozone treatment of cyclophosphamide and ifosfamide in various water sources (McDowell *et al.*, 2005; Venta *et al.*, 2005; Chen *et al.*, 2008; Garcia-Ac *et al.*, 2010). Venta *et al.* (2005) investigated cyclophosphamide degradation in a gaseous ozonation reactor; the authors reported the pseudo-first order rate constant for cyclophosphamide degradation in the peroxone process (the molar ratio of $\text{H}_2\text{O}_2/\text{O}_3$ was varied from 0.15 to 0.39) system and identified 4-ketocyclophosphamide as an intermediate oxidation product; detection of the reactive mustards was not reported. Garcia-Ac *et al.* (2010) determined the second-order rate constant for cyclophosphamide reaction with ozone in ultrapure water to be $k''_{\text{O}_3,\text{CYP}} = 3.3 \text{ M}^{-1}\text{s}^{-1}$; in contrast, Chen *et al.* (2008) determined the second-order rate constant for cyclophosphamide transformation by ozone to be nearly two orders of magnitude greater ($k''_{\text{O}_3,\text{CYP}} = 143 \text{ M}^{-1}\text{s}^{-1}$) than that determined by Garcia-Ac *et al.* (2010). In both of these studies, highly concentrated aqueous ozone was injected into a batch solution containing cyclophosphamide; samples were taken over time and analyzed for ozone and cyclophosphamide concentrations. Both papers report similar values for the second-order rate constant for

cyclophosphamide transformation by hydroxyl radicals: $2.0 \times 10^9 \text{ M}^{-1}\text{s}^{-1}$ (Garcia-Ac *et al.*, 2010) and $2.1 \times 10^9 \text{ M}^{-1}\text{s}^{-1}$ (Chen *et al.*, 2008). The work of McDowell *et al.* (2005) demonstrates removal of cyclophosphamide and ifosfamide as a function of applied ozone dose. Of the nine compounds investigated by these investigators, cyclophosphamide and ifosfamide exhibited the lowest percent transformation for all applied ozone doses. The transformation kinetics of ifosfamide with ozone and hydroxyl radicals has not previously been reported.

In this paper, we report on the use of a novel continuous liquid ozone addition reactor to determine the kinetics of cyclophosphamide and ifosfamide transformation through reactions with ozone (O_3) and hydroxyl radicals ($\text{HO}\cdot$). This method for determining kinetics is especially relevant for compounds that react slowly with ozone, because ozone concentrations can be effectively controlled without the limitations incurred by ozone decay or the complications associated with modeling of aqueous ozone concentrations. In addition, the impact of natural organic matter (NOM) on the transformation of cyclophosphamide and ifosfamide at specific applied ozone doses was investigated. Finally, we provide initial characterization of major intermediate oxidation products produced during ozone and hydroxyl radical oxidation of cyclophosphamide and ifosfamide. The value of studying both of these closely related compounds was to determine how the placement of the two chloroethyl functional groups affects both the transformation kinetics with ozone and hydroxyl radicals and the structures of the resultant intermediate oxidation products.

MATERIALS AND METHODS

Chemicals and stock solutions. Cyclophosphamide monohydrate and ifosfamide were purchased through VWR from MP Biomedicals (Solon, OH) and US Pharmacopeia (Rockville, MD), respectively. Stock solutions of cyclophosphamide (CYP) and ifosfamide (IFO) were prepared at 1 mg/mL in deionized water and stored in amber bottles in the dark at 4°C. *para*-chlorobenzoic acid (*p*CBA) stock solutions (100 μM)

were made in deionized water and stored in the dark at 4°C. LC-MS grade methanol and water were employed in LC-MS and LC-MS/MS analysis of cyclophosphamide and ifosfamide. HPLC grade methanol was employed in HPLC-UV analysis of *p*CBA. NOM was isolated from Lake Austin (Austin, TX) using the procedures described by Aiken *et al.* (1992). The hydrophobic organic acids (HPOA) fraction of Lake Austin NOM was isolated using XAD-8 resin. Lake Austin HPOA was chosen as a representative NOM source; furthermore, because the Lake Austin HPOA was available in extract form, the DOC concentration could be controlled. A stock solution of hydrogen peroxide was made from 30% H₂O₂; the H₂O₂ stock solution (0.105 M H₂O₂) was placed in an amber bottle and stored in the dark at 4°C.

Ozone reactor setup. A schematic of the ozone supply system and reactor is shown in Figure 4-1a. Oxygen gas flowed into the ozone generator at 30 cm³/min; a fraction of that oxygen was converted to ozone. This combined gas stream was directed into a gas-washing bottle, which served as a stock ozone solution. The ozone stock solution was maintained on ice ($T_{\text{solution}} \sim 0.5^{\circ}\text{C}$) to increase the solubility of ozone. After 4-6 hours, the ozone concentration in the stock solution reached a plateau at 50-60 mg O₃/L. In this research, the ozone stock solution was employed in three different ozone reactors: continuous aqueous ozone addition, continuous peroxone addition, and batch ozone experiments. The continuous aqueous ozone addition experiments were used to calculate the rate constants for cyclophosphamide and ifosfamide transformation by ozone and hydroxyl radicals; the rate constants for cyclophosphamide and ifosfamide transformation with hydroxyl radicals were verified using the continuous peroxone addition reactor. The batch ozone experiments were utilized to (1) describe the impact of NOM on cyclophosphamide and ifosfamide transformation and (2) characterize the intermediate oxidation products of cyclophosphamide and ifosfamide transformation for specific ozone doses.

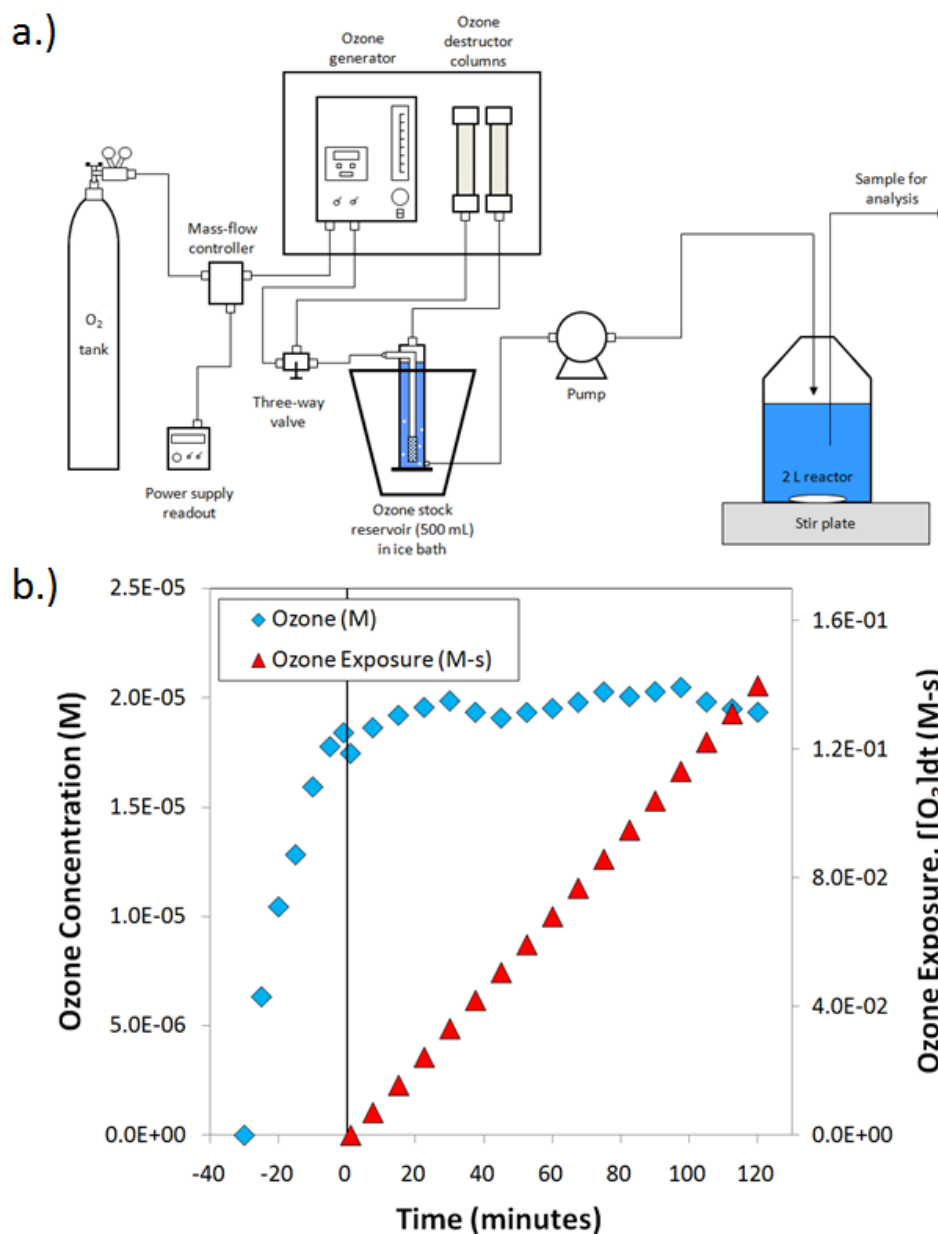


Figure 4-1. (a) Schematic of the continuous liquid ozone addition reactor; (b) Behavior of ozone concentrations and ozone exposure throughout a continuous ozone addition experiment. (In (b), the solution is composed of 1.71×10^{-3} M NaCl, 2.38×10^{-3} M NaHCO₃, and 10^{-2} M *t*-BuOH at pH 6.3. At time equal to zero, 3.83×10^{-7} M cyclophosphamide and 3.83×10^{-7} M ifosfamide were dosed into solution.)

Continuous ozone addition experiments. The ozone stock solution was pumped into the 2-L reactor for 30 minutes; the aqueous ozone concentration in the 2-L reactor was controlled by adjusting the pumping rate from the stock reservoir. After 30 minutes of pre-ozonation, a small volume of solution (400 μL) containing cyclophosphamide (1.92×10^{-3} M) and ifosfamide (1.92×10^{-3} M) was dosed into the 2-L reactor to achieve concentrations of 3.83×10^{-7} M of cyclophosphamide and 3.83×10^{-7} M of ifosfamide. Samples were taken at regular time intervals and analyzed for ozone, cyclophosphamide, and ifosfamide concentrations, as described below. An example of ozone concentrations and ozone exposure ($\int [\text{O}_3] dt$) throughout a typical experiment is shown in Figure 4-1b. Clearly, the ozone exposure in the continuous liquid addition reactor increases in a linear fashion throughout experimentation. In contrast, for a batch ozonation experiment aimed at determining the kinetics for compounds that react slowly with ozone ($k''_{\text{app}, \text{O}_3, \text{PhAC}} < 10^2 \text{ M}^{-1} \text{ s}^{-1}$), the ozone exposure approaches an asymptote as the aqueous ozone concentration decreases to zero. The continuous ozone reactor provides a unique advantage over more traditional methods for determining the kinetics of compounds that react slowly with ozone because the ozone concentration in the reactor is controllable and non-zero for an extended time. Nevertheless, batch kinetics experiments are useful for determining the transformation kinetics of compounds that react quickly with ozone (Marron, 2010; Huang, 2011). Batch experiments are also useful for determining removal efficiency as a function of applied ozone dose (transformation as a function of the molar ratio of applied ozone to the initial PhAC concentration) as indicated below.

Continuous peroxone addition experiments. A stock hydrogen peroxide solution was also employed in the continuous peroxone addition experiments. The molar ratio of hydrogen peroxide to ozone was essentially controlled by the pumping rates of the ozone stock solution (Q_{O_3}) and the hydrogen peroxide stock solution ($Q_{\text{H}_2\text{O}_2}$), since the ozone and hydrogen peroxide concentrations are measured. Then, using Eq. 4-1, the molar ratio of applied H_2O_2 to O_3 is calculated.

$$\frac{H_2O_2}{O_3} \text{ (mol/mol)} = \frac{[H_2O_2]_{stock} \times Q_{H_2O_2}}{[O_3]_{stock} \times Q_{O_3}} \quad \text{Eq. 4-1}$$

Batch ozone experiments. Small aliquots of ozone stock solution were added to culture tubes containing a small volume (2-7 mL) of solutions containing cyclophosphamide and/or ifosfamide in the background matrix of choice. After ozone addition, samples were immediately shaken, capped, and placed in a dark environment for 24 hours before analysis to ensure that the applied ozone was completely exhausted. Samples were measured for residual ozone concentrations using the indigotrisulfonate method (APHA *et al.*, 2006); as expected, no samples demonstrated residual ozone after the reaction period. This type of experiment was used to determine the transformation of cyclophosphamide and ifosfamide in different NOM matrices and to generate intermediate oxidation products for LC-MS characterization. For experiments investigating the impact of organic matter on the transformation of cyclophosphamide and ifosfamide, the initial concentrations of cyclophosphamide and ifosfamide were 1.15×10^{-5} M; the applied ozone dose varied from 0 to 1.09×10^{-4} M. Experiments used to characterize intermediate oxidation products employed initial cyclophosphamide and ifosfamide concentrations of 3.83×10^{-4} M; ozone doses were calculated to achieve molar ratios of applied ozone to initial PhAC in the range of 0 to 7.5 mol/mol.

Analytical Procedures. Dissolved ozone concentrations of stock solutions were measured directly at 258 nm on a UV-VIS spectrophotometer (Agilent). Aqueous ozone concentrations in the 2-L continuous liquid ozone addition reactor were measured using the indigo blue method (Bader and Hoigné, 1981) and employing Indigo Reagent II (Standard Method 4500.B; APHA *et al.*, 2006). Hydrogen peroxide concentrations were measured using the potassium permanganate titration (Schumb *et al.*, 1955).

Cyclophosphamide and ifosfamide samples pertaining to kinetics and the impact of organic matter on percent transformation experiments were measured with LC-MS/MS

(Thermo Finnigan, TSQ Quantum). The injection volume was 10 μ L and the flow rate was 700 μ L/min. HPLC separation was achieved with a C₁₈ (Shimadzu 150 \times 4.6 mm; particle size, 5 μ m) column; the eluent gradient was 5% MeOH, 95% H₂O (0-3 min); ramp to 80% MeOH, 20% H₂O (3-10 min); 80% MeOH, 20% H₂O (10-12 min); ramp to 100% MeOH, 0% H₂O (12-12.1 min); 100% MeOH, 0% H₂O (12.1-16 min); ramp to 5% MeOH, 95% H₂O (16-16.1 min); 5% MeOH, 95% H₂O (16.1-18 min). The electrospray ionization tandem mass spectrometer was operated in positive ion mode. Method parameters include the following: parent mass, 261.0 mg; product mass, 139.8 mg (CYP) and 153.9 (IFO); collision gas pressure, 1.5 mTorr; collision energy, 20 V; spray voltage, 4000 V; vaporizer temperature, 400 $^{\circ}$ C; sheath gas pressure, 50 psi (CYP) and 30 psi (IFO); and auxiliary gas pressure, 30 psi (CYP) and 10 psi (IFO). Ifosfamide was eluted at 11.7 minutes; cyclophosphamide was eluted at 12.0 minutes.

Samples from the batch experiments employed for characterization of cyclophosphamide and ifosfamide intermediate oxidation products were analyzed using LC-MS; the measured m/z range was 30–1500. The injection volume was 20 μ L and the flow rate was 350 μ L/min. The eluent gradient was 5% MeOH, 95% H₂O (0-15 min); ramp to 80% MeOH, 20% H₂O (15-22 min); 80% MeOH, 20% H₂O (22-29 min); ramp to 100% MeOH, 0% H₂O (29-29.1 min); 100% MeOH, 0% H₂O (29.1-33 min); ramp to 5% MeOH, 95% H₂O (33-33.1 min); 5% MeOH, 95% H₂O (33.1-35 min). The electrospray ionization tandem mass spectrometer was operated in positive ion mode. Method parameters include the following: parent mass, 261.0 mg; collision gas pressure, 1.5 mTorr; collision energy, 20 V; spray voltage, 4000 V; vaporizer temperature, 400 $^{\circ}$ C; sheath gas pressure, 25 psi (CYP) and 15 psi (IFO); and auxiliary gas pressure, 15 psi (CYP) and 5 psi (IFO).

The hydroxyl radical probe compound, *p*CBA, was measured at 234 nm using an HPLC (Waters Corporation) with photo-diode array (PDA). HPLC separation was achieved with a C₁₈ column (Sonoma C18(2), 3 μ 100 Å). The eluent, 60% MeOH, 40%

25 mM H₃PO₄, was pumped at a constant flow rate (0.5 mL/min). *p*CBA was eluted after 5.35 minutes.

RESULTS

In this section, the results of the transformation kinetics experiments using the continuous aqueous ozone addition reactor are presented. The impact of NOM on the transformation of cyclophosphamide and ifosfamide achievable for a specific ozone dose and characterization of the intermediate oxidation products formed during ozonation of cyclophosphamide and ifosfamide are also discussed.

Kinetics

The continuous peroxone addition reactor was employed to determine the second-order rate constant for PhAC transformation with hydroxyl radicals. In this system, hydroxyl radicals are the dominant oxidant; therefore, the change in PhAC concentration with respect to time can be described by Eq. 4-2.

$$\frac{d[PhAC]}{dt} = -k''_{HO\cdot,app,PhAC} [HO\cdot][PhAC] \quad \text{Eq. 4-2}$$

$[PhAC]$ is the pharmaceutical concentration at time, t ; $k''_{HO\cdot,app,PhAC}$ is the second-order rate constant for PhAC transformation by hydroxyl radicals; and, $[HO\cdot]$ is the hydroxyl radical concentration at time, t . Integration of Eq. 4-2 with respect to time yields Eq. 4-3.

$$\ln \frac{[PhAC]}{[PhAC]_0} = -k''_{HO\cdot,app,PhAC} \int_0^t [HO\cdot] dt \quad \text{Eq. 4-3}$$

The term, $\int [HO\cdot] dt$, is called the hydroxyl radical exposure, and it can be calculated using data from transformation of the hydroxyl radical probe compound, *para*-chlorobenzoic acid (*p*CBA). The second-order rate constants for *p*CBA with ozone and hydroxyl radical are known from the literature: $k''_{O_3,pCBA} = 0.15 \text{ M}^{-1}\text{s}^{-1}$ (Yao and Haag, 1991) and

$k''_{HO\cdot,pCBA} = 5.2 \times 10^9 \text{ M}^{-1}\text{s}^{-1}$ (Buxton *et al.*, 1988). Because of the low reactivity with ozone, changes in $[pCBA]$ in a batch reactor (with respect to $pCBA$) are attributed solely to reaction with hydroxyl radicals. Then, the transformation of $pCBA$ with respect to time is similar to Eq. 4-3; thus, the hydroxyl radical exposure at any time, t , can be calculated as shown in Eq. 4-4.

$$\int_0^t [HO\cdot] dt = - \frac{\ln \frac{[pCBA]}{[pCBA]_0}}{k''_{HO\cdot,app,pCBA}} \quad \text{Eq. 4-4}$$

Using the hydroxyl radical exposure determined from the $pCBA$ transformation data with the PhAC transformation data allows calculation of the second-order rate constant for PhAC transformation by hydroxyl radicals.

Two separate solutions containing $1.71 \times 10^{-3} \text{ M NaCl}$, $2.38 \times 10^{-3} \text{ M NaHCO}_3$, $10^{-5} \text{ M } pCBA$, and $7.66 \times 10^{-7} \text{ M}$ of either cyclophosphamide or ifosfamide were created. The pH of both solutions was 8.2. The ozone concentration in the ozone stock solution was measured, and pumping rates were set for the O_3 and H_2O_2 systems. For both experiments, the H_2O_2 to O_3 molar ratio was set at 0.88. At time, $t = 0$, both pumps were started and measurements commenced, *i.e.*, pre-ozonation was not performed due to rapid hydroxyl radical decomposition. The results from these experiments can be seen in Figure 4-2. The slope of the data plotted in Figure 4-2 is equal to the second-order rate constant for PhAC transformation by hydroxyl radicals as demonstrated by Eq. 4-3. In this case, the second-order rate constants (with 95% confidence intervals) for cyclophosphamide and ifosfamide transformation by hydroxyl radicals were $2.69(\pm 0.17) \times 10^9 \text{ M}^{-1}\text{s}^{-1}$ and $2.73(\pm 0.16) \times 10^9 \text{ M}^{-1}\text{s}^{-1}$, respectively.

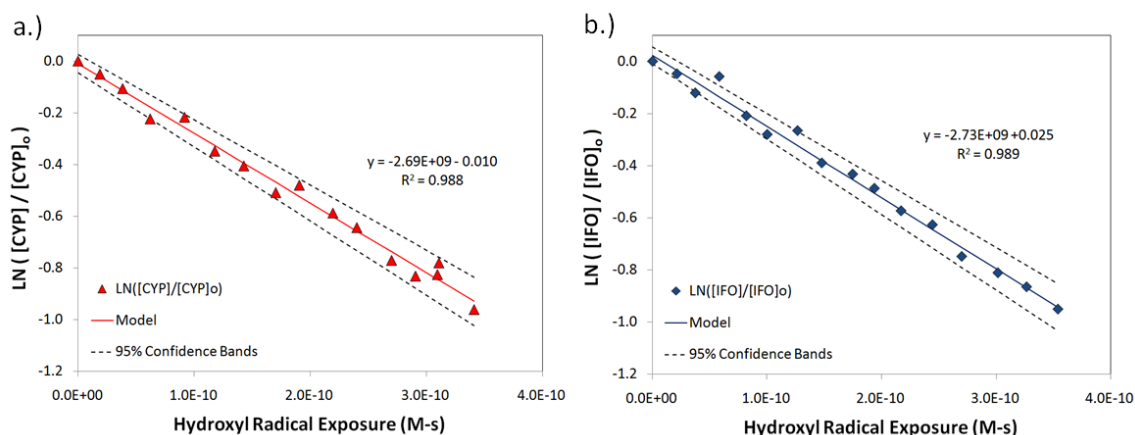
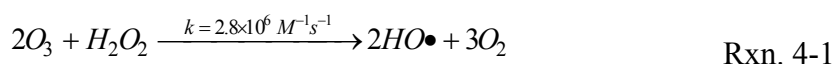


Figure 4-2. Determination of second order rate constant for hydroxyl radical reaction with cyclophosphamide (a) and ifosfamide (b) using the continuous addition peroxone reactor. (Dashed lines are 95% confidence bands.)

The aqueous ozone concentrations were found to be below the detection limit (8.0×10^{-8} mol/L using the indigo method with indigo reagent II) throughout these experiments. Given these observations, the maximal ozone exposure for the experiments shown in Figure 4-2 is approximately 1.44×10^{-4} M-s, which would only correspond to $\sim 0.1\%$ PhAC removal efficiency; clearly, the majority of the transformation, then, is due to PhAC transformation by hydroxyl radicals. These observations reflect the rapid reaction of ozone with hydrogen peroxide (Rxn. 4-1; Glaze and Kang, 1989; Alsheyab and Muñoz, 2006):



The rate constants for cyclophosphamide and ifosfamide transformation by ozone were found using the continuous liquid ozone addition reactor. The aqueous ozone concentration was built up, and then the PhACs were dosed into the reactor. To isolate PhAC reaction with ozone, 10 mM *t*-BuOH was added to the reactor solution. *t*-BuOH reacts slowly with ozone ($k_{O_3, t\text{-BuOH}} = 0.003 \text{ M}^{-1} \text{ s}^{-1}$; Hoigné and Bader, 1983a) but

quickly with hydroxyl radicals ($k''_{\text{HO}\cdot, t\text{-BuOH}} = 6 \times 10^8 \text{ M}^{-1}\text{s}^{-1}$; Buxton *et al.*, 1988). For this reason, *t*-BuOH does not affect the aqueous ozone exposure but, at sufficient concentration, will scavenge virtually all of the hydroxyl radicals in solution. At a concentration of 10mM *t*-BuOH, the molar ratio of *t*-BuOH to the total PhAC concentration ($3.83 \times 10^{-7} \text{ M}$) is over 26,000; for this molar ratio, *t*-BuOH will scavenge 99.998% of hydroxyl radicals in solution. Therefore, in these experiments, any changes in cyclophosphamide or ifosfamide concentration can be attributed to reaction with ozone, as described in Eq. 4-5. Integration of Eq. 4-5 with respect to time yields Eq. 4-6.

$$\frac{d[\text{PhAC}]}{dt} = -k''_{\text{O}_3, \text{app}, \text{PhAC}} [\text{O}_3][\text{PhAC}] \quad \text{Eq. 4-5}$$

$$\ln \frac{[\text{PhAC}]}{[\text{PhAC}]_0} = -k''_{\text{O}_3, \text{app}, \text{PhAC}} \int_0^t [\text{O}_3] dt \quad \text{Eq. 4-6}$$

It should be noted that the reactor volume varies with time in these experiments due to the continuous flow of ozone stock solution into the reactor and sample withdrawal. Here, a modified constant volume equation was employed; in this case, the effects of dilution on PhAC concentrations were accounted for in the data analysis by multiplying the pharmaceutical concentration by the ratio of the initial reactor volume to the reactor volume at time, *t*. Appendix E demonstrates that this assumption has a negligible impact on calculation of the rate constant for pharmaceutical transformation by ozone; therefore, the modified constant volume model was used here.

By plotting $\ln [\text{PhAC}]/[\text{PhAC}]_0$ vs. the ozone exposure ($\int [\text{O}_3] dt$), the second order rate constant for PhAC transformation by ozone ($k''_{\text{O}_3, \text{app}, \text{PhAC}}$) can be measured. Figure 4-3 shows determination of the second-order rate constants for cyclophosphamide ($[\text{CYP}]_0 = 3.83 \times 10^{-7} \text{ M}$) and ifosfamide ($[\text{IFO}]_0 = 3.83 \times 10^{-7} \text{ M}$) transformation by ozone; the background matrix includes $1.71 \times 10^{-3} \text{ M}$ NaCl, $2.38 \times 10^{-3} \text{ M}$ NaHCO₃, 10^{-2} M *t*-BuOH, and the pH was 6.3. Similar experiments were completed at pH 4.4 and 8.3 (not

shown), the second-order rate constant for ifosfamide and cyclophosphamide with ozone was similar at all pH values studied. The ozone concentration was held at different concentrations for each experiment; those concentrations ranged from $1.6\text{--}4.6 \times 10^{-5}$ M. Recall from Table 4-1 that the pK_a values for cyclophosphamide and ifosfamide reported by different investigators show some discrepancies; regardless, no differences in the rate constants were found in the investigated pH range. For the experimental results shown in Figure 4-3, the rate constants were found to be $k''_{O_3,app,CYP} = 2.27(\pm 0.31) \text{ M}^{-1}\text{s}^{-1}$ and $k''_{O_3,app,IFO} = 6.07(\pm 0.44) \text{ M}^{-1}\text{s}^{-1}$, respectively. Experiments were conducted at other pH values in the range of 4.4–8.3 to yield specific rate constants (with 95% confidence intervals) of $k''_{O_3,app,CYP} = 3.03 (\pm 0.48) \text{ M}^{-1}\text{s}^{-1}$ and $k''_{O_3,app,IFO} = 7.38 (\pm 0.27) \text{ M}^{-1}\text{s}^{-1}$, respectively. The specific rate constants (and 95% confidence intervals) were determined using the cumulative data from all experiments.

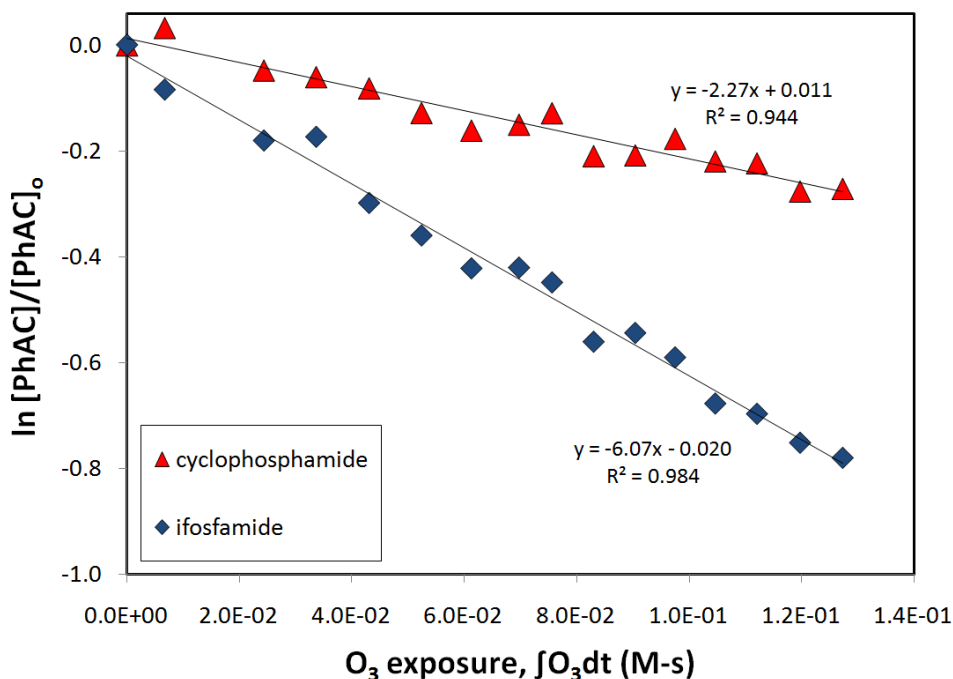


Figure 4-3. Determination of cyclophosphamide and ifosfamide second-order rate constants with ozone. (The data in this figure correspond to a background solution containing 1.71×10^{-3} M NaCl, 2.38×10^{-3} M NaHCO_3 , 10^{-2} M *t*-BuOH, 3.83×10^{-7} M cyclophosphamide, and 3.83×10^{-7} $\mu\text{g/L}$ ifosfamide at pH 6.3.)

The apparent rate constants for cyclophosphamide and ifosfamide transformation by hydroxyl radicals at pH 8.2 and the average rate constants for cyclophosphamide and ifosfamide transformation by ozone across the investigated pH values are shown in Table 4-2. The second-order rate constant for the reaction of cyclophosphamide with ozone ($k''_{O_3,CYP} = 3.03 (\pm 0.48) M^{-1}s^{-1}$) found in this study is reasonably similar to that found by Garcia-Ac *et al.* (2010), $3.3 M^{-1}s^{-1}$, and almost two orders of magnitude less than that found by Chen *et al.* (2008), $143 M^{-1}s^{-1}$. The second-order rate constant for cyclophosphamide reaction with hydroxyl radicals ($k''_{HO\cdot,CYP} = 2.69 (\pm 0.17) \times 10^9 M^{-1}s^{-1}$) compares reasonably well with the values found by both Garcia-Ac *et al.* (2010), $2.0 \times 10^9 M^{-1}s^{-1}$, and Chen *et al.* (2008), $2.1 \times 10^9 M^{-1}s^{-1}$.

Table 4-2. Rate constants for cyclophosphamide and ifosfamide with ozone and hydroxyl radicals.

Rate constants	Cyclophosphamide	Ifosfamide
$k''_{O_3,PhAC} (M^{-1}s^{-1})$	$3.03 (\pm 0.48)$	$7.38 (\pm 0.27)$
$k''_{HO\cdot,PhAC} (M^{-1}s^{-1})$	$2.69 (\pm 0.17) \times 10^9$	$2.73 (\pm 0.16) \times 10^9$

The validity of these rate constants was verified by running the continuous ozone addition reactor under conditions where both oxidants (O_3 and $HO\cdot$) are significant. For these experiments, the 2-L reactor contained $1.71 \times 10^{-3} M$ NaCl, $2.38 \times 10^{-3} M$ $NaHCO_3$, $10^{-5} M$ $pCBA$, $3.83 \times 10^{-7} M$ cyclophosphamide, and $3.83 \times 10^{-7} \mu g/L$ ifosfamide at the pH of interest; as above, the pH range investigated was 4.4-8.3. In this scenario, Eq. 4-4 can be rearranged as shown in Eq. 4-7.

$$\ln \frac{[pCBA]}{[pCBA]_0} = -k''_{HO\cdot,app,pCBA} \times \int_0^t [HO\cdot] dt \quad \text{Eq. 4-7}$$

Elovitz and von Gunten's (1999) R_{ct} term (Eq. 4-8), which is defined as the molar ratio of hydroxyl radical exposure to ozone exposure, can be substituted into Eq. 4-7 to yield Eq. 4-9.

$$R_{ct} = \frac{\int_0^t [HO\cdot] dt}{\int_0^t [O_3] dt} \quad \text{Eq. 4-8}$$

$$\ln \frac{[pCBA]}{[pCBA]_0} = -k''_{HO\cdot, app, pCBA} \times R_{ct} \times \int_0^t [O_3] dt \quad \text{Eq. 4-9}$$

Then, R_{ct} can be calculated as the slope of a plot of $\ln [pCBA]/[pCBA]_0$ versus $k''_{HO\cdot, pCBA} \times \int [O_3] dt$, as shown in Figure 4-4a. In this case, the value of R_{ct} is 2.16×10^{-8} mol $HO\cdot$ / mol O_3 .

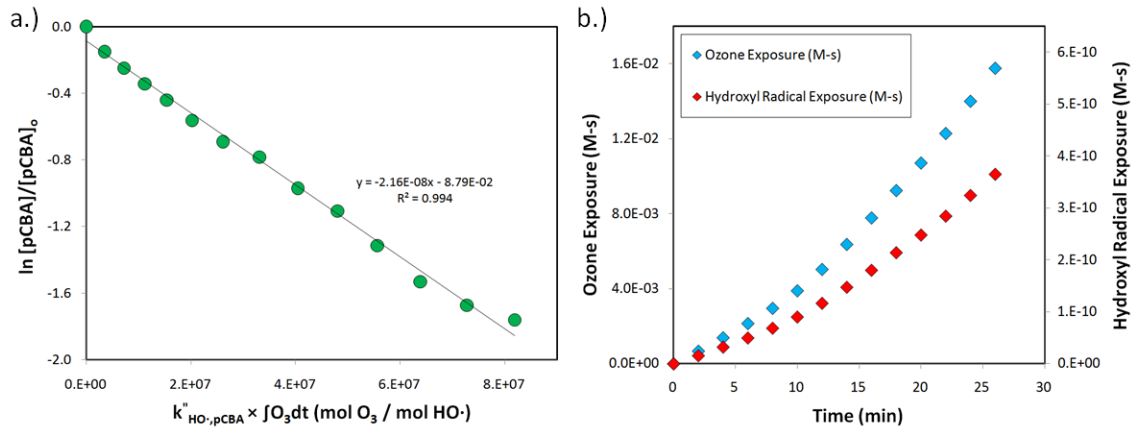


Figure 4-4. (a) Determination of R_{ct} and (b) plots of ozone and hydroxyl radical exposure corresponding to ozonation of a solution containing 1.71×10^{-3} M NaCl, 2.38×10^{-3} M $NaHCO_3$, 10^{-5} M $pCBA$, 3.83×10^{-7} M cyclophosphamide, and 3.83×10^{-7} $\mu g/L$ ifosfamide at pH 8.3.

Figure 4-4b presents the ozone ($0-1.6 \times 10^{-2}$ M-s) and hydroxyl radical ($0-3.7 \times 10^{-10}$ M-s) exposure throughout this experiment. The presence of non-negligible ozone and hydroxyl radical exposure indicates that ozone and hydroxyl radicals are available for reaction with cyclophosphamide and ifosfamide and so both must be accounted for in the reaction rate expression (Eq. 4-10):

$$\frac{d[PhAC]}{dt} = -k''_{O_3,app,PhAC} [O_3][PhAC] - k''_{HO\cdot,app,PhAC} [HO\cdot][PhAC] \quad \text{Eq. 4-10}$$

Integration of Eq. 4-10 with respect to time, and substitution of Eq. 4-8 yields Eq. 4-11.

$$\ln \frac{[PhAC]}{[PhAC]_0} = -\left(k''_{O_3,app,PhAC} + k''_{HO\cdot,app,PhAC} \times R_{ct}\right) \int_0^t [O_3] dt \quad \text{Eq. 4-11}$$

This equation was used to test whether the rate constants found above could be used to predict what would occur in scenarios where both oxidants are present. The results shown in Figure 4-5 correspond to a solution containing 1.71×10^{-3} M NaCl, 2.38×10^{-3} M NaHCO_3 , 10^{-5} M *p*CBA, 3.83×10^{-7} M cyclophosphamide, and 3.83×10^{-7} $\mu\text{g/L}$ ifosfamide at pH 8.3. The lines labeled “model” employ the rate constants listed in Table 4-2, which were determined from other experiments besides those modeled here, and the R_{ct} determined in Figure 4-4, which stems from analysis of *p*CBA concentrations in this experiment. The 95% confidence intervals were calculated by propagating the 95% confidence intervals associated with $k''_{O_3,PhAC}$, $k''_{HO\cdot,PhAC}$, and R_{ct} . In this case, the rate constants for cyclophosphamide and ifosfamide transformation by ozone and hydroxyl radicals do an excellent job of describing the transformation of cyclophosphamide and ifosfamide in a scenario where both ozone and hydroxyl radicals are relevant.

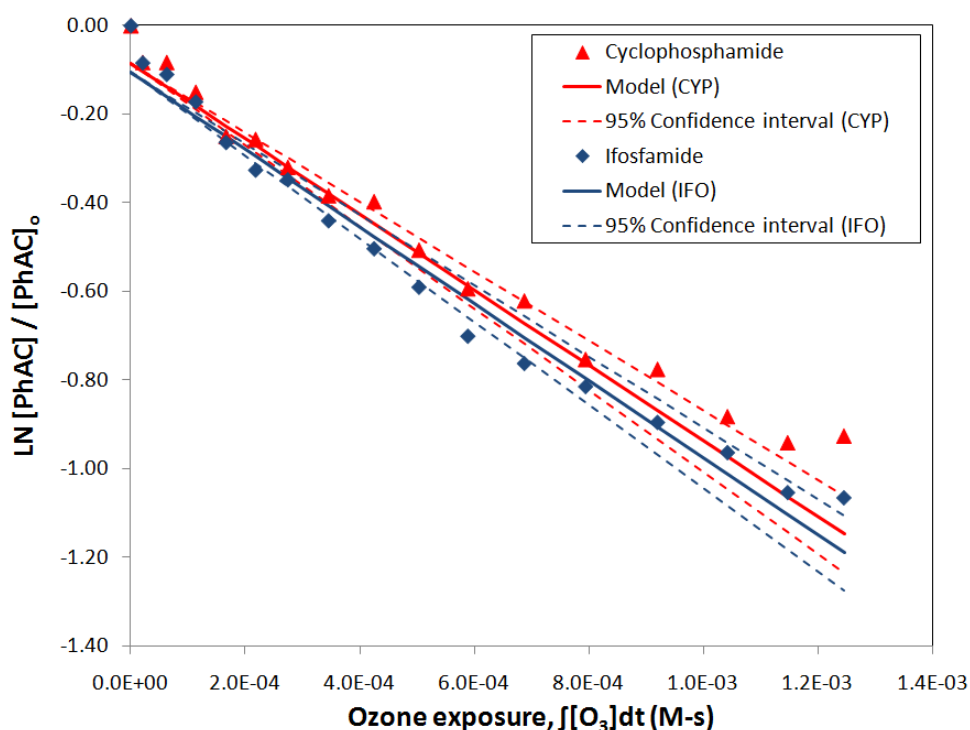


Figure 4-5. Transformation of cyclophosphamide and ifosfamide in a system that demonstrates ozone and hydroxyl radical exposure. (The solution composition is 1.71×10^{-3} M NaCl, 2.38×10^{-3} M NaHCO₃, 10^{-5} M *p*CBA, 3.83×10^{-7} M cyclophosphamide, and 3.83×10^{-7} μ g/L ifosfamide at pH 8.3. The lines labeled “model” employ the rate constants listed in Table 4-2 and the R_{ct} determined in Figure 4-4.)

Percent Transformation

The transformation of cyclophosphamide (1.15×10^{-5} M) and ifosfamide (1.15×10^{-5} M) was studied in three background matrices: (1) DI with 1.71×10^{-3} M NaCl, 2.38×10^{-3} M NaHCO₃, 10^{-5} M *p*CBA, (2) solution (1) with 0.276 mg/L DOC (2.3×10^{-5} M as C) from Lake Austin hydrophobic organic acids (HPOA), and (3) solution (1) with 27.6 mg/L DOC (2.3×10^{-3} M as C) from Lake Austin HPOA. The pH of all solutions was adjusted to 8.30. Solution 1 contained no organic matter; in solutions 2 and 3, the molar ratio of dissolved organic carbon (as mol C) to the total moles of cyclophosphamide and ifosfamide was 1 and 100 mol C (from LA HPOA) / mol PhACs, respectively. *p*CBA was included in all solutions to determine the hydroxyl radical

exposure associated with specific applied ozone doses. Incremental volumes of highly concentrated ozone from a stock solution (8.75×10^{-4} M O_3) were added to 7-mL of solutions 1-3 to get applied ozone doses in the range of 0 to 1.1×10^{-4} M O_3 . Dilution effects were accounted for in subsequent calculations. Hence the data in Figure 4-6 represents the transformation of cyclophosphamide and ifosfamide, as well as the hydroxyl radical exposure, obtained for a given applied ozone dose.

From Figure 4-6a, the impact of the increasing concentrations of DOC from Lake Austin HPOA is clearly observable; as the DOC concentration increases, less cyclophosphamide is transformed. The same trend exists for ifosfamide (Figure 4-6b). In Solution 3 (100 mol DOC (as C) / mol PhAC), the transformation efficiencies of cyclophosphamide and ifosfamide for an ozone dose of 9.92×10^{-5} M were approximately 38% and 28%, respectively, of the transformations observed in the no DOC solution (Solution 1). Hence, the impact of DOC at environmentally relevant concentrations can be significant for compounds that react slowly with ozone. That impact also extends to advanced oxidation processes (AOPs). The change in *p*CBA concentration was used to calculate the hydroxyl radical exposure (Eq. 4-4). As seen in Figure 4-6c, the hydroxyl radical exposure observed in Solution 3 was significantly lower than that in Solutions 1 and 2. For the ozone dose discussed above (9.92×10^{-5} M), the hydroxyl radical exposure observed in Solution 3 was only 19% of that observed in Solution 1. For all ozone doses but two, the hydroxyl radical exposure in Solution 3 was 19-23% of that observed in Solution 1; the other two samples exhibited 29% and 38% of the hydroxyl radical exposure. It is important to note that although the reduction of hydroxyl radical exposure in the presence of DOC (Solution 3) was only 20%, the reduction of the removal of CYP and IFO were 38% and 28%, respectively. Predicted removals of CYP and IFO (using the calculated values of hydroxyl radical exposure and known rate constants for reaction with hydroxyl radicals) were somewhat lower than measured removals. For example, for an applied ozone dose of 9.92×10^{-5} M in Solution 1, the predicted CYP and IFO remaining were $33.1(\pm 2.2)\%$ and $32.6(\pm 2.1)\%$, respectively; measured values of CYP

and IFO remaining were 38.7% and 40.3%, respectively. Regardless, the reduction in hydroxyl radical exposure seems to be the major contributor to the reduced transformation of cyclophosphamide and ifosfamide observed in Figure 4-6.

These results are interesting in the context of the ozone demand of the NOM matrix. Cyclophosphamide and ifosfamide do not react quickly with ozone; therefore, most of the cyclophosphamide and ifosfamide transformation observed in these experiments derives from reaction with hydroxyl radicals. At a molar ratio of 1 mol C (from DOC) to 1 mol PhAC, the effects of NOM on hydroxyl radical exposure are minor; however, as that ratio shifts up to 100 mol C (from DOC) / mol PhAC, the impact of NOM on the treatment process becomes more important. In this scenario, a significant portion of the applied ozone likely reacts with NOM; this situation results in a lower hydroxyl radical exposure (due to less ozone available for decomposition) and a changed ozone decomposition rate (due to ability for NOM to inhibit and/or propagate ozone decomposition; Figure 2-2). For these reasons, it would be interesting to employ the continuous ozone (or peroxone) addition reactor toward CYP and IFO treatment in the context of how different NOM matrices affect the transformation of these compounds. In Chapter 5, the ability for the continuous aqueous ozone addition reactor to treat ciprofloxacin in the presence of various organic matter matrices is demonstrated.

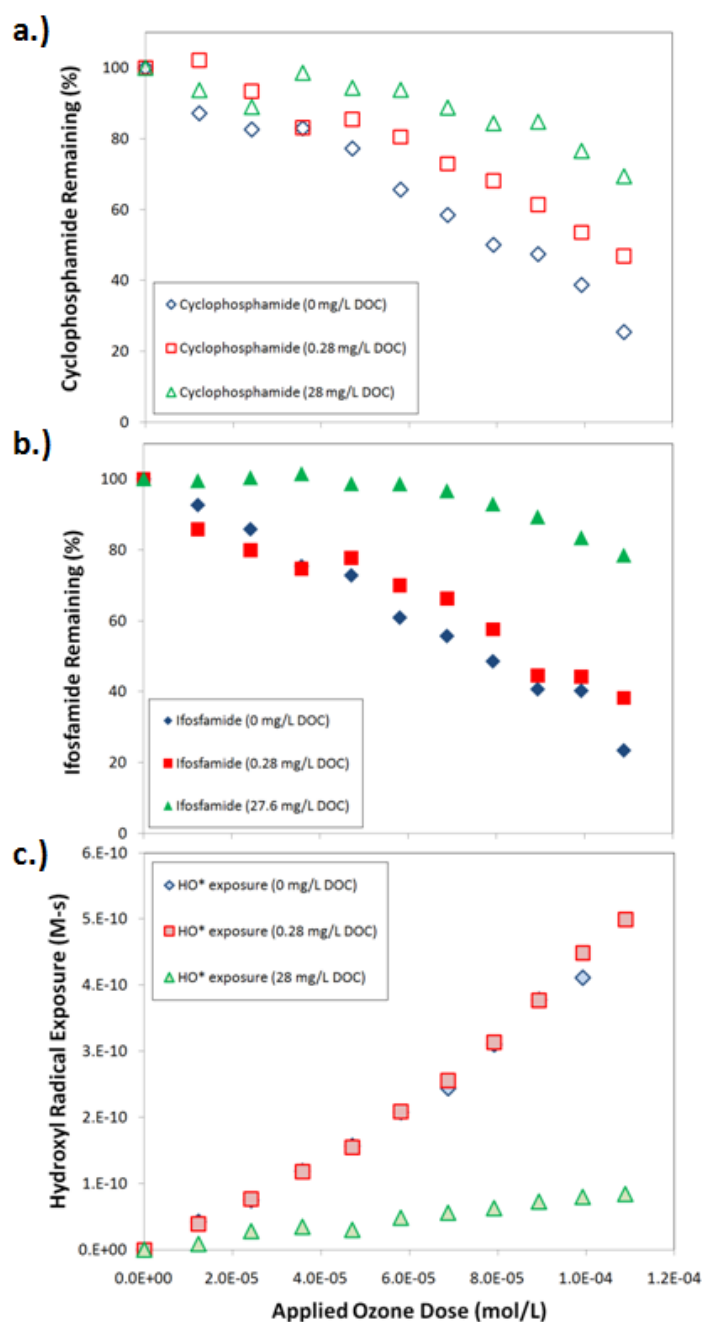


Figure 4-6. The impact of three different concentrations (0, 0.28, and 27.6 mg/L DOC) of organic matter (Lake Austin HPOA) on (a) Cyclophosphamide and (b) Ifosfamide removal as a function of the applied ozone dose (mol/L). (The hydroxyl radical exposure (M-s) for solutions (1)-(3) is plotted against the applied ozone dose in (c). The molar ratio of LA HPOA (as mol C / L) to the total concentration of PhACs is 0, 1, and 100 for solutions (1)-(3), respectively.)

Intermediate Product Identification

To study the formation and transformation of intermediate oxidation products generated by ozone and hydroxyl radical reaction with cyclophosphamide and ifosfamide, solutions containing 3.83×10^{-4} M of cyclophosphamide or ifosfamide were prepared. Four separate solutions were employed; two (pH 2.5 and pH 9.6) containing cyclophosphamide and two (pH 2.5 and pH 9.6) containing ifosfamide. All solutions contained 1.71×10^{-3} M NaCl, 2.38×10^{-3} M NaHCO₃, and 3.83×10^{-4} M of either cyclophosphamide or ifosfamide. Solution pH was adjusted by adding a small volume of 5N H₂SO₄ or 5N NaOH. The low pH solutions contained 10 mM *t*-BuOH to isolate O₃-based transformative mechanisms. On the other hand, 10 μ M *p*CBA was added to the high pH solutions to quantify the hydroxyl radical exposure. At pH 9.6, ozone decay kinetics are fairly fast ($k_{d,O_3} = 4.70 \times 10^{-2} \text{ s}^{-1}$, extrapolated from Elovitz *et al.*, 2000); the fast ozone decay kinetics combined with the slow reaction between ozone and cyclophosphamide ($k''_{O_3,CYP} = 3.03 (\pm 0.48) \text{ M}^{-1}\text{s}^{-1}$) and ifosfamide ($k''_{O_3,IFO} = 7.38 (\pm 0.27) \text{ M}^{-1}\text{s}^{-1}$) allow us to examine hydroxyl radical-initiated transformations.

Small (2-mL) aliquots of each of these four solutions were dosed with incremental volumes of ozone stock solution (1.15×10^{-3} M O₃), corresponding to a specific applied ozone dose. The response associated with select *m/z* values versus the molar ratio of applied ozone to initial cyclophosphamide (Figure 4-7a-b) and initial ifosfamide (Figure 4-7c-d) confirm the presence of several intermediate oxidation products. A number of other intermediate oxidation products were identified; however, *m/z* values that did not demonstrate at least one data point that was at least 10% of the initial cyclophosphamide or ifosfamide response were not included in this analysis. From these plots, it is clear that several major intermediate oxidation products are formed during the transformation of cyclophosphamide and ifosfamide via ozone- and hydroxyl radical-based pathways. Furthermore, a large overlap existed in the *m/z* values that were observed between ozone and hydroxyl radical pathways. Given the structural similarity of cyclophosphamide to ifosfamide, it is not surprising that many of the *m/z* values for intermediate oxidation

products formed from cyclophosphamide transformation (Figure 4-7a-b) are also observed for ifosfamide oxidation (Figure 4-7c-d).

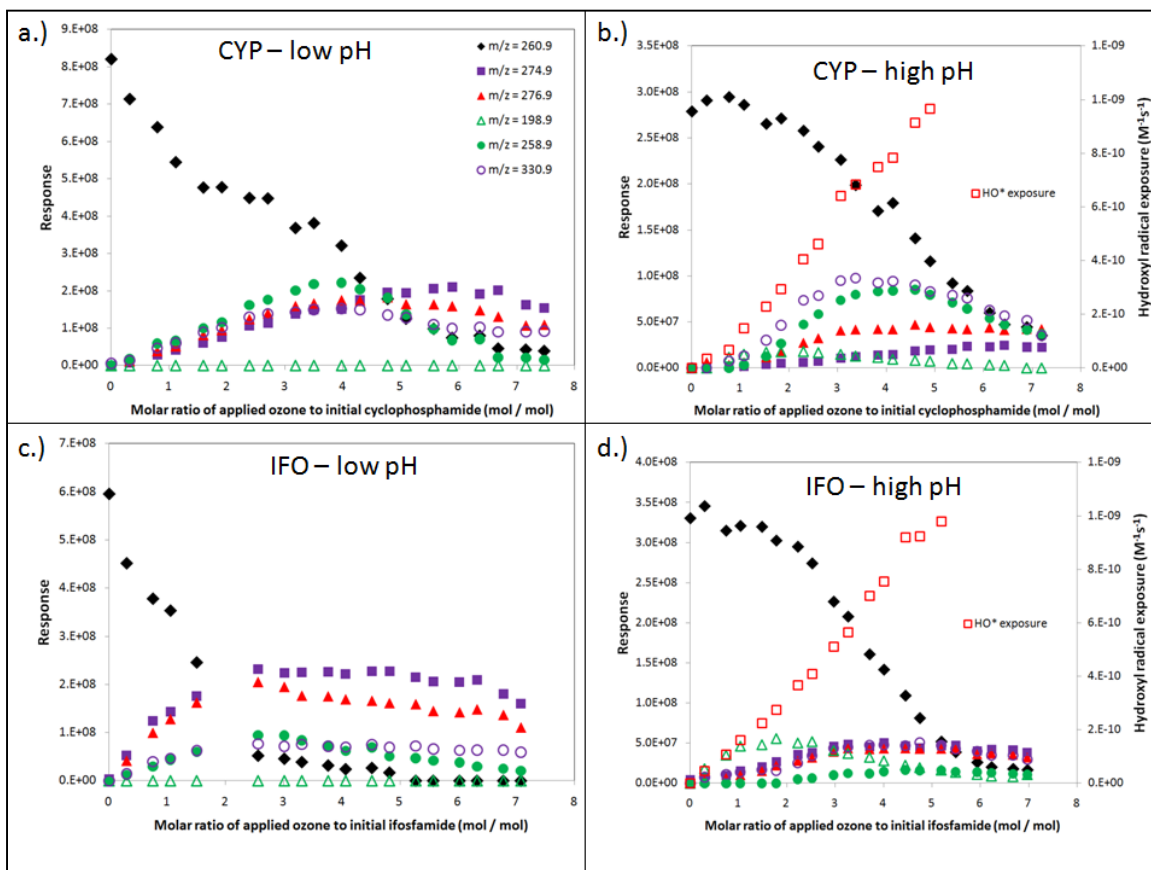


Figure 4-7. Cyclophosphamide transformation and production of intermediate products as a function of the molar ratio of applied ozone to the initial cyclophosphamide concentration (mol O_3 / mol CYP) at a.) pH 2.5 and b.) pH 9.6. Ifosfamide transformation and production of intermediate products as a function of the molar ratio of applied ozone to the initial ifosfamide concentration (mol O_3 / mol IFO) at c.) pH 2.5 and d.) pH 9.6. (All solutions also contained 100 mg/L NaCl and 200 mg/L $NaHCO_3$; pH was adjusted using 5N H_2SO_4 or 5N NaOH. The pH 2.5 solutions contained 10mM *t*-BuOH to isolate O_3 -based transformative mechanisms. The pH 9.6 solutions contained an initial concentration of 10 μ M pCBA, to quantify the hydroxyl radical exposure as seen in b.) and d.).)

While these experiments were allowed to proceed until completion, the rate constants found above can provide some insight to the data. In comparing Figure 4-7a-d,

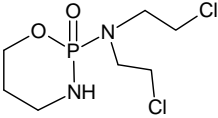
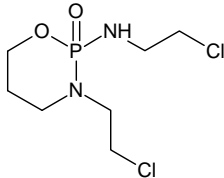
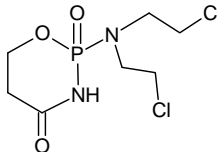
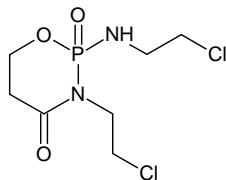
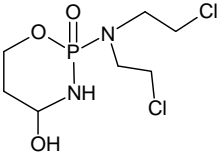
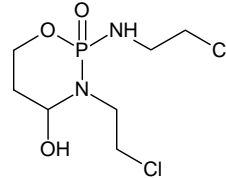
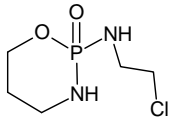
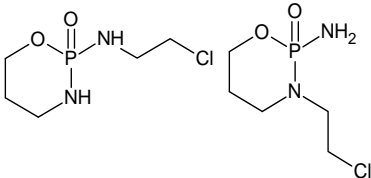
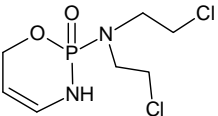
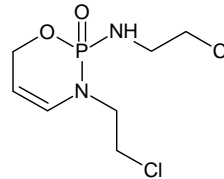
it is clear that more ifosfamide is transformed for a given ozone dose as compared to cyclophosphamide at both low and high pH. The molar ratios of applied ozone to initial PhAC corresponding to 50% transformation of cyclophosphamide (Figure 4-7a-b) and ifosfamide (Figure 4-7c-d) were 2.93, 4.61, 1.29, and 3.67 mol O₃/ mol PhAC, respectively. As expected, the ratio of the 50% transformation values for ifosfamide to cyclophosphamide at low pH (0.44) is similar to the ratio of the second order ratio constant for ifosfamide with ozone to that of cyclophosphamide with ozone (0.47). Additionally, the ratio of the 50% transformation values for ifosfamide to cyclophosphamide at high pH (0.80) is similar to the ratio of the second order ratio constant for ifosfamide with hydroxyl radicals to that of cyclophosphamide with hydroxyl radicals (0.71). These results are consistent with the higher rate constants for ifosfamide transformation by ozone and hydroxyl radicals, as compared to cyclophosphamide.

For the most part, the formation and transformation of $m/z = 274.9$ and $m/z = 276.9$ are closely related. These species appear to be the dominant intermediate products for ozone-based reaction of cyclophosphamide and ifosfamide in the range of ozone doses reported. The $m/z = 198.9$ peak was only identified in the high pH solutions, suggesting that this compound is formed primarily through HO· attack on cyclophosphamide and ifosfamide. One major difference between the intermediate products identified for cyclophosphamide transformation, as compared to ifosfamide transformation, is the magnitude of the $m/z = 258.9$ peak; the formation of this compound is more pronounced in cyclophosphamide oxidation for the ozone- and hydroxyl radical-initiated scenarios.

Venta *et al.* (2005) investigated treatment of cyclophosphamide using peroxone; in that study the intermediate oxidation product associated with the $m/z = 274.9$ peak was identified as 4-ketocyclophosphamide. In this study, that peak was identified for both cyclophosphamide and also ifosfamide; given the structural similarity of these

compounds, we postulate that the $m/z = 274.9$ peak corresponds to 4-ketoifosfamide, which is formed through ozone attack on the C4 atom. Another peak was observed at $m/z = 276.9$ for both compounds; this m/z value corresponds to the addition of one oxygen atom into the molecule. Given, the production of 4-ketocyclophosphamide and 4-ketoifosfamide, it is likely that the $m/z = 276.9$ peaks correspond to 4-hydroxycyclophosphamide and 4-hydroxyifosfamide. The $m/z = 198.9$ peak, which is only significant for the high pH solution containing ifosfamide, appears to form due to the loss of one chloroethyl group from the parent cyclophosphamide and ifosfamide structures. An attack on the hydroxyl group of the 4-hydroxy derivative of cyclophosphamide or ifosfamide results in the loss of an H_2O molecule and the formation of a double bond between the C4 and C5 atoms; this compound corresponds to $m/z = 258.9$. The proposed structures of these intermediate oxidation products are shown in Table 4-3. The other major intermediate product shown in Table 4-3 is $m/z = 330.9$. A proposed molecular formula for this compound is provided in Table 4-3; however, at this time, no structure has been proposed.

Table 4-3. Proposed intermediate products formed via ozonation of cyclophosphamide and ifosfamide.

<i>m/z</i> measured	Proposed molecular formula	Change	Proposed structure (from cyclophosphamide)	Proposed structure (from ifosfamide)
260.9 (parent)	C ₇ H ₁₅ Cl ₂ N ₂ O ₂ P	---		
			cyclophosphamide	ifosfamide
274.9	C ₇ H ₁₃ Cl ₂ N ₂ O ₃ P	-2H +1O		
			4-ketocyclophosphamide	4-ketoifosfamide
276.9	C ₇ H ₁₅ Cl ₂ N ₂ O ₃ P	+1O		
			4-hydroxycyclophosphamide	4-hydroxyifosfamide
198.9	C ₅ H ₁₂ ClN ₂ O ₂ P	-2C -3H -1Cl		
			Dechloroethylcyclophosphamide	2-dechloroethylifosfamide 3-dechloroethylifosfamide
258.9	C ₇ H ₁₃ Cl ₂ N ₂ O ₂ P	-2H		
			Iminocyclophosphamide	Iminoifosfamide
330.9	C ₇ H ₁₃ Cl ₄ N ₂ O ₂ P	-1H +2Cl	None proposed	None proposed

While the m/z values shown in Figure 4-7 and Table 4-3 correspond to those products that demonstrated the most significant instrument response, m/z ratios of 221.0 and 56.1 were also monitored. These m/z values correspond to phosphoramidate and isophosphoramidate mustard ($m/z = 221.0$) and acrolein ($m/z = 56.1$). Recall that cyclophosphamide and ifosfamide are prodrugs that are first metabolized into the 4-hydroxy derivatives and then further metabolized to the active form of the drugs, phosphoramidate mustard and isophosphoramidate mustard, respectively. The ratio of the response for $m/z = 221.0$ to the response of the initial PhAC concentration (for the corresponding data set) for all four data sets are plotted in Figure 4-8. No peaks were observed for $m/z = 56.1$; however, that might be a function of the LC-MS method, which was optimized for cyclophosphamide and ifosfamide elution. For cyclophosphamide and ifosfamide, similar trends were observed in the formation/transformation of the $m/z = 221.0$ peak. At high pH, the $m/z = 221.0$ peak demonstrated relatively high formation for molar ratios of ozone to the initial PhAC concentration ranging from 1.0–3.5 mol O_3 / mol PhAC. The highest response (as a percent of the initial PhAC response) was approximately 5%. As the molar ratio of ozone to cyclophosphamide/ifosfamide was increased the peak at $m/z = 221.0$ declined. However, at low pH, no apparent formation of the reactive mustards occurred. It should be noted that while the peak areas were small in magnitude, distinct peaks were observed (Figure 4-9).

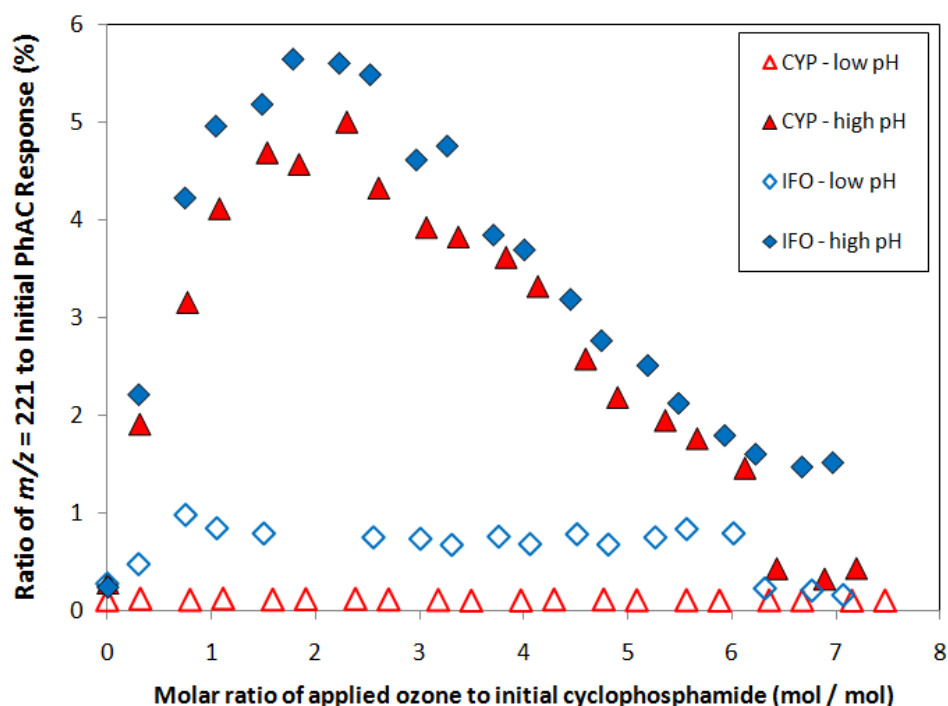


Figure 4-8. Formation and transformation of $m/z = 221.0$, which corresponds to phosphoramidate mustard (cyclophosphamide) and isophosphoramidate mustard (ifosfamide) as a percentage of the initial cyclophosphamide/ifosfamide response.

Recently, Li *et al.* (2010) investigated the metabolism of cyclophosphamide and ifosfamide in a mouse model. That research identified several metabolites of cyclophosphamide and ifosfamide, including those discussed above, with the exception of $m/z = 330.9$. The overlap between the intermediate products identified in this study with the metabolites found in Li *et al.*'s (2010) work is of special interest because it demonstrates that ozone- and hydroxyl radical- based water treatment processes have the potential to replicate metabolic transformative processes in terms of what products are formed. In fact, Hohorst *et al.* (1976) employed ozone to synthetically generate the 4-hydroxy derivatives, 4-hydroxycyclophosphamide and 4-hydroxyifosfamide (Low *et al.*, 1983; Fleming, 1997). Furthermore, the chloroethyl group, lost from cyclophosphamide and ifosfamide during formation of the $m/z = 198.9$ peak, may form chloroacetaldehyde, which is a known alkylating agent (Guengerich *et al.*, 1979). The potential for ozonation

to form pharmacologically active intermediate products is a topic of debate in the field of environmental engineering. For prodrugs, this scenario is of increasing interest due to the potential of water treatment to actually increase the toxicological activity of a water. Here, initial characterization of intermediate oxidation products resulting from ozonation of cyclophosphamide and ifosfamide was described; the literature suggests that some of these compounds can exert pharmacological activity. These results suggest that further research to explore the residual pharmacological activity of cyclophosphamide and ifosfamide intermediate oxidation products throughout ozone treatment processes is justified. Attempts were made to measure the residual pharmacological activity of treated solutions containing cyclophosphamide and ifosfamide; however, the corresponding cytotoxicity assay was never successfully employed (Appendix D).

In the next Chapter, the residual pharmacological activity associated with ciprofloxacin and its intermediate oxidation products was measured and the results were used to draw conclusions regarding the ability of intermediate oxidation products to retain pharmacological activity.

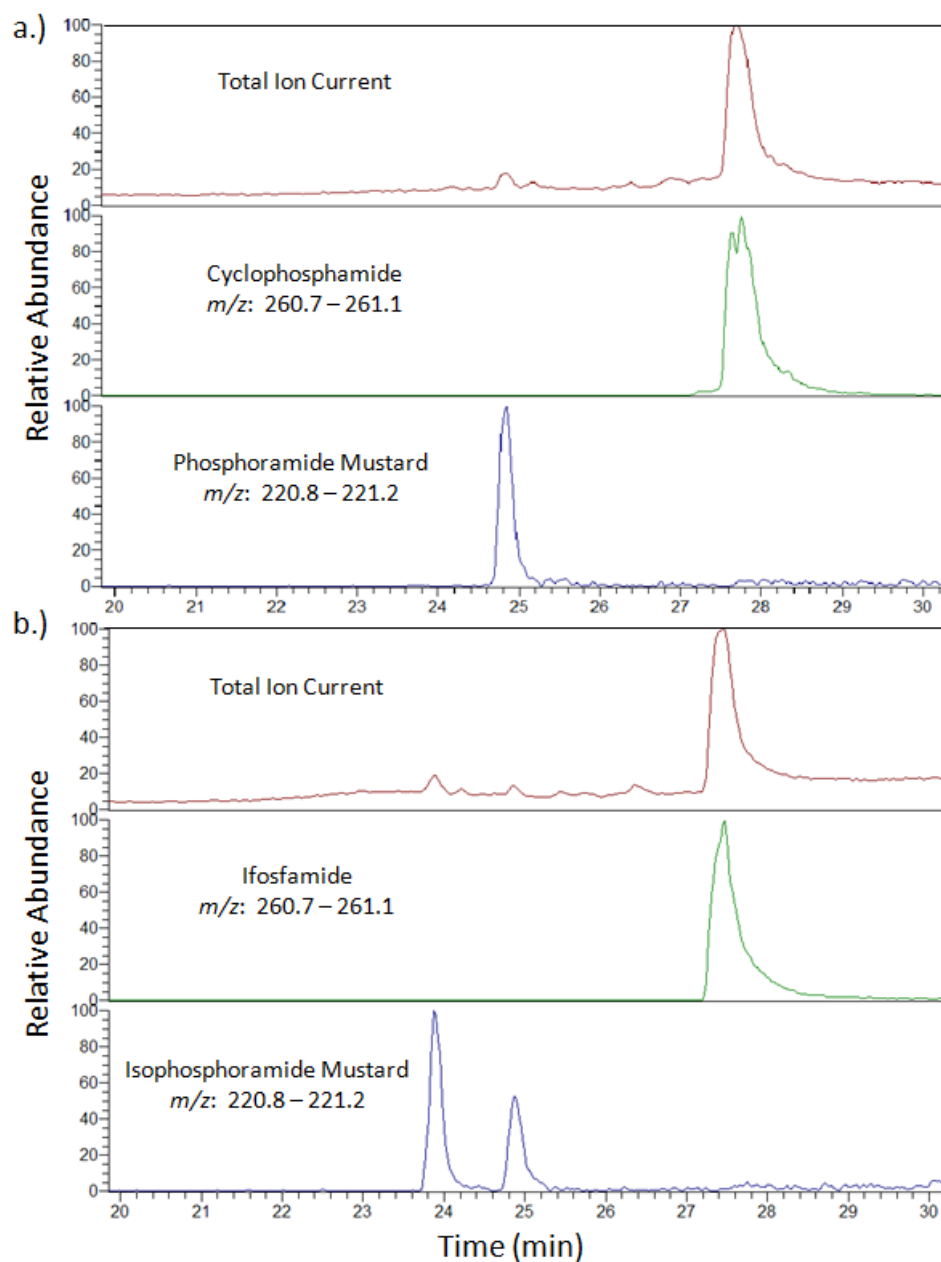


Figure 4-9. Typical LC-MS peaks for (a) cyclophosphamide and phosphoramidate mustard and (b) ifosfamide and isophosphamide mustard. (The total ion current for these samples are provided for magnitude comparison. The sample demonstrated in (a) corresponds to a sample containing 1.71×10^{-3} M NaCl, 2.38×10^{-3} M NaHCO_3 , 10^{-5} M *p*CBA, and 3.83×10^{-4} M cyclophosphamide (at pH 9.6) that was dosed with 1.53 mol O_3 / mol CYP. In (b), the sample contained the same background compounds, but with 3.83×10^{-4} M ifosfamide rather than cyclophosphamide; the ozone dose for the sample shown in (b) was 1.04 mol O_3 / mol IFO.)

CHAPTER 5: EFFECTS OF NATURAL ORGANIC MATTER ON OZONATION OF CIPROFLOXACIN AND REMOVAL OF ANTIMICROBIAL ACTIVITY

ABSTRACT

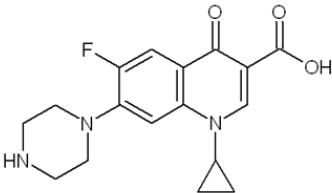
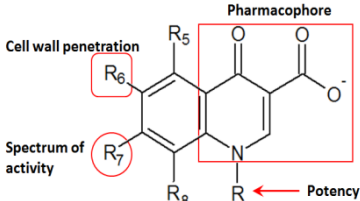
Elimination of the fluoroquinolone antibiotic, ciprofloxacin, was evaluated during aqueous ozonation in the presence of natural organic matter from various sources. The impacts of natural organic matter (NOM) concentration, source (Lake Austin, TX and Claremore Lake, OK), and composition (hydrophobic organic acids and transphilic organic acids) on ciprofloxacin transformation were determined. Additionally, the residual pharmacological activity of treated samples was determined using an antimicrobial susceptibility assay. Two metrics, ciprofloxacin transformed and antimicrobial activity eliminated, were used to describe treatment efficiency. Each NOM source, at equivalent dissolved organic carbon (DOC) concentrations, was found to alter the applied ozone dose required to remove 50% of the initial ciprofloxacin and antimicrobial activity. DOC concentration and NOM composition also affected the required applied ozone dose. The inhibition profile of treated samples suggests that pharmacologically active intermediate oxidation products were formed during treatment.

Key words: ciprofloxacin, natural organic matter, ozone, antimicrobial activity, residual pharmacological activity

INTRODUCTION

Ciprofloxacin, a second generation fluoroquinolonic antibiotic, has been detected in water supplies around the world (Golet *et al.*, 2002; Kolpin *et al.*, 2002; Zuccato *et al.*, 2005; Larsson *et al.*, 2007). Ciprofloxacin inhibits the DNA gyrase and topoisomerase IV enzymes, which are involved in the DNA replication process of many microorganisms (Drlica and Zhao, 1997). The widespread detection of ciprofloxacin in water supplies reflects its longstanding popularity as a prescribed drug (Prescription, 2009); by 2006, ciprofloxacin had recorded a lifetime sales profit of \$19 billion dollars (Finch and Hunter, 2006). The structure and properties of ciprofloxacin are shown in Table 5-1.

Table 5-1. Salient properties of ciprofloxacin and depiction of structure-activity relationship for quinolones.

Property	Ciprofloxacin	Generalized Quinolone (Lemke and Williams, 2008)
Structure		
Formula	C ₁₇ H ₁₈ FN ₃ O ₃	
Molecular Weight (g/mol)	331.35	
pK _{a1}	6.2	
pK _{a2}	8.8	

Due to ciprofloxacin's widespread popularity and use, it is not surprising that ciprofloxacin has been detected in raw wastewater, treated wastewater, and surface waters (Golet *et al.*, 2002; Kolpin *et al.*, 2002; Zuccato *et al.*, 2005; Larsson *et al.*, 2007). Golet *et al.* (2002) tracked ciprofloxacin concentrations in raw wastewater (300-600 ng/L), treated wastewater (60-110 ng/L), and in downstream river locations (5-18 ng/L) throughout the Glatt River Valley in Switzerland. Similarly, Zuccato *et al.* (2005) found ciprofloxacin concentrations as high as 251 ng/L in wastewater effluents and 14-26 ng/L in two Italian river systems. A 2002 USGS study (2002) identified ciprofloxacin in three

of the 139 surface water sampling locations across the continental United States; the highest concentration detected was 30 ng/L. In at least one case, high ciprofloxacin concentrations have been discharged to the environment; specifically, Larsson *et al.* (2007) found 28-31 mg/L of ciprofloxacin in effluent from an industrial wastewater treatment plant near Hyderabad, India.

The release of pharmacologically active compounds (PhACs), such as ciprofloxacin, into the environment is thought to have negative effects on environmental and human health. Pomati and coworkers (2006; 2008) have investigated the effects of 13 pharmaceuticals on *Escherichia coli*, human embryonic kidney, and human ovarian carcinoma cells. These investigators found that environmentally relevant levels of pharmaceuticals can inhibit the proliferation of human embryonic kidney cells by up to 30% (Pomati *et al.*, 2006) and that the pharmacological activity of drug mixtures can vary from that predicted solely on the basis of additive effects for individual compounds (Pomati *et al.*, 2008). While the impact of trace levels of pharmaceuticals on human development is still widely debated, concern over the contribution of low levels of antibiotics in wastewater to the acceleration of antibiotic resistance is increasing (Kummerer, 2004). Evidence of antibiotic resistant organisms and antibiotic resistance genes in wastewater and wastewater treatment plants (Schwartz *et al.*, 2003; Szczepanowski *et al.*, 2009) corroborates these concerns. Finally, increasing attention is being paid to characterization of the sub-lethal effects on bacterial cells caused by PhACs, and antibiotics in particular; the ability of antibiotics to act as signaling agents may have negative environmental impacts (Davies *et al.*, 2006; Fajardo and Martínez, 2008).

With the emerging concern over this class of contaminants, several research efforts have focused on removing pharmaceuticals from water using a variety of separation treatment processes: ion exchange, activated carbon, or membrane-based technologies (Adams *et al.*, 2002; Westerhoff *et al.*, 2005; Xu *et al.*, 2005). While

reverse osmosis treatment provided good removal (>90%) of all test compounds, the other processes offered widely variant removal efficiencies (0-98%) due to the range of polarity and hydrophobicity of different pharmaceutical compounds. However, process flexibility, ease of installation, and competitive economics have propelled oxidation processes to the forefront of this emerging field.

Given the superior capabilities of oxidation processes for treatment of trace organic contaminants, several research efforts have focused on the ability of ozone and ozone-based advanced oxidation processes to remove PhACs from water and wastewater streams. Huber *et al.* (2003) investigated the ability of aqueous ozone to treat nine pharmaceuticals in batch reactors; their results indicated that pharmaceutical structure, solution alkalinity, and the dissolved organic carbon (DOC) concentration of the water source are the most important variables in determining the percent of parent compound transformed during batch ozonation. Ternes and coworkers (2002; 2003) conducted full- and pilot-scale studies with various ozone-based advanced oxidation processes (AOPs) and showed successful removal of over twenty pharmaceuticals. Hua *et al.* (2006) operated two side-by-side pilot plants, one with coagulation, flocculation, and sedimentation followed by GAC filtration and the other with pre-ozonation before the same processes. The pilot plant containing ozone treatment demonstrated better removal of the four PhACs (carbamazepine, cotinine, caffeine, and atrazine).

Because of its widespread popularity and use, ciprofloxacin has emerged as a model PhAC and has been previously studied in the context of ozone-based treatment processes (Dodd *et al.*, 2006; DeWitte *et al.*, 2008; DeWitte *et al.*, 2009; Dodd *et al.*, 2009). The reaction kinetics of ciprofloxacin with ozone and hydroxyl radicals has been studied in gaseous addition (DeWitte *et al.*, 2009) and liquid addition (Dodd *et al.*, 2006) schemes. Dodd *et al.* (2006) observed significant variations in the second order (*i.e.*, first order with respect to both ozone and ciprofloxacin) rate constants for the protonated (dominant at $\text{pH} < 6.2$), zwitterionic (dominant at $6.2 < \text{pH} < 8.8$), and deprotonated

(dominant at pH > 8.8) ciprofloxacin species: $4.0 \times 10^2 \text{ M}^{-1}\text{s}^{-1}$, $7.5 \times 10^3 \text{ M}^{-1}\text{s}^{-1}$, and $9.0 \times 10^5 \text{ M}^{-1}\text{s}^{-1}$, respectively. The second order rate constant for ciprofloxacin with hydroxyl radicals was determined to be $4.1 \times 10^9 \text{ M}^{-1}\text{s}^{-1}$ at pH 7. In that work, Dodd *et al.* (2006) postulate that ozone and hydroxyl radicals attack ciprofloxacin at sites other than the pharmacophore (see Table 5-1 for the structure-activity relationship for fluoroquinolones). This hypothesis is of great interest due to the potential for pharmaceutical metabolites and intermediate oxidation products (*i.e.*, those compounds formed as products of PhAC reaction with ozone or hydroxyl radicals) to exert the same pharmacological activity as the original parent compound in environment systems.

Lemke and Williams (2008) delineated the structure-activity relationship for quinolonic compounds, as seen in Table 5-1. The pharmacophore is the core structure required for the compound to exert pharmacological activity; furthermore, three important functional groups that determine the pharmacological capabilities of the compound. The R₆ group contributes to the ability of the compound to penetrate cell walls; fluoroquinolones, such as ciprofloxacin, have a fluoro group at R₆. The R₇ group relates to the compound's spectrum of activity, *i.e.*, this functional group establishes what microorganisms will be affected by the compound. The R group determines the relative potency of the compound. Recent work by DeWitte and coworkers (2008; 2009) suggested structures for intermediate oxidation products formed during gaseous ozonation of ciprofloxacin. Of the twelve intermediate oxidation products determined by DeWitte *et al.* (2008), all twelve structures retained the fluoro group on R₆, all twelve compounds retained the same potency group as ciprofloxacin, and six intermediate oxidation products retained the pharmacophore. The majority of oxidative transformations target the piperazinyl group (R₇) (DeWitte *et al.*, 2008; 2009), which may change the spectrum of microorganisms affected by the compound but does not necessarily remove pharmacological activity. Therefore, the potential for formation of pharmacologically active oxidative intermediate products via ozonation of ciprofloxacin is high.

In the past few years, several researchers (Suarez *et al.*, 2007; Baeza, 2008; Dodd *et al.*, 2009; Paul *et al.*, 2010) have used an antimicrobial susceptibility assay (NCCLS, 2004) to describe treatment efficacy in terms of pharmacological activity. Suarez *et al.* (2007) treated triclosan with aqueous ozone and showed that antibacterial activity against *E. coli* ATCC 23716 closely followed triclosan concentration. Baeza (2008) used this assay (with *E. coli* ATCC 25922) in combination with UV photolysis and photochemical UV/H₂O₂ treatment of four antimicrobials to demonstrate that the impact of the background water matrix varied depending on the treatment conditions. Dodd *et al.* (2009) employed an antimicrobial susceptibility assay (with *E. coli* ATCC 23716 and *Bacillus subtilis* ATCC 6051) to track the pharmacological activity of 14 antimicrobial compounds, including ciprofloxacin, during ozone treatment; in this work, the authors concluded that ciprofloxacin intermediate products did not demonstrate any quantifiable antimicrobial activity. These findings seemingly contradict the hypothesis put forth in Dodd *et al.*'s earlier work (2006), which suggested that because ozone and hydroxyl radicals mainly attack at ciprofloxacin's piperazinyl group (R₇, spectrum of activity) the intermediate oxidation products may demonstrate antimicrobial activity. A recent paper by Paul *et al.* (2010) indicates that ciprofloxacin degradation products from photolytic (UV) and photocatalytic (UV-TiO₂) processes exert some antimicrobial activity against *E. coli* ATCC 23716. In summary, many questions still surround the pharmacological activity of ciprofloxacin's intermediate oxidation products.

The objectives of the present study were threefold: (1) to determine the impact of different NOM matrices on ciprofloxacin transformation by continuous addition of a high-strength aqueous ozone solution, (2) to employ an antimicrobial activity assay to track residual antimicrobial activity throughout treatment, and (3) to compare ciprofloxacin transformation with elimination of antimicrobial activity. This work should be considered an extension of the work already performed by others (Dodd *et al.*, 2006; DeWitte *et al.*, 2008; DeWitte *et al.*, 2009; Dodd *et al.*, 2009; Paul *et al.*, 2010) on ciprofloxacin oxidation. The data presented in this paper offers key insights on the use of

ozone for transformation of ciprofloxacin and removal of residual antimicrobial activity, in the presence of NOM. This two-pronged approach of measuring ciprofloxacin concentration and residual antimicrobial activity allows determination of the treatment required to remove pharmacological activity and provides a framework for treatment of other antimicrobial PhACs encountered in water treatment plants.

MATERIALS AND METHODS

Chemicals and stock solutions. Stock solutions of ciprofloxacin were prepared at 10 mg/L in deionized water and stored in the dark at 4°C. HPLC-grade acetonitrile (ACN) and ACS-grade phosphoric acid (H₃PO₄) were used for HPLC analysis of ciprofloxacin. Mueller-Hinton broth (MHB) was purchased in powder form and was prepared according to the manufacturer's guidelines, autoclaved at 121°C for 20 minutes, and stored in the dark at 4°C.

Natural organic matter sources. NOM was isolated from Lake Austin (Austin, TX) and Claremore Lake (Claremore, OK) using the procedures described by Aiken *et al.* (1992). Lake Austin NOM was available as the hydrophobic organic acids (HPOA) fraction, which was isolated using XAD-8 resin. Organic matter isolation of the Claremore Lake NOM was completed with XAD-8 followed by XAD-4. The XAD-8 isolate represents the HPOA fraction and contains aliphatic carboxylic acids of 5-9 carbons, one- and two-ring aromatic carboxylic acids, one- and two-ring phenols, and aquatic humic substances. The XAD-4 isolate contains the transphilic organic acids (TPIA), *i.e.*, polyfunctional organic acids and aliphatic acids with five or fewer carbon atoms. Characteristics, including SUVA₂₅₄, of the NOM and HPOA / TPIA isolates are summarized in Table 5-2.

Table 5-2. Source water and NOM characteristics.

Parameter	Claremore Lake	Lake Austin
pH	7.52	8.01
Alkalinity (mg CaCO ₃ /L)	57	164.5
DOC (mg/L)	6.4	3.5
SUVA ₂₅₄ (L/mg-m)	2.89	1.76
HPOA (%)	45	35
HPOA SUVA ₂₅₄ (L/mg-m)	3.7	2.9
TPIA (%)	19	20
TPIA SUVA ₂₅₄ (L/mg-m)	2.9	1.7

Ozone reactor setup. Oxygen gas flowed into the ozone generator at 30 cm³/min; some fraction of that oxygen was converted to ozone. This combined gas stream was directed into a 500-mL gas-washing bottle, which served as a stock ozone solution. The ozone stock solution was kept on ice to increase the solubility of ozone. After 4-6 hours, the ozone concentration in the stock solution reached a plateau at 55-65 mg/L O₃. A schematic of the ozone supply system and reactor is shown in Figure 3-15.

Two types of ozonation experiments, namely, continuous liquid addition and batch, are described in this paper. In the continuous liquid addition experiments, the ozone stock solution was pumped at rates between 2.2 and 4.5 mL/min into a 2-L solution in a closed reactor, which contained ciprofloxacin and the background matrix of choice. No drop in aqueous ozone concentration was observed between the stock solution and the tubing entering the reactor. Experiments were run for 30 minutes with continuous ozone addition from the stock solution; the flow rate of that solution was adjusted for different experiments to capture the treatment window of ciprofloxacin in different background matrices. Changes in volume were accounted for and ciprofloxacin concentrations were normalized. The applied ozone dose ($[O_3]_{\text{applied}}$) was computed by dividing the product of the flow rate of the stock solution, the ozone concentration of the stock solution, and the time that the sample was taken by the volume of solution in the reactor.

For the batch kinetics experiments, a small aliquot of ozone stock solution, corresponding to a specific ozone dose, was introduced into a 1-L reactor containing ciprofloxacin and the background matrix of choice. A bottle-top dispenser with Teflon tubing was used to rapidly sample at small time intervals. Two types of batch experiments were conducted. The first type of experiment involved the introduction of 10 mM *t*-BuOH, a recognized hydroxyl radical scavenger (Dodd *et al.*, 2006), into the 1-L reactor. Hence, this experiment allows determination of the second order rate constant for ciprofloxacin reaction with ozone. The apparent rate constant (corresponding to a specific pH) can be calculated by plotting the transformation of ciprofloxacin ($\ln [CIP]/[CIP]_0$) vs. ozone exposure ($\int [O_3]dt$), as described in Eq. 5-1.

$$\ln \frac{[CIP]}{[CIP]_0} = -k''_{O_3,app,CIP} \int_0^t [O_3]dt \quad \text{Eq. 5-1}$$

The other batch experiment employed 1 μ M *p*CBA, which is known to react minimally with ozone ($k''_{O_3,pCBA} = 0.15 \text{ M}^{-1}\text{s}^{-1}$; Yao and Haag, 1991), but quickly with hydroxyl radicals ($k''_{HO\cdot,pCBA} = 5.2 \times 10^9 \text{ M}^{-1}\text{s}^{-1}$; Neta and Dorfman, 1968). By monitoring the transformation of *p*CBA, R_{ct} ($\int [HO\cdot]dt / \int [O_3]dt$) can be determined (Elovitz and von Gunten, 1999). R_{ct} is calculated by dividing the slope of $\ln [pCBA]/[pCBA]_0$ vs. $\int [O_3]dt$ by $k''_{HO\cdot,pCBA}$, as shown in Eq. 5-2.

$$\ln \frac{[pCBA]}{[pCBA]_0} = -k''_{HO\cdot,pCBA} \times R_{ct} \times \int_0^t [O_3]dt \quad \text{Eq. 5-2}$$

Finally, the second order rate constant between ciprofloxacin and hydroxyl radicals was determined by plotting $\ln [CIP]/[CIP]_0$ vs. ozone exposure for the *p*CBA experiment. In this case, both O_3 and $HO\cdot$ contribute to the transformation of ciprofloxacin, and so both terms are included in Eq. 5-3. The slope of Eq. 5-3 can be manipulated to yield $k''_{HO\cdot,app,CIP}$ since $k''_{O_3,app,CIP}$ and R_{ct} were determined above.

$$\ln \frac{[PhAC]}{[PhAC]_0} = - \left(k_{O_3,app,PhAC}'' + k_{HO\cdot,app,PhAC}'' \times R_{ct} \right) \int_0^t [O_3] dt \quad \text{Eq. 5-3}$$

Modeling ciprofloxacin transformation in the continuous aqueous ozone addition reactor. The NOM in solution exerts a large ozone demand. Essentially, as each drop of ozone stock solution is introduced into the reactor, it quickly reacts with ciprofloxacin and the DOC matrix. In such scenarios, hydroxyl radical exposure is negligible. Then, ciprofloxacin transformation can be modeled according to Eq. 5-4.

$$\frac{d[CIP]}{dt} = -k_{O_3,app,CIP} \times [CIP] \times [O_3] \quad \text{Eq. 5-4}$$

[CIP] is the ciprofloxacin concentration, $k_{O_3,app,CIP}$ is the apparent rate constant for ciprofloxacin reaction with ozone, and $[O_3]$ is the aqueous ozone concentration. In this case, the aqueous ozone concentrations were low due to rapid ozone reaction with ciprofloxacin and NOM. Then, over the course of an experiment (or until ciprofloxacin and the reactive fraction of the NOM matrix are exhausted), the ozone concentration in the reactor will remain nearly steady at a very low value. In this case, samples were analyzed using the indigo blue method; however, no change in absorbance was observed, that is, the concentration of aqueous ozone in the reactor was below detection (6×10^{-8} M) for solutions containing DOC. For the synthetic water (without DOC), the aqueous ozone concentration was directly proportional to the applied ozone dose in the region of ciprofloxacin transformation. For these reasons, a proportionality constant (k_{prop}) was used to relate the aqueous ozone exposure with the applied ozone exposure (Eq. 5-5).

$$k_{prop} = \frac{\int_0^t [O_3]_{aqueous} \times dt}{\int_0^t [O_3]_{applied} \times dt} \quad \text{Eq. 5-5}$$

The aqueous ozone exposure is the integration of the aqueous ozone concentration in the reactor with respect to time, whereas the applied ozone exposure is the integration of the applied ozone dose (constant) over time. Therefore, k_{prop} describes the proportion of the applied ozone exposure that is available as aqueous ozone exposure. Lower values of k_{prop} correspond to high ozone demands from the background water matrix (*i.e.*, NOM).

Integration of Eq. 5-4 with substitution of Eq. 5-5 yields the model represented in Equation 5-6.

$$[CIP] = [CIP]_o \times \exp \left(-k_{O_3,app,CIP} \times k_{prop} \times \int_0^t [O_3]_{applied} \times dt \right) \quad \text{Eq. 5-6}$$

Application of this model provided a good ($R^2 > 0.93$, in all cases) fit to all experimental data for ciprofloxacin; that is, the curves in these figures represent fits of Eq. 5-6 to the data, with the only fitting parameter being k_{prop} .

Analytical procedures. The ozone concentration of the stock solution was calculated directly using the absorbance at 258 nm and the molar absorptivity of ozone ($3000 \text{ M}^{-1}\text{cm}^{-1}$; Acero and von Gunten, 2000). Aqueous ozone measurements for kinetics experiments were measured using the indigo blue method (Bader and Hoigné, 1981).

Ciprofloxacin was measured by high performance liquid chromatography (HPLC; Waters 2795, Waters Corporation, Milford, MA) with a fluorescence detector; a Phenomenex (Torrence, CA) Luna 5u C₁₈(2) (250×4.6mm, 5μm) column was utilized for analyte separation. 50-μL aliquots were injected directly into the HPLC. The analytical method is based on the procedure developed by Golet *et al.* (2001) but several changes were made to optimize the response on our instrument. The eluent gradient was 7% acetonitrile (ACN), 93% 25-mM H₃PO₄ for 2 min; 3 min ramp to 12% ACN, 88% 25-mM H₃PO₄; 2 min ramp to 15% ACN, 85% 25-mM H₃PO₄; 3 min ramp to 20% ACN,

80% 25-mM H₃PO₄; 10 min isocratic. The flow rate was 0.70 mL/min, and the column temperature was set at 40°C. Excitation and emission wavelengths were set at 278 nm and 445 nm, respectively.

Microorganisms. *Escherichia coli* #25922 was purchased from the American Type Culture Collection (ATCC). A small amount of the freeze-dried *E. coli* was scraped into 10-mL of MHB and incubated in ambient air at 37°C for 24 hours. After the incubation period, the *E. coli* suspension was mixed 1:1 with 50% glycerol and stored at -80°C. Before experimentation, a small amount of the frozen *E. coli* stock was scraped into 10 mL of MHB and incubated aerobically at 37°C for 12-18 hours. To prepare the inoculum, the stock *E. coli* solution was diluted with MHB to obtain the same absorbance (*ABS*) at 600 nm as a BaSO₄ turbidity standard equivalent to a 0.5 McFarland standard.

Antimicrobial susceptibility assay. The antimicrobial susceptibility assay, which was based on the NCCLS protocol (2004), was run in 96-well microplates. Wells were partially filled with 50 µL of either a standard containing a known concentration of ciprofloxacin in the background matrix of choice or a sample from ozonation experiments; then, 50 µL of the *E. coli* inoculum was added to each well. Positive growth controls consisted of 50 µL of the background matrix without the drug and 50 µL of inoculum; negative growth controls contained 50 µL of the background matrix and 50 µL of MHB. All standards and samples were prepared in triplicate. Microplates were covered in Parafilm to prevent evaporative water loss and incubated in ambient air at 37°C for 20 hours, while being shaken at 75 rpm; no condensation appeared on the inside of the Parafilm. After this incubation period, plates were shaken for 5 minutes in a microplate reader (BioTek), and the wells were aspirated using a micropipette. The absorbance at 600 nm was recorded. The absorbance at 600 nm for the positive/negative growth controls was used to calculate the percent of *E. coli* inhibition for a given sample.

This assay has been employed previously in two different ways to describe the removal of antimicrobial activity associated with antimicrobial compounds throughout water treatment processes. Some researchers (Dodd *et al.*, 2009; Paul *et al.*, 2010) have serially diluted individual samples to describe residual antimicrobial activity as a stoichiometric measure of ciprofloxacin remaining using potency equivalents ($PEQ = IC_{50,standard} / IC_{50,sample}$). This technique allows description of the residual antimicrobial activity for PhAC concentrations that are greater than the minimum concentration required to completely inhibit microbial growth, as the serially diluted samples will still demonstrate a spectrum of inhibitory activity. If intermediate oxidation products do not contribute to the residual antimicrobial activity, the PEQ data should be equivalent to the fraction of ciprofloxacin remaining in solution ($[CIP]/[CIP]_0$); however, if intermediate oxidation products exert some antimicrobial activity, then the PEQ data will fall above the 1:1 line. This approach is especially useful for quantifying the contribution of early intermediate products to residual antimicrobial activity when the concentrations of the parent compound and intermediates are high.

The assay has also been employed for triclosan, sulfamethoxazole, sulfamethazine, sulfadiazine, trimethoprim, bisphenol-A, and diclofenac without serial dilution of individual samples (Suarez *et al.*, 2007; Baeza, 2008). The variation of antimicrobial activity as a function of extent of treatment is measured for samples containing undiluted concentrations of parent and intermediate oxidation products. In this scenario, the percent of *E. coli* inhibition (*i.e.*, the residual antimicrobial activity) is plotted as a function of the aqueous concentration of the parent compound or applied ozone dose. Antimicrobial activity contributions from intermediate oxidation products can be assessed via the presence of shifts in the inhibition profile of treated samples as compared to the inhibition profile of standard solutions obtained from serial dilution of the parent compound in the background matrix. As the focus of this research was to demonstrate ciprofloxacin transformation and antimicrobial activity removal in the presence of different background water matrices, this assay configuration was employed.

RESULTS AND DISCUSSION

Ciprofloxacin oxidation. Synthetic water was prepared by adding 200 mg/L NaHCO₃, 100 mg/L NaCl, and 100 µg/L ciprofloxacin to deionized water; the solution pH was approximately 8.3. Two other solutions were created by adding 2 mg/L DOC and 4 mg/L DOC of Lake Austin HPOA to the synthetic water recipe; the pH was 8.4 for both of these solutions. Ozone was applied to these solutions using the continuous liquid addition process described above, and represented in Figure 3-15. The ciprofloxacin degradation for these three solutions as a function of applied ozone dose is shown in Figure 5-1. For the synthetic water matrix (no organic matter), the aqueous ozone concentration was found to be directly correlated to the applied ozone dose in the region of ciprofloxacin transformation. In contrast, aqueous ozone concentrations in solutions containing organic matter were below detection ($[O_3] < 6 \times 10^{-8}$ M) with the indigo blue method throughout experimentation due to the high ozone demand of the NOM; the low aqueous ozone concentration is discussed in more detail below. For these reasons, the applied ozone dose was used as the principal descriptor of ozone introduced to the reactor. The data in Figure 5-1 represent the extent of reaction for the specific ozone dose and background matrix.

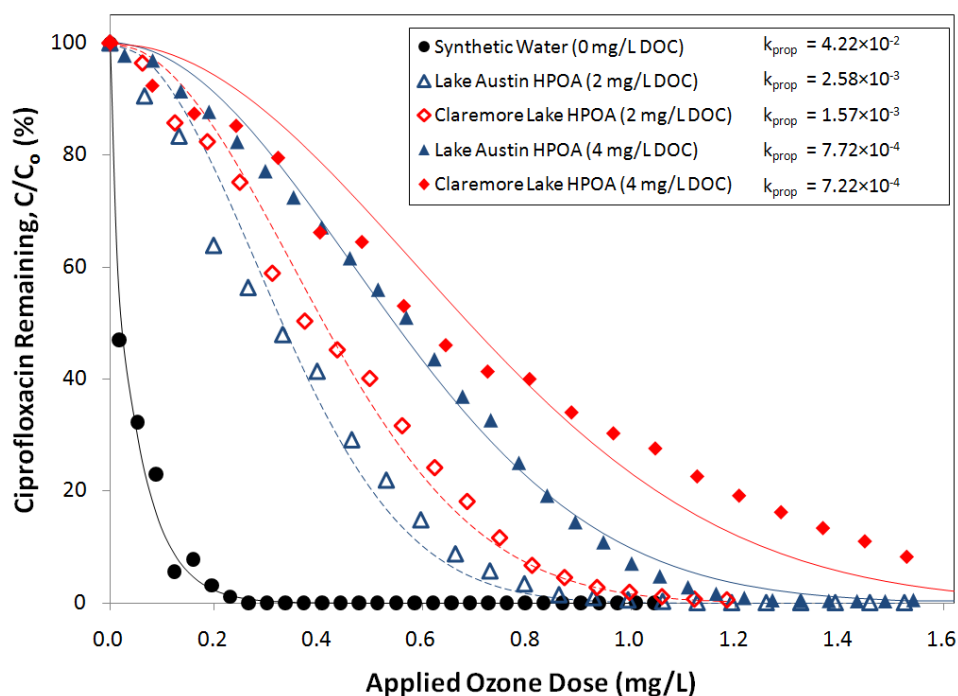


Figure 5-1. The impact of NOM source (no organic matter, Lake Austin HPOA, and Claremore Lake HPOA) and concentration (0, 2, and 4 mg/L DOC) on ciprofloxacin oxidation. (Symbols represent experimental data; curves represent model fits using Eq. 5-6. Initial ciprofloxacin concentration = 100 µg/L)

In the synthetic water (no DOC), ciprofloxacin was transformed at a low applied dose of ozone, with 50% removal at an applied ozone dose of approximately 0.06 mg/L. The water samples containing 2 and 4 mg/L DOC of Lake Austin HPOA showed markedly higher 50% removal treatment requirements, 0.33 and 0.54 mg/L applied O_3 , respectively. These differences manifest because the HPOA exert an ozone demand, thereby decreasing the amount of ozone (and its primary degradation product, hydroxyl radicals) available to react with ciprofloxacin. At higher DOC concentrations, the number of organic matter sites available for reaction with ozone increases yielding a higher degree of competition between NOM and ciprofloxacin for ozone. Therefore, a smaller fraction of the applied oxidant is available for ciprofloxacin oxidation in the

presence of 4 mg/L DOC from Lake Austin HPOA as compared to 2 mg/L DOC, and higher applied ozone doses are required to remove ciprofloxacin.

The results from ozonating solutions containing Claremore Lake HPOA (pH 8.4) are shown along with the Lake Austin HPOA data sets in Figure 5-1. The solutions containing 2 mg/L DOC and 4 mg/L DOC from Claremore Lake HPOA demonstrated 50% removal treatment requirements of 0.41 and 0.69 mg/L applied O_3 , respectively; these treatment requirements are higher than the corresponding values for the Lake Austin HPOA solutions. Recall from Figure 5-1 that the $SUVA_{254}$ of Claremore Lake HPOA (3.9 L/mg-m) is markedly greater than that of the Lake Austin HPOA (2.5 L/mg-m). The data suggest a relationship between the $SUVA_{254}$ of the HPOA and the 50% treatment requirement. Such a relationship follows from the work of Westerhoff *et al.* (1999a), who demonstrated that the oxidant rate parameters for NOM reaction with ozone and hydroxyl radicals are directly related to $SUVA_{254}$. Therefore, NOM with higher $SUVA_{254}$ are expected to exert a greater ozone demand than those with lower $SUVA_{254}$. Then, the increased organic matter reactivity (with respect to ozone and hydroxyl radicals) causes greater oxidant consumption by the Claremore Lake HPOA as compared to Lake Austin HPOA. The difference in NOM reactivity with ozone results in less oxidant reaction with ciprofloxacin in the Claremore Lake HPOA matrix, and hence, less ciprofloxacin transformation for a given applied ozone dose. Figure 5-1, then, demonstrates the significance of Westerhoff *et al.*'s (1999a) findings regarding NOM reactivity with ozone and hydroxyl radicals for oxidation processes targeting trace organic contaminants. While these results are expected, it is interesting to note that in an ozone limited treatment scenario, such as that presented here, NOM can have major impacts (*i.e.*, the 50% treatment requirements varied widely for the 0 mg/L DOC, 4 mg/L DOC from LA HPOA, and 4 mg/L DOC from CL HPOA cases: 0.06, 0.54, and 0.69 mg/L applied ozone, respectively).

It is interesting to consider these 50% treatment requirements as a function of the mass ratio of applied ozone to DOC. While the required ozone dose depends on the DOC composition, mass ratios of applied ozone to DOC of 1-2 mg O₃/mg DOC are generally recommended for ozonation processes (van der Kooij *et al.*, 1989; Langlais *et al.*, 1991). In this case, 50% removal was observed at applied ozone to DOC mass ratios ranging from 0.14-0.21 mg applied O₃/mg DOC. These results indicate that ciprofloxacin competes rather well with Lake Austin HPOA and Claremore Lake HPOA for reaction with ozone.

The competition between NOM and ciprofloxacin for the oxidant is a function of the transformation kinetics of these compounds by ozone and hydroxyl radicals. To demonstrate that the transformation kinetics of ciprofloxacin with ozone and hydroxyl radicals does not change in the presence of organic matter, kinetics tests were run in the absence and presence of Claremore Lake HPOA. Figure 5-2 shows data and model fits for the two types of batch kinetics experiments described above. The second order rate constants for ciprofloxacin reaction with ozone ($k''_{O_3,app,CIP} = 1.55(\pm 0.13) \times 10^4 \text{ M}^{-1}\text{s}^{-1}$ at pH 7.0) and hydroxyl radicals ($k''_{HO\cdot,app,CIP} = 1.19(\pm 0.69) \times 10^{10} \text{ M}^{-1}\text{s}^{-1}$ at pH 7.0) do not significantly change in the presence of 0.5 mg/L DOC from Claremore Lake HPOA ($k''_{O_3,app,CIP} = 1.33(\pm 0.25) \times 10^4 \text{ M}^{-1}\text{s}^{-1}$; $k''_{HO\cdot,app,CIP} = 1.32(\pm 0.55) \times 10^{10} \text{ M}^{-1}\text{s}^{-1}$). No significant difference in the rate constants for ciprofloxacin with ozone and hydroxyl radicals were observed in presence/absence of NOM. These results confirm that the differences between the data sets shown in Figure 5-1 derive from the oxidant demand exerted by the DOC concentration and HPOA composition.

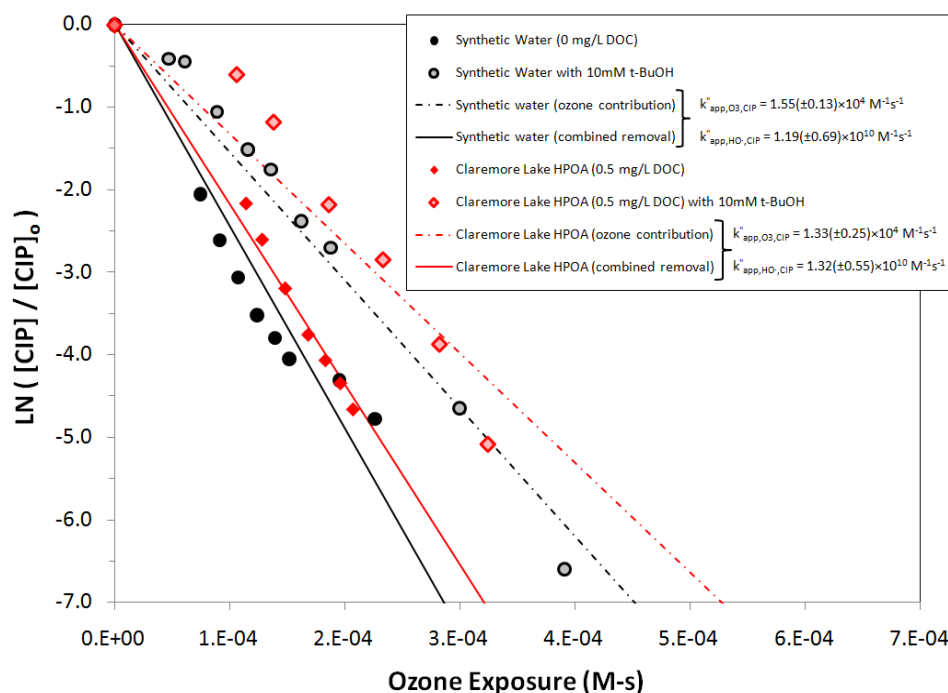


Figure 5-2. Kinetics of ciprofloxacin reaction with ozone and hydroxyl radical at pH 7 with 1mM NaHCO₃ in two solutions, one without organic matter and one with 0.5 mg/L DOC from Claremore Lake HPOA. (Symbols represent experimental data; curves represent second-order kinetics model fits. Initial ciprofloxacin concentration = 100 µg/L)

These values are comparable to rate constants available in the literature. For example, Dodd *et al.* (2006) found an apparent second order rate constant of $1.9 \times 10^4 \text{ M}^{-1}\text{s}^{-1}$ for the reaction between ciprofloxacin and ozone at pH 7. An *et al.* (2010) conducted pulse radiolysis experiments to obtain a value of $2.15(\pm 0.1) \times 10^{10} \text{ M}^{-1}\text{s}^{-1}$ for $k''_{\text{HO}\cdot, \text{app}, \text{CIP}}$; contrarily, Dodd *et al.* (2006) reported a value of $4.1(\pm 0.3) \times 10^9 \text{ M}^{-1}\text{s}^{-1}$. The value found in this work, $k''_{\text{HO}\cdot, \text{app}, \text{CIP}} = 1.19(\pm 0.69) \times 10^{10} \text{ M}^{-1}\text{s}^{-1}$ (at pH 7.0), falls between these two reported values. Ultimately, the high rate constant for ciprofloxacin transformation by ozone indicates that ozone processes can effectively treat water sources containing ciprofloxacin; furthermore, as demonstrated above, this reaction is also competitive in the presence of high DOC concentrations.

The impact of NOM composition was also investigated using the continuous liquid ozone addition reactor. Figure 5-3 shows ciprofloxacin transformation for the synthetic water and 2 and 4 mg/L DOC from Claremore Lake HPOA and TPIA. The 50% removal treatment requirement for the solutions containing 2 and 4 mg/L DOC from Claremore Lake TPIA were 0.29 and 0.42 mg/L applied O₃, respectively, as compared to 0.41 and 0.69 mg/L applied O₃ for the solutions with 2 and 4 mg/L DOC from Claremore Lake HPOA. Table 5-2 lists the SUVA₂₅₄ values for the Claremore Lake HPOA and TPIA isolates as 3.9 and 2.5 L/mg-m, respectively. As noted above, Westerhoff *et al.* (1999a) demonstrated that the reactivity of NOM with ozone and hydroxyl radicals is directly related to SUVA₂₅₄. The data in Figure 5-3, and the resulting treatment requirements, agree with this relationship; however, to more fully describe this relationship more NOM sources should be studied. Regardless, it is clear that NOM composition can have a significant influence on the treatability of PhACs with ozone. Finally, it is important to note that the applied ozone to DOC mass ratio required for 50% ciprofloxacin transformation was relatively low, 0.11-0.15 mg applied O₃ / mg DOC.

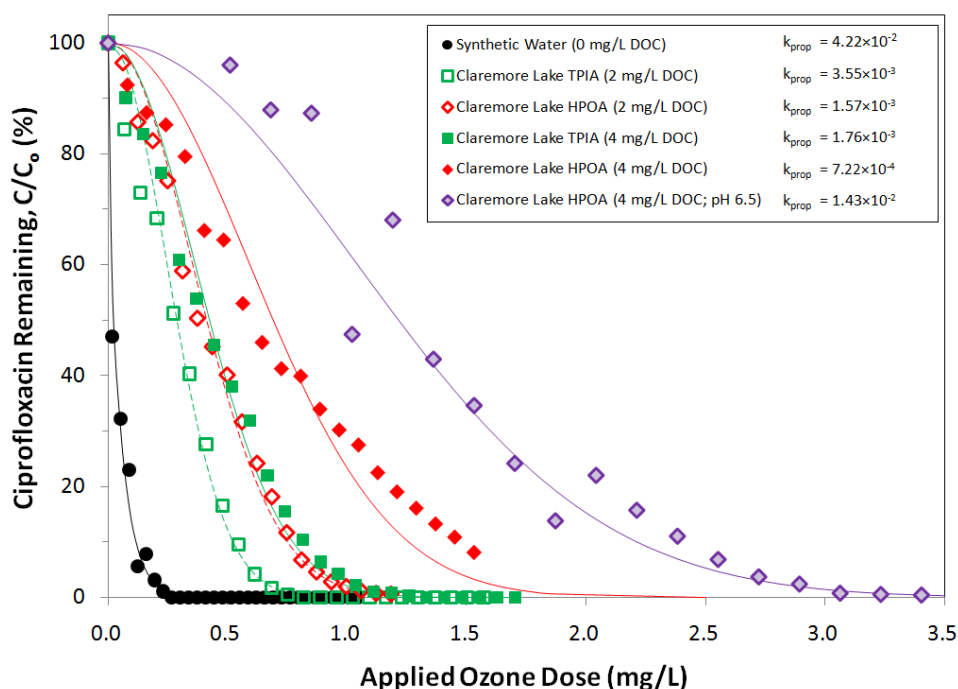


Figure 5-3. The impact of NOM composition (hydrophobic organic acids and transphilic organic acids fractions) and pH (8.4 and 6.5) of Claremore Lake organic matter on ciprofloxacin oxidation. (All data sets correspond to pH 8.4, unless otherwise noted. Symbols represent experimental data; curves represent model fits using Eq. 5-6. Initial ciprofloxacin concentration = 100 µg/L)

Solution pH can also play a significant role in ciprofloxacin transformation in different organic matter matrices because the second-order rate constant between ciprofloxacin and ozone is species dependent. Recall that the second-order rate constants found by Dodd *et al.* (2006) of the zwitterionic ($6.2 < \text{pH} < 8.8$) ciprofloxacin species with ozone is $7.5 \times 10^3 \text{ M}^{-1}\text{s}^{-1}$ and that of the deprotonated ($\text{pH} > 8.8$) species is $9.0 \times 10^5 \text{ M}^{-1}\text{s}^{-1}$; therefore, the rate constant is almost two orders of magnitude smaller at pH 6.5 than at pH 8.4. A set of continuous liquid ozone addition experiments (Figure 5-3) was run with 100 mg/L NaCl, 200 mg/L NaHCO₃, 100 µg/L ciprofloxacin, and 4 mg/L DOC from Claremore Lake HPOA at two distinct pH values: 6.5 and 8.4. The data in Figure 5-3 show that lower applied ozone doses are required to treat ciprofloxacin at pH 8.4, as compared to pH 6.5. Indeed, the 50% treatment requirement increased from 0.69 mg/L at

pH 8.4 to 1.29 mg/L applied O₃ at pH 6.5. Even though the apparent second-order rate constant for the reaction between ciprofloxacin and ozone is over 30 times lower at pH 6.5 than at pH 8.4, the ozone dose required to remove 50% of the ciprofloxacin only increases by a factor of approximately 1.9. As the aqueous ozone that is introduced to the reactor is used rapidly (*i.e.*, no significant buildup of aqueous ozone concentrations in the reactor throughout the experiment), no significant impact from the faster ozone decomposition rate at pH 8.4 (as compared to pH 6.5) can be expected. That is, as an excess of ozone is not available, ozone reaction with NOM and ciprofloxacin outcompete ozone decay. Hence, these results indicate that it is possible to effectively transform ciprofloxacin in the presence of high DOC concentrations for the pH range of interest (even when the second order rate constant with ozone varies within the 10³-10⁵ M⁻¹s⁻¹ range) to water treatment processes.

Inhibition profile. The inhibition profile of ciprofloxacin can be constructed by performing the antimicrobial susceptibility assay over a range of ciprofloxacin concentrations to determine regions of inhibition, partial inhibition, and no inhibition. In a specific background matrix, the inhibition profile will indicate the maximum drug concentration that shows no effect on the test microorganism, the minimum concentration that leads to complete inhibition (no growth of the microorganism), and an intermediate region with partial inhibition. The ciprofloxacin inhibition profile for *E. coli* ATCC #25922 in a background matrix containing 100 mg/L NaCl, 200 mg/L NaHCO₃, and 4 mg/L of Lake Austin DOC is shown in Figure 5-4. Note that the concentrations listed on the abscissa correspond to the ciprofloxacin concentration of the sample (not the microplate well).

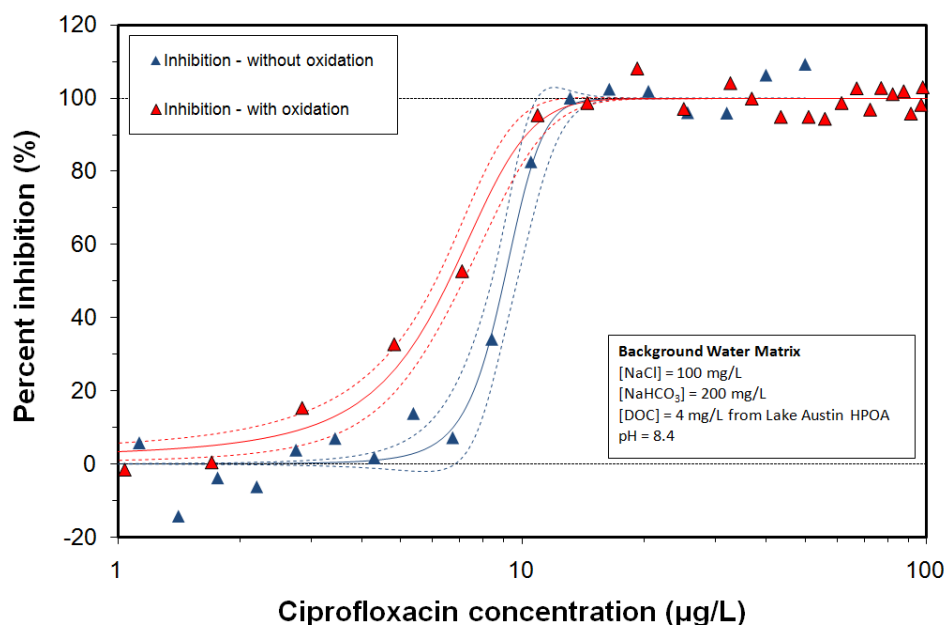


Figure 5-4. *E.coli* inhibition profiles with ciprofloxacin for standards (“without oxidation”) and ozonated samples (“with oxidation”). (The curves represent the Hill equation fit to the data ($R^2 = 0.966$ for both data sets); the dotted lines represent the 95% confidence bands found with GraphPad Prism software.)

The Hill curve (Equation 5-7) has been shown to describe dose-response curves (Suarez *et al.*, 2007; Baeza, 2008; Dodd *et al.*, 2009; Paul *et al.*, 2010) for antimicrobial compounds and was used to fit the data in Figure 5-4.

$$\% \text{ Inhibition} = \left[I_{\min} + \frac{I_{\max} - I_{\min}}{1 + \left(\frac{IC_{50}}{C_{\text{sample}}} \right)^H} \right] \times 100\% \quad \text{Eq. 5-7}$$

I_{\min} is the minimum inhibition (0%), I_{\max} is the maximum inhibition (100%), IC_{50} is the ciprofloxacin concentration that corresponds to 50% inhibition, C_{sample} is the sample’s ciprofloxacin concentration, and H is the Hill slope. The fitting parameters for this

equation are the values of IC_{50} and H . GraphPad Prism (GraphPad Software, Inc.) was used to solve for IC_{50} and H . The focus of the current discussion is on the data set labeled, “without oxidation”; the “with oxidation” data set is discussed subsequently. The values of the “without oxidation” model line in Figure 5-4 are $IC_{50} = 9.0 \mu\text{g/L}$ and $H = 0.42$ ($R^2 = 0.966$); the surrounding dotted lines represent the 95% confidence intervals determined by GraphPad Prism. Use of this equation provides a convenient way to quantify the effects of other parameters (such as the treatment conditions or NOM content) on the inhibition profile. Furthermore, by substituting Eq. 5-6 into Eq. 5-7, we can measure the antimicrobial activity (in terms of *E. coli* inhibition) as a function of the applied treatment, *i.e.*, applied ozone dose.

The most important facet of Figure 5-4 is that the relationship between ciprofloxacin concentration and antimicrobial activity follows a sharp S-shaped curve. This characteristic results in a narrow window of partial activity; for ciprofloxacin with *E. coli* #29522, that window is only about $7 \mu\text{g/L}$ wide (Figure 5-4). For other pharmaceuticals and personal care products, the width of that region of partial antimicrobial activity may differ (Suarez *et al.*, 2007; Baeza, 2008; Dodd *et al.*, 2009; Paul *et al.*, 2010).

Removal of antimicrobial activity. With the ability to monitor antimicrobial activity through the antimicrobial susceptibility assay, the relationships between applied ozone dose, ciprofloxacin concentration, and antimicrobial activity can be described. Figure 5-5 shows model fits for ciprofloxacin remaining and data and model fits for antimicrobial activity (as a percent of *E. coli* inhibition, see Eq. 5-7) as a function of the applied ozone dose for the synthetic and Lake Austin HPOA solutions shown in Figure 5-1. For all three solutions, the antimicrobial activity remains nearly constant ($100(\pm 10)\%$ *E. coli* inhibition) until the ciprofloxacin remaining approaches approximately 20% (*i.e.*, $20 \mu\text{g/L}$) for the 0 and 2 mg/L DOC solutions and approximately 15% for the 4 mg/L DOC solution. At those points, the antimicrobial activity drops from 100% to 0% over a

narrow window of applied ozone dose (approximately 0.1-0.2 mg/L applied O_3). The treatment requirements for 50% removal of antibiotic activity for the synthetic (0 mg/L DOC) and Lake Austin HPOA (2 and 4 mg/L DOC) solutions are shown in Table 5-3. Clearly, the impact of organic matter on ciprofloxacin transformation is the major cause for the differences in the applied ozone dose required to remove the antimicrobial activity from these three solutions.

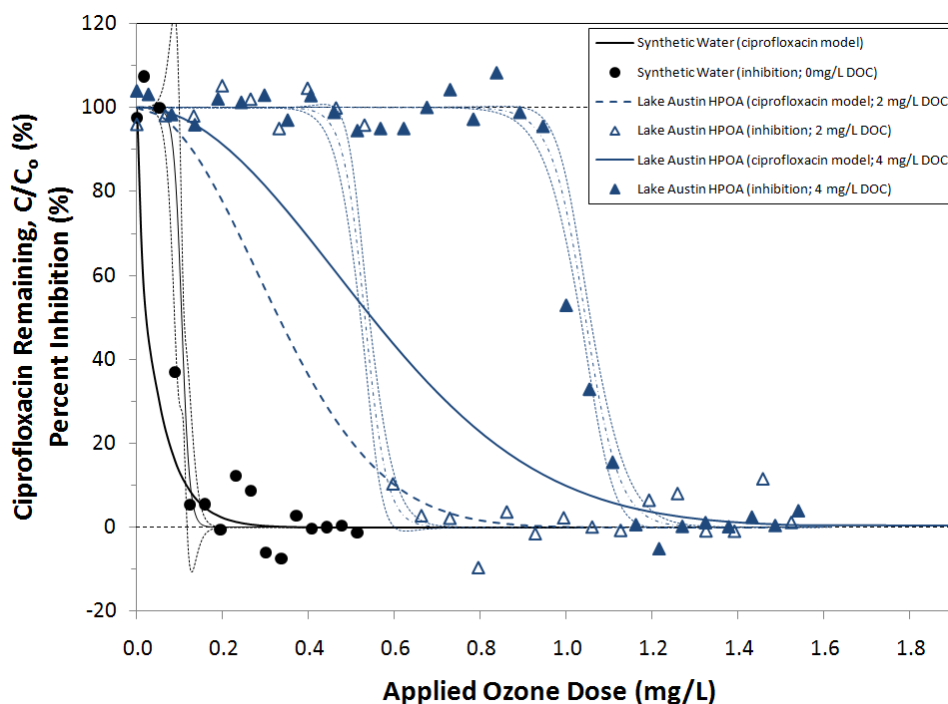


Figure 5-5. Simultaneous removal of ciprofloxacin (heavy curves; corresponding to the model fits from Figure 5-1) and antimicrobial activity (hollow symbols) in the synthetic (0 mg/L DOC) and Lake Austin HPOA (2 and 4 mg/L DOC) solutions. (The Hill curve ($R^2 > 0.91$ in all cases) and accompanying 95% confidence bands (light curves) are shown for the antimicrobial activity data. Initial ciprofloxacin concentration = 100 $\mu\text{g/L}$)

The effects of NOM concentration, source, and composition on elimination of antimicrobial activity with ozone are further expounded in Figure 5-6, which shows the antimicrobial activity history for ciprofloxacin in the synthetic water, the Lake Austin

HPOA solution (4 mg/L DOC), and the Claremore Lake HPOA and TPIA solutions (4 mg/L DOC); in all cases the R^2 associated with the Hill curve was greater than 0.91. As expected from Figure 5-1 and Figure 5-3, the ciprofloxacin solution containing Claremore Lake HPOA requires the greatest applied ozone dose to eliminate antimicrobial activity; excepting the synthetic water, the lowest treatment requirement was observed in the Claremore Lake TPIA matrix. The elimination of antimicrobial activity in the solutions containing 2 mg/L DOC exhibited lower ozone treatment requirements than the 4 mg/L DOC solutions and followed the same order (*i.e.*, Claremore Lake TPIA < Lake Austin HPOA < Claremore Lake HPOA) in all cases; these data were not included in Figure 5-6 to maintain clarity.

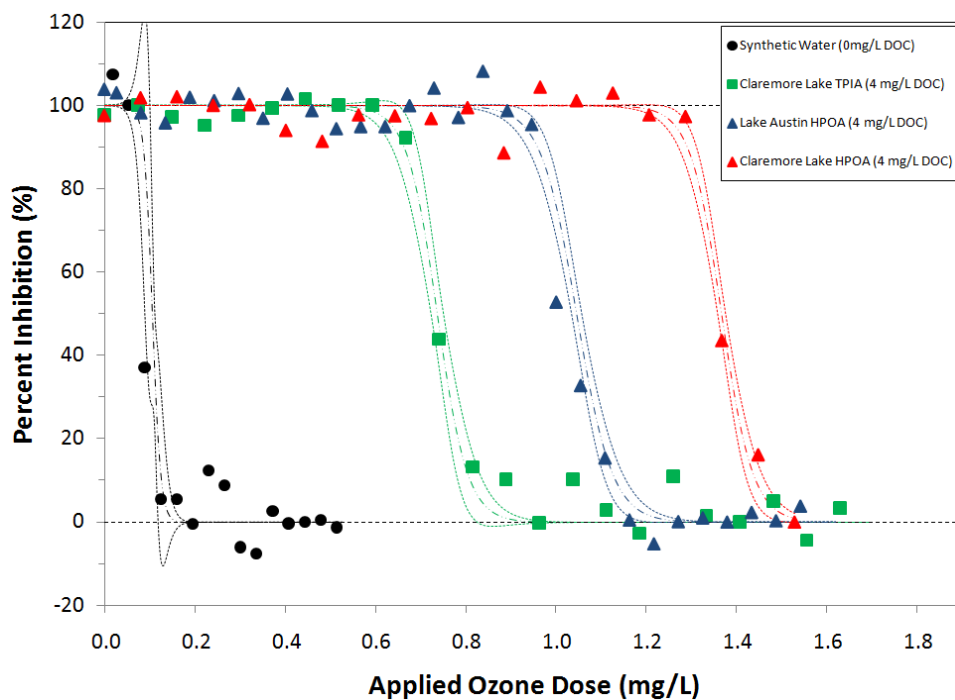


Figure 5-6. Elimination of antimicrobial activity in the synthetic (0 mg/L DOC), Lake Austin HPOA (4 mg/L DOC), and Claremore Lake HPOA and TPIA (4 mg/L DOC) water matrices. (The Hill curve ($R^2 > 0.91$ in all cases) and accompanying 95% confidence bands are shown. Initial ciprofloxacin concentration = 100 $\mu\text{g/L}$)

The treatment requirements for 50% removal of ciprofloxacin and antibiotic activity for the synthetic (0 mg/L DOC), Lake Austin HPOA (2 and 4 mg/L DOC), and Claremore Lake HPOA and TPIA (2 and 4 mg/L DOC) waters are shown in Table 5-3. The treatment requirements for 50% removal of ciprofloxacin correlate well to the treatment requirements for 50% removal of antimicrobial activity ($R^2 = 0.992$; not shown). This result would be expected if ciprofloxacin is the most potent compound present in solution. The treatment required for 50% removal of ciprofloxacin and antimicrobial activity in the 0 mg/L DOC solution was subtracted from that of the 2 and 4 mg/L DOC solutions. Then, the ratio of the normalized 50% treatment requirements was calculated (not shown). The ratio of the treatment requirement for 50% removal of ciprofloxacin in the 2 mg/L DOC solution to that of the 4 mg/L DOC solution was approximately 59%; for antimicrobial activity, the value of the ratio is 51%. With only three NOM sources, no conclusive relationships can be made regarding these treatment requirement ratios; however, these data suggest that the 50% treatment requirements for antimicrobial activity scale relatively well with DOC concentration.

Table 5-3. Applied ozone dose (mg/L) necessary for 50% removal of ciprofloxacin and antimicrobial activity for a variety of NOM matrices.

Solution	50% Removal of ciprofloxacin	50% Removal of antimicrobial activity
Synthetic (0 mg/L DOC)	0.06	0.11
Claremore Lake TPIA (2 mg/L DOC)	0.29	0.45
Lake Austin HPOA (2 mg/L DOC)	0.33	0.53
Claremore Lake HPOA (2 mg/L DOC)	0.41	0.76
Claremore Lake TPIA (4 mg/L DOC)	0.42	0.74
Lake Austin HPOA (4 mg/L DOC)	0.54	1.04
Claremore Lake HPOA (4 mg/L DOC)	0.69	1.37
Claremore Lake HPOA (4 mg/L DOC; pH 6.5)	1.29	2.54

Impact of intermediate products on antimicrobial activity. While the data in Figure 5-5 suggest that ciprofloxacin is the major contributor to antimicrobial activity in these experiments, the pharmacology fundamentals discussed earlier demonstrate the potential for forming pharmacologically active intermediate oxidation products. This issue can be

more closely investigated by comparing ciprofloxacin inhibition profiles deriving from standards and ozonated samples. In Figure 5-4, the “without oxidation” curve represents the inhibition profile of standard solutions while the “with oxidation” curve corresponds to the inhibition profile of treated samples. Therefore, the “with oxidation” data exemplifies not only the antimicrobial activity of ciprofloxacin at the concentrations listed on the abscissa but also any pharmacological impact from intermediate oxidation products and/or treatment byproducts. The IC_{50} for the “no oxidation” data set is 9.0 $\mu\text{g/L}$, while the IC_{50} for the “with oxidation” data set was 6.6 $\mu\text{g/L}$. Furthermore, the partially inhibited region was “stretched” in the “with oxidation” data set as evidenced by the smaller Hill slope value: 0.42 and 0.26 for “no oxidation” and “with oxidation,” respectively. The shift in the data indicates that equivalent antimicrobial activities manifest in the presence of lower ciprofloxacin concentrations within ozone treated samples, suggesting that some other compounds are exerting pharmacological activity. It should be noted that samples from control experiments run by ozonating the three NOM sources did not exert any antimicrobial activity, *i.e.*, the inhibition profile and the resultant shift were observed for all background water matrices. In similar experiments, Dodd *et al.* (2009) did not find evidence of pharmacologically active intermediate products from ciprofloxacin ozonation; however, Paul *et al.* (2010) recently reported that early ciprofloxacin intermediate products formed through photolysis (UV) and photocatalysis (UV/TiO₂) did exert some pharmacological activity. Both of these studies employed the serial dilution scheme (see Chapter 3 and Appendix C) for running the antimicrobial activity assay.

In the serial dilution scheme employed by Dodd *et al.* (2009) and Paul *et al.* (2010), ciprofloxacin concentrations are being serially diluted, but so are intermediate oxidation products. As the region of partial inhibition for ciprofloxacin is narrow (approximately, 7 $\mu\text{g/L}$), it is reasonable to assume the region of partial inhibition for intermediate products is also narrow. Hence, if the antimicrobial potency of intermediate oxidation products is less than that of the parent compound and the inhibition profile is

sharp, any antimicrobial activity stemming from the presence of intermediate oxidation products may be masked in the serial dilution scheme. This is an important point, because it acknowledges the utility of the serial dilution scheme for employing the antimicrobial activity assay at high antibiotic concentrations but it also suggests that the employment of this technique at lower drug concentrations may mask the contributions of intermediate oxidation products to the ultimate antimicrobial activity. For ciprofloxacin, the serial dilution scheme is more useful at ciprofloxacin concentrations greater than 11 µg/L, and the direct antimicrobial activity measurement scheme is most useful at concentrations lower than 11 µg/L.

Another reason for the difference between our results and those of Dodd *et al.* (2009) lies in the inherent difference in the initial ciprofloxacin concentration employed. In the Dodd *et al.* (2009) and Paul *et al.* (2010) papers, the initial ciprofloxacin concentration was 330-1650 and 33,100 µg/L, respectively; we used initial ciprofloxacin concentrations of 100 µg/L. In the Paul *et al.* (2010) paper, the data suggests a slight contribution of intermediate oxidation products to the residual antimicrobial activity; however, Dodd *et al.* (2009) saw no impact from ciprofloxacin's intermediate oxidation products. This difference may be due to the initial ciprofloxacin concentrations employed. The higher initial concentration in the Paul *et al.* (2010) study would result in higher concentrations of intermediate oxidation products. Therefore, dilution of those samples would result in greater intermediate oxidation product concentrations being introduced into the assay, allowing the contribution of those products to the residual antimicrobial activity to be observed. Although our initial ciprofloxacin concentration (100 µg/L) was lower than that employed in the Dodd *et al.* (2009) and Paul *et al.* (2010) papers, intermediate oxidation products were not diluted and, therefore, the contribution of those compounds to the residual antimicrobial activity was observed. Both methods for running the antimicrobial activity assay have merit and provide meaningful data; however, it is clear that the best method for characterizing the antimicrobial potency of intermediate products is through isolation of those compounds and developing their

individual inhibition profiles. For that reason, further investigation is necessary to positively identify the cause for the shift in the inhibition profile of partially treated samples observed in Figure 5-4.

The organic matter source, concentration, and composition have all been shown to impact ciprofloxacin transformation in ozonation. That impact significantly affects the removal of antimicrobial activity. Furthermore, the presence of pharmacologically active intermediate oxidation products has been shown to be theoretically possible, and the data presented above suggests that active intermediate products are present in experimental samples. The combined determination of ciprofloxacin concentration and antimicrobial activity throughout treatment provides a useful metric for determining the treatment requirement. Ultimately, the application of an ozone model that incorporates the kinetics of ozone decomposition and oxidation of NOM should be able to predict destruction of parent PhACs; however, the development of such a model will eventually have to include pharmacologically active intermediate oxidation products.

CHAPTER 6: OZONATION OF ERYTHROMYCIN: RATE CONSTANTS, MAJOR INTERMEDIATE PRODUCTS, AND REMOVAL OF ANTIMICROBIAL ACTIVITY

ABSTRACT

Ozone experiments were run with erythromycin A, which is the only antibiotic/antimicrobial compound listed on the US EPA Candidate Contaminant List 3. The rate constant for erythromycin A transformation by ozone was found to be $4.36(\pm 0.14) \times 10^6 \text{ M}^{-1}\text{s}^{-1}$. Additionally, the rate constant for anhydroerythromycin A, the common form of erythromycin present in the environment, with ozone was determined to be $6.00(\pm 0.25) \times 10^6 \text{ M}^{-1}\text{s}^{-1}$. The dominant intermediate oxidation products for erythromycin A and anhydroerythromycin A were determined to be erythromycin A N-oxide and anhydroerythromycin A N-oxide. An antimicrobial activity assay was employed to determine the inhibition profile of erythromycin A against *E. coli* (ATCC 25922), and an IC_{50} of approximately $4.87(\pm 0.55) \times 10^{-5} \text{ M}$ was determined. Treated samples were introduced to an antimicrobial activity assay; however, the presence of intermediate oxidation products did not alter the residual antimicrobial activity, that is, the intermediate oxidation products were not pharmacologically active. Ozonation effectively removed the antimicrobial activity associated with erythromycin A; furthermore, the antimicrobial activity of anhydroerythromycin A was determined to be negligible. That fact, along with the irreversible formation of anhydroerythromycin A (from erythromycin A), downplay the need for treatment of anhydroerythromycin A.

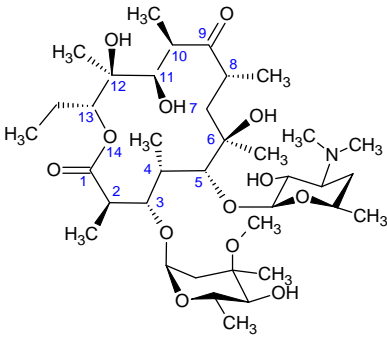
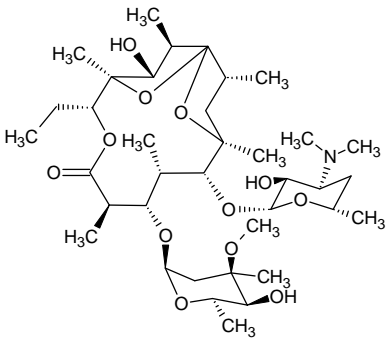
Key words: erythromycin A, anhydroerythromycin A, ozone, residual antimicrobial activity, reaction kinetics, intermediate oxidation products

Manuscript to be submitted to *Environmental Science and Technology*

INTRODUCTION

The U.S. Environmental Protection Agency recently released its Candidate Contaminant List 3 (CCL3; EPA, 2009). Of the 104 chemical compounds present on that list, erythromycin is the only antimicrobial; most compounds are pesticides, herbicides, insecticides, or estrogenic chemicals (EPA, 2009). Erythromycin is a macrolide antimicrobial compound containing a large 14-membered lactone ring with two sugar moieties (C-3 L-cladinose and C-5 D-desosamine). Under environmental conditions, erythromycin exists as two major forms: erythromycin A, which is the conventional structure of erythromycin, and anhydroerythromycin A, which is an acid-catalyzed degradation product of erythromycin A. Salient information for erythromycin A and anhydroerythromycin A is presented in Table 6-1. In this paper, erythromycin corresponds to the total erythromycin (*i.e.*, the sum of erythromycin A and anhydroerythromycin A) present in solution; however, the individual behavior of erythromycin A and anhydroerythromycin A throughout treatment processes is also described.

Table 6-1. Salient information for erythromycin.

Property	Erythromycin A	Anhydroerythromycin A
Chemical Formula	C ₃₇ H ₆₇ NO ₁₃	C ₃₇ H ₆₅ NO ₁₂
Molecular Weight (g/mol)	733.93	715.92
CAS Number	114-07-8	23893-13-2
Structure		
pK _a	8.8	8.8 *

* The pK_a of anhydroerythromycin A was estimated at 8.8 (Harang and Westerlund, 1999).

Erythromycin was discovered in 1952 when it was isolated from the metabolic products of a strain of *Streptomyces erythreus* (McGuire *et al.*, 1952). Since the discovery of erythromycin, a number of other macrolide compounds have been developed, including clarithromycin (1970s), azithromycin (1980), roxithromycin (1987), and telithromycin (1998), among others; generally, for the most part macrolides containing 14-membered rings are employed in the United States, whereas 16-membered rings are popular in Europe (Lemke and Williams, 2008). Over 2000 macrolides have been identified, including at least 153 and 362 compounds with 14- and 16-membered rings, respectively; research into the isolation and synthesis of new macrolide compounds is ongoing (Omura, 2002). Regardless of the development of these other macrolides, erythromycin is one of the most successful drugs of all time (Pal, 2006). Erythromycin is used to treat bacterial infections like bronchitis; diphtheria; Legionnaires' disease; pertussis; pneumonia; and ear, urinary tract, and skin infections (Wishart *et al.*, 2008). Macrolides are bacteriostatic and work by binding to the 23S rRNA in the 50S subparticle and thereby inhibit production of peptidyltransferase (Mao and Robishaw, 1972). Lemke and Williams (2008) indicated that the C-5 D-desosamine moiety is particularly important in inhibition, and that removal of the C-3 L-cladinose results in an 100-fold decrease in biological activity. Therefore, ozone attack at these sites is likely to significantly decrease the ultimate antimicrobial activity of solutions containing erythromycin.

With an annual production of approximately 4000 tons (Minas, 2004), erythromycin is one of the most popular macrolides prescribed. Given that popularity, it is not surprising that trace concentrations of erythromycin have been detected in wastewater supplies. Hirsch *et al.* (1999) detected 6 µg/L of erythromycin in a German sewage treatment plant. In a critical review by Oulton *et al.* (2010), erythromycin was shown to exhibit one of the lowest removal efficiencies of the 43 compounds investigated in traditional wastewater treatment plants; therefore, erythromycin is expected to pass through wastewater treatment and enter the environment. In a 2002 US Geological

Survey (USGS) survey, erythromycin was detected at 21.5% of the 139 streams tested; the maximum erythromycin concentration detected was 1.70 µg/L (Kolpin *et al.*, 2002). Only one antibiotic (trimethoprim) exhibited a higher detection frequency (27.4%; Kolpin *et al.*, 2002). In another USGS-sponsored study, Kinney *et al.* (2006) measured erythromycin concentrations up to 611 ng/L in reclaimed wastewater; the soil irrigated with that reclaimed wastewater demonstrated erythromycin concentrations of 1-6 ng/g. Given the widespread presence of erythromycin in the environment and the listing of erythromycin on the EPA CCL3, investigation of water treatment processes aimed at removing erythromycin is merited.

Ozone-based treatment processes have demonstrated potential for transforming erythromycin. In their landmark paper, Ternes *et al.* (2003) treated 0.62 µg/L erythromycin in sewage treatment plant effluent to below 50 ng/L with an ozone dose of 5 mg/L. Westerhoff *et al.* (2005) investigated the abilities of several water treatment processes to remove trace organic contaminants from water supplies; approximately 33%, 54%, and 97% of erythromycin was removed through addition of alum, addition of powdered activated carbon, and ozonation, respectively. Erythromycin has also been shown to be more effectively treated using conventional ozonation as compared to advanced oxidation through the peroxone (O_3/H_2O_2) system (Lin *et al.*, 2009).

Some research efforts have identified the rate constants for other macrolide compounds with ozone and hydroxyl radicals (Huber *et al.*, 2005; Dodd *et al.*, 2006; Lange *et al.*, 2006); however, to our knowledge, the kinetics of erythromycin transformation with ozone have not been reported previously. Lange *et al.* (2006) reported that the free tertiary amine present on the D-desosamine moiety of most macrolide antibiotics (including erythromycin, clarithromycin, roxithromycin, and azithromycin, among others) reacts with ozone with a rate constant near $4 \times 10^6 \text{ M}^{-1} \text{ s}^{-1}$; that site is the main ozone attack site and controls the kinetics of the transformation of most macrolides with ozone. In that same paper, Lange *et al.* (2006) provided the

apparent second order rate constant of clarithromycin with ozone at pH 7 as $7 \times 10^4 \text{ M}^{-1} \text{ s}^{-1}$. The literature yields pK_a values for clarithromycin ranging from 8.6–9.0 (Gustavson *et al.*, 1995; Liu and Ren, 2006), meaning that the specific rate constant for clarithromycin with ozone is $2.9\text{--}7.1 \times 10^6 \text{ M}^{-1} \text{ s}^{-1}$. The specific rate constants for roxithromycin ($k''_{\text{O}_3, \text{RX}} = 1.0(\pm 0.1) \times 10^7 \text{ M}^{-1} \text{ s}^{-1}$) and azithromycin ($k''_{\text{O}_3, \text{AZ}} = 6.0(\pm 1.1) \times 10^6 \text{ M}^{-1} \text{ s}^{-1}$) were reported by Dodd *et al.* (2006). The apparent rate constant for roxithromycin at pH 7 was listed as $7 \times 10^4 \text{ M}^{-1} \text{ s}^{-1}$ by Huber *et al.* (2005); taking the pK_a of roxithromycin ($\text{pK}_a = 8.8$) into account, the specific rate constant for roxithromycin would be $4.49 \times 10^6 \text{ M}^{-1} \text{ s}^{-1}$. Discrepancies exist between the rate constants for macrolide interaction with ozone reported in the literature; however, Lange *et al.*'s (2006) prediction that these rate constants would be clustered around $4 \times 10^6 \text{ M}^{-1} \text{ s}^{-1}$ seems to be consistent.

Increasingly, antimicrobial activity assays have been employed to describe treatment of antimicrobial pharmaceuticals and to determine if intermediate oxidation products exert antimicrobial activity (Suarez *et al.*, 2007; Baeza, 2008; Dodd *et al.*, 2009; Paul *et al.*, 2010). Dodd *et al.* (2009) investigated ozonation of other macrolide compounds, namely, roxithromycin, azithromycin, and tylosin. The chemical structures of roxithromycin and azithromycin are similar to that of erythromycin A. For most macrolides, the free tertiary amine located on the desosamine moiety (see Table 6-1) represents the primary ozone attack site. Using the serial dilution technique, Dodd *et al.* (2009) concluded that intermediate oxidation products formed via ozonation of the macrolides listed above did not exert any significant residual antimicrobial activity. To our knowledge, no work has been completed regarding the elimination of antimicrobial activity of erythromycin in water treatment processes. In this paper, the intermediate oxidation products of erythromycin transformation by ozone are identified, and the theoretical antimicrobial activity of those products is compared with measured values of residual antimicrobial activity. Therefore, this paper provides the first documentation of how the antimicrobial activity associated with erythromycin, and erythromycin intermediate oxidation products, changes throughout ozone treatment.

Given the documented evidence of erythromycin presence in water supplies, as well as the importance of erythromycin with regard to the EPA CCL3, erythromycin transformation in an ozone-based water treatment process was studied. In this work, we discuss the importance of erythromycin speciation between erythromycin A (EA) and anhydroerythromycin A (AEA) from environmental detection and antimicrobial activity standpoints, the transformation kinetics of EA and AEA with aqueous ozone, the characterization of primary oxidation products formed through ozone reaction with EA and AEA, and the residual antimicrobial activity of treated waters containing EA, AEA, and their intermediate oxidation products. Ultimately, we hope to demonstrate effective treatment of erythromycin using ozone-based processes not only in terms of erythromycin transformation, but also in terms of elimination of residual antimicrobial activity.

MATERIALS AND METHODS

Chemicals. Erythromycin (50 mg/mL in ethanol) was purchased from VWR; that solution was kept in a dark environment at -20°C. Working solutions of 1 mg/mL were made by diluting the erythromycin stock solution into DI water; working solutions were stored in the dark at 4°C to prevent erythromycin degradation. LC-MS grade acetonitrile was employed in LC-MS and LC-MS/MS analysis of erythromycin. LC-MS analysis also required 0.1% formic acid, which was made by diluting 88% formic acid with DI. NOM was isolated from Lake Austin (Austin, TX) and Claremore Lake (Claremore, OK) using the procedures described by Aiken *et al.* (1992). The details of these NOM sources have been described earlier (Chapters 3 and 5), and as the role of NOM is not crucial to the results presented in this paper, the characteristics of these NOM isolates are not discussed here.

Ozone Stock Solution and Analysis. An ozone generator (Yanco Industries) was used to generate an aqueous ozone stock solution. Oxygen gas was introduced to the ozone generator at a flow rate of 30 cm³/min. The ozone generator was set to the maximum

setting, which resulted in a mass ozone flow rate of approximately 4.08 mg/min. The combined (oxygen and ozone) gas stream was bubbled into deionized water in a 500-mL gas washing bottle, which was placed in an ice bath. The temperature of the solution in the gas-washing bottle was approximately 0.5°C. The aqueous ozone concentration of the ozone stock solution quickly increased; the ozone concentration was greater than 40 mg/L after only 30 minutes of ozonation. The aqueous ozone concentration continued to increase to approximately 60 mg/L after three hours of ozonation. The ozone reactor is shown in the schematic presented in Figure 6-1a, and the development of the aqueous ozone concentration in the stock solution is shown in Figure 6-1b.

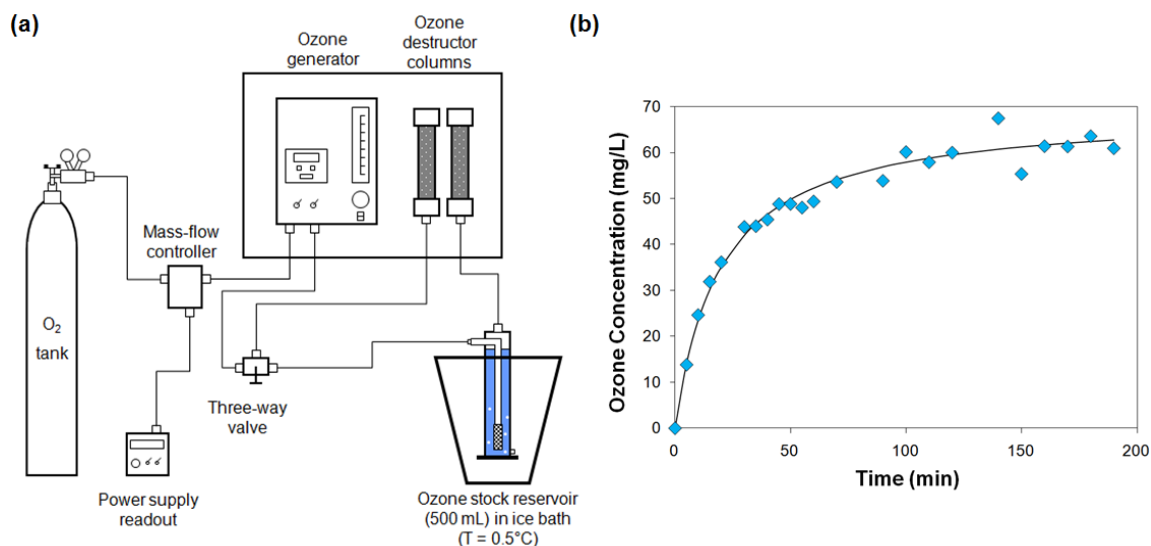


Figure 6-1. (a) Ozone reactor setup; (b) aqueous ozone concentration with time.

Aqueous ozone concentrations were measured in two ways: direct measurement at 258 nm and indirect measurement of indigotrisulfonate at 600 nm (Bader and Hoigné, 1981). The ozone concentration of the stock solution was always measured directly at 258 nm because of the high steady state ozone concentrations reached in that reactor (typically, 45-55 mg/L). For batch kinetics experimentation, the aqueous ozone concentrations were measured using indigotrisulfonate as an ozone probe compound. Indigotrisulfonate reacts quickly with ozone ($k''_{\text{O}_3, \text{indigo}} = 9.4 \times 10^7 \text{ M}^{-1} \text{ s}^{-1}$; Munoz and von

Sonntag, 2000); therefore, as long as a molar excess of indigotrisulfonate to ozone is added to the solution, the indigotrisulfonate compound, which absorbs light at 600 nm, can be used as an ozone probe compound. In this work, Indigo Reagent II (Standard Method 4-104; APHA *et al.*, 2006) was employed to measure low ($6 \times 10^{-8} \text{ M} < [\text{O}_3] < 1.04 \times 10^{-4} \text{ M}$) aqueous ozone concentrations with a 4-cm quartz cuvette.

Batch Experimentation. Ozone experiments were run in two different configurations. In the first configuration, a predetermined ozone dose ($2.92\text{--}8.32 \times 10^{-6} \text{ M}$) was introduced into a 2-L reactor containing $1.36 \times 10^{-6} \text{ M}$ erythromycin and the background matrix of interest to determine the kinetics of erythromycin A transformation with ozone. Experiments were run with 10^{-2} M *t*-BuOH to isolate ozone kinetics from that associated with hydroxyl radicals. The 2-L reactor was equipped with a bottle-top dispenser to enable rapid sampling; the first sample was generally taken approximately 11-13 seconds after introduction of aqueous ozone, and several samples were taken during the short period of one to two minutes after ozone introduction. Samples were analyzed for aqueous ozone using the indigotrisulfonate method (Bader and Hoigné, 1981) and for anhydroerythromycin A using the LC-MS/MS method described below.

The other experimental configuration consisted of adding specific applied ozone doses to solutions containing $1.36 \times 10^{-4} \text{ M}$ erythromycin and a background matrix of interest. In this case, the predetermined ozone dose was introduced to the sample; samples were kept in a 21°C dark environment for at least 12 hours, allowing complete aqueous ozone degradation ($[\text{O}_3] < 6 \times 10^{-8} \text{ M}$). At this time, samples were analyzed for residual ozone concentration using the indigotrisulfonate method (Bader and Hoigné, 1981) to ensure complete ozone degradation; erythromycin A, anhydroerythromycin A, and erythromycin intermediate oxidation products were analyzed using the LC-MS method described below. This experimental configuration was employed to calculate the rate constant for anhydroerythromycin A transformation with ozone and to identify the

intermediate oxidation products corresponding to ozonation of erythromycin A and anhydroerythromycin A.

Erythromycin Analysis. Erythromycin A was measured using an LC-MS/MS (Thermo Finnigan, TSQ Quantum) method based on that employed by Calamari *et al.* (2003). The injection volume was 20 μ L and the flow rate was 700 μ L/min. LC separation was achieved with a C₁₈ column (Shimadzu Premier C18 5 μ 150 \times 4.6-mm); the eluent gradient was 100% 0.1% Formic acid (FA), 0% Acetonitrile (ACN) (0-3 min); ramp to 88% 0.1% FA, 12% ACN (3-10 min); 75% 0.1% FA, 25% ACN (10-12 min); ramp to 50% 0.1% FA, 50% ACN (12-12.1 min); 50% 0.1% FA, 50% ACN (12.1-16 min); ramp to 50% 0.1% FA, 50% ACN (16-16.1 min); 12% 0.1% FA, 88% ACN (16.1-18 min). The electrospray ionization tandem mass spectrometer was operated in positive ion mode. Method parameters include the following: parent mass, 716.4 mg; product mass, 558.3 mg; collision gas pressure, 1.5 mTorr; collision energy, 24 V; spray voltage, 4000 V; vaporizer temperature, 400 $^{\circ}$ C; sheath gas pressure, 25 psi; and auxiliary gas pressure, 5 psi. The parent mass of 716.4 corresponds to anhydroerythromycin A, which was formed from erythromycin A due to the low pH of samples containing Indigo Reagent II (from aqueous ozone measurement). At low pH, erythromycin A is quickly degraded into anhydroerythromycin A. Erythromycin A was eluted at 15.6 minutes.

Erythromycin A and anhydroerythromycin A were also analyzed in LC-MS mode to characterize the formation and transformation of intermediate oxidation products resulting from erythromycin reaction with ozone. The injection volume was 20 μ L and the flow rate was 350 μ L/min. The eluent gradient was 100% 0.1% FA, 0% ACN (0-2 min); ramp to 88% 0.1% FA, 12% ACN (2-12 min); 75% 0.1% FA, 25% ACN (12-16 min); ramp to 50% 0.1% FA, 50% ACN (16-21 min); 50% 0.1% FA, 50% ACN (21-28 min); ramp to 50% 0.1% FA, 50% ACN (28-30 min); 88% 0.1% FA, 12% ACN (30-35). The electrospray ionization tandem mass spectrometer was operated in positive ion mode and the *m/z* range of 150–1500 was monitored. Method parameters include the

following: parent mass, 734.4 mg; collision gas pressure, 1.5 mTorr; collision energy, 24 V; spray voltage, 4000 V; vaporizer temperature, 400 °C; sheath gas pressure, 25 psi; and auxiliary gas pressure, 20 psi. Erythromycin A, anhydroerythromycin A, and their major intermediate oxidation products were generally eluted between 25 and 29 minutes.

Antimicrobial Activity Assay. An *E. coli* -based antimicrobial activity assay (NCCLS, 2004) was employed to monitor changes in antimicrobial activity throughout treatment. In this work, *E. coli* ATCC 25922 was utilized. After purchase, a small aliquot of the purchased *E. coli* was grown in 10 mL Mueller-Hinton Broth. After a significant growth period, a streak plate was run, and an inoculation loop was used to select a single colony forming unit from the streak plate. Stock *E. coli* solutions were created in Mueller-Hinton Broth from that original colony forming unit. The stock solution was incubated at 37°C in an aerobic environment until the suspension was quite turbid, at that point, the *E. coli* suspension was mixed 1:1 with 50% glycerol and stored in a dark environment at -80°C. During experimentation, an *E. coli* working solution was maintained at 37°C in an aerobic environment.

Antimicrobial activity assays were run in 96-well microplates. First, standards and samples (100 µL) were added to the microplate wells. After the standard / sample solutions were added to the wells, the *E. coli* inoculum was prepared by diluting the *E. coli* stock solution with Mueller-Hinton Broth to attain an absorbance at 625 nm equivalent to a 0.5 McFarland standard. The inoculum (100 µL) was immediately added to each well. Positive and negative growth controls were created by adding the inoculum (100 µL) and Mueller-Hinton Broth (100 µL) to DI (100 µL), respectively. All samples were run in triplicate. Microplates were then incubated at 37°C in an aerobic environment for 20 hours while being shaken at 75 rpm. After the 20-hour incubation period, the absorbance at 600 nm of each well in the microplate was recorded using a microplate reader (BioTek). The absorbance data was converted into percent inhibition using Eq. 6-1.

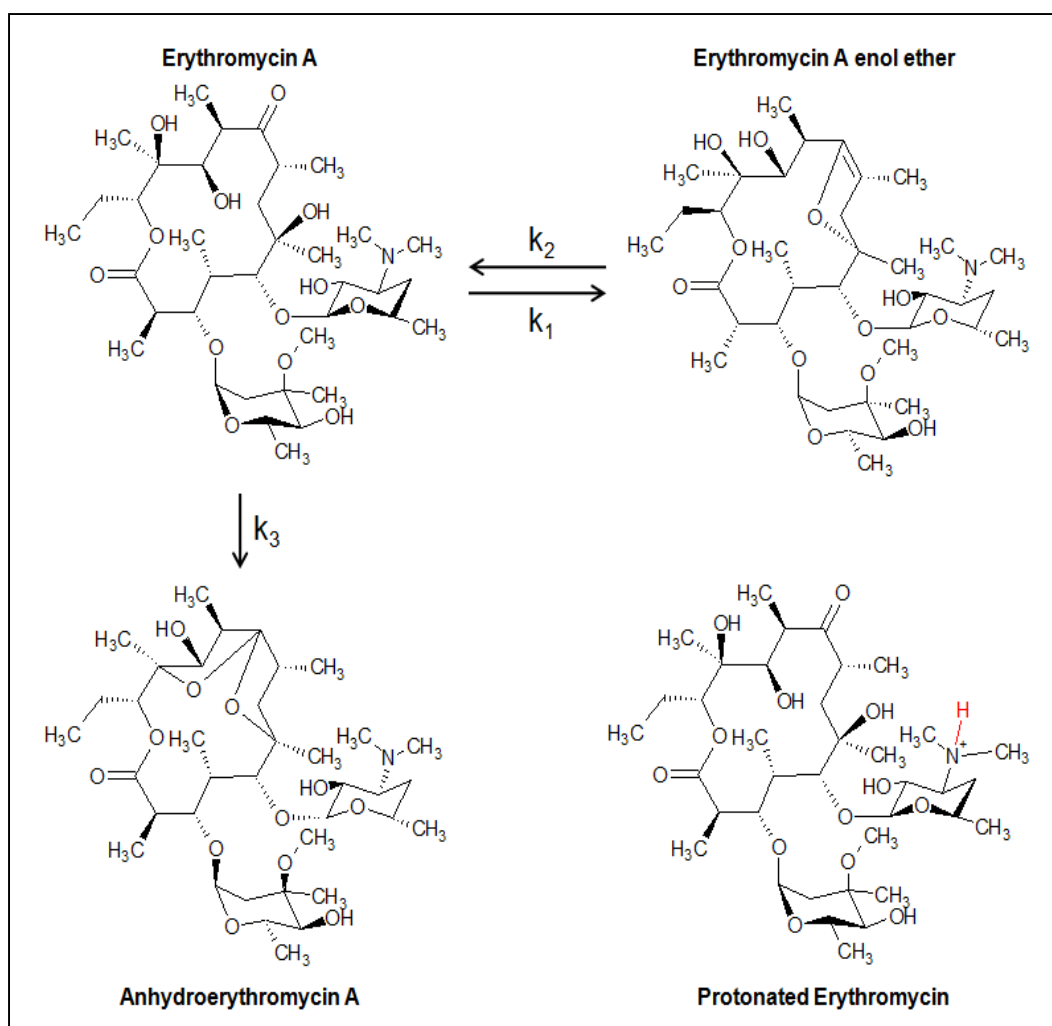
$$\% \text{ Inhibition} = \left(1 - \frac{ABS_{600nm, sample} - ABS_{600nm, positivecontrol}}{ABS_{600nm, positivecontrol} - ABS_{600nm, negativecontrol}} \right) \times 100\% \quad \text{Eq. 6-1}$$

The resulting antimicrobial activity data was analyzed using the GraphPad Prism software; the specific GraphPad equations used are discussed below.

RESULTS

Chemical Structure of Erythromycin and Erythromycin Degradation Products

Based on the pK_a for erythromycin A, the dominant species at low pH ($pH < pK_a = 8.8$) would be the erythromycin molecule with a proton on the tertiary amine located on the desosamine sugar, resulting in the protonated form of erythromycin shown in the bottom right of Scheme 6-1. In actuality, at these lower pH values, erythromycin is acid-catalyzed to form erythromycin A enol ether and anhydroerythromycin A (Kurath *et al.*, 1971; Atkins *et al.*, 1986; Cachet *et al.*, 1989; Vinckier *et al.*, 1989). Cachet *et al.* (1989) described the kinetics of the system shown in Scheme 6-1. At pH 5.83, k_1 , k_2 , and k_3 were $0.76(\pm 0.11) \times 10^{-4} \text{ min}^{-1}$, $6.23(\pm 1.44) \times 10^{-4} \text{ min}^{-1}$, $1.20(\pm 0.02) \times 10^{-4} \text{ min}^{-1}$, respectively (Cachet *et al.*, 1989). As k_2 is greater than k_1 , the ultimate product of erythromycin degradation is anhydroerythromycin A. One other important observation is that the reaction between erythromycin A and anhydroerythromycin A is not reversible; therefore, once anhydroerythromycin A is formed, no anhydroerythromycin A conversion back to erythromycin A is possible. The implications of this irreversible reaction are discussed below.



Scheme 6-1. Erythromycin degradation products (adapted from Cachet *et al.*, 1989) and clarification of erythromycin A and anhydroerythromycin A structures.

Hirsch *et al.* (1999) discussed the speciation of erythromycin A and anhydroerythromycin A and determined that environmental samples contain mostly anhydroerythromycin A; given the degradation kinetics described above and oral administration of erythromycin (exposure to acidic conditions during digestion), this finding is not surprising. Previous researchers have listed anhydroerythromycin A as “erythromycin” or “erythromycin- H_2O ,” which is often incorrectly described using the molecular weight and CAS number of erythromycin A. This name is slightly misleading

as the water molecule that is lost from erythromycin A causes drastic structural changes as demonstrated by the chemical structure of anhydroerythromycin A as shown in Table 6-1 and Scheme 6-1. Furthermore, it is important to note that environmental sampling and preservation techniques may result in undesired erythromycin speciation. For example, the landmark report by Kolpin *et al.* (2002) used an LC-MS based analytical technique that acidified samples to pH 3 before analytical measurement, which would cause erythromycin A to degrade to anhydroerythromycin A. Given the importance of erythromycin with respect to the EPA CCL3 list, it is important to clarify the chemical structures of erythromycin and degradation products that are expected to exist in the environment. The implications of erythromycin speciation with respect to antimicrobial activity are discussed below.

Erythromycin Kinetics with Ozone

Kinetic experiments were run at several different pH values ranging from 5.35 to 6.81. The solutions were composed of 1.36×10^{-6} M erythromycin A (EA), 1×10^{-3} M phosphate buffer, and 1×10^{-3} M *t*-BuOH. Ozone was spiked into these solutions at applied doses of $2.92\text{--}8.32 \times 10^{-6}$ M. The ozone concentration data from each experiment was integrated with respect to time to yield ozone exposure ($\int [O_3] dt$). Then, $\ln ([EA]/[EA]_o)$ was plotted against ozone exposure. As hydroxyl radicals were being scavenged by *t*-BuOH, Eq. 6-2 describes erythromycin A transformation.

$$\frac{d[EA]}{dt} = -k_{O_3,app,EA} [O_3][EA] \quad \text{Eq. 6-2}$$

In Eq. 6-2, $[EA]$ is the erythromycin A concentration at time t , $[O_3]$ is the aqueous ozone concentration at time t , and $k_{O_3,app,EA}$ is the apparent rate constant for erythromycin A with ozone at a particular pH. Integrating Eq. 6-2 yields Eq. 6-3.

$$\ln \frac{[EA]}{[EA]_o} = -k_{O_3,app,EA} \int_{t=0}^t [O_3] dt \quad \text{Eq. 6-3}$$

This equation can be further simplified by substituting the specific rate constants for each erythromycin species with ozone and the ionization factor (α_0 and α_1) terms for the apparent rate constant, as shown in Eq. 6-4.

$$\ln \frac{[EA]}{[EA]_0} = - \left[\alpha_0 \times k_{O_3,EA-H^+} + \alpha_1 \times k_{O_3,EA} \right] \int_{t=0}^t [O_3] dt \quad \text{Eq. 6-4}$$

In this case, α_0 and α_1 correspond to the fraction of protonated and deprotonated, respectively, erythromycin A compared to the total erythromycin A present in solution.

The data from the experiments described above are plotted as $\ln [EA]/[EA]_0$ vs. ozone exposure in Figure 6-2a. These data were modeled using Eq. 6-3; therefore, the slope of the trend lines fitted to each data set represents the apparent second order rate constant for erythromycin A at the corresponding pH value. The apparent second order rate constants for erythromycin at pH 5.35-6.81 are provided in Table 6-2.

Table 6-2. Apparent second order rate constants ($k_{O_3,app,EA}$) for the transformation of erythromycin A by ozone at pH 5.35-6.81.

Solution pH	$k_{O_3,app,EA} (M^{-1}s^{-1})$	α_1
5.35	1.89×10^3	3.55×10^{-4}
5.66	4.45×10^3	7.24×10^{-4}
6.00	7.11×10^3	1.58×10^{-3}
6.40	2.04×10^4	3.97×10^{-3}
6.81	4.02×10^4	1.01×10^{-2}

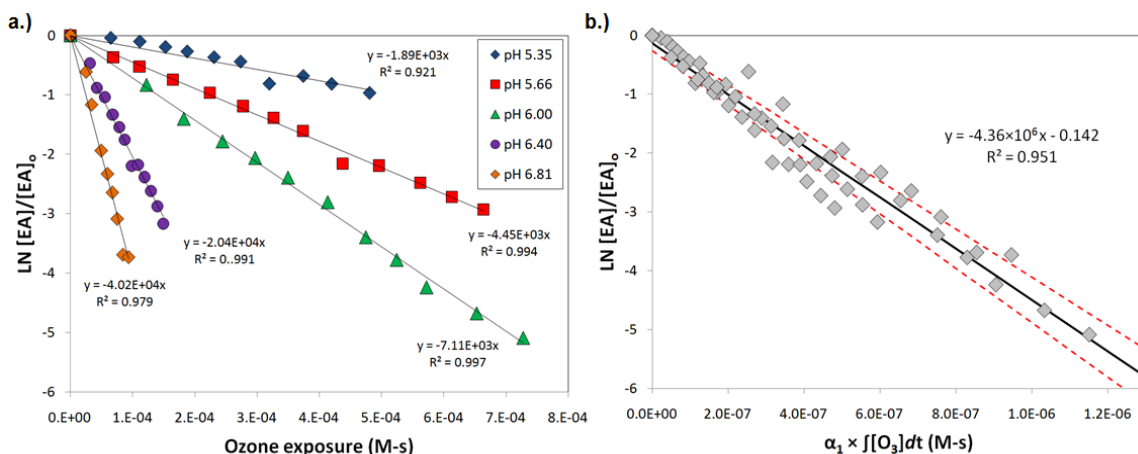


Figure 6-2. (a) Erythromycin transformation at different pH values; (b) determination of specific second order rate constant for erythromycin with ozone. (The solutions contained 1.36×10^{-6} M erythromycin, 1×10^{-3} M phosphate buffer, and 1×10^{-3} M *t*-BuOH at the pH values listed in the legend. The dotted red lines represent the 95% confidence bands.)

Previous researchers have assumed that reaction between the protonated forms of other macrolides (roxithromycin, azithromycin, and clarithromycin, in particular) and ozone is negligible (Dodd *et al.*, 2006; Lange *et al.*, 2006). This assumption stems from work by previous researchers demonstrating low rate constants for compounds containing protonated amine groups with ozone (Hoigné and Bader, 1983b; Munoz and von Sonntag, 2000). In contrast, ozone reacts quickly with deprotonated amine groups due to the presence of a lone pair of electrons on the nitrogen atom; therefore, high apparent rate constants between the deprotonated form of erythromycin and ozone are expected. For these reasons, we considered the reaction between the protonated form of erythromycin A and ozone to be negligible ($k''_{O_3,EA-H^+} < 1.0 \text{ M}^{-1}\text{s}^{-1}$). To determine the specific second order rate constant for erythromycin A, the data from Figure 6-2a were replotted as $\ln [EA]/[EA]_0$ vs. the product of the ionization factor (α_1) for the deprotonated form of erythromycin A and ozone exposure in Figure 6-2b (Eq. 6-4). The resultant data collapses into one curve. The slope of that curve is the specific second order rate constant for transformation of the deprotonated form of erythromycin A by ozone; the rate constant ($\pm 95\%$ confidence interval) is $4.36 (\pm 0.14) \times 10^6 \text{ M}^{-1}\text{s}^{-1}$.

Similar experiments were run to determine the rate constant of erythromycin A with hydroxyl radicals, which are the most important ozone degradation product in terms of oxidant activity. In those experiments, 1 μM para-chlorobenzoic acid (*p*CBA) was added to the reactor solution in the place of the 10 mM *t*-BuOH used to isolate ozone kinetics. While erythromycin A and *p*CBA transformation were both observed, the degradation of these compounds did not occur in the same time range; that is, erythromycin A was completely degraded before *p*CBA demonstrated any removal. Ultimately, the high reactivity of erythromycin A with ozone precludes determination of $k''_{\text{HO}\cdot, \text{AEA}}$ using an ozone-based method. Other authors have employed UV- and radiation-based methods for determination of the second order rate constants of wastewater derived organic contaminants with hydroxyl radicals (Dodd *et al.*, 2009; An *et al.*, 2010). The second order rate constant for azithromycin and roxithromycin with hydroxyl radicals at pH 7 were determined by Dodd *et al.* (2006) to be $2.9(\pm 0.6) \times 10^9 \text{ M}^{-1} \text{ s}^{-1}$ and $5.4(\pm 0.3) \times 10^9 \text{ M}^{-1} \text{ s}^{-1}$, respectively. Given the similarity of these macrolides with erythromycin A and anhydroerythromycin A, we expect the rate constants with hydroxyl radicals for erythromycin A (and anhydroerythromycin A) would be in the same range, namely $2\text{--}6 \times 10^9 \text{ M}^{-1} \text{ s}^{-1}$.

Batch experiments were run by dosing $6.0\text{--}12.7 \times 10^{-5} \text{ M}$ of ozone into solutions containing $4.81\text{--}13.6 \times 10^{-5} \text{ M}$ erythromycin, $2.38 \times 10^{-3} \text{ M}$ NaHCO_3 , $1.71 \times 10^{-3} \text{ M}$ NaCl , and 10^{-5} M *p*CBA at pH 8.4. At this pH, the initial samples, approximately 24.5% of the total erythromycin in solution was present as anhydroerythromycin A and the other 75.5% was present as erythromycin A; this speciation was determined using LC-MS. These solutions also contained various concentrations of DOC; the mass ratio of applied ozone to initial DOC ranged from 0–0.164 mg O_3 / mg DOC. In this experiment, a select volume of the ozone stock solution was added to each solution to correspond to a molar ratio of applied ozone to initial erythromycin of 1.25 mol O_3 / mol ERY (ERY is the total erythromycin in solution, that is the sum of erythromycin A and the anhydroerythromycin A). The solutions were allowed to react over the course of at least 12 hours. Aqueous

ozone concentrations were measured before measuring erythromycin concentrations via LC-MS; all solutions showed no ozone residual after the 12-hour reaction period. The samples were analyzed in LC-MS mode and erythromycin A and anhydroerythromycin A concentrations were measured. The normalized erythromycin A and anhydroerythromycin A (anhydroerythromycin A response divided by the initial erythromycin A response) remaining are plotted against the mass ratio of applied ozone to initial DOC in Figure 6-3. The rapid reaction kinetics of erythromycin and DOC with ozone effectively quenched aqueous ozone before ozone decomposition to hydroxyl radicals occurred, *i.e.*, no hydroxyl radical exposure was observed for any of the samples. Furthermore, the rapid transformation kinetics of erythromycin with ozone allowed highly effective erythromycin competition with DOC for reaction with ozone; for that reason, minimal differences were observed between the three DOC sources.

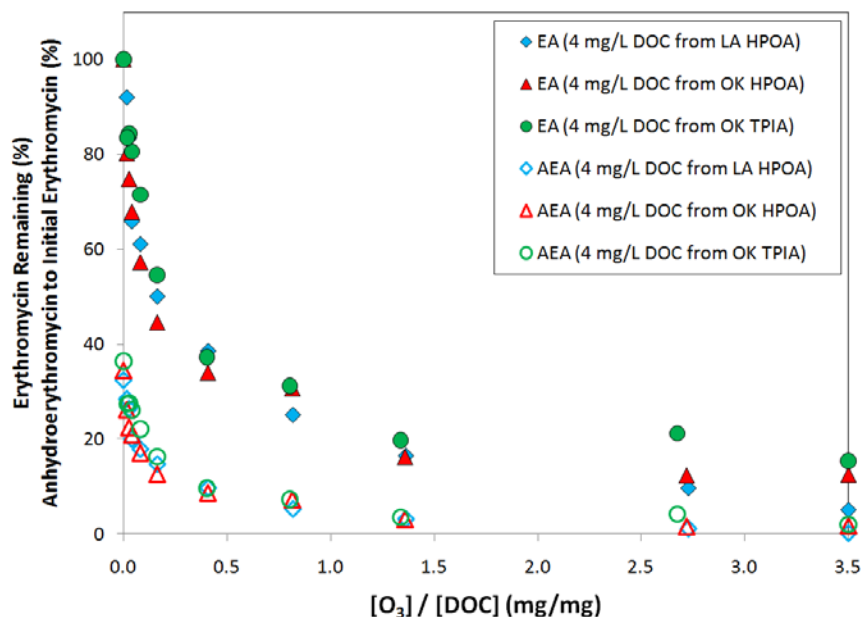


Figure 6-3. Changes in erythromycin and anhydroerythromycin concentrations as a function of the mass ratio of applied ozone to DOC concentration. (The molar ratio of applied ozone to initial erythromycin was held constant at 1.25 mol O₃ / mol ERY (ERY is the total erythromycin in solution, that is the sum of erythromycin A and the anhydroerythromycin A). The background water quality matrix contained 1.36×10⁻⁶ M erythromycin, 2.38 ×10⁻⁵ M NaHCO₃, 1.71 ×10⁻³ M NaCl, and 4 mg/L DOC at pH 8.4.)

In Chapter 5, the rate constant for ciprofloxacin transformation by ozone did not change in the presence of NOM. Here, we assume the same conclusion for erythromycin transformation kinetics. This data was also used to calculate the second-order rate constant for anhydroerythromycin A transformation by ozone. Using the change in erythromycin A ($\ln [EA]/[EA]_o$), the change in anhydroerythromycin A ($\ln [AEA]/[AEA]_o$) and the apparent second order rate constant for erythromycin A at pH 8.4 ($\alpha_1 = 0.285$; $k''_{O3,app,EA} = 1.24 \times 10^6 \text{ M}^{-1}\text{s}^{-1}$), the apparent second order rate constant describing anhydroerythromycin A reaction with ozone was calculated, as shown in Eq. 6-5.

$$k''_{O3,app,AEA} = k''_{O3,app,EA} \times \frac{\ln\left(\frac{[AEA]}{[AEA]_o}\right)}{\ln\left(\frac{[EA]}{[EA]_o}\right)} \quad \text{Eq. 6-5}$$

The apparent rate constant for anhydroerythromycin A at pH 8.4 was determined to be $1.71(\pm 0.07) \times 10^6 \text{ M}^{-1}\text{s}^{-1}$. This approach is mathematically equivalent to calculating the ozone exposure using the erythromycin A data, and then using the calculated ozone exposure and the change in the anhydroerythromycin A ($\ln [AEA]/[AEA]_o$) to get the second order rate constant for anhydroerythromycin A reaction with ozone; the range of ozone exposures observed was $6.74 \times 10^{-8} - 2.41 \times 10^{-6} \text{ M}\cdot\text{s}$. As with erythromycin A, the apparent rate constant was divided by the ionization factor of anhydroerythromycin A at pH 8.4 ($\alpha_1 = 0.285$) to yield the specific rate constant, $k''_{O3,AEA} = 6.00(\pm 0.25) \times 10^6 \text{ M}^{-1}\text{s}^{-1}$. As the primary ozone attack site is the free tertiary amine, the specific rate constants for erythromycin A ($k''_{O3,EA} = 4.36(\pm 0.14) \times 10^6 \text{ M}^{-1}\text{s}^{-1}$) and anhydroerythromycin A ($k''_{O3,AEA} = 6.00(\pm 0.25) \times 10^6 \text{ M}^{-1}\text{s}^{-1}$) are both close to the $4 \times 10^6 \text{ M}^{-1}\text{s}^{-1}$ value predicted by Lange *et al.* (2006).

These rate constants were verified using data from a separate experiment, in which ozone doses of $0-2.23 \times 10^{-4} \text{ M}$ of ozone were spiked into solutions containing $1.36 \times 10^{-4} \text{ M}$ erythromycin, $2.38 \times 10^{-3} \text{ M}$ NaHCO_3 , $1.71 \times 10^{-3} \text{ M}$ NaCl , and 10^{-5} M

*p*CBA at pH 8.4. No organic matter was present in these solutions. The molar ratio of the applied ozone to initial erythromycin was spread across the range of 0 to 2.12 mol O₃ / mol erythromycin. The LC-MS response for both erythromycin A and anhydroerythromycin A was measured, and those values, along with the apparent rate constants calculated above for pH 8.4, were employed to determine the ozone exposure. In this case, the ozone exposure was found using both sets of data, *i.e.*, the erythromycin A data and the anhydroerythromycin A data. Figure 6-4 shows the ozone exposure calculated using the erythromycin A data plotted against the ozone exposure calculated using the anhydroerythromycin A data. A 1:1 dashed line is overlaid on the plot. Clearly, the ozone exposure calculated for each individual compound compare nicely with each other. This relationship suggests that the rate constants calculated above (from different data sets) accurately describe erythromycin A and anhydroerythromycin A transformation by ozone. In these experiments, the hydroxyl radical exposure was minimal (*i.e.*, no change in *p*CBA concentration).

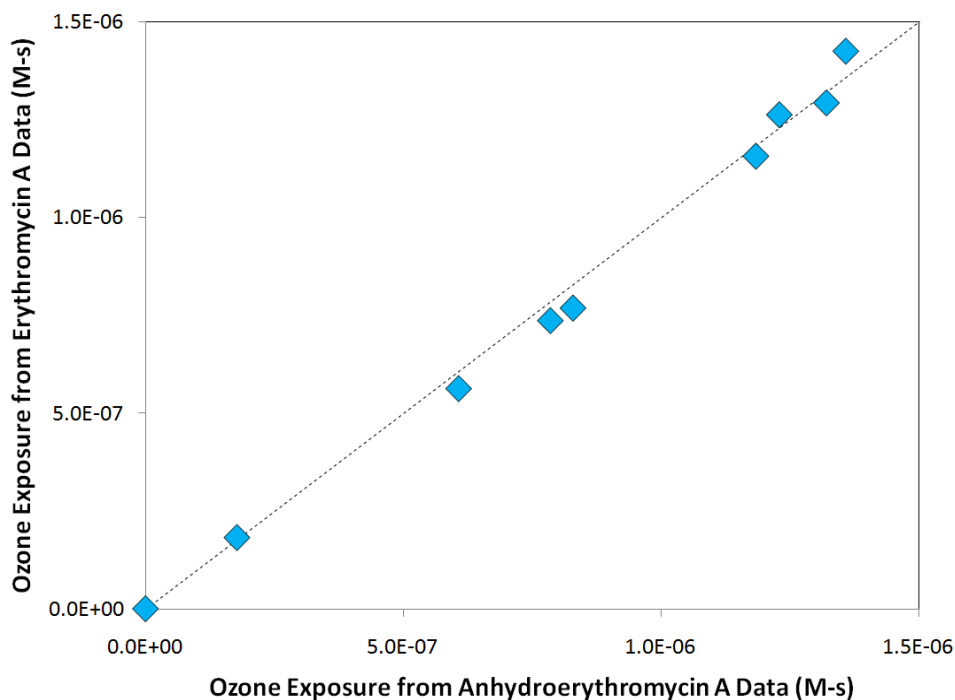


Figure 6-4. Verification of erythromycin rate constants through comparison of ozone exposure calculated from changes in erythromycin A and anhydroerythromycin A concentrations.

Inhibition Profile of Erythromycin

The inhibition profile *E. coli* ATCC #25922 for erythromycin was generated by performing the antimicrobial susceptibility assay over a range of erythromycin concentrations using standard solutions. The inhibition profile of erythromycin standards prepared in sterile DI with 2.38×10^{-3} M NaHCO_3 and 1.71×10^{-3} M NaCl at pH 8.3 is shown in Figure 6-5. The model line in Figure 6-5 follows the Hill equation (Eq. 6-6), which has been used to describe inhibition profiles (Suarez *et al.*, 2007; Baeza, 2008; Dodd *et al.*, 2009); the Hill Equation model parameters were determined by the GraphPad Prism software.

$$\% \text{ Inhibition} = \left[I_{\min} + \frac{I_{\max} - I_{\min}}{1 + \left(\frac{IC_{50}}{C_{\text{sample}}} \right)^H} \right] \times 100\%$$

Eq. 6-6

I_{\min} is the minimum inhibition, I_{\max} is the maximum inhibition, IC_{50} is the erythromycin concentration that corresponds to 50% inhibition, C_{sample} is the erythromycin concentration of the sample, and H is the Hill slope. The equation used in the GraphPad Prism software automatically sets the minimum and maximum inhibition at 0% and 100%, respectively; therefore, IC_{50} and H were the only fitting parameters.

The Hill curve and the 95% confidence bands (dotted red lines) were generated using the “log(inhibitor) vs. normalized response – variable slope” equation in the GraphPad Prism software. In Figure 6-5, the erythromycin concentrations on the abscissa correspond to the concentration of erythromycin present in the sample/standard solution added to the well; recall that 100 μL of the *E. coli* inoculum was added to wells containing 100 μL of standards/samples. The IC_{50} and Hill slope (with 95% confidence intervals) were $4.9(\pm 0.55) \times 10^{-5}$ M and $1.7(\pm 0.32) \times 10^4$, respectively; the correlation coefficient (R^2) was 0.83. It should be noted that erythromycin demonstrates a relatively large window of partial inhibition. In Chapter 5, we discussed ozone treatment of ciprofloxacin and the antimicrobial activity associated with ciprofloxacin and its intermediate oxidation products (Chapter 5). The region of partial inhibition (20-80% inhibition of *E. coli*) was 1.39×10^{-8} M for ciprofloxacin (Chapter 5); for erythromycin, the same region is more than two orders of concentration wider (7.00×10^{-5} M). While a sharp inhibition profile (*e.g.*, ciprofloxacin) elucidates a clear treatment goal, the impacts of the background water quality (especially, the DOC content) are more likely to be problematic for compounds with wider inhibition profiles.

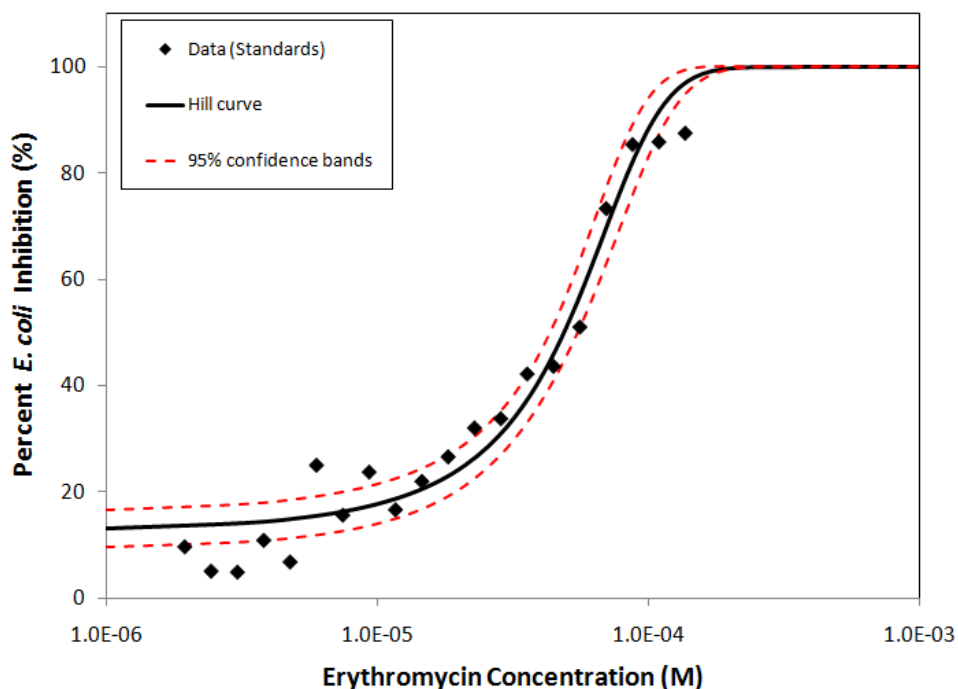


Figure 6-5. Inhibition profile for erythromycin A against *E. coli* at pH 8.3.

Experimentation demonstrated that anhydroerythromycin A is not antimicrobially active in the same concentration range of erythromycin A. Figure 6-6 shows the results of two experiments where specific ozone doses were applied to solutions containing 1.36×10^{-4} M erythromycin, 2.38×10^{-3} M NaHCO_3 , 1.71×10^{-3} M NaCl , 10^{-5} M *p*CBA, and 4 mg/L of DOC from Lake Austin HPOA at two distinct pH values, 8.5 and 4.1. In the pH 8.5 solution, approximately 24.5% of the erythromycin was present as anhydroerythromycin A, whereas anhydroerythromycin A made up 94.7% of the total erythromycin present in the pH 4.1 solution. Aliquots of these solutions were dosed with ozone (the molar ratio of applied ozone to initial erythromycin was 0-2.47 mol O_3 / mol ERY) and samples were kept in a dark environment at room temperature for at least 12 hours before LC-MS analysis. All samples demonstrated no ozone residual and no hydroxyl radical exposure.

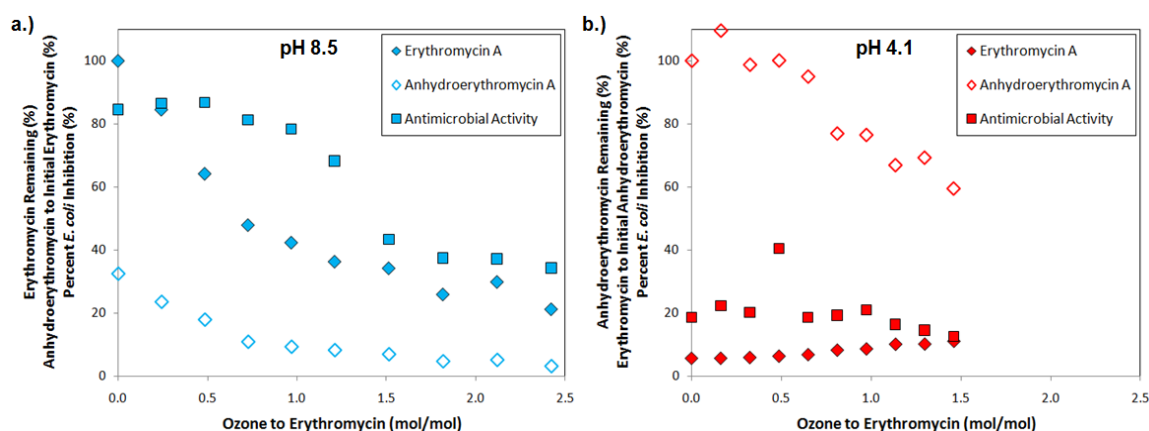


Figure 6-6. Difference between solutions containing erythromycin A and anhydroerythromycin A as the dominant species in solution on the *E. coli*-based antimicrobial activity assay. (In (a) samples were ozonated at pH 8.5 and erythromycin A was the dominant erythromycin species; in (b), samples were ozonated at pH 4.1 and anhydroerythromycin A was the dominant species. For both cases, the initial erythromycin concentration was 1.36×10^{-4} M erythromycin.)

These samples were also run in the antimicrobial activity assay; it should be noted that even though experimental samples were at pH 8.5 and 4.1, the MHB growth medium is sufficiently buffered at pH ~ 7.2 . Hence, the pH of experimental samples did not lead to differences in the biological response measured in the antimicrobial activity assay. The most interesting aspect of Figure 6-6 is that the initial sample did not demonstrate any significant antimicrobial activity. These data suggest that anhydroerythromycin A is not antimicrobially active. Kibwage *et al.* (1985) provided minimum inhibitory concentrations (MICs) for erythromycin A and anhydroerythromycin A against a number of gram-positive and gram-negative bacteria; in all cases, the MIC of anhydroerythromycin A was greater than that of erythromycin A. For *E. coli* ATCC 25922, the MIC of erythromycin A and anhydroerythromycin A were listed as 32 and >64 $\mu\text{g/mL}$, respectively. As the highest concentration employed in that study was 64 $\mu\text{g/mL}$, it is difficult to compare the relative antimicrobial activity of anhydroerythromycin A to that of erythromycin A for *E. coli* ATCC 25922; however, for two other gram-negative bacteria (*Neisseria meningitides* 1 and *Pasteurella ureae*) the

MIC listed for anhydroerythromycin A was over 60 and 500 times greater, respectively, than that listed for erythromycin A (Kibwage *et al.*, 1985). These findings align well with the results shown in Figure 6-6 and demonstrate the importance of erythromycin speciation with respect to antimicrobial activity.

Recall that the reaction from erythromycin A to anhydroerythromycin A is not reversible; hence sampling/preservation protocols that acidify environmental samples will convert erythromycin A to anhydroerythromycin A, thereby eliminating antimicrobial activity. Therefore, later analysis of the samples for residual pharmacological activity may not accurately describe the environmental sample. While the antimicrobial activity of other macrolide antibiotics and their degradation products is outside of the scope of this research, it should be noted that other macrolides (clarithromycin and azithromycin, among others) do not undergo the type of acid-catalyzed transformations described in Scheme 6-1 (Hirsch *et al.*, 1999). Hence, the effects of sampling/preservation techniques on the speciation of these compounds are not expected to generate drastic changes in antimicrobial activity.

Antimicrobial Activity of Erythromycin Intermediate Oxidation Products

Figure 6-7 shows the antimicrobial activity (as percent *E. coli* inhibition) versus the erythromycin A concentration of the treated samples that were plotted earlier in Figure 6-3. These samples were generated by dosing $0\text{--}2.47\times 10^{-4}$ M of ozone into samples containing 1.36×10^{-4} M erythromycin, 2.38×10^{-3} M NaHCO_3 , 1.71×10^{-3} M NaCl , 10^{-5} M *p*CBA, and 4 mg/L of DOC (with the exception being the “No NOM” data set, which did not contain any DOC). As described earlier, this dosing scheme resulted in applied ozone to initial erythromycin molar ratios of $0\text{--}2.42$ mol O_3 / mol ERY. On this type of plot, any contribution of intermediate oxidation products to the overall antimicrobial activity would cause a shift up in the percent inhibition data; however, if the intermediate oxidation products do not exert any significant antimicrobial activity, the data should fall on the inhibition profile shown in Figure 6-5. In Figure 6-7, it is clear

that most of the data from these four data sets fall within or quite close to the 95% confidence bands of the erythromycin A inhibition profile.

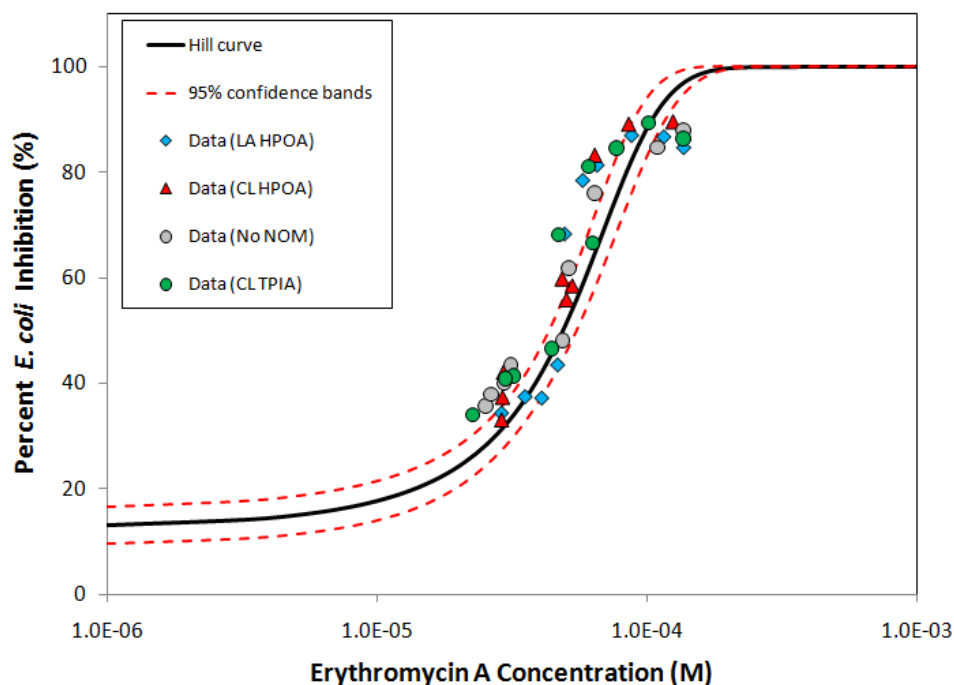


Figure 6-7. Antimicrobial activity data for experimental samples overlaid on the inhibition profile of erythromycin. (The data correspond to samples containing 1.36×10^{-4} M erythromycin, 2.38×10^{-3} M NaHCO_3 , 1.71×10^{-3} M NaCl, and 4 mg/L of DOC (with the exception being the “No NOM” data set, which did not contain any DOC) that were dosed with $0\text{--}2.47 \times 10^{-4}$ M of ozone.)

Recall from Chapter 5 that the intermediate oxidation products generated by ozonation of ciprofloxacin resulted in a shift in the inhibition profile of ciprofloxacin. In that work, the IC_{50} of the standard inhibition profile exhibited an IC_{50} of 9.0 $\mu\text{g/L}$ and an H of 0.42; the inhibition profile of treated samples (*i.e.*, those containing ciprofloxacin and intermediate oxidation products formed through ciprofloxacin reaction with ozone) had an IC_{50} of 6.6 $\mu\text{g/L}$ and an H of 0.26. The difference in IC_{50} illustrates the contribution of intermediate oxidation products to the residual antimicrobial activity, while the change in the Hill slope corresponds to a wider region of partial inhibition,

presumably due to a difference in potency between ciprofloxacin and its antimicrobially active intermediate products. For erythromycin, model (Hill curve with 95% confidence bands) fits to the four data sets all intersect; therefore, we can conclude that the intermediate oxidation products generated from ozone attack on erythromycin A do not demonstrate considerable antimicrobial activity. Furthermore, the differences observed for ciprofloxacin and erythromycin demonstrate the need to consider the transformation chemistry of individual compounds when considering residual pharmacological activity.

As intermediate oxidation products did not appear to exert any antimicrobial activity, we investigated the chemical structures of the compounds produced through ozone attack to determine if the structures of the intermediate oxidation products agree with experimental evidence suggesting that they do not express antimicrobial activity. LC-MS analysis of the samples previously plotted in Figure 6-3 and Figure 6-7 demonstrated four major *m/z* peaks: 733.9, 715.9, 749.9, and 731.9; these peaks are shown in Figure 6-8.

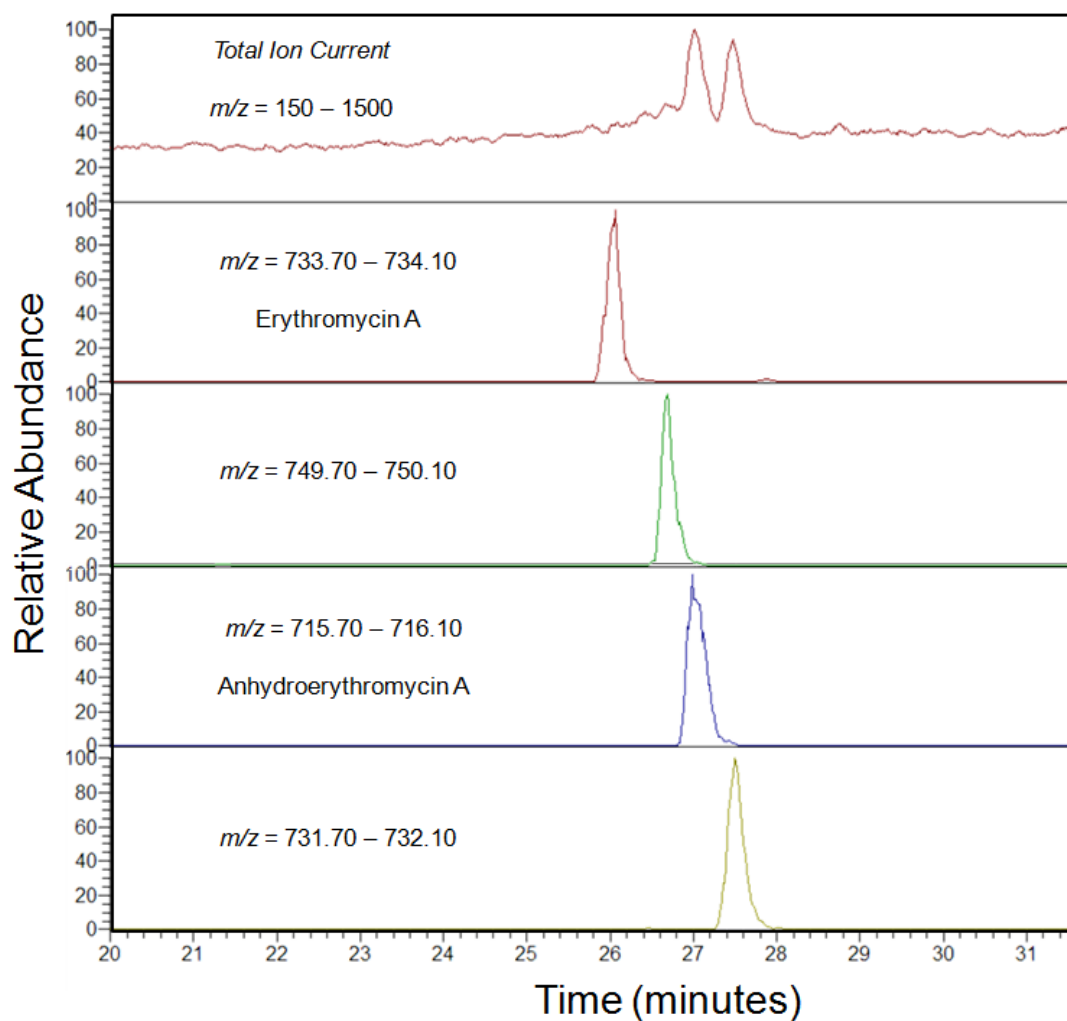
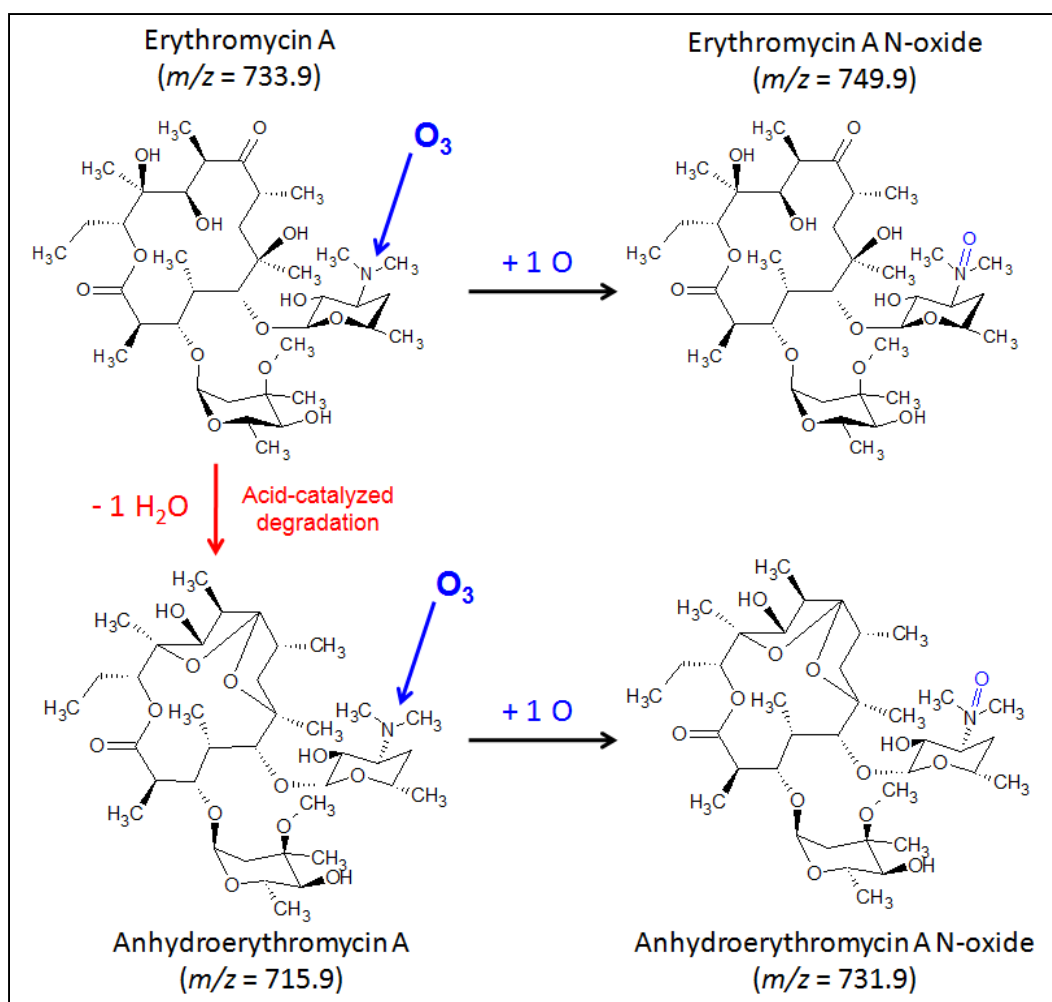


Figure 6-8. Peaks for intermediate oxidation products generated by ozonation of erythromycin and anhydroerythromycin. (The individual chromatograms stem from two different samples: one at pH 8.5 where erythromycin A dominates, and the other at pH 4.1, where anhydroerythromycin A dominates. The $m/z = 733.9$ and $m/z = 749.9$ chromatograms come from a sample that was dosed with ozone to achieve a molar ratio of applied ozone to erythromycin of 0.97 mol/mol; the pH of the sample was 8.5. The total ion current, $m/z = 715.9$, and $m/z = 731.9$ chromatograms correspond to a sample that was dosed with ozone to achieve a molar ratio of applied ozone to erythromycin of 1.46 mol/mol; the pH of the sample was 4.1.)

The 733.9 and 715.9 m/z peaks correspond to erythromycin A and anhydroerythromycin A, respectively; the $m/z = 749.9$ and $m/z = 731.9$ peaks correspond to intermediate oxidation products. Lange *et al.* (2006) identified clarithromycin-N-oxide (MW = 764 g/mol) as a major product of clarithromycin (MW = 748 g/mol) reaction with ozone. In this case, ozone attacks the lone pair of electrons on the tertiary amine present on the desosamine group, resulting in addition of a double-bonded oxygen onto the nitrogen atom in the desosamine sugar (Lange *et al.*, 2006). In that work, Lange *et al.* (2006) postulated that formation of the macrolide-N-oxide product can be expected for erythromycin, roxithromycin, and “all the other macrolide drugs.” From the major peaks identified in our samples, the $m/z = 749.9$ peak would correspond to the addition of an oxygen atom to the $m/z = 733.9$ peak. Furthermore, the difference between the $m/z = 715.9$ peak (anhydroerythromycin A) and the $m/z = 731.9$ peak is also 16 units, which corresponds to addition of an oxygen atom to the molecule. Both of these products can be described by the same ozone attack mechanism that was proposed by Lange *et al.* (2006). For these reasons, the evidence suggests that the two major oxidation products identified in this work correspond to erythromycin A N-oxide (CAS #992-65-4) and anhydroerythromycin A N-oxide (CAS #63950-90-3). In Scheme 6-2, we show the proposed site of ozone attack on the erythromycin A and anhydroerythromycin A molecules as well as the structures of the proposed transformation products.



Scheme 6-2. Erythromycin A and anhydroerythromycin A oxidation mechanisms.

These transformations essentially remove the antimicrobial activity of the erythromycin molecule as demonstrated above in Figure 6-6 and Figure 6-7. This result corresponds well to the known pharmacology of macrolides. As described earlier, Lemke and Williams (2008) indicated that the C-5 D-desosamine moiety is especially important to inhibition. As the transformation from erythromycin A to erythromycin A N-oxide affects the predominant active site of the D-desosamine functional group, it is not surprising that binding to the 23S rRNA would be affected, thereby, eliminating inhibition of peptidyltransferase and the bacteriostatic activity of erythromycin.

CONCLUSIONS

The behavior of erythromycin was studied throughout an oxidative treatment process:

- At acidic pH, erythromycin A degrades to form anhydroerythromycin A;
- While erythromycin A demonstrates antimicrobial activity ($IC_{50} = 4.87(\pm 0.55) \times 10^{-5}$ M, $H = 1.72(\pm 0.32) \times 10^4$ for *E. coli* ATCC #25922), anhydroerythromycin A is a much less potent antimicrobial compound and no significant activity was observed in this study;
- The specific rate constants for erythromycin A and anhydroerythromycin A transformation by ozone were determined to be $4.36(\pm 0.14) \times 10^6 \text{ M}^{-1} \text{ s}^{-1}$ and $6.00(\pm 0.25) \times 10^6 \text{ M}^{-1} \text{ s}^{-1}$, respectively. These rate constants correspond to the deprotonated species; rate constants for the reaction of protonated erythromycin species with ozone are negligible ($< 1 \text{ M}^{-1} \text{ s}^{-1}$);
- Both erythromycin A and anhydroerythromycin A underwent the same oxidative mechanism, namely, the addition of an oxygen atom on the free tertiary amine located on the D-desosamine moiety to form erythromycin A N-oxide ($C_{37}H_{67}NO_{14}$, MW = 749.9 g/mol) and anhydroerythromycin A N-oxide ($C_{37}H_{65}NO_{13}$, MW = 731.9 g/mol), respectively;
- The intermediate oxidation products identified in this study did not contribute to the residual antimicrobial activity of samples, that is, erythromycin A was the only antimicrobially active substance present in our samples.

The implications of this research for the field of environmental engineering demonstrate that not only does erythromycin degrade to form anhydroerythromycin A, which is much less antimicrobially potent than erythromycin A, but also erythromycin intermediate oxidation products do not possess antimicrobial potency. These findings relieve some of the concern over erythromycin presence in the environment because it demonstrates that ozone-based treatment of erythromycin will eliminate most (due to the rapid reaction of erythromycin with ozone) of the corresponding antimicrobial activity. The rapid erythromycin transformation kinetics with ozone allow for highly effective

erythromycin treatment in ozone processes; in advanced oxidation processes, erythromycin will not compete as well because transformation will be a direct function of the relative concentration of erythromycin with respect to background NOM. Questions still abound regarding non-lethal concerns of antimicrobial presence in the environment especially with regards to antibiotic resistance (Kummerer, 2004) and interruption of cell-signaling processes (Davies *et al.*, 2006; Fajardo and Martínez, 2008).

CHAPTER 7 – CONCLUSIONS

In *The Sea Around Us*, Rachel Carson, arguably the mother of the environmental movement, stated “For all at last returns to the sea...” (Carson, 1951) As technology, chemical production, and pharmaceutical development progresses, we must remember that the chemicals that we produce and consume do indeed find their way into our water supplies. To protect environmental and human health, water and wastewater treatment processes that are capable of removing the threat from trace organic contaminants need to be developed and tested. The ability of ozone-based treatment processes to transform four model pharmaceuticals was demonstrated in this research. The scientific understanding of how those chemicals are transformed and the potential for the intermediate oxidation products to exert pharmacological activity was investigated. Additionally, novel methods for employing ozone-based processes to determine the transformation kinetics of PhACs with ozone and hydroxyl radicals were presented. Below, three sets of bulleted lists describing the major conclusions drawn from the research results from Chapters 4-6 are presented below. Those lists describe major conclusions stemming from ozone experimentation with four pharmaceuticals: cyclophosphamide (Chapter 4), ifosfamide (Chapter 4), ciprofloxacin (Chapter 5), and erythromycin (Chapter 6). These compounds were chosen for a variety of reasons, including their predicted reactivity with ozone and their pharmacological mechanisms of action. Subsequent to the summation of findings for individual pharmaceuticals, an overview that ties these separate results together into a unified story of the significance of the research is given.

Based on the experimental findings presented in Chapter 4, which focuses on determination of the transformation kinetics of cyclophosphamide and ifosfamide by

ozone and hydroxyl radicals, identification of the impact of NOM on cyclophosphamide and ifosfamide transformation, and characterization of intermediate oxidation products, the following conclusions were reached.

- A highly concentrated ozone stock solution can be continuously pumped into a separate reactor, and the aqueous ozone concentration and ozone exposure can be controlled by the flow rate.
- A similar experimental design, with inclusion of continuous addition of hydrogen peroxide, can be employed to achieve a controllable level of hydroxyl radical exposure.
- The rate constants for cyclophosphamide and ifosfamide reaction with hydroxyl radicals were determined using the continuous peroxone addition reactor. The use of this reactor to determine transformation kinetics of PhACs with hydroxyl radicals is novel. The rate constants for the transformation cyclophosphamide and ifosfamide by hydroxyl radicals are $2.69(\pm 0.17) \times 10^9 \text{ M}^{-1}\text{s}^{-1}$ and $2.73(\pm 0.16) \times 10^9 \text{ M}^{-1}\text{s}^{-1}$, respectively.
- The continuous ozone reactor can be employed to determine the rate constants for compounds that react slowly with ozone (*i.e.*, cyclophosphamide and ifosfamide), and this methodology is an improvement over standard batch reactors with a single ozone addition at time zero due to the ability to control the ozone concentration throughout experimentation. The rate constants for the transformation of cyclophosphamide and ifosfamide with ozone are $3.03(\pm 0.48) \text{ M}^{-1}\text{s}^{-1}$ and $7.38 (\pm 0.27) \text{ M}^{-1}\text{s}^{-1}$, respectively.
- The presence of NOM impacts the rate of transformation of cyclophosphamide and ifosfamide mainly through NOM reaction with ozone, which reduces the achievable hydroxyl radical exposure for a specific ozone dose.
- Many intermediate oxidation products are observed for cyclophosphamide and ifosfamide, and an overlap exists for the *m/z* values associated with cyclophosphamide and ifosfamide transformation products; furthermore, these products are similar to known metabolites of cyclophosphamide and ifosfamide,

including the 4-keto-, 4-hydroxy-, and imino- derivatives of the parent compounds.

- The pharmacologically active metabolites of cyclophosphamide (phosphoramidate mustard) and ifosfamide (isophosphoramidate mustard) were formed at pH 9.6 but not pH 2.5; these results suggest that the pharmacological activity associated with these compounds was not removed by ozonation.

In Chapter 5, the ability of the continuous ozone addition reactor to treat ciprofloxacin and its associated antimicrobial activity in the presence of NOM was demonstrated. The major conclusions from that work include the following.

- Ciprofloxacin reacts quickly with ozone ($k''_{O_3,app,CIP} = 1.55(\pm 0.13) \times 10^4 \text{ M}^{-1}\text{s}^{-1}$ at pH 7) and hydroxyl radicals ($k''_{HO\cdot,app,CIP} = 1.19(\pm 0.69) \times 10^{10} \text{ M}^{-1}\text{s}^{-1}$ at pH 7).
- In the continuous ozone addition reactor, ciprofloxacin is quickly transformed in the absence of any background DOC.
- In the presence of NOM, ciprofloxacin removal for particular applied ozone doses depended on the DOC concentration and NOM composition.
- Of the three NOM sources tested, the hydrophobic organic acids isolated from Claremore Lake exerted the greatest impact on ciprofloxacin transformation. The Claremore Lake transphilic organic acids isolate exerted the lowest impact on ciprofloxacin transformation, while the Lake Austin hydrophobic organic acids were intermediate in their effect. These results are consistent with the composition and $SUVA_{254}$ of the NOM isolates.
- Ciprofloxacin inhibits *E. coli* at relatively low concentrations, and the inhibition profile is exceptionally sharp with the difference between complete and no inhibition being approximately 7 $\mu\text{g/L}$ (4-11 $\mu\text{g/L}$). The IC_{50} and Hill slope of the ciprofloxacin inhibition profile are 9.0 $\mu\text{g/L}$ and 0.42, respectively.
- The residual antimicrobial activity of samples from continuous ozone addition experiments was measured, and the inhibition profile of oxidized samples was

shifted to lower ciprofloxacin concentrations, suggesting that intermediate oxidation products exert a non-negligible antimicrobial activity.

- The applied ozone dose required for complete removal of residual antimicrobial activity depends on the presence, concentration, and composition of the background NOM present in solution.

The rate constants for erythromycin transformation by ozone, identification of the intermediate oxidation products formed through erythromycin reaction with ozone, and characterization of the antimicrobial activity of erythromycin and its major intermediate oxidation products were presented in Chapter 6. In solution, erythromycin A readily degrades to anhydroerythromycin A; this reaction is irreversible. As erythromycin A and anhydroerythromycin A were present in samples, experimentation addressed the points listed above for both compounds. The following conclusions were reached.

- The rate constants for transformation of the deprotonated forms of erythromycin A and anhydroerythromycin A by ozone were determined to be $k''_{O_3,EA} = 4.36(\pm 0.14) \times 10^6 \text{ M}^{-1}\text{s}^{-1}$ and $k''_{O_3,AEA} = 6.00(\pm 0.25) \times 10^6 \text{ M}^{-1}\text{s}^{-1}$, respectively.
- The kinetics of erythromycin transformation by ozone are so rapid that no hydroxyl radical exposure was observed (while erythromycin remained in solution).
- The inhibition profile of erythromycin exhibited a gentler slope (*i.e.*, a larger range of pharmaceutical concentrations result in partial *E. coli* inhibition) than that of ciprofloxacin. The IC_{50} and Hill slope of the erythromycin inhibition profile were $4.87(\pm 0.55) \times 10^{-5} \text{ M}$ and $1.72(\pm 0.32) \times 10^4$, respectively.
- The antimicrobial activity against *E. coli* of anhydroerythromycin A was found to be negligible compared to that of erythromycin A; therefore, one approach to removing the antimicrobial activity of solutions containing erythromycin A is to lower the pH.

- The major intermediate oxidation products formed via ozone attack on erythromycin A and anhydroerythromycin A were identified as erythromycin A N-oxide and anhydroerythromycin A N-oxide.
- Erythromycin A N-oxide and anhydroerythromycin A N-oxide demonstrated negligible antimicrobial activity against *E. coli*.

SIGNIFICANCE

As comprehension of the extent of pharmaceutical contamination increases, the understanding of engineered processes aimed at effectively removing these compounds from water and wastewater sources is crucial. In this research, the ability of ozone to treat four pharmacologically active compounds was demonstrated. The dual oxidation mechanism (*i.e.*, ozone and hydroxyl radicals) present in ozone processes ensures effective treatment of PhACs. For this reason, ozone-based processes have a unique advantage with respect to treatment of wastewater-derived organic contaminants.

The individual findings from Chapters 4-6 can be merged to demonstrate the higher level findings of this research. From the calculated rate constants, it is clear that cyclophosphamide and ifosfamide react slowly with ozone and that ciprofloxacin and erythromycin react quickly with ozone. The four compounds demonstrate rate constants for reaction with hydroxyl radicals of $2.7\text{--}12 \times 10^9 \text{ M}^{-1}\text{s}^{-1}$. Typical values of ozone exposure and hydroxyl radical exposure after 30 minutes in the continuous aqueous ozone addition reactor were $9.1 \times 10^{-3} \text{ M-s}$ and $4.0 \times 10^{-10} \text{ M-s}$, respectively. At pH 7, these exposures would lead to complete ciprofloxacin and erythromycin transformation; the removal efficiencies of cyclophosphamide and ifosfamide would be approximately 66%. With a hydroxyl radical exposure of $2 \times 10^{-9} \text{ M-s}$, over 99% removal of cyclophosphamide and ifosfamide can be achieved. In the continuous ozone and peroxone addition reactors, the ozone and hydroxyl radical exposures can be easily controlled; therefore, depending on the PhAC composition of the untreated water, the process can be optimized. For conventional ozone reactors, the applied ozone dose that corresponds to a sufficient

ozone exposure (and by extension, hydroxyl radical exposure) for the water of interest must be determined. The rate constants for transformation of these four compounds by ozone span the range of expected values for a much broader array of PhACs; therefore, ozone-based treatment processes aimed at PhAC treatment should be capable of achieving an ozone exposure of at least 9.1×10^{-3} M-s and a hydroxyl radical exposure of at least of 2×10^{-9} M-s, even in the presence of background NOM.

The findings of this study indicate that concern over the formation of pharmacologically active intermediate oxidation products during ozonation of pharmaceuticals is valid. Erythromycin was the only compound that did not theoretically or experimentally demonstrate the ability to form pharmacologically active compounds through reaction with ozone. During treatment of the two prodrugs, cyclophosphamide and ifosfamide, the active metabolites, phosphoramidate mustard and isophosphoramidate mustard, were formed. Other metabolic products of cyclophosphamide and ifosfamide were also detected, indicating the ability of hydroxyl radical driven oxidation processes to emulate metabolic processes. Additionally, intermediate oxidation products stemming from ciprofloxacin transformation contributed to the residual antimicrobial activity of treated samples. For this reason, detailed analyses of other pharmaceuticals are expected to indicate that the potential to form pharmacologically active products is widespread. Therefore, this work should be considered as part of a model relating ozone and hydroxyl radical attacks to the structure-pharmacological activity relationships of various classes of drugs.

The rise of wastewater reclamation and indirect water reuse has propelled the issue of trace organic contaminants into media and academic spotlight. Due to mounting pressure from their customers, municipal water utilities are concerned about the presence of trace constituents in finished drinking water and wastewater. In these treatment scenarios, it is important to consider compounds that compete with pharmaceuticals for reaction with ozone and hydroxyl radicals. For the most part, competition will be

manifested through the oxidant demand of the background NOM matrix. A major focus of the research presented herein was to determine the impact of organic matter on oxidation of the four target pharmaceuticals. Results demonstrate that the presence and composition of NOM can significantly alter the applied ozone dose required to achieve the desired removal efficiency. While others have demonstrated how NOM composition affects NOM reactivity with ozone, this research goes further to show the impact that NOM reaction with ozone has on not only ciprofloxacin and erythromycin removal, but also elimination of residual antimicrobial activity.

With the increasing attention on treating trace constituents in water and wastewater processes, pioneering changes to traditional ozonation experiments are vital. Traditionally, ozone has been applied in the gaseous form, necessitating the presence of gaseous diffusers in the ozone contact tanks. Moving forward, it would be interesting to assess the effectiveness of the continuous ozone and peroxone addition reactors in pilot-scale projects. These pilot-scale reactors would supply highly concentrated liquid ozone (and hydrogen peroxide in the case of peroxone treatment) in a similar manner as liquid chlorination processes. In addition, opportunities exist for using the off-gas from the ozone stock solution in other stages of the treatment train, applying higher ozone doses, and improving occupational safety. Given these possibilities and the operational ease of employing aqueous ozone, these novel ozone-based processes might demonstrate significant advantages in water and wastewater treatment plants.

RECOMMENDATIONS FOR FUTURE WORK

This research has demonstrated the ability for ozone-based water treatment processes to effectively treat four pharmaceuticals (two antimicrobials and two chemotherapy agents) in a variety of background water matrices. The experimental design of the research activities described within this dissertation has connected key parameters in oxidation processes aimed at treating trace organic contaminants, and in particular, pharmacologically active compounds. While key connections have been made

regarding the impact of organic matter on treatment of pharmaceuticals, the ability for pharmacologically active intermediate oxidation products to be formed in oxidation processes, and the removal of residual antimicrobial activity throughout treatment of pharmaceuticals, this field is still relatively young. Therefore, I propose the following recommendations for future work aimed at furthering the scientific and engineering understanding of ozone-based processes aimed at water treatment of organic wastewater-derived contaminants.

- 1.) *Isolation of intermediate products.* While the antimicrobial activity assay employed in this research (and that of other researchers) can suggest the impact of intermediate oxidation products on residual antimicrobial activity, a direct measure of the inhibition profile of all intermediate products will provide a clearer evaluation of how intermediate oxidation products contribute to the ultimate antimicrobial activity. At this time, no such work has been done; however, with advanced analytical equipment (LC-MS/MS) and the versatile collection of solid-phase extraction materials, isolation of individual intermediate oxidation products should be possible. By isolating individual products and measuring their inhibition profile, a detailed library of compound potencies can be created for individual pharmaceuticals. Such work would allow a more thorough understanding of the overall potency of intermediate oxidation products as compared to that of the parent pharmaceuticals.
- 2.) *Residual pharmacological activity of water sources containing multiple pharmaceuticals.* In this research, the behavior of the residual pharmacological activity of a water containing a mixture of pharmaceuticals from the same class of drugs (*e.g.*, antibiotics) was not investigated. Can the ultimate pharmacological activity of the mixture be determined by considering the additive effects of the individual pharmaceuticals? If not, is the ultimate pharmacological activity of mixtures synergistic (the combined effect is greater than the additive effects of the

individual components) or antagonistic (the combined effect is less than the additive effects of the individual components)? Furthermore, this question applies to the additive effects of a parent compound and its intermediate oxidation products. Does the formation of intermediate oxidation products affect the residual antimicrobial activity on a per mole of parent compound basis?

- 3.) *Consideration of non-lethal impacts.* The work on the pharmacological activity of both parent compounds and transformation products presented in this dissertation focused only on antimicrobial activity, which was measured as a function of *E. coli* proliferation. While such work is pioneering, the next step in this hybrid association of water treatment with environmental toxicology is consideration of non-lethal impacts that pharmaceuticals exert on environmental and human health. How does the presence of anti-inflammatory, antihypertensive, antidepressant, anti-diabetic, and other drugs in water affect environmental and human health? Furthermore, research in the antibiotic community has demonstrated that, at sub-lethal concentrations, antibiotics can affect cell-signaling processes. As environmentally-relevant concentrations are typically in the sub-lethal regime, it would be interesting to extend this research into how water and wastewater treatment processes affect the ability of water containing PhACs to impact cell-signaling processes.
- 4.) *Model development for predicting PhAC transformation efficiency.* Using known rate constants for PhACs, PhAC intermediate oxidation products, and NOM, and typical values of ozone exposure and hydroxyl radical exposure experienced in oxidation and advanced oxidation processes, the transformation efficiency of PhACs can be modeled for specified systems. Given the wide range of rate constants observed for PhAC transformation by ozone, this model would be particularly useful in delineating PhAC transformation efficiencies for solutions containing mixtures of pharmaceuticals.

5.) *Pilot scale testing of the continuous aqueous ozone addition reactor.* While the above efforts are mainly focused on environmental toxicology extensions of this work, future work on the engineering aspects of this project also exist. In particular, it would be interesting to study the ability of the continuous aqueous ozone addition reactor to operate in a pilot-scale setting. In this case, I envisage a process that is similar to liquid chlorination processes. Engineering challenges include (1) maintaining the stock ozone supply while introducing enough ozone to effectively treat trace organic contaminants in a continuous flow scheme, (2) efficiently using the off-gas from the ozone stock solution in other stages of the treatment train, and (3) conducting an energy audit of the continuous aqueous ozone reactor and comparing the treatment cost (kWh/1000 gallons) with a gaseous ozonation system operating at the same level of PhAC transformation.

APPENDIX A – DISH WASHING AND AUTOCLAVE PROTOCOLS

Dish Washing Protocol

All glassware underwent stringent washing protocol. First dishes were rinsed with tap water and submerged in an Alconox solution for at least 30 minutes. Dishes were rinsed with Alconox solution at least three times, rinsed five times with tap water, and submerged in a Micro-90® (an alkaline detergent; Micro-90(R), 2009) bath overnight. After rinsing at least three times with the Micro-90® solution, the dishes were rinsed five times with DI and submerged in a 10% nitric acid bath overnight. The dishes were rinsed at least three times with the acid bath solution, rinsed five times with DI, and left to dry overnight. To remove any organic carbon from the glassware, dishes were baked in a muffle furnace set to 550°C for at least three hours. After cooling, dishes were covered with Parafilm to prevent accumulation of dust or particles in the glassware.

Autoclave Procedure

All dishware and solutions used in the antimicrobial activity assay were autoclaved prior to use. The autoclave was the Sterilmatic model from Market Forge Industries, Inc. Dishware was either loosely capped or covered with aluminum foil and autoclaved for 21 minutes using a fast temperature ramp. Solutions, including DI and Mueller-Hinton Broth (MHB), were autoclaved for 21 minutes using a slower temperature ramp. All solid microbial waste was collected in an autoclavable bag, autoclaved for at least 30 minutes, marked with a “Treated in Accordance with Section 1.136 of the TAC Special Waste from Health Care Related Facilities Regulations” sticker, and disposed of into normal-use waste bins. All liquid waste was placed into a bottle containing approximately 10% bleach and autoclaved for at least 30 minutes, and disposed of into hazardous waste bins for subsequent disposal by the University of Texas Environmental Health and Safety team.

APPENDIX B – FLUORESCENCE EEM DATA FOR NOM ISOLATES

Recently, several authors (Baker, 2001; 2002a; b; Chen *et al.*, 2003; Her *et al.*, 2003) have used fluorescence mapping as a tool for describing the makeup of organic matter in water sources. Chen *et al.* (2003) published a Fluorescence Excitation-Emission Matrix (EEM) map (Figure B-1) that listed the location of several classes of organic compounds. Several authors have employed this tool to show how NOM matrices are altered in treatment processes (Win *et al.*, 2000; Holbrook *et al.*, 2005).

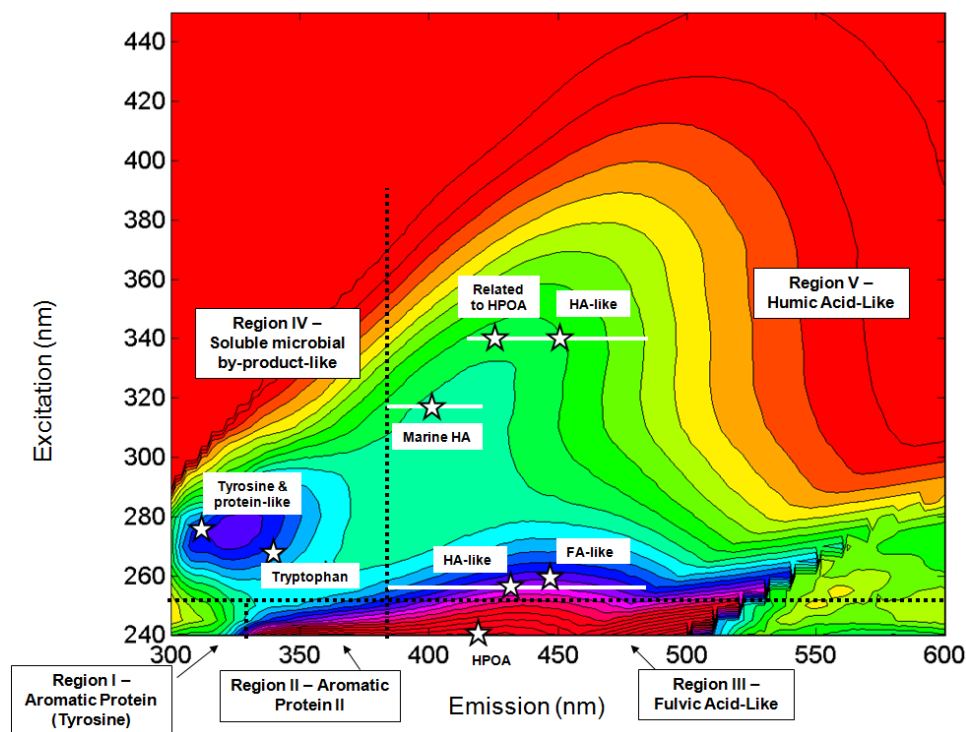


Figure B-1. Description of the major regimes of a Fluorescence EEM map.

Below, in Figure B-2, the fluorescence maps for the Claremore Lake HPOA and TPIA isolates, and the Lake Austin whole water and HPOA isolate are presented. The EEMs for these NOM matrices are different; also, note the difference in magnitude of the fluorescence signal amongst the four samples. These Fluorescence EEMs contain a lot of data; therefore, several authors have taken to calculating the fluorescence index as the ratio of the emission at 470 nm by the emission at 520 nm at an excitation wavelength of 370 nm (Jaffe *et al.*, 2008). The fluorescence indices for the NOM matrices presented in Figure B-2 are provided in Table B-1.

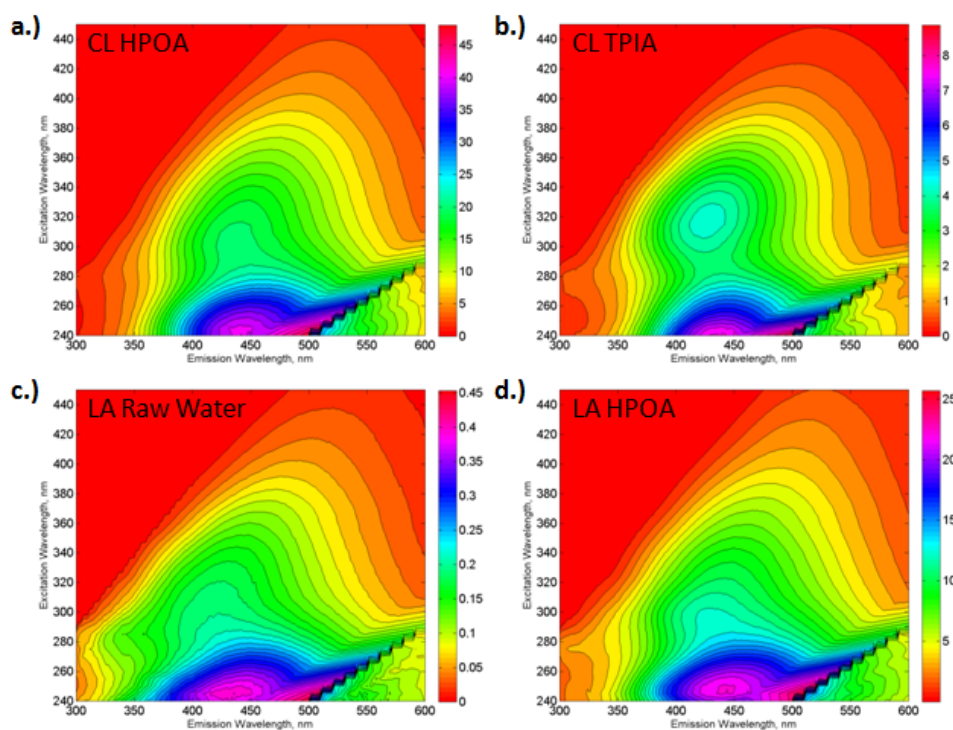


Figure B-2. Fluorescence maps of (a) Claremore Lake HPOA, b.) Claremore Lake TPIA, c.) Lake Austin raw water, and d.) Lake Austin HPOA.

Table B-1. Fluorescence index for organic matter isolates.

Solution	Fluorescence Index
Claremore Lake HPOA	1.31
Claremore Lake TPIA	1.55
Lake Austin Raw Water	1.52
Lake Austin HPOA	1.34

In Chapters 4-6, the impact of organic matter on oxidation of the four pharmacologically active compounds of concern was investigated. As only three NOM isolates were available, no overriding conclusions were drawn from that data with respect to the Fluorescence Excitation-Emission Matrix data. Regardless, this information is provided here for future researchers employing the Lake Austin and Claremore Lake isolates employed in this research.

APPENDIX C: ANTIMICROBIAL ACTIVITY ASSAY DATA ANALYSIS

This Appendix explains the analysis of antimicrobial activity data using the inhibition profile and the potency equivalents protocols that were discussed in Chapters 5-6.

Inhibition Profile Protocol

Wells were partially filled with 100 μL of a standard or sample; then, 100- μL of the *E. coli* inoculum is added to the well. Triplicates are run for all standards and samples. The plate setup for a microplate containing standard solutions of ciprofloxacin is shown below; please note, that the positive and negative growth controls were present on another plate for this particular experiment.

PLATE SETUP												
CIP ($\mu\text{g/L}$)	1	2	3	4	5	6	7	8	9	10	11	12
A	100.00	80.00	64.00	51.20	40.96	32.77	26.21	20.97	16.78	13.42	10.74	8.59
B	100.00	80.00	64.00	51.20	40.96	32.77	26.21	20.97	16.78	13.42	10.74	8.59
C	100.00	80.00	64.00	51.20	40.96	32.77	26.21	20.97	16.78	13.42	10.74	8.59
D												
E	6.87	5.50	4.40	3.52	2.81	2.25	1.80	1.44	1.15	0.92	0.74	0.59
F	6.87	5.50	4.40	3.52	2.81	2.25	1.80	1.44	1.15	0.92	0.74	0.59
G	6.87	5.50	4.40	3.52	2.81	2.25	1.80	1.44	1.15	0.92	0.74	0.59
H												

In this example, standard solutions containing various concentrations (0.59-100 $\mu\text{g/L}$) of ciprofloxacin were added to microplate. After 100- μL of each standard was added to the wells, 100- μL of the *E. coli* inoculum was added to each well. The plate was incubated for 20 hours at 37°C in ambient air. After the incubation period, the

absorbance at 600 nm for each well was read using a microplate reader. The absorbance of a microplate containing no solution (*i.e.*, a blank plate) was subtracted from the raw data. The raw data and the corrected data are presented below:

RAW ABSORBANCE DATA												
ABS _{600 nm}	1	2	3	4	5	6	7	8	9	10	11	12
A	0.149	0.159	0.146	0.150	0.149	0.145	0.159	0.146	0.164	0.167	0.196	0.198
B	0.146	0.143	0.139	0.142	0.144	0.136	0.152	0.146	0.144	0.144	0.161	0.213
C	0.137	0.136	0.131	0.138	0.140	0.141	0.150	0.136	0.139	0.142	0.178	0.187
D	0.095	0.094	0.095	0.096	0.099	0.099	0.097	0.093	0.099	0.097	0.089	0.098
E	0.204	0.225	0.224	0.246	0.245	0.254	0.246	0.242	0.242	0.237	0.248	0.250
F	0.216	0.230	0.240	0.239	0.234	0.235	0.243	0.221	0.247	0.242	0.241	0.257
G	0.216	0.229	0.246	0.240	0.233	0.228	0.251	0.241	0.251	0.258	0.235	0.251
H	0.094	0.096	0.091	0.098	0.095	0.105	0.104	0.098	0.101	0.098	0.103	0.105

CORRECT ABSORBANCE DATA												
ABS _{600 nm}	1	2	3	4	5	6	7	8	9	10	11	12
A	0.338	0.018	0.335	0.328	0.323	0.315	0.311	0.280	0.263	0.259	0.261	0.254
B	0.325	0.012	0.273	0.196	0.196	0.226	0.289	0.221	0.258	0.258	0.250	0.227
C	0.231	0.012	0.201	0.324	0.331	0.256	0.233	0.172	0.235	0.167	0.236	0.219
D	0.011	0.004	0.009	0.005	0.005	0.011	0.009	0.004	0.007	0.000	0.003	-0.002
E	0.211	0.197	0.202	0.179	0.167	0.129	0.052	0.035	0.045	0.034	0.012	0.010
F	0.221	0.209	0.198	0.152	0.171	0.149	0.072	0.040	0.040	0.044	0.014	-0.004
G	0.226	0.205	0.197	0.191	0.171	0.166	0.124	0.068	0.053	0.046	0.019	0.008
H	0.013	0.009	0.008	0.010	0.010	0.015	0.011	0.010	-0.008	0.003	0.022	0.028

For this example, the corrected absorbance values for the negative and positive growth controls were 0.033 and 0.144, respectively. The corrected raw data was then normalized using Eq. C-1, and converted to percent of *E. coli* inhibition using Eq. C-2. These equations set the negative and positive growth controls to 0 and 100% inhibition, respectively.

$$ABS_{600-nm,norm.} = \frac{ABS_{600-nm,sample} - ABS_{600-nm,negative}}{ABS_{600-nm,positive} - ABS_{600-nm,negative}} \quad \text{Eq. C-1}$$

$$\% \text{ Inhibition} = (1 - ABS_{600-nm,norm.}) \times 100\% \quad \text{Eq. C-2}$$

Table C-1 shows the ciprofloxacin concentration, the corrected and normalized absorbance at 600 nm data, and the percent of *E. coli* inhibition for the microplate described above.

Table C-1. Summary of inhibition data for antimicrobial activity assay with ciprofloxacin.

CIP ($\mu\text{g/L}$)	ABS _{600 nm}			ABS _{600 nm, norm.}			Percent <i>E. coli</i> Inhibition		
	Rep. 1	Rep. 2	Rep. 3	Rep. 1	Rep. 2	Rep. 3	Rep. 1	Rep. 2	Rep. 3
100.00	0.0333	0.0270	0.0387	0.0012	-0.0558	0.0491	99.9	105.6	95.1
80.00	0.0347	0.0410	0.0213	0.0132	0.0701	-0.1067	98.7	93.0	110.7
64.00	0.0390	0.0367	0.0353	0.0521	0.0311	0.0191	94.8	96.9	98.1
51.20	0.0360	0.0310	0.0363	0.0251	-0.0198	0.0281	97.5	102.0	97.2
40.96	0.0297	0.0427	0.0423	-0.0318	0.0851	0.0821	103.2	91.5	91.8
32.77	0.0217	0.0203	0.0307	-0.1037	-0.1157	-0.0228	110.4	111.6	102.3
26.21	0.0443	0.0437	0.0450	0.1000	0.0941	0.1060	90.0	90.6	89.4
20.97	0.0300	0.0443	0.0417	-0.0288	0.1000	0.0761	102.9	90.0	92.4
16.78	0.0430	0.0337	0.0293	0.0881	0.0042	-0.0348	91.2	99.6	103.5
13.42	0.0527	0.0423	0.0423	0.1750	0.0821	0.0821	82.5	91.8	91.8
10.74	0.0863	0.0603	0.0790	0.4776	0.2439	0.4117	52.2	75.6	58.8
8.59	0.0830	0.1067	0.0833	0.4476	0.6604	0.4506	55.2	34.0	54.9
6.87	0.1130	0.1240	0.1203	0.7173	0.8162	0.7833	28.3	18.4	21.7
5.50	0.1330	0.1397	0.1350	0.8971	0.9571	0.9151	10.3	4.3	8.5
4.40	0.1260	0.1467	0.1503	0.8342	1.0200	1.0529	16.6	-2.0	-5.3
3.52	0.1427	0.1387	0.1443	0.9840	0.9481	0.9990	1.6	5.2	0.1
2.81	0.1490	0.1420	0.1300	1.0410	0.9780	0.8702	-4.1	2.2	13.0
2.25	0.1510	0.1280	0.1227	1.0589	0.8522	0.8042	-5.9	14.8	19.6
1.80	0.1400	0.1360	0.1503	0.9600	0.9241	1.0529	4.0	7.6	-5.3
1.44	0.1457	0.1150	0.1337	1.0110	0.7353	0.9031	-1.1	26.5	9.7

The first column (ciprofloxacin concentration) and the last three columns (Percent of *E. coli* Inhibition) were copied into GraphPad Prism. The data was analyzed using the “log(inhibitor) vs. normalized response – Variable slope” model using a least squares fit. In addition to calculation of the standard error associated with the model fits on IC₅₀ and H, the 95% confidence bands were generated. Model input/output are shown in Figure C-1, below.

Table format XY		X	A		
		CIP (µg/L)	Percent Inhibition (%)		
		X	A:Y1	A:Y2	A:Y3
1	Title	100.00	99.9	105.6	95.1
2	Title	80.00	98.7	93.0	110.7
3	Title	64.00	94.8	96.9	98.1
4	Title	51.20	97.5	102.0	97.2
5	Title	40.96	103.2	91.5	91.8
6	Title	32.77	110.4	111.6	102.3
7	Title	26.21	90.0	90.6	89.4
8	Title	20.97	102.9	90.0	92.4
9	Title	16.78	91.2	99.6	103.5
10	Title	13.42	82.5	91.8	91.8
11	Title	10.74	52.2	75.6	58.8
12	Title	8.59	55.2	34.0	54.9
13	Title	6.87	28.3	18.4	21.7
14	Title	5.50	10.3	4.3	8.5
15	Title	4.40	16.6	-2.0	-5.3
16	Title	3.52	1.6	5.2	0.1
17	Title	2.81	-4.1	2.2	13.0
18	Title	2.25	-5.9	14.8	19.6
19	Title	1.80	4.0	7.6	-5.3
20	Title	1.44	-1.1	26.5	9.7
21	Title	1.15	7.3	-5.0	8.8
22	Title	0.92	3.1	-0.5	-13.7
23	Title	0.74	-7.7	-1.7	1.9
24	Title	0.59	-6.8	-18.5	-8.6

Nonlin fit Table of results		A
		Percent Inhibition (%)
		Y
1	log(inhibitor) vs. normalized response -- Variable slope	
2	Best-fit values	
3	LOGIC50	9.338
4	HILLSLOPE	0.2216
5	IC50	2.175e+009
6	Std. Error	
7	LOGIC50	0.2423
8	HILLSLOPE	0.02172
9	95% Confidence Intervals	
10	LOGIC50	8.854 to 9.821
11	HILLSLOPE	0.1782 to 0.2650
12	IC50	7.141e+008 to 6.626e+009
13	Goodness of Fit	
14	Degrees of Freedom	70
15	R ²	0.9662
16	Absolute Sum of Squares	5031
17	Sy.x	8.478
18	Number of points	
19	Analyzed	72

Figure C-1. GraphPad Prism input/output for analysis of the ciprofloxacin and percent inhibition data presented above in Table C-1.

In this case, the IC₅₀ of the data is given as the LOG(IC₅₀) value (9.338 µg/L) presented in Figure C-1. The standard error on the IC₅₀ is ±0.2423 µg/L, and the 95% confidence band on the IC₅₀ ranges from 8.854 – 9.821 µg/L. Similarly, the Hill slope for this data is 0.2216, with a standard error of 0.002172; the 95% confidence band for the Hill slope ranges from 0.1782 to 0.2650. The coefficient of correlation provided by GraphPad Prism is R² = 0.9662. In Figure C-2, the average (of the three replicate samples) for the percent inhibition data is plotted against ciprofloxacin concentration. The Hill curve and 95% confidence bands were plotted using the fitted values for IC₅₀ and H described in Figure C-1.

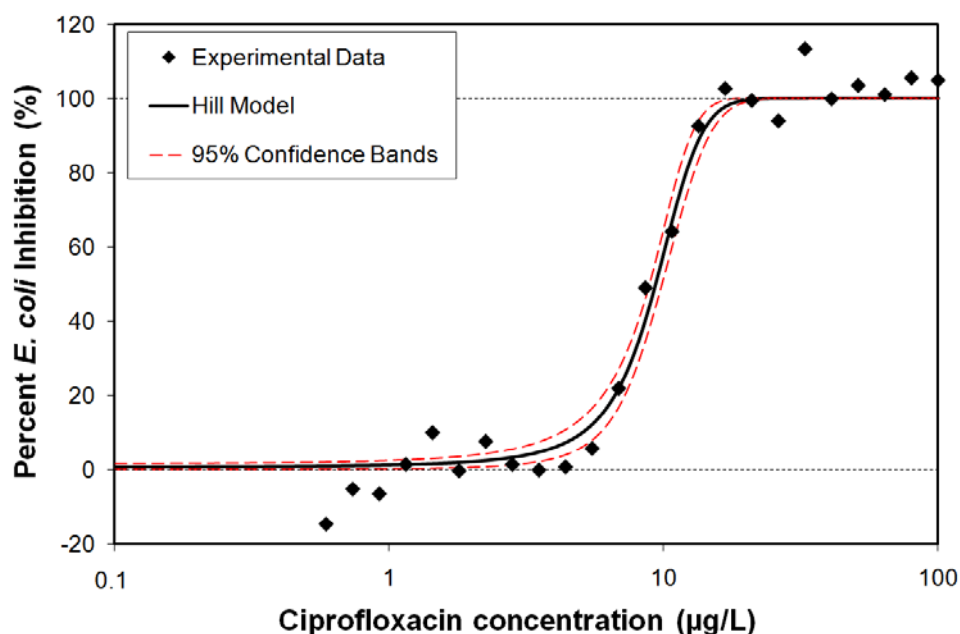


Figure C-2. The inhibition profile of ciprofloxacin against *E. coli*. (The Hill curve and the 95% confidence bands were generated in GraphPad Prism.)

Potency Equivalents Protocol

In this example, a 1000 mg/L erythromycin solution was generated. That solution was serially diluted ten times using a dilution factor of 0.50; the final solution contained 1.95 mg/L ERY. These solutions (1000 µL) were added to the first row of the microplate (A2 through A11). Sterile DI water (100 µL) was added to every other well on the plate (A1, A12, B1:H12). The standards in A2-A11 were then serially diluted by a factor of 0.6. For example, 150 µL of the solution (1000 mg/L ERY) in well A11 was added to well B11, which already contained 100 µL of DI, thereby generating a solution with 27.99 mg/L ERY. It should be noted that 100 µL of sample/standard was left in each well. This process was completed for each initial standard solution (A2-A11), working down the plate. Hence, seven dilutions were created. Column 1 (A1-H1) were reserved for positive growth controls, while Column 12 (A12-H12) were set aside for negative growth controls; all of these wells contained sterile DI water and the background matrix. A schematic of the erythromycin concentrations in each well is provided below:

PLATE SETUP												
ERY (mg/L)	1	2	3	4	5	6	7	8	9	10	11	12
A	Pos.	1.95	3.91	7.81	15.63	31.25	62.50	125.00	250.00	500.00	1000.00	Neg.
B	Pos.	1.17	2.34	4.69	9.38	18.75	37.50	75.00	150.00	300.00	600.00	Neg.
C	Pos.	0.70	1.41	2.81	5.63	11.25	22.50	45.00	90.00	180.00	360.00	Neg.
D	Pos.	0.42	0.84	1.69	3.38	6.75	13.50	27.00	54.00	108.00	216.00	Neg.
E	Pos.	0.25	0.51	1.01	2.03	4.05	8.10	16.20	32.40	64.80	129.60	Neg.
F	Pos.	0.15	0.30	0.61	1.22	2.43	4.86	9.72	19.44	38.88	77.76	Neg.
G	Pos.	0.09	0.18	0.36	0.73	1.46	2.92	5.83	11.66	23.33	46.66	Neg.
H	Pos.	0.05	0.11	0.22	0.44	0.87	1.75	3.50	7.00	14.00	27.99	Neg.

After the samples were added to the plate, 100- μ L of the *E. coli* inoculum was added to Columns 1-11; 100 μ L of MHB was added to Column 12, which contained negative growth controls. The raw data was then normalized using Eq. C-1, and converted to percent of *E. coli* inhibition using Eq. C-2. The raw and corrected data are shown below:

RAW ABSORBANCE DATA												
ABS _{600 nm}	1	2	3	4	5	6	7	8	9	10	11	12
A	0.434	0.374	0.330	0.297	0.250	0.180	0.160	0.147	0.157	0.159	0.150	0.121
B	0.406	0.363	0.343	0.308	0.258	0.243	0.157	0.145	0.152	0.149	0.150	0.114
C	0.411	0.370	0.351	0.328	0.288	0.242	0.191	0.153	0.139	0.139	0.140	0.103
D	0.389	0.367	0.353	0.338	0.312	0.270	0.220	0.161	0.145	0.146	0.133	0.113
E	0.387	0.371	0.366	0.352	0.332	0.303	0.260	0.217	0.150	0.145	0.133	0.105
F	0.380	0.380	0.360	0.352	0.345	0.316	0.291	0.239	0.210	0.146	0.132	0.105
G	0.387	0.386	0.375	0.369	0.352	0.330	0.313	0.279	0.233	0.181	0.138	0.106
H	0.396	0.399	0.402	0.383	0.365	0.364	0.345	0.306	0.275	0.227	0.166	0.116

CORRECTED ABSORBANCE DATA												
ABS _{600 nm}	1	2	3	4	5	6	7	8	9	10	11	12
A	0.315	0.250	0.222	0.184	0.126	0.052	0.046	0.030	0.042	0.043	0.040	0.007
B	0.296	0.264	0.240	0.197	0.155	0.134	0.049	0.041	0.043	0.046	0.049	0.007
C	0.309	0.268	0.253	0.227	0.183	0.132	0.084	0.057	0.029	0.039	0.042	0.006
D	0.293	0.262	0.253	0.231	0.205	0.155	0.105	0.058	0.036	0.030	0.027	0.005
E	0.291	0.270	0.262	0.246	0.229	0.197	0.152	0.112	0.042	0.040	0.038	0.007
F	0.289	0.291	0.266	0.254	0.250	0.208	0.183	0.125	0.102	0.051	0.040	0.003
G	0.292	0.291	0.282	0.274	0.260	0.232	0.216	0.184	0.133	0.088	0.047	0.011
H	0.284	0.300	0.301	0.280	0.266	0.255	0.244	0.208	0.166	0.123	0.052	0.013

Table C-2 shows the erythromycin concentration and the serial dilutions for each sample, the corrected and normalized absorbance at 600 nm data, and the percent of *E. coli* inhibition for the microplate described above.

The second column (Erythromycin concentration) was plotted against the last column (LOG(C/C₀)) for all ten data sets using GraphPad Prism®, as seen in Figure C-3. The data was analyzed using the “log(inhibitor) vs. normalized response – Variable slope” model using a least squares fit; the standard error was also computed. The GraphPad Prism software was not able to fit sample set #1 (serial dilutions of 1000 mg/L) or sample set #9 (serial dilutions of 3.91 mg/L).

Table C-2. Summary of inhibition data for antimicrobial activity assay with erythromycin run using the potency equivalents protocol.

Top level	ERY (mg/L)	ABS _{600 nm}	ABS _{600 nm,norm}	Percent <i>E. coli</i> Inhibition (%)	LOG(C/C ₀)
Pos.	Pos.	0.296	1.000	0.0	
Neg.	Neg.	0.003	0.000	100.0	
1.95	1.95	0.250	0.842	15.8	0.000
	1.17	0.264	0.891	10.9	-0.222
	0.70	0.268	0.905	9.5	-0.444
	0.42	0.262	0.884	11.6	-0.666
	0.25	0.270	0.912	8.8	-0.887
	0.15	0.291	0.983	1.7	-1.109
	0.09	0.291	0.983	1.7	-1.331
	0.05	0.300	1.013	-1.3	-1.553
3.91	3.91	0.222	0.746	25.4	0.000
	2.34	0.240	0.809	19.1	-0.222
	1.41	0.253	0.852	14.8	-0.444
	0.84	0.253	0.852	14.8	-0.666
	0.51	0.262	0.884	11.6	-0.887
	0.30	0.266	0.896	10.4	-1.109
	0.18	0.282	0.953	4.7	-1.331
	0.11	0.301	1.016	-1.6	-1.553
7.81	7.81	0.184	0.616	38.4	0.000
	4.69	0.197	0.662	33.8	-0.222
	2.81	0.227	0.763	23.7	-0.444
	1.69	0.231	0.777	22.3	-0.666
	1.01	0.246	0.828	17.2	-0.887
	0.61	0.254	0.855	14.5	-1.109
	0.36	0.274	0.924	7.6	-1.331
	0.22	0.280	0.946	5.4	-1.553
15.63	15.63	0.126	0.420	58.0	0.000
	9.38	0.155	0.519	48.1	-0.222
	5.63	0.183	0.613	38.7	-0.444
	3.38	0.205	0.690	31.0	-0.666
	2.03	0.229	0.770	23.0	-0.887
	1.22	0.250	0.843	15.7	-1.109
	0.73	0.260	0.876	12.4	-1.331
	0.44	0.266	0.897	10.3	-1.553
31.25	31.25	0.052	0.166	83.4	0.000
	18.75	0.134	0.448	55.2	-0.222
	11.25	0.132	0.440	56.0	-0.444
	6.75	0.155	0.517	48.3	-0.666
	4.05	0.197	0.661	33.9	-0.887
	2.43	0.208	0.701	29.9	-1.109
	1.46	0.232	0.782	21.8	-1.331
	0.87	0.255	0.859	14.1	-1.553
62.50	62.50	0.046	0.146	85.4	0.000
	37.50	0.049	0.157	84.3	-0.222

	22.50	0.084	0.276	72.4	-0.444
	13.50	0.105	0.347	65.3	-0.666
	8.10	0.152	0.508	49.2	-0.887
	4.86	0.183	0.614	38.6	-1.109
	2.92	0.216	0.726	27.4	-1.331
	1.75	0.244	0.821	17.9	-1.553
125.00	125.00	0.030	0.093	90.7	0.000
	75.00	0.041	0.131	86.9	-0.222
	45.00	0.057	0.185	81.5	-0.444
	27.00	0.058	0.189	81.1	-0.666
	16.20	0.112	0.372	62.8	-0.887
	9.72	0.125	0.417	58.3	-1.109
	5.83	0.184	0.616	38.4	-1.331
	3.50	0.208	0.698	30.2	-1.553
250.00	250.00	0.042	0.132	86.8	0.000
	150.00	0.043	0.135	86.5	-0.222
	90.00	0.029	0.090	91.0	-0.444
	54.00	0.036	0.111	88.9	-0.666
	32.40	0.042	0.134	86.6	-0.887
	19.44	0.102	0.337	66.3	-1.109
	11.66	0.133	0.442	55.8	-1.331
	7.00	0.166	0.557	44.3	-1.553
500.00	500.00	0.043	0.135	86.5	0.000
	300.00	0.046	0.147	85.3	-0.222
	180.00	0.039	0.123	87.7	-0.444
	108.00	0.030	0.091	90.9	-0.666
	64.80	0.040	0.127	87.3	-0.887
	38.88	0.051	0.163	83.7	-1.109
	23.33	0.088	0.290	71.0	-1.331
	14.00	0.123	0.409	59.1	-1.553
1000.00	1000.00	0.040	0.126	87.4	0.000
	600.00	0.049	0.157	84.3	-0.222
	360.00	0.042	0.133	86.7	-0.444
	216.00	0.027	0.083	91.7	-0.666
	129.60	0.038	0.119	88.1	-0.887
	77.76	0.040	0.127	87.3	-1.109
	46.66	0.047	0.149	85.1	-1.331
	27.99	0.052	0.168	83.2	-1.553

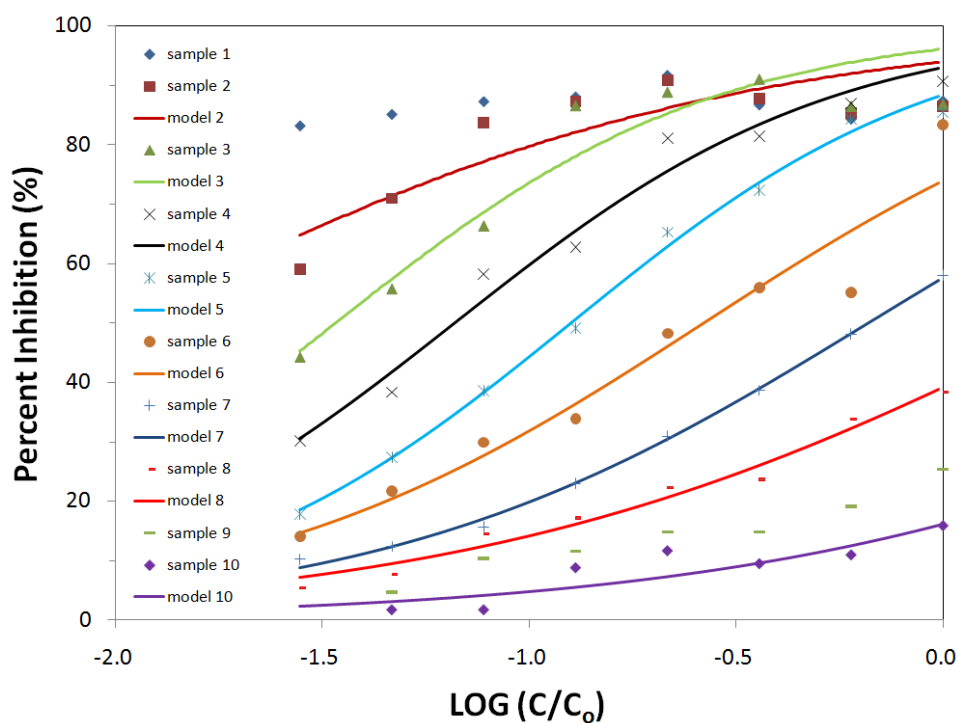


Figure C-3. Percent inhibition plotted against $\text{LOG}(C/C_0)$ for the ten data sets described in Table C-2. (GraphPad Prism was not able to fit a model to sample set #1 (1000 mg/L) and #9 (3.91 mg/L).)

The equivalent of IC_{50} (*i.e.*, the value of $\text{LOG}(C/C_0)$ that corresponds to 50% inhibition) for these curves was calculated by GraphPad Prism. Using those values, the potency equivalents (PEQ) were calculated according to Equation 3 (Suarez *et al.*, 2007). As data set #2 did not demonstrate less than 50% inhibition, that data was not used for calculation of potency equivalents. Therefore in Eq. C-3, the numerator refers to the antilog of the value of $\text{LOG}(C/C_0)$ that corresponds to 50% inhibition for sample set #3 (serial dilutions of 250 mg/L); the term in the denominator corresponds to the corresponding value for the other sample sets. As expected for standard solutions, the

PEQ data demonstrates a 1:1 relationship (Figure C-4) with the normalized erythromycin concentration (C/C_0).

$$PEQ = \frac{\left(\frac{C_i}{C_o} \right)_{50,o}}{\left(\frac{C_i}{C_o} \right)_{50,x}} \quad \text{Eq. C-3}$$

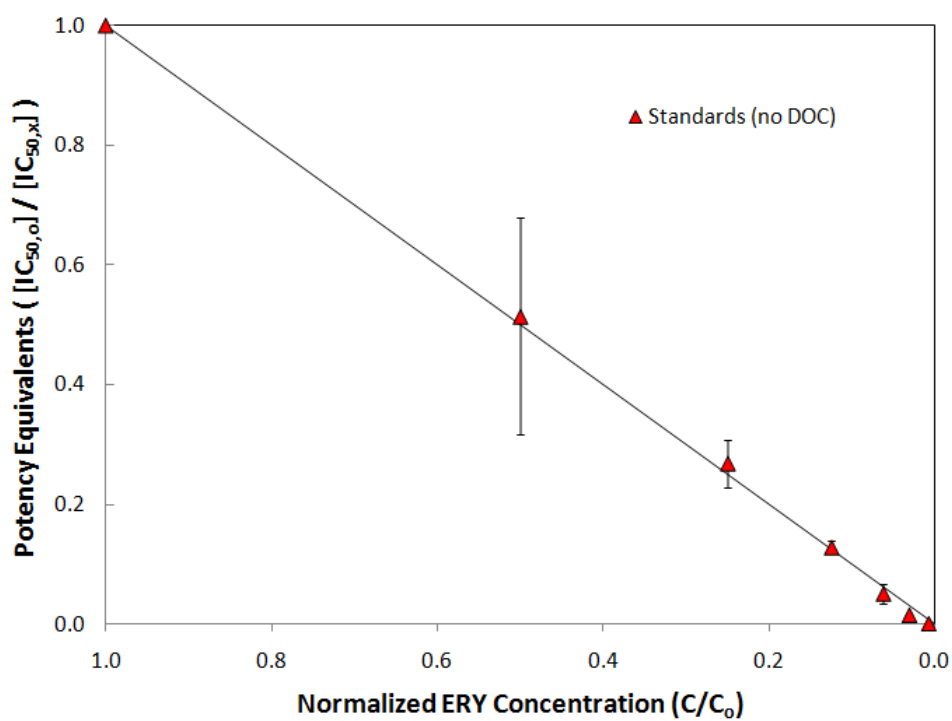


Figure C-4. Potency equivalents plotted against normalized erythromycin concentration.

APPENDIX D: CYTOTOXICITY ASSAY

The Promega CellTiter 96® Aqueous Non-Radioactive Cell Proliferation Assay was utilized in attempts to measure the residual cytotoxic activity of solutions containing cyclophosphamide and ifosfamide. Below, the procedures employed are documented to provide a starting point for future research efforts aimed at assessment of this parameter.

Human embryonic kidney cells (HEK-293) were grown in Dulbecco's Modified Eagles Medium (DMEM) with 10% Fetal Bovine Serum (FBS) in T25 culture flasks. At approximately 80% confluence, the cells were rinsed with 3-mL of phosphate buffered saline (PBS). The cells were then exposed to 2-mL of 0.53-mM EDTA-trypsin, which detaches the cells from the culture flask's growing surface. After 5 minutes of exposure to the EDTA-trypsin solution, the cell suspension was aspirated using a micropipette. The cell suspension was then centrifuged at 10000 rpm for 5 minutes. The supernatant was wasted, and the cells were resuspended in 1-mL of PBS. 50-μL of the cell suspension was mixed with 50-μL of 0.4% trypan blue. The trypan blue stain passes through the membrane of nonviable (dead) cells and colors the cells blue; therefore, the trypan blue stain allows counting of viable and nonviable cells. 10-μL of the cell-trypan blue mixture was added to a hemacytometer. The hemacytometer was viewed at 200× magnification (Figure D-1a), and cells were counted as described by Eq. D-1 and Figure D-1b.

$$Cell\ conc. (cells/mL) = \frac{(Cells\ in\ A - D) \times 10^4}{4 \times \frac{1}{2}} \quad Eq. D-1$$

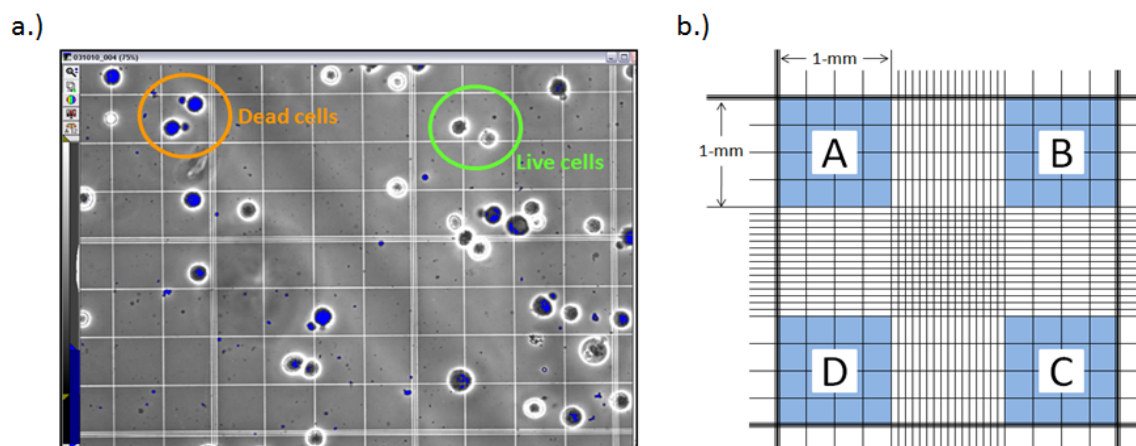


Figure D-1. a.) A microphotograph of a portion of the hemacytometer grid; each of the small boxes shown is 0.0625-mm \times 0.0625-mm. b.) An illustration of the grid pattern on the hemacytometer and presentation of what areas (A-D) are used for cell counting.

After counting the cells, the cell suspension (in PBS) was centrifuged at 10000 rpm for 5 minutes. The supernatant was wasted, and the HEK-293 cells were resuspended in 1-mL of DMEM with 10% FBS. Next, different numbers of cells were added to the microplate wells in a total volume of 100- μ L DMEM with 10% FBS. In Figure D-2, six different cell concentrations (0, 7800, 19,500, 39,000, 58,500, and 78,000 cells/well) were employed. After the cells were added to the wells, the plate was incubated at 37°C with 5% CO₂ for one hour. Then, 20- μ L of the assay solution (a mixture of 3-(4,5-dimethylthiazol-2-yl)-5-(3-carboxymethoxyphenyl)-2-(4-sulfophenyl)-2H-tetrazolium (MTS) and phenazine methosulfate (PMS), an electron coupling reagent) was introduced to the well. Viable cells convert MTS into a formazan product that absorbs light at 490 nm. Hence, the absorbance at 490 nm can be used as an indirect measure of the number of viable cells in each well; the absorbance at 650 nm was used as a reference wavelength. After addition of the MTS/PMS solution, the microplate was incubated for 2 hours at 37°C with 5% CO₂. The microplate was then analyzed using a microplate reader (BioTek), and the absorbance at 490 nm and 650 nm (reference) were recorded.

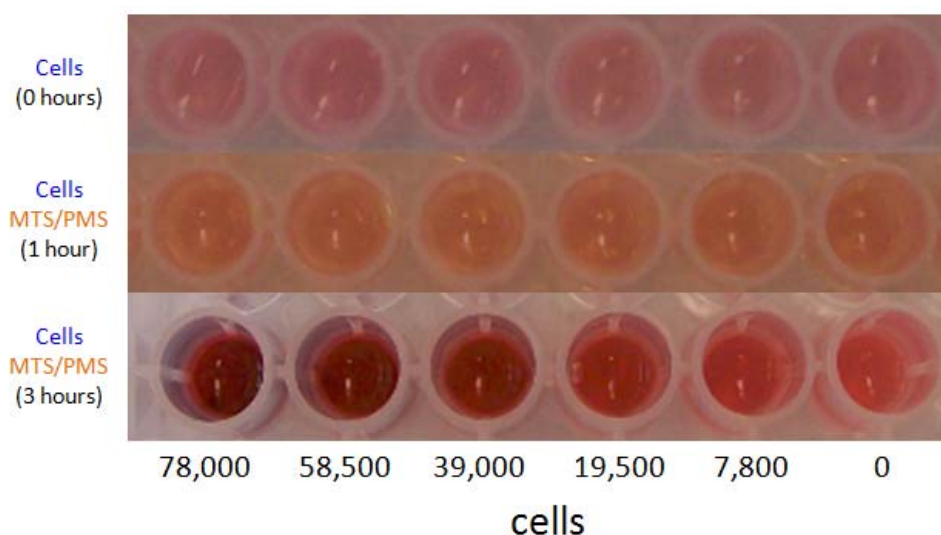


Figure D-2. Photograph of the solution coloring throughout the cell-response calibration experiment using HEK-293 cells and the MTS/PMS reagent solution.

The calibration protocol described above and the photographs shown in Figure D-2 only employed single measurements of six cell concentrations. Figure D-3 represents the same type of calibration experiment; however, more cell concentrations were employed, and samples were prepared in triplicate. The difference in the absorbance at 490 nm and the absorbance at 650 nm is plotted against the original number of cells added to each well in Figure D-3. The calibration curve demonstrates a linear fit with good correlation coefficient ($R^2 = 0.992$) from 0 to 70,000 cells. At cell counts greater than 70,000, the difference in absorbance at 490 nm and 650 nm leveled out. Observation of the strong purple color of the solutions in these wells suggests that the absorbance at 490 nm maxes out at these high cell counts because all of the MTS in solution was converted to formazan.

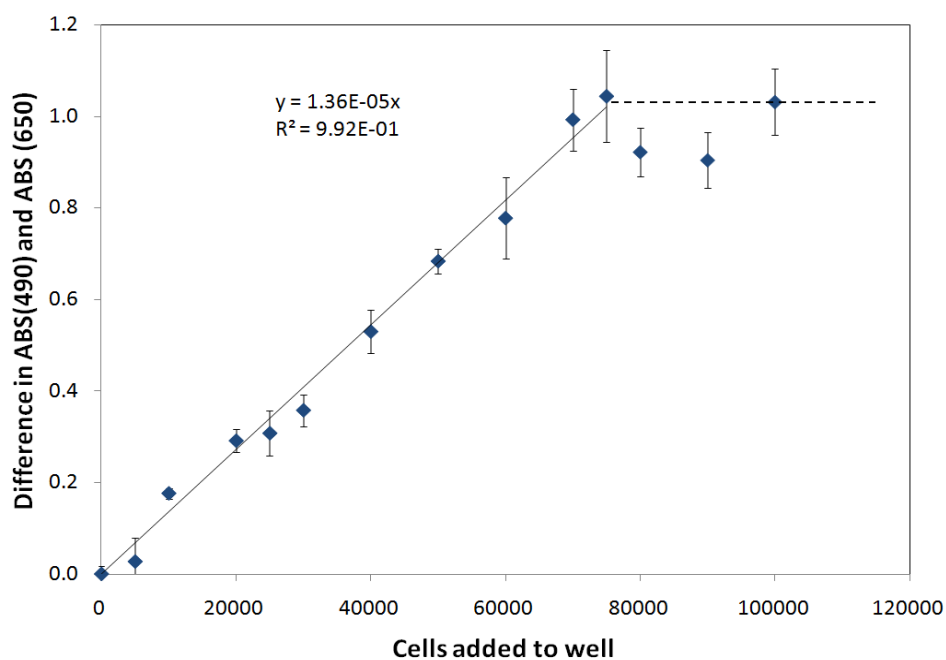


Figure D-3. Calibration curve of initial number of HEK-293 cells added to the microplate wells with the response determined using the difference in absorbance at 490 nm and 650 nm.

Unfortunately, we were unsuccessful in our attempts to standardize this assay with standard solutions containing cyclophosphamide. The results of one attempt to build a standard calibration curve using known concentrations of cyclophosphamide are shown in Figure D-4. Clearly, no trend was observed. Based on the intermediate oxidation products identified in Chapter 4, we believe that future application of a similar assay to measure the residual pharmacological activity associated with ozonation of cyclophosphamide or ifosfamide would provide interesting results.

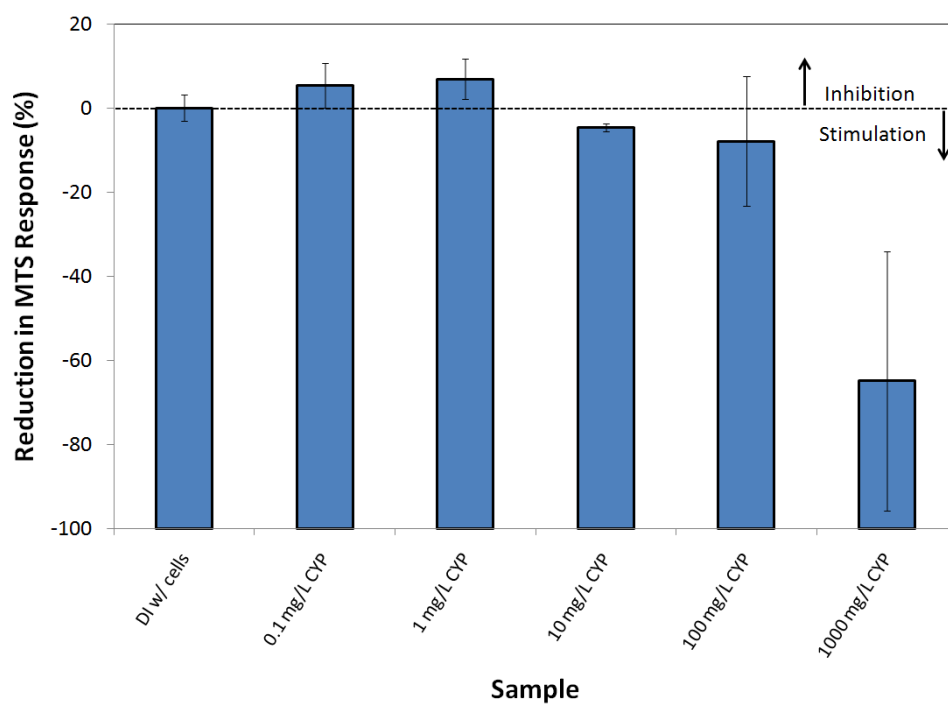


Figure D-4. Results from an attempt to standardize the response of the MTS cytotoxicity assay to standard solutions of cyclophosphamide. (No calibration curve could be generated.)

APPENDIX E: COMPARISON OF THE VARIABLE VOLUME, CONSTANT VOLUME, AND MODIFIED CONSTANT VOLUME MODELS FOR PHARMACEUTICAL TRANSFORMATION IN THE CONTINUOUS OZONE ADDITION REACTOR

Variable Volume Model

The continuous ozone addition reactor is essentially a continuous flow stirred tank reactor (CFSTR). The change in concentration of any species in a CFSTR can be modeled using Eq. E-1. In this case, two general assumptions were made: sample withdrawal was assumed to be a flow rate, that is, the sample volume was divided by the sampling interval to obtain Q_{out} ; and, both flow rates (Q_{in} and Q_{out}) were considered to be constant throughout experimentation.

$$\frac{d(VC_{out})}{dt} = V \frac{dC_{out}}{dt} + C_{out} \frac{dV}{dt} = Q_{in}C_{in} - Q_{out}C_{out} + Vr \quad \text{Eq. E-1}$$

Substituting in the variables relevant to this problem yields Eq. E-2. In this case, the pharmaceutical concentration is the variable of interest. For this example, we are only considering pharmaceutical transformation by ozone. As the influent is the ozone stock solution, $[PhAC]_{in}$ is zero and the influent mass flow term goes to zero.

$$V \frac{d[PhAC]}{dt} + [PhAC] \frac{dV}{dt} = -Q_{out}[PhAC] - V \times k_{O_3, PhAC}'' [O_3][PhAC] \quad \text{Eq. E-2}$$

V is the volume of solution in the reactor, which is a function of the initial solution volume (V_o), influent flow rate (Q_{in}), the effluent flow rate (Q_{out}), and time (t), as shown

in Eq. E-3; $[PhAC]$ is the pharmaceutical concentration at time t ; dV/dt is the derivative of the volume with respect to time (Eq. E-4); $k''_{O_3,PhAC}$ is the second-order rate constant for transformation of the pharmaceutical by ozone; and $[O_3]$ is the ozone concentration at time t .

$$V = V_o + (Q_{in} - Q_{out}) \times t \quad \text{Eq. E-3}$$

$$\frac{dV}{dt} = (Q_{in} - Q_{out}) \quad \text{Eq. E-4}$$

Dividing both sides of Eq. E-2 by V yields Eq. E-5.

$$\frac{d[PhAC]}{dt} + \frac{[PhAC]}{V} \frac{dV}{dt} = -\frac{Q_{out}}{V} [PhAC] - k''_{O_3,PhAC} [O_3] [PhAC] \quad \text{Eq. E-5}$$

Substituting Eq. E-4 into Eq. E-5 yields Eq. E-6.

$$\frac{d[PhAC]}{dt} + \frac{[PhAC]}{V} (Q_{in} - Q_{out}) = -\frac{Q_{out}}{V} [PhAC] - k''_{O_3,PhAC} [O_3] [PhAC] \quad \text{Eq. E-6}$$

Eq. E-3 can be substituted into Eq. E-6; rearrangement and simplification of the resulting equation leads to Eq. E-7.

$$\frac{d[PhAC]}{dt} = -[PhAC] \left(\frac{Q_{in}}{V_o + (Q_{in} - Q_{out}) \times t} + k''_{O_3,PhAC} [O_3] \right) \quad \text{Eq. E-7}$$

Multiplying Eq. E-7 by $dt/[PhAC]$ and integrating both sides with respect to time yields Eq. E-8.

$$\int_0^t \frac{d[PhAC]}{[PhAC]} = - \int_0^t \left(\frac{Q_{in}}{[V_o + (Q_{in} - Q_{out}) \times t]} + k''_{O3,PhAC} [O_3] \right) dt \quad \text{Eq. E-8}$$

Integration of the left hand side of Eq. E-8 is relatively straightforward. The right hand side of Eq. E-8 can be integrated in parts (Eq. E-9).

$$\ln \left(\frac{[PhAC]}{[PhAC]_o} \right) = - \int_0^t \left(\frac{Q_{in}}{[V_o + (Q_{in} - Q_{out}) \times t]} \right) dt + \int_0^t (k''_{O3,PhAC} [O_3]) dt \quad \text{Eq. E-9}$$

Consider the first term on the right hand side of Eq. E-9. The denominator can be called u , as shown in Eq. E-10. The derivative of Eq. E-10 with respect to time (du) is shown in Eq. E-11.

$$u = V_o + (Q_{in} - Q_{out}) \times t \quad \text{Eq. E-10}$$

$$du = (Q_{in} - Q_{out}) dt \quad \text{Eq. E-11}$$

Substitution of Eqs. E-10 and E-11 into the first term on the right hand side of Eq. E-9 allows integration of that term with respect to time as shown in Eqs. E-12 and E-13.

$$\int_0^t \left(\frac{Q_{in}}{[V_o + (Q_{in} - Q_{out}) \times t]} \right) dt = \frac{Q_{in}}{(Q_{in} - Q_{out})} \times \int_0^t \frac{du}{u} \quad \text{Eq. E-12}$$

$$\int_0^t \left(\frac{Q_{in}}{[V_o + (Q_{in} - Q_{out}) \times t]} \right) dt = \frac{Q_{in}}{(Q_{in} - Q_{out})} \times [\ln(V_o + (Q_{in} - Q_{out}) \times t) - \ln(V_o)] \quad \text{Eq. E-13}$$

Integration of the second term on the right hand side of Eq. E-9 is relatively straightforward. For this analysis the ozone concentration ($[O_3]$) was set to a constant value, *i.e.*, $[O_3]$ did not vary with time. This assumption is well grounded in the ozone data from experimentation, and it allows straightforward analysis of the change in pharmaceutical concentration as a function of time. Then, integration of Eq. E-9 with respect to time yields Eq. E-14.

$$\ln\left(\frac{[PhAC]}{[PhAC]_o}\right) = -\left(\frac{Q_{in}}{(Q_{in} - Q_{out})} \times [\ln(V_o + (Q_{in} - Q_{out}) \times t) - \ln(V_o)] + k_{O_3, PhAC}'' \times [O_3] \times t\right) \quad \text{Eq. E-14}$$

Rearrangement of Eq. E-14 yields Eq. E-15, which can be directly compared to Eq. E-5 to assess the effect of the constant volume assumption. Eq. E-15 is the general solution for a CFSTR resembling the continuous ozone addition reactor. The solution for a scenario where $Q_{in} = Q_{out}$ is shown in Eq. E-15*.

$$[PhAC] = [PhAC]_o \times e^{-\left(\frac{Q_{in}}{(Q_{in} - Q_{out})} \times [\ln(V_o + (Q_{in} - Q_{out}) \times t) - \ln(V_o)] + k_{O_3, PhAC}'' \times [O_3] \times t\right)} \quad \text{Eq. E-15}$$

$$[PhAC] = [PhAC]_o \times e^{-\left(\frac{Q_{out}}{V_o} + k_{O_3, PhAC}'' \times [O_3]\right) \times t} \quad \text{Eq. E-15*}$$

Constant Volume Model

The change in pharmaceutical concentration in a batch reactor (constant volume) can also be modeled. In this case, the overriding assumption is that there are no inputs or outputs to the reactor (*i.e.*, $Q_{in} = 0$, $Q_{out} = 0$). Using these assumptions, the change in pharmaceutical concentration in a batch reactor was modeled using Eq. E-16.

$$V \frac{dC}{dt} = Vr \quad \text{Eq. E-16}$$

As expected, the volume term cancels itself out in Eq. E-16. Substituting the pharmaceutical concentration at time t [PhAC] in for C , and the second-order reaction term in for r , Eq. E-16 becomes Eq. E-17.

$$\frac{d[PhAC]}{dt} = -k''_{O_3, PhAC} [O_3][PhAC] \quad \text{Eq. E-17}$$

Rearrangement of Eq. E-17 and integration with respect to time yields Eq. E-18.

$$\int_0^t \frac{d[PhAC]}{[PhAC]} = - \int_0^t k''_{O_3, PhAC} [O_3] dt \quad \text{Eq. E-18}$$

Integration of these two terms was completed above for Eq. E-9. The resultant expression is shown in Eq. E-19.

$$\ln \left(\frac{[PhAC]}{[PhAC]_0} \right) = -k''_{O_3, PhAC} [O_3] \times t \quad \text{Eq. E-19}$$

Rearranging Eq. E-19 allows us to solve for the pharmaceutical concentration at any time, t , as shown in Eq. E-20.

$$[PhAC] = [PhAC]_0 \times e^{-(k''_{O_3, PhAC} [O_3] \times t)} \quad \text{Eq. E-20}$$

Modified Constant Volume Model

Clearly, the constant volume model (Eq. E-20) oversimplifies the mass transfer system present in the continuous ozone addition reactor. However, the variable volume model (Eq. E-15) is complex and difficult to employ for data that demonstrates several time dependent parameters. Therefore, a modified constant volume model was employed to describe pharmaceutical transformation in the continuous ozone addition reactor. In this model, Eq. E-20 is multiplied by the ratio of the initial reactor volume to the reactor volume at time, t , as shown in Eq. E-21. The inclusion of this parameter allows us to account for the changing volume in the reactor.

$$[PhAC] = [PhAC]_o \times \frac{V_o}{V} \times e^{-(k_{O_3, PhAC}^{''} [O_3] \times t)} \quad \text{Eq. E-21}$$

Comparison of the Three Models

Typical values of the relevant parameters were employed to demonstrate the differences between the variable volume model (Eq. E-15), the constant volume model (Eq. E-20), and the modified constant volume model (Eq. E-21) that was used in Chapters 3-5.

For the first example, consider the following values: Q_{in} was 2.73 mL/min, Q_{out} was 1.2 mL/min; V_o was 2000 mL, $[IFO]_o$ was 3.83×10^{-7} M, $k_{O_3, IFO}^{''}$ was $6.84 \text{ M}^{-1} \text{ s}^{-1}$, and $[O_3]$ was 3.90×10^{-5} M. In these scenarios, the second-order rate constant for IFO transformation by ozone refers to the value measured using the constant volume model; that value is used in the variable volume and constant volume models. For the modified constant volume model, the rate constant determined in the *t*-BuOH experiment incorporates the dilution adjustment (V_o/V) that is present in Eq. E-21. For this example, the second-order rate constant for IFO transformation by ozone in the modified constant

volume model is $k''_{O_3,PhAC} = 7.38 \text{ M}^{-1}\text{s}^{-1}$. In this example, the volume change throughout experimentation is approximately 9%. The resultant curves for the variable volume, constant volume, and modified constant volume solutions are shown below in Figure E-1.

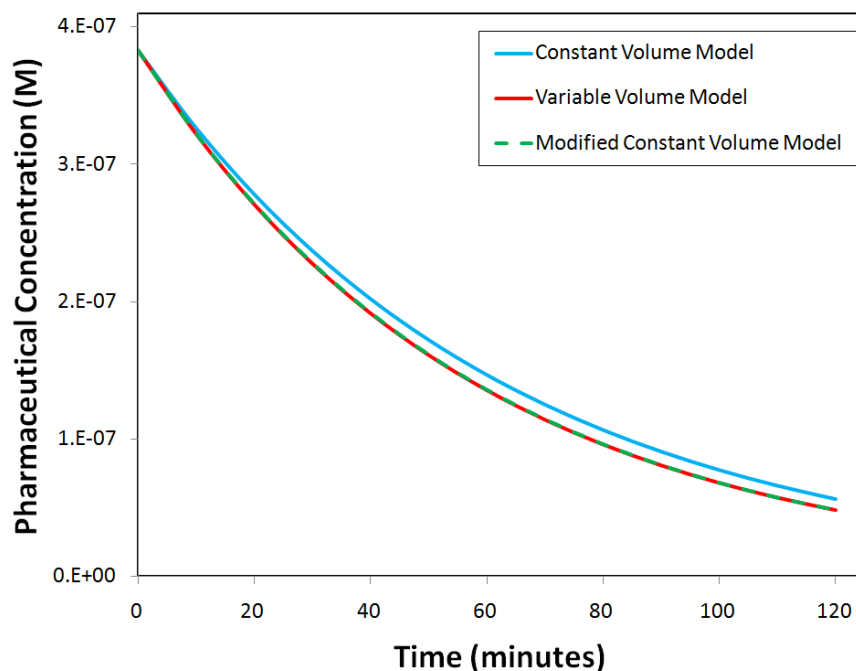


Figure E-1. Comparison of the constant volume, variable volume, and modified constant volume models for ifosfamide transformation. (In this example, the volume changed by approximately 9% during experimentation.)

In this case, the constant volume assumption results in a rate constant ($6.84(\pm 0.27) \text{ M}^{-1}\text{s}^{-1}$) approximately 8.4% lower than that of the variable volume model ($7.47 \text{ M}^{-1}\text{s}^{-1}$). The rate constant for the modified constant volume model was found to be $7.38(\pm 0.27) \text{ M}^{-1}\text{s}^{-1}$, which is approximately 1.2% less than that predicted by the variable volume model; however, the 95% confidence interval on the rate constant found using the modified constant volume model overlaps the value predicted by the variable volume model.

Similar results were attained for cyclophosphamide. Consider the same example as that just discussed, but now the rate constants for the constant volume and modified constant volume models are $k''_{O_3,CYP}$ was $2.50(\pm 0.48) \text{ M}^{-1}\text{s}^{-1}$ and $k''_{O_3,CYP}$ was $3.03(\pm 0.48) \text{ M}^{-1}\text{s}^{-1}$, respectively (Figure E-2). Recall that these parameters were calculated from experimental data as described above. In the variable volume model, the calculated rate constant is $3.05 \text{ M}^{-1}\text{s}^{-1}$. Clearly, the modified constant volume model (with 95% confidence intervals) overlaps with the variable volume rate constant.

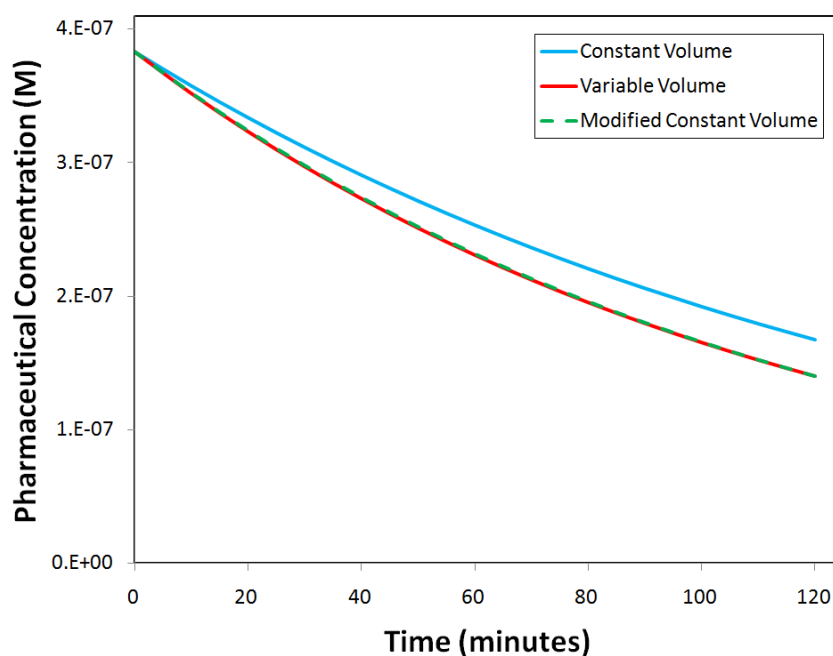


Figure E-2. Comparison of the constant volume, variable volume, and modified constant volume models for cyclophosphamide transformation.

Next, consider an example with a greater difference in Q_{in} and Q_{out} . The values of the parameters were: Q_{in} was 3.23 mL/min , Q_{out} was 0.27 mL/min ; V_o was 2000 mL , $[PhAC]_o$ was $3.83 \times 10^{-7} \text{ M}$, $k''_{O_3,IFO}$ was $6.84 \text{ M}^{-1}\text{s}^{-1}$, and $[O_3]$ was $4.60 \times 10^{-5} \text{ M}$. In this case, the total volume change is approximately 18%. The resultant curves for the constant volume and variable volume solutions are shown below in Figure E- 3.

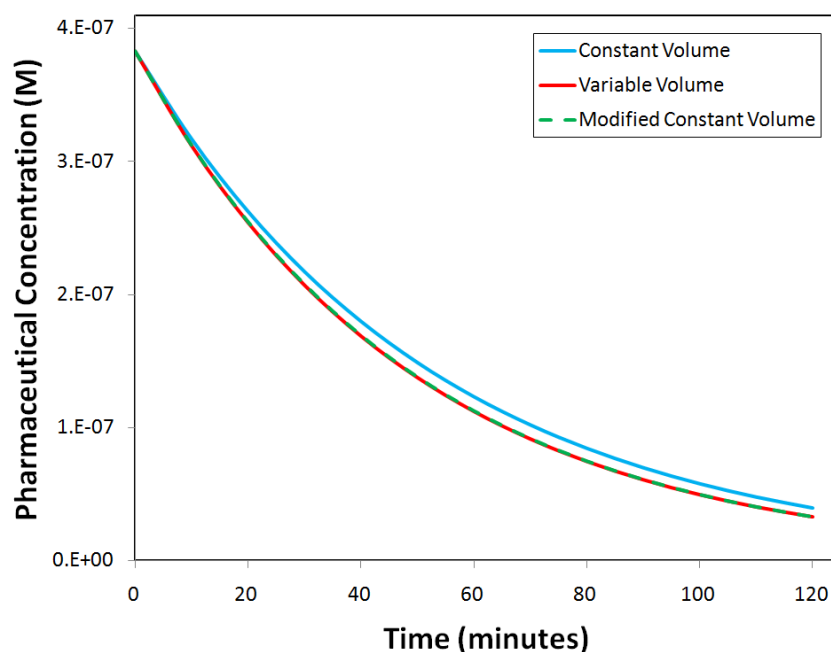


Figure E- 3. Comparison of the constant volume, variable volume, and modified constant volume models for ifosfamide transformation. (In this example, the volume changed by approximately 18% during experimentation.)

The rate constant measured using the constant volume model ($k''_{O_3,IFO} = 6.84(\pm 0.27) \text{ M}^{-1}\text{s}^{-1}$) is approximately 7.4% lower than that described by the variable volume reactor ($k''_{O_3,IFO} = 7.39 \text{ M}^{-1}\text{s}^{-1}$). Again, the modified constant volume model ($k''_{O_3,IFO} = 7.38(\pm 0.27) \text{ M}^{-1}\text{s}^{-1}$) compares well to the variable volume model.

The impact of the volume change in the reactor was also studied to understand how the increase or decrease in reactor volume affects the rate constant (for cyclophosphamide) calculated in the variable volume model. For this scenario, the same values for the relevant parameters were used as in the previous example. Volume changes of -40%, -20%, -10%, 10%, 20%, and 40% were studied. The negative volume changes were modeled by changing Q_{out} to achieve the necessary volume change over the course of the experiment; the positive volume changes were achieved by adjusting Q_{in} . Eq. E-15* was also plotted to describe a scenario where there is an influent stream (ozone stock solution) and an effluent stream (sample withdrawal) but the reactor volume

remains constant (*e.g.*, $V(t) = 2000$ mL). From Figure E-4, it is clear that variable reactor volume does affect the rate constant found using the variable volume model; however, a volume change of approximately +36% or -71% is required before the rate constant from the variable volume reactor falls outside of the 95% confidence interval for the modified constant volume model. All but two of the experiments were within 10% volume change (one experiment exhibited an 18% change and another showed 15%); therefore, we expect that the modified constant volume model successfully describes pharmaceutical transformation in the continuous ozone addition reactor.

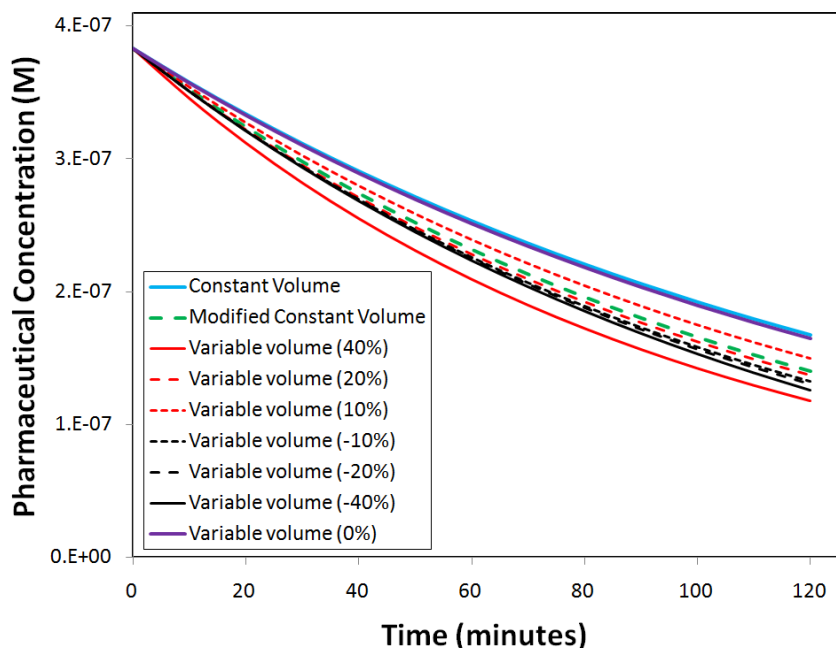


Figure E-4. Comparison of the constant volume, variable volume, and modified constant volume models for cyclophosphamide transformation. (In this example, the volume change in the reactor was controlled by adjusting Q_{in} and Q_{out} . Note, that a scenario where volume change in 0%, but influent and effluent streams are present (Eq. E-15*) is also plotted.)

REFERENCES

- Acero, J.L., Stemmler, K. and von Gunten, U. (2000). Degradation Kinetics of Atrazine and Its Degradation Products with Ozone and OH Radicals: A Predictive Tool for Drinking Water Treatment. *Environ. Sci. Technol.* 34(4), 591-597.
- Acero, J.L. and von Gunten, U. (2000). Influence of carbonate on the ozone/hydrogen peroxide based advanced oxidation process for drinking water treatment. *Ozone: Sci. Eng.* 22(3), 305-328.
- Acero, J.L. and von Gunten, U. (2001). Characterization of oxidation processes: ozonation and the AOP O₃/H₂O₂. *J. Am. Water Works Assoc.* 93(10), 90-100.
- Adams, C., Wang, Y., Loftin, K. and Meyer, M. (2002). Removal of antibiotics from surface and distilled water in conventional water treatment processes. *J. Environ. Eng.* 128(3), 253-260.
- Aiken, G.R., McKnight, D.M., Thorn, K.A. and Thurman, E.M. (1992). Isolation of hydrophilic organic acids from water using nonionic macroporous resins. *Org. Geochem.* 18(4), 567-573.
- Alsheyab, M.A. and Muñoz, A.H. (2006). Reducing the formation of trihalomethanes (THMs) by ozone combined with hydrogen peroxide (H₂O₂/O₃). *Desalination* 194(1-3), 121-126.
- An, T., Yang, H., Li, G., Song, W., Cooper, W.J. and Nie, X. (2010). Kinetics and mechanism of advanced oxidation processes (AOPs) in degradation of ciprofloxacin in water. *Appl. Catal., B* 94(3-4), 288-294.
- Andreozzi, R., Canterino, M., Marotta, R. and Paxeus, N. (2005). Antibiotic removal from wastewaters: The ozonation of amoxicillin. *J. Hazard. Mater.* 122(3), 243-250.
- Andreozzi, R., Caprio, V., Marotta, R. and Radovnikovic, A. (2003). Ozonation and H₂O₂/UV treatment of clofibric acid in water: a kinetic investigation. *J. Hazard. Mater.* 103(3), 233-246.
- APHA, AWWA and WPCF (1989). Standard Methods for the Examination of Water and Wastewater, APHA, Washington, D.C.

- APTwater (2011). APTwater Receives Contract to Build First Ozone-based Water Reuse System for the City of Anaheim, CA. February 2, 2011.
<http://www.aptwater.com/about-aptwater/press-room/press-releases/item/298-aptwater-receives-contract-to-build-first-ozone-based-water-reuse-system-for-the-city-of-anaheim>
- Atkins, P.J., Herbert, T.O. and Jones, N.B. (1986). Kinetic studies on the decomposition of erythromycin A in aqueous acidic and neutral buffers. *Int. J. Pharm.* 30(2-3), 199-207.
- Bader, H. and Hoigné, J. (1981). Determination of ozone in water by the indigo method. *Water Research* 15(4), 449-456.
- Baeza, A.C. (2008). Removal of pharmaceutical and endocrine disrupting chemicals by sequential photochemical and biological oxidation processes. PhD Dissertation, North Carolina State University, Raleigh.
- Baker, A. (2001). Fluorescence Excitation-Emission Matrix Characterization of Some Sewage-Impacted Rivers. *Environmental Science & Technology* 35(5), 948-953.
- Baker, A. (2002a). Fluorescence Excitation-Emission Matrix Characterization of River Waters Impacted by a Tissue Mill Effluent. *Environmental Science & Technology* 36(7), 1377-1382.
- Baker, A. (2002b). Fluorescence properties of some farm wastes: implications for water quality monitoring. *Water Research* 36(1), 189-195.
- Baquero, F., Martínez, J.L. and Cantón, R. (2008). Antibiotics and antibiotic resistance in water environments. *Current Opinion in Biotechnology* 19(3), 260-265.
- Barnes, K.K., Kolpin, D.W., Furlong, E.T., Zaugg, S.D., Meyer, M.T. and Barber, L.B. (2008). A national reconnaissance of pharmaceuticals and other organic wastewater contaminants in the United States -- I) Groundwater. *Science of The Total Environment* 402(2-3), 192-200.
- Beltran, F.J. (2003). *Ozone Reaction Kinetics for Water & Wastewater Systems*. CRC Press, Boca Raton, FL.
- Bhandari, A., Close, L.I., Kim, W., Hunter, R.P., Koch, D.E. and Surampalli, R.Y. (2008). Occurrence of ciprofloxacin, sulfamethoxazole, and azithromycin in municipal wastewater treatment plants. *Pract. Period. Hazard., Toxic, Radioact. Waste Manage.* 12(4), 275-281.
- Bhavnani, S.M., Callen, W.A., Forrest, A., Gilliland, K.K., Collins, D.A., Paladino, J.A. and Schentag, J.J. (2003). Effect of fluoroquinolone expenditures on susceptibility of *Pseudomonas aeruginosa* to ciprofloxacin in U.S. hospitals. *American Journal of Health-System Pharmacy* 60(19), 1962.
- Bound, J.P., Kitsou, K. and Voulvoulis, N. (2006). Household disposal of pharmaceuticals and perception of risk to the environment. *Environmental Toxicology and Pharmacology* 21(3), 301-307.

- Braund, R., Peake, B.M. and Shieffebien, L. (2009). Disposal practices for unused medications in New Zealand. *Environment International* 35(6), 952-955.
- Brunton, L., Lazo, J., and Parker, K. (2006). Goodman & Gilman's The Pharmacological Basis of Therapeutics, 11th Edition. McGraw-Hill, Columbus, OH.
- Buehler, R.E., Staehelin, J. and Hoigne, J. (1984). Ozone decomposition in water studied by pulse radiolysis. 1. Perhydroxyl (HO_2)/hyperoxide (O_2^-) and HO_3/O_3^- as intermediates. *The Journal of Physical Chemistry* 88(12), 2560-2564.
- Buerge, I.J., Buser, H.R., Poiger, T. and Mueller, M.D. (2006). Occurrence and Fate of the Cytostatic Drugs Cyclophosphamide and Ifosfamide in Wastewater and Surface Waters. *Environ. Sci. Technol.* 40(23), 7242-7250.
- Buffle, M.O., Galli, S. and von Gunten, U. (2004). Enhanced Bromate Control during Ozonation: The Chlorine-Ammonia Process. *Environmental Science & Technology* 38(19), 5187-5195.
- Buffle, M.O., Schumacher, J., Meylan, S., Jekel, M. and von, G.U. (2006). Ozonation and advanced oxidation of wastewater: effect of O_3 dose, pH, DOM and HO radical scavengers on ozone decomposition and HO radical generation. *Ozone: Sci. Eng.* 28(4), 247-259.
- Bus, J.S., Gibson, J.E. and Reinke, D.A. (1973). Teratogenicity and neonatal toxicity of ifosfamide in mice. *Proc Soc Exp Biol Med* 143(4), 965-970.
- Buxton, G.V., Greenstock, C.L., Helman, W.P. and Ross, A.B. (1988). Critical review of rate constants for reactions of hydrated electrons, hydrogen atoms and hydroxyl radicals ($\cdot\text{OH}/\cdot\text{O}$) in aqueous solution. *J. Phys. Chem. Ref. Data* 17(2), 513-886.
- Cachet, T., Van, d.M.G., Hauchecorne, R., Vinckier, C. and Hoogmartens, J. (1989). Decomposition kinetics of erythromycin A in acidic aqueous solutions. *Int. J. Pharm.* 55(1), 59-65.
- Calamari, D., Zuccato, E., Castiglioni, S., Bagnati, R. and Fanelli, R. (2003). Strategic Survey of Therapeutic Drugs in the Rivers Po and Lambro in Northern Italy. *Environ. Sci. Technol.* 37(7), 1241-1248.
- California (2007). California Code - Article 3.4: Drug Waste Management and Disposal, Public Resources Code § 47120-47126.
- Carson, R. (1962) *Silent Spring*, Houghton Mifflin, New York, NY.
- Carson, R. (1951) *The Sea Around Us*, Oxford University Press, New York, NY.
- Castiglioni, S., Fanelli, R., Calamari, D., Bagnati, R. and Zuccato, E. (2004). Methodological approaches for studying pharmaceuticals in the environment by comparing predicted and measured concentrations in River Po, Italy. *Regul. Toxicol. Pharmacol.* 39(1), 25-32.

- Chen, W., Westerhoff, P., Leenheer, J.A. and Booksh, K. (2003). Fluorescence Excitation-Emission Matrix Regional Integration to Quantify Spectra for Dissolved Organic Matter. *Environmental Science & Technology* 37(24), 5701-5710.
- Chen, Z., Park, G., Herckes, P. and Westerhoff, P. (2008). Physicochemical treatment of three chemotherapy drugs: irinotecan, tamoxifen, and cyclophosphamide. *J. Adv. Oxid. Technol.* 11(2), 254-260.
- Daughton, C.G. (2007). "Pharmaceuticals in the environment: sources and their management" in *Analysis, Fate and Removal of Pharmaceuticals in the Water Cycle*. Elsevier Science, 1-58.
- Daughton, C.G. and Ternes, T.A. (1999). Pharmaceuticals and personal care products in the environment: agents of subtle change? *Environ. Health Perspect. Suppl.* 107(6), 907-938.
- Davies, J., Spiegelman, G.B. and Yim, G. (2006). The world of subinhibitory antibiotic concentrations. *Current Opinion in Microbiology* 9(5), 445-453.
- De Souza, M.V.N. (2005). New Fluoroquinolones: A Class of Potent Antibiotics. *Mini Reviews in Medicinal Chemistry* 5(11), 1009-1017.
- Descheemaeker, P., Chapelle, S., Lammens, C., Hauchecorne, M., Wijdooghe, M., Vandamme, P., Ieven, M. and Goossens, H. (2000). Macrolide resistance and erythromycin resistance determinants among Belgian *Streptococcus pyogenes* and *Streptococcus pneumoniae* isolates. *Journal of Antimicrobial Chemotherapy* 45(2), 167-173.
- DeWitte, B., Dewulf, J., Demeestere, K., Van De Vyvere, V., De Wispelaere, P. and Van Langenhove, H. (2008). Ozonation of Ciprofloxacin in Water: HRMS Identification of Reaction Products and Pathways. *Environ. Sci. Technol.* 42(13), 4889-4895.
- DeWitte, B., Dewulf, J., Demeestere, K. and Van Langenhove, H. (2009). Ozonation and advanced oxidation by the peroxone process of ciprofloxacin in water. *J. Hazard. Mater.* 161(2-3), 701-708.
- Dodd, M.C., Buffle, M.O. and von Gunten, U. (2006). Oxidation of Antibacterial Molecules by Aqueous Ozone: Moiety-Specific Reaction Kinetics and Application to Ozone-Based Wastewater Treatment. *Environ. Sci. Technol.* 40(6), 1969-1977.
- Dodd, M.C., Kohler, H.P.E. and von Gunten, U. (2009). Oxidation of antibacterial compounds by ozone and hydroxyl radical: elimination of biological activity during aqueous ozonation processes. *Environ. Sci. Technol.* 43(7), 2498-2504.

- Dodd, M.C., Zuleeg, S., von Gunten, U. and Pronk, W. (2008). Ozonation of Source-Separated Urine for Resource Recovery and Waste Minimization: Process Modeling, Reaction Chemistry, and Operational Considerations. *Environmental Science & Technology* 42(24), 9329-9337.
- Donn, J., Mendoza, M. and Pritchard, J. (2008). Associated Press investigation: Pharmaceuticals found in drinking water, affecting wildlife and maybe humans. March 9, 2008.
- Drlica, K. and Zhao, X. (1997). DNA gyrase, topoisomerase IV, and the 4-quinolones. *Microbiol. Mol. Biol. Rev.* 61(3), 377-392.
- Duong, H.A., Pham, N.H., Nguyen, H.T., Hoang, T.T., Pham, H.V., Pham, V.C., Berg, M., Giger, W. and Alder, A.C. (2008). Occurrence, fate and antibiotic resistance of fluoroquinolone antibacterials in hospital wastewaters in Hanoi, Vietnam. *Chemosphere* 72(6), 968-973.
- Elovitz, M.S. and von Gunten, U. (1999). Hydroxyl radical/ozone ratios during ozonation processes. I. The Rct concept. *Ozone: Sci. Eng.* 21(3), 239-260.
- Elovitz, M.S., von Gunten, U. and Kaiser, H.P. (2000). Hydroxyl radical/ozone ratios during ozonation processes. II. The effect of temperature, pH, alkalinity, and DOM properties. *Ozone: Sci. Eng.* 22(2), 123-150.
- EPA, U.S. (2008). Amendment to the Universal Waste Rule: Addition of Pharmaceuticals; Proposed Rule. Federal Register 73(232).
- EPA, U.S. (2009). Drinking Water Contaminant Candidate List 3—Final. EPA document EPA-HQ-OW-2007-1189.
- Fajardo, A. and Martínez, J.L. (2008). Antibiotics as signals that trigger specific bacterial responses. *Current Opinion in Microbiology* 11(2), 161-167.
- Falconer, I.R., Chapman, H.F., Moore, M.R. and Ranmuthugala, G. (2006). Endocrine-disrupting compounds: a review of their challenge to sustainable and safe water supply and water reuse. *Environ. Toxicol.* 21(2), 181-191.
- FDA (2004). Cipro(R). Federal Drug Administration document 08918468,R.0.
- FDA (2010). Disposal of Unused Medicines: What You Should Know. Accessed on May 27, 2011.
<http://www.fda.gov/Drugs/ResourcesForYou/Consumers/BuyingUsingMedicineSafely/EnsuringSafeUseofMedicine/SafeDisposalofMedicines/ucm186187.htm#MEDICINES>
- Finch, R. and Hunter, P.A. (2006). Antibiotic resistance--action to promote new technologies: report of an EU Intergovernmental Conference held in Birmingham, UK, 12-13 December 2005. *J. Antimicrob. Chemother.* 58 Suppl 1, i3-i22.
- Fleming, R.A. (1997). An overview of cyclophosphamide and ifosfamide pharmacology. *Pharmacotherapy* 17(5, Pt. 2), 146S-154S.

- Garcia-Ac, A., Broséus, R., Vincent, S., Barbeau, B., Prévost, M. and Sauvé, S. (2010). Oxidation kinetics of cyclophosphamide and methotrexate by ozone in drinking water. *Chemosphere* 79(11), 1056-1063.
- Glassmeyer, S.T., Hinchey, E.K., Boehme, S.E., Daughton, C.G., Ruhoy, I.S., Conerly, O., Daniels, R.L., Lauer, L., McCarthy, M., Nettesheim, T.G., Sykes, K. and Thompson, V.G. (2009). Disposal practices for unwanted residential medications in the United States. *Environment International* 35(3), 566-572.
- Glaze, W.H. and Kang, J.W. (1989). Advanced oxidation processes. Description of a kinetic model for the oxidation of hazardous materials in aqueous media with ozone and hydrogen peroxide in a semibatch reactor. *Industrial & Engineering Chemistry Research* 28(11), 1573-1580.
- Golet, E., M., Alder, A., C. and Giger, W. (2002). Environmental exposure and risk assessment of fluoroquinolone antibacterial agents in wastewater and river water of the Glatt Valley Watershed, Switzerland. *Environ. Sci. Technol.* 36(17), 3645-3651.
- Golet, E.M., Alder, A.C., Hartmann, A., Ternes, T.A. and Giger, W. (2001). Trace Determination of Fluoroquinolone Antibacterial Agents in Urban Wastewater by Solid-Phase Extraction and Liquid Chromatography with Fluorescence Detection. *Analytical Chemistry* 73(15), 3632-3638.
- Guengerich, F.P., Crawford, W.M. and Watanabe, P.G. (1979). Activation of vinyl chloride to covalently bound metabolites: roles of 2-chloroethylene oxide and 2-chloroacetaldehyde. *Biochemistry* 18(23), 5177-5182.
- Gustavson, L.E., Kaiser, J.F., Edmonds, A.L., Locke, C.S., DeBartolo, M.L. and Schneck, D.W. (1995). Effect of omeprazole on concentrations of clarithromycin in plasma and gastric tissue at steady state. *Antimicrobial Agents and Chemotherapy* 39(9), 2078-2083.
- Haag, W.R. and Yao, C.C.D. (1992). Rate constants for reaction of hydroxyl radicals with several drinking water contaminants. *Environ. Sci. Technol.* 26(5), 1005-1013.
- Hale, R.C., Kim, S.L., Harvey, E., La Guardia, M.J., Mainor, T.M., Bush, E.O. and Jacobs, E.M. (2008). Antarctic Research Bases: Local Sources of Polybrominated Diphenyl Ether (PBDE) Flame Retardants. *Environmental Science & Technology* 42(5), 1452-1457.
- Halliday, S. (2006). Ozone In The Water Reclamation Process At South Caboolture, Queensland, Australia. Watertex Engineering, South Caboolture, Queensland, Australia.
- Halling-Sorensen, B., Nielsen, S.N., Lanzky, P.F., Ingerslev, F., Lutzht, H.C.H. and Jorgensen, S.E. (1998). Occurrence, fate and effects of pharmaceutical substances in the environment - a review. *Chemosphere* 36(2), 357-393.

- Hamad, B. (2010). The antibiotics market. *Nat Rev Drug Discov* 9(9), 675-676.
- Hansch, C., Leo, A. and Hoekman, D. (1995). *Exploring QSAR: Hydrophobic, Electronic, and Steric Constants*, American Chemical Society, Washington, DC.
- Hao, C., Lissemore, L., Nguyen, B., Kleywegt, S., Yang, P. and Solomon, K. (2006). Determination of pharmaceuticals in environmental waters by liquid chromatography/electrospray ionization/tandem mass spectrometry. *Anal. Bioanal. Chem.* 384(2), 505-513.
- Harang, V. and Westerlund, D. (1999). Optimization of an HPLC method for the separation of erythromycin and related compounds using factorial design. *Chromatographia* 50(9/10), 525-531.
- Her, N., Amy, G., McKnight, D., Sohn, J. and Yoon, Y. (2003). Characterization of DOM as a function of MW by fluorescence EEM and HPLC-SEC using UVA, DOC, and fluorescence detection. *Water Research* 37(17), 4295-4303.
- Hirsch, R., Ternes, T., Haberer, K. and Kratz, K.L. (1999). Occurrence of antibiotics in the aquatic environment. *Sci. Total Environ.* 225(1,2), 109-118.
- Ho, S.K. and Ho, Y.L. (1976). The Role of Hydroxyl Radicals in Radiation-Induced Single-Strand Breaks of Bacterial DNA Sensitized by Parachloromercuribenzoate. *Radiation Research* 67(2), 277-285.
- Hohorst, H.J., Peter, G. and Struck, R.F. (1976). Synthesis of 4-Hydroperoxy Derivatives of Ifosfamide and Trofosfamide by Direct Ozonation and Preliminary Antitumor Evaluation in Vivo. *Cancer Research* 36(7 Part 1), 2278-2281.
- Hoigne, J. and Bader, H. (1983a). Rate constants of reactions of ozone with organic and inorganic compounds in water. I. Nondissociating organic compounds. *Water Res.* 17(2), 173-183.
- Hoigne, J. and Bader, H. (1983b). Rate constants of reactions of ozone with organic and inorganic compounds in water. II. Dissociating organic compounds. *Water Res.* 17(2), 185-194.
- Hoigné, J. and Bader, H. (1975). Ozonation of Water: Role of Hydroxyl Radicals as Oxidizing Intermediates. *Science* 190(4216), 782-784.
- Hoigné, J. and Bader, H. (1976). The role of hydroxyl radical reactions in ozonation processes in aqueous solutions. *Water Research* 10(5), 377-386.
- Hoigné, J., Bader, H., Haag, W.R. and Staehelin, J. (1985). Rate constants of reactions of ozone with organic and inorganic compounds in water - III. Inorganic compounds and radicals. *Water Res.* 19(8), 993-1004.
- Holbrook, R.D., Breidenich, J. and DeRose, P.C. (2005). Impact of Reclaimed Water on Select Organic Matter Properties of a Receiving Stream Fluorescence and Perylene Sorption Behavior *Environmental Science & Technology* 39(17), 6453-6460.

- Hollender, J., Zimmermann, S.G., Koepke, S., Krauss, M., McArdell, C.S., Ort, C., Singer, H., von, G.U. and Siegrist, H. (2009). Elimination of Organic Micropollutants in a Municipal Wastewater Treatment Plant Upgraded with a Full-Scale Post-Ozonation Followed by Sand Filtration. *Environ. Sci. Technol.* 43(20), 7862-7869.
- Hua, W., Bennett, E.R. and Letcher, R.J. (2006). Ozone treatment and the depletion of detectable pharmaceuticals and atrazine herbicide in drinking water sourced from the upper Detroit River, Ontario, Canada. *Water Res.* 40(12), 2259-2266.
- Huang, L. (2011). Ozonation of Erythromycin and the Effects of pH, Carbonate System, Phosphate Buffer and Initial Ozone Dose. Master's Thesis, The University of Texas at Austin, Austin, TX.
- Huang, R., Southall, N., Wang, Y., Yasgar, A., Shinn, P., Jadhav, A., Nguyen, D.-T. and Austin, C.P. (2011). The NCGC Pharmaceutical Collection: a comprehensive resource of clinically approved drugs enabling repurposing and chemical genomics. *Sci. Transl. Med.* 3(80), 80ps16, 12 pp.
- Huber, M.M., Canonica, S., Park, G.-Y. and von Gunten, U. (2003). Oxidation of Pharmaceuticals during Ozonation and Advanced Oxidation Processes. *Environ. Sci. Technol.* 37(5), 1016-1024.
- Huber, M.M., Gabel, A., Joss, A., Hermann, N., Laffler, D., McArdell, C.S., Ried, A., Siegrist, H., Ternes, T.A. and von Gunten, U. (2005). Oxidation of Pharmaceuticals during Ozonation of Municipal Wastewater Effluents: A Pilot Study. *Environmental Science & Technology* 39(11), 4290-4299.
- Huber, M.M., Ternes, T.A. and von, G.U. (2004). Removal of Estrogenic Activity and Formation of Oxidation Products during Ozonation of 17 α -Ethinylestradiol. *Environ. Sci. Technol.* 38(19), 5177-5186.
- Humphreys, A. (2007). Med Ad News 200 - World's Best-Selling Medicines. *Med Ad News* 13(7).
- IMS Health (2007). Global Pharmaceutical Market Prognosis. Accessed on June 17, 2011. http://www.market-forecasting.com/europe2007/presentations/2007/Jerry_Rosenblatt.pdf
- Iowa (2007). Senate File 579 - Pharmaceutical Collection and Disposal Pilot Project.
- Jaffe, R., McKnight, D., Maie, N., Cory, R., McDowell, W.H. and Campbell, J.L. (2008). Spatial and temporal variations in DOM composition in ecosystems: the importance of long-term monitoring of optical properties. *J. Geophys. Res., [Biogeosci.]* 113(G4), G04032/04031-G04032/04015.
- Jjemba, P.K. (2008). *Pharma-Ecology: the Occurrence and Fate of Pharmaceuticals and Personal Care Products in the Environment*, John Wiley & Sons, Inc, Hoboken, NJ.

- Johnson, A.C., Juergens, M.D., Williams, R.J., Kuemmerer, K., Kortenkamp, A. and Sumpter, J.P. (2007). Do cytotoxic chemotherapy drugs discharged into rivers pose a risk to the environment and human health? An overview and UK case study. *J. Hydrol.* 348(1-2), 167-175.
- Karlowsky, J.A., Kelly, L.J., Thornsberry, C., Jones, M.E. and Sahm, D.F. (2002). Trends in Antimicrobial Resistance among Urinary Tract Infection Isolates of *Escherichia coli* from Female Outpatients in the United States. *Antimicrobial Agents and Chemotherapy* 46(8), 2540-2545.
- Kibwage, I.O., Hoogmartens, J., Roets, E., Vanderhaeghe, H., Verbist, L., Dubost, M., Pascal, C., Petitjean, P. and Levot, G. (1985). Antibacterial activities of erythromycins A, B, C, and D and some of their derivatives. *Antimicrobial Agents and Chemotherapy* 28(5), 630-633.
- Kiffmeyer, T., Goetze, H.J., Jursch, M. and Lueders, U. (1998). Trace enrichment, chromatographic separation, and biodegradation of cytostatic compounds in surface water. *Fresenius' J. Anal. Chem.* 361(2), 185-191.
- Kim, I., Yamashita, N. and Tanaka, H. (2009). Performance of UV and UV/H₂O₂ processes for the removal of pharmaceuticals detected in secondary effluent of a sewage treatment plant in Japan. *J. Hazard. Mater.* 166(2-3), 1134-1140.
- Kim, S.D., Cho, J., Kim, I.S., Vanderford, B.J. and Snyder, S.A. (2007). Occurrence and removal of pharmaceuticals and endocrine disruptors in South Korean surface, drinking, and waste waters. *Water Res.* 41(5), 1013-1021.
- Kinney, C.A., Furlong, E.T., Werner, S.L. and Cahill, J.D. (2006). Presence and distribution of wastewater-derived pharmaceuticals in soil irrigated with reclaimed water. *Environmental Toxicology and Chemistry* 25(2), 317-326.
- Kolpin, D.W., Furlong, E.T., Meyer, M.T., Thurman, E.M., Zaugg, S.D., Barber, L.B. and Buxton, H.T. (2002). Pharmaceuticals, Hormones, and Other Organic Wastewater Contaminants in U.S. Streams, 1999-2000: A National Reconnaissance. *Environ. Sci. Technol.* 36(6), 1202-1211.
- Kummerer, K. (2004). Resistance in the environment. *Journal of Antimicrobial Chemotherapy* 54(2), 311-320.
- Kummerer, K., Steger-Hartmann, T. and Meyer, M. (1997). Biodegradability of the anti-tumor agent ifosfamide and its occurrence in hospital effluents and communal sewage. *Water Res.* 31(11), 2705-2710.
- Kurath, P., Jones, P.H., Egan, R.S. and Perun, T.J. (1971). Acid degradation of erythromycin A and erythromycin B. *Experientia* 27(4), 362.
- Lange, F., Cornelissen, S., Kubac, D., Sein, M.M., von Sonntag, J., Hannich, C.B., Golloch, A., Heipieper, H.J., Möder, M. and von Sonntag, C. (2006). Degradation of macrolide antibiotics by ozone: A mechanistic case study with clarithromycin. *Chemosphere* 65(1), 17-23.

- Langlais, B., Reckhow, D.A. and Brink, D.R. (1991) Ozone in water treatment : application and engineering : cooperative research report / American Water Works Association Research Foundation, Compagnie generale des eaux, Lewis Publishers, Chelsea, MI.
- Larsson, D.G.J., de Pedro, C. and Paxeus, N. (2007). Effluent from drug manufacturers contains extremely high levels of pharmaceuticals. *Journal of Hazardous Materials* 148(3), 751-755.
- Lee, C.O., Howe, K.J. and Thomson, B.M. (2010). Ozone and biofiltration as an alternative to reverse osmosis for removing PPCPs and EDCs from Wastewater. Report to New Mexico Environment Department. The University of New Mexico, May 19, 2010.
- Lemke, T.L. and Williams, D.A. (2008). *Foye's Principles of Medicinal Chemistry*; Sixth Edition. Lippincott, Williams & Wilkins, Baltimore, MD.
- Li, F., Patterson, A.D., Höfer, C.C., Krausz, K.W., Gonzalez, F.J. and Idle, J.R. (2010). Comparative metabolism of cyclophosphamide and ifosfamide in the mouse using UPLC-ESI-QTOFMS-based metabolomics. *Biochemical Pharmacology* 80(7), 1063-1074.
- Lienert, J., Gadel, K. and Escher, B.I. (2007). Screening Method for Ecotoxicological Hazard Assessment of 42 Pharmaceuticals Considering Human Metabolism and Excretory Routes. *Environmental Science & Technology* 41(12), 4471-4478.
- Lin, A.Y.C., Lin, C.F., Chiou, J.M. and Hong, P.K.A. (2009). O₃ and O₃/H₂O₂ treatment of sulfonamide and macrolide antibiotics in wastewater. *J. Hazard. Mater.* 171(1-3), 452-458.
- Linares, J.F., Gustafsson, I., Baquero, F. and Martinez, J.L. (2006). Antibiotics as intermicrobial signaling agents instead of weapons. *Proceedings of the National Academy of Sciences* 103(51), 19484-19489.
- Liu, J. and Ren, H.P. (2006). Tuberculosis: Current Treatment and New Drug Development. *Anti-Infective Agents in Medicinal Chemistry* 5(4), 331-344.
- Lopez, A., Bozzi, A., Mascolo, G. and Kiwi, J. (2003). Kinetic investigation on UV and UV/H₂O₂ degradations of pharmaceutical intermediates in aqueous solution. *J. Photochem. Photobiol., A* 156(1-3), 121-126.
- Low, J.E., Borch, R.F. and Sladek, N.E. (1983). Further Studies on the Conversion of 4-Hydroxyoxazaphosphorines to Reactive Mustards and Acrolein in Inorganic Buffers. *Cancer Research* 43(12 Part 1), 5815-5820.
- Ma, H., Allen, H.E. and Yin, Y. (2001). Characterization of isolated fractions of dissolved organic matter from natural waters and a wastewater effluent. *Water Res.* 35(4), 985-996.

- Mahoney, B.P., Raghunand, N., Baggett, B. and Gillies, R.J. (2003). Tumor acidity, ion trapping and chemotherapeutics: I. Acid pH affects the distribution of chemotherapeutic agents in vitro. *Biochemical Pharmacology* 66(7), 1207-1218.
- Maine (2005). Title 22 §2700. Unused Pharmaceutical Disposal Program.
- Mao, J.C.H. and Robishaw, E.E. (1972). Erythromycin, a peptidyltransferase effector. *Biochemistry* 11(25), 4864-4872.
- Marron, C. (2010). Kinetics of Ciprofloxacin Degradation by Ozonation: Effects of Natural Organic Matter, the Carbonate System, and pH. Master's Thesis, The University of Texas at Austin, Austin, TX.
- McDowell, D.C., Huber, M.M., Wagner, M., von Gunten, U. and Ternes, T.A. (2005). Ozonation of Carbamazepine in Drinking Water: Identification and Kinetic Study of Major Oxidation Products. *Environ. Sci. Technol.* 39(20), 8014-8022.
- McGuire, J.M., Bunch, R.L., Anderson, R.C., Boaz, H.E., Flynn, E.H., Powell, H.M. and Smith, J.W. (1952). Ilotycin, a new antibiotic. *Antibiot. Chemother. (Washington, D. C.)* 2, 281-283.
- Metcalf, C.D., Miao, X.S., Koenig, B.G. and Struger, J. (2003). Distribution of acidic and neutral drugs in surface waters near sewage treatment plants in the lower Great Lakes, Canada. *Environ. Toxicol. Chem.* 22(12), 2881-2889.
- Meyerhoff, A., Albrecht, R., Meyer, J.M., Dionne, P., Higgins, K. and Murphy, D. (2004). US Food and Drug Administration Approval of Ciprofloxacin Hydrochloride for Management of Postexposure Inhalational Anthrax. *Clinical Infectious Diseases* 39(3), 303-308.
- Miao, X.S., Bishay, F., Chen, M. and Metcalfe, C.D. (2004). Occurrence of Antimicrobials in the Final Effluents of Wastewater Treatment Plants in Canada. *Environ. Sci. Technol.* 38(13), 3533-3541.
- Micro-90(R) (2009). MSDS Sheet for Micro-90(R) Concentrated Cleaning Solution.
- Minas, W. (2004). Production of erythromycin with *Saccharopolyspora erythraea*. Humana Press, Totowa, NJ
- Mispagel, H. and Gray, J.T. (2005). Antibiotic resistance from wastewater oxidation ponds. *Water Environ. Res.* 77(7), 2996-3002.
- Mohn, G.R. and Ellenberger, J. (1976). Genetic effects of cyclophosphamide, ifosfamide, and trofosfamide. *Mutat. Res.* 32(3-4), 331-360.
- Munoz, F. and von Sonntag, C. (2000). Determination of fast ozone reactions in aqueous solution by competition kinetics. *Journal of the Chemical Society, Perkin Transactions 2* (4), 661-664.

- Murthy, V.V., Becker, B.A. and Steele, W.J. (1973). Effects of dosage, phenobarbital, and 2-diethylaminoethyl-2,2-diphenylvalerate on the binding of cyclophosphamide and/or its metabolites to the DNA, RNA, and protein of the embryo and liver in pregnant mice. *Cancer Res.* 33(4), 664-670.
- NCCLS (2004). *Methods for Antimicrobial Susceptibility Testing of Anaerobic Bacteria: Approved Standard*, 6th edition. National Committee for Clinical Laboratory Standards, Wayne, Pennsylvania.
- Neta, P. and Dorfman, L.M. (1968). Pulse radiolysis studies. XIII. Rate constants for the reactions of hydroxyl radicals with aromatic compounds in aqueous solutions. *Advan. Chem. Ser.* No. 81, 222-230.
- Norrby, S.R. and Lietman, P.S. (1993). Safety and tolerability of fluoroquinolones. *Drugs* 45 Suppl 3, 59-64.
- Okuda, T., Kobayashi, Y., Nagao, R., Yamashita, N., Tanaka, H., Tanaka, S., Fujii, S., Konishi, C. and Houwa, I. (2008). Removal efficiency of 66 pharmaceuticals during wastewater treatment process in Japan. *Water Sci. Technol.* 57(1), 65-71.
- Olson, T.M. and Barbier, P.F. (1994). Oxidation kinetics of natural organic matter by sonolysis and ozone. *Water Res.* 28(6), 1383-1391.
- Omura, S. (2002). *Macrolide Antibiotics: Chemistry, Biology, and Practice*, Second Edition, Academic Press, San Diego, CA.
- ONDCP (2009). Proper Disposal of Prescription Drugs. Office of National Drug Control Policy. Accessed on May 27, 2011.
http://www.whitehousedrugpolicy.gov/publications/pdf/prescrip_disposal.pdf
- Oregon (2007). Senate Bill 737 - Implementation: Addressing Priority Persistent Pollutants in Oregon's Water.
- Oulton, R.L., Kohn, T. and Cwiertny, D.M. (2010). Pharmaceuticals and personal care products in effluent matrices: A survey of transformation and removal during wastewater treatment and implications for wastewater management. *Journal of Environmental Monitoring* 12(11), 1956-1978.
- Pal, S. (2006). A journey across the sequential development of macrolides and ketolides related to erythromycin. *Tetrahedron* 62(14), 3171-3200.
- Paul, T., Dodd, M.C. and Strathmann, T.J. (2010). Photolytic and photocatalytic decomposition of aqueous ciprofloxacin: Transformation products and residual antibacterial activity. *Water Research* 44(10), 3121-3132.
- Pennsylvania (2008). House Bill 2073 - Pharmaceutical Drug Disposal Act.
- Pomati, F., Castiglioni, S., Zuccato, E., Fanelli, R., Vigetti, D., Rossetti, C. and Calamari, D. (2006). Effects of a Complex Mixture of Therapeutic Drugs at Environmental Levels on Human Embryonic Cells. *Environ. Sci. Technol.* 40(7), 2442-2447.

- Pomati, F., Cotsapas, C.J., Castiglioni, S., Zuccato, E. and Calamari, D. (2007). Gene expression profiles in zebrafish (*Danio rerio*) liver cells exposed to a mixture of pharmaceuticals at environmentally relevant concentrations. *Chemosphere* 70(1), 65-73.
- Pomati, F., Orlandi, C., Clerici, M., Luciani, F. and Zuccato, E. (2008). Effects and Interactions in an Environmentally Relevant Mixture of Pharmaceuticals. *Toxicol. Sci.* 102(1), 129-137.
- Prescription (2009). Top 200 prescription drugs. Accessed on September 22, 2009. http://www.prescriptiondrug-info.com/top_prescription_drugs.asp
- Prescription (2011). Top 200 Prescription Drugs. Accessed on May 20, 2011. http://www.prescriptiondrug-info.com/top_prescription_drugs.asp
- Ridley, A. and Threlfall, E.J. (1998). Molecular epidemiology of antibiotic resistance genes in multiresistant epidemic *Salmonella typhimurium* DT 104. *Microb. Drug Resist.* (Larchmont, N. Y.) 4(2), 113-118.
- Rosal, R., Rodriguez, A., Perdigon-Melon, J.A., Mezcuca, M., Hernando, M.D., Leton, P., Garcia-Calvo, E., Agueera, A. and Fernandez-Alba, A.R. (2008). Removal of pharmaceuticals and kinetics of mineralization by O₃/H₂O₂ in a biotreated municipal wastewater. *Water Res.* 42(14), 3719-3728.
- Schulz, R. and Peall, S.K.C. (2000). Effectiveness of a Constructed Wetland for Retention of Nonpoint-Source Pesticide Pollution in the Lourens River Catchment, South Africa. *Environmental Science & Technology* 35(2), 422-426.
- Schumb, W.C., Satterfield, C.N. and Wentworth, R.L. (1955). Hydrogen Peroxide. Am. Chem. Soc. Monograph No. 128, Reinhold Pub. Corp.
- Schwartz, T., Kohnen, W., Jansen, B. and Obst, U. (2003). Detection of antibiotic-resistant bacteria and their resistance genes in wastewater, surface water, and drinking water biofilms. *FEMS Microbiology Ecology* 43(3), 325-335.
- Seppala, H., Nissinen, A., Jarvinen, H., Huovinen, S., Henriksson, T., Herva, E., Holm, S.E., Jahkola, M., Katila, M.-L., Klaukka, T., Kontiainen, S., Liimatainen, O., Oinonen, S., Passi-Metsomaa, L. and Huovinen, P. (1992). Resistance to Erythromycin in Group A Streptococci. *New England Journal of Medicine* 326(5), 292-297.
- Siddiqui, M.S., Amy, G.L. and Murphy, B.D. (1997). Ozone enhanced removal of natural organic matter from drinking water sources. *Water Res.* 31(12), 3098-3106.
- Sirivedhin, T. and Gray, K.A. (2005a). Part 1. Identifying anthropogenic markers in surface waters influenced by treated effluents: a tool in potable water reuse. *Water Research* 39(6), 1154-1164.
- Sirivedhin, T. and Gray, K.A. (2005b). Part 2. Comparison of the disinfection by-product formation potentials between a wastewater effluent and surface waters. *Water Research* 39(6), 1025-1036.

- Snyder, S.A., Adham, S., Redding, A.M., Cannon, F.S., DeCarolis, J., Oppenheimer, J., Wert, E.C. and Yoon, Y. (2007). Role of membranes and activated carbon in the removal of endocrine disruptors and pharmaceuticals. *Desalination* 202(1-3), 156-181.
- Snyder, S.A., Wert, E.C., Rexing, D.J., Zegers, R.E. and Drury, D.D. (2006). Ozone oxidation of endocrine disruptors and pharmaceuticals in surface water and wastewater. *Ozone: Sci. Eng.* 28(6), 445-460.
- Sotelo, J.L., Beltrán, F.J., Benitez, F.J. and Beltrán-Heredia, J. (1989). Henry's law constant for the ozone-water system. *Water Research* 23(10), 1239-1246.
- Sottani, C., Rinaldi, P., Leoni, E., Poggi, G., Teragni, C., Delmonte, A. and Minoia, C. (2008). Simultaneous determination of cyclophosphamide, ifosfamide, doxorubicin, epirubicin and daunorubicin in human urine using high-performance liquid chromatography/electrospray ionization tandem mass spectrometry: bioanalytical method validation. *Rapid Communications in Mass Spectrometry* 22(17), 2645-2659.
- Stackelberg, P.E., Furlong, E.T., Meyer, M.T., Zaugg, S.D., Henderson, A.K. and Reissman, D.B. (2004). Persistence of pharmaceutical compounds and other organic wastewater contaminants in a conventional drinking-water-treatment plant. *Science of The Total Environment* 329(1-3), 99-113.
- Staehelin, J., Buehler, R.E. and Hoigne, J. (1984). Ozone decomposition in water studied by pulse radiolysis. 2. Hydroxyl and hydrogen tetroxide (HO₄) as chain intermediates. *The Journal of Physical Chemistry* 88(24), 5999-6004.
- Staehelin, J. and Hoigne, J. (1982). Decomposition of ozone in water: rate of initiation by hydroxide ions and hydrogen peroxide. *Environ. Sci. Technol.* 16(10), 676-681.
- Steger-Hartmann, T., Kummerer, K. and Hartmann, A. (1997). Biological degradation of cyclophosphamide and its occurrence in sewage water. *Ecotoxicol. Environ. Saf.* 36(2), 174-179.
- Stumpf, M., Ternes, T.A., Wilken, R.D., Rodrigues, S.V. and Baumann, W. (1999). Polar drug residues in sewage and natural waters in the State of Rio de Janeiro, Brazil. *Sci. Total Environ.* 225(1,2), 135-141.
- Suarez, S., Dodd, M.C., Omil, F. and von Gunten, U. (2007). Kinetics of triclosan oxidation by aqueous ozone and consequent loss of antibacterial activity: Relevance to municipal wastewater ozonation. *Water Res.* 41(12), 2481-2490.
- Szczepanowski, R., Linke, B., Krahn, I., Gartemann, K.H., Gotzkow, T., Eichler, W., Puhler, A. and Schluter, A. (2009). Detection of 140 clinically relevant antibiotic resistance genes in the plasmid metagenome of wastewater treatment plant bacteria showing reduced susceptibility to selected antibiotics. *Microbiology*, mic.0.028233-028230.

- Tamtam, F., Mercier, F., Le Bot, B., Eurin, J., Dinh, Q.T., Clement, M. and Chevreuil, M. (2008). Occurrence and fate of antibiotics in the Seine River in various hydrological conditions. *Sci. Total Environ.* 393(1), 84-95.
- Ternes, T.A. (1998). Occurrence of drugs in German sewage treatment plants and rivers. *Water Res.* 32(11), 3245-3260.
- Ternes, T.A., Meisenheimer, M., McDowell, D., Sacher, F., Brauch, H.-J., Haist-Gulde, B., Preuss, G., Wilme, U. and Zulei-Seibert, N. (2002). Removal of Pharmaceuticals during Drinking Water Treatment. *Environ. Sci. Technol.* 36(17), 3855-3863.
- Ternes, T.A., Stuber, J., Herrmann, N., McDowell, D., Ried, A., Kampmann, M. and Teiser, B. (2003). Ozonation: a tool for removal of pharmaceuticals, contrast media and musk fragrances from wastewater? *Water Res.* 37(8), 1976-1982.
- Thomas, K.V., Dye, C., Schlabach, M. and Langford, K.H. (2007). Source to sink tracking of selected human pharmaceuticals from two Oslo city hospitals and a wastewater treatment works. *J. Environ. Monit.* 9(12), 1410-1418.
- Thurman, E.M. and Malcolm, R.L. (1981). Preparative isolation of aquatic humic substances. *Environmental Science & Technology* 15(4), 463-466.
- Tomiyasu, H., Fukutomi, H. and Gordon, G. (1985). Kinetics and mechanism of ozone decomposition in basic aqueous solution. *Inorg. Chem.* 24(19), 2962-2966.
- Tyler, C.R., Jobling, S. and Sumpter, J.P. (1998). Endocrine Disruption in Wildlife: A Critical Review of the Evidence. *Critical Reviews in Toxicology* 28(4), 319-361.
- van der Kooij, D., Hijnen, W.A.M. and Kruithof, J.C. (1989). The Effects of Ozonation, Biological Filtration and Distribution on the Concentration of Easily Assimilable Organic Carbon (AOC) in Drinking Water. *Ozone: Science & Engineering: The Journal of the International Ozone Association* 11(3), 297-311.
- Vasconcelos, T.G., Kuemmerer, K., Henriques, D.M. and Martins, A.F. (2009). Ciprofloxacin in hospital effluent: Degradation by ozone and photoprocesses. *J. Hazard. Mater.* 169(1-3), 1154-1158.
- Venta, M.B., Castro, C.H., Garcia, L.A.F., Marzo, A.L., Lorenzo, E.V. and Alvarez, C.A. (2005). Effect of O₃/H₂O₂ molar concentration ratio at different pH values on cyclophosphamide degradation. *J. Water Supply: Res. Technol.--AQUA* 54(7), 403-410.
- Vieno, N.M., Haerikki, H., Tuhkanen, T. and Kronberg, L. (2007). Occurrence of Pharmaceuticals in River Water and Their Elimination in a Pilot-Scale Drinking Water Treatment Plant. *Environ. Sci. Technol.* 41(14), 5077-5084.
- Vinckier, C., Hauchecorne, R., Cachet, T., van den Mooter, G. and Hoogmartens, J. (1989). A new mechanism for the decomposition of erythromycin A in acidic aqueous solutions. *Int. J. Pharm.* 55(1), 67-76.

- Virginia (2008). House Bill 86 - Unused Pharmaceuticals Disposal Program.
- Volk, C., Roche, P., Joret, J.C. and Paillard, H. (1997). Comparison of the effect of ozone, ozone-hydrogen peroxide system and catalytic ozone on the biodegradable organic matter of a fulvic acid solution. *Water Res.* 31(3), 650-656.
- Volkman, H., Schwartz, T., Bischoff, P., Kirchen, S. and Obst, U. (2004). Detection of clinically relevant antibiotic-resistance genes in municipal wastewater using real-time PCR (TaqMan). *Journal of Microbiological Methods* 56(2), 277-286.
- von Gunten, U. (2003). Ozonation of drinking water: Part I. Oxidation kinetics and product formation. *Water Res.* 37(7), 1443-1467.
- von Gunten, U. and Hoigne, J. (1994). Bromate Formation during Ozonization of Bromide-Containing Waters: Interaction of Ozone and Hydroxyl Radical Reactions. *Environmental Science & Technology* 28(7), 1234-1242.
- Vos, J.G., Dybing, E., Greim, H.A., Ladefoged, O., Lambre, C., Tarazona, J.V., Brandt, I. and Vethaak, A.D. (2000). Health effects of endocrine-disrupting chemicals on wildlife, with special reference to the European situation. *Crit. Rev. Toxicol.* 30(1), 71-133.
- Vosmaer, A. (1916). *Ozone: Its Manufacture, Properties, and Uses*. Van Nostrand Co., New York, NY.
- Wang, L., Albasi, C., Faucet-Marquis, V., Pfohl-Leszkowicz, A., Dorandeu, C., Marion, B. and Causserand, C. (2009). Cyclophosphamide removal from water by nanofiltration and reverse osmosis membrane. *Water Res.* 43(17), 4115-4122.
- Westerhoff, P., Aiken, G., Amy, G. and Debroux, J. (1999a). Relationships between the structure of natural organic matter and its reactivity towards molecular ozone and hydroxyl radicals. *Water Res.* 33(10), 2265-2276.
- Westerhoff, P., Debroux, J., Aiken, G. and Amy, G. (1999b). Ozone-induced changes in natural organic matter (NOM) structure. *Ozone: Sci. Eng.* 21(6), 551-570.
- Westerhoff, P., Song, R., Amy, G. and Minear, R. (1997). Applications of Ozone Decomposition Models. *Ozone: Science & Engineering: The Journal of the International Ozone Association* 19(1), 55-73.
- Westerhoff, P., Yoon, Y., Snyder, S. and Wert, E. (2005). Fate of Endocrine-Disruptor, Pharmaceutical, and Personal Care Product Chemicals during Simulated Drinking Water Treatment Processes. *Environ. Sci. Technol.* 39(17), 6649-6663.
- Win, Y.Y., Kumke, M.U., Specht, C.H., Schindelin, A.J., Kolliopoulos, G., Ohlenbusch, G., Kleiser, G., Hesse, S. and Frimmel, F.H. (2000). Influence of oxidation of dissolved organic matter (DOM) on subsequent water treatment processes. *Water Research* 34(7), 2098-2104.
- Windhoek (2011). The City of Windhoek: Water reclamation, Windhoek, Namibia. Accessed June 17, 2011. <http://www.windhoekcc.org.na/Default.aspx?page=117>

Wisconsin (2007). Senate Bill 40.

Wishart, D.S., Knox, C., Guo, A.C., Cheng, D., Shrivastava, S., Tzur, D., Gautam, B. and Hassanali, M. (2008). DrugBank: a knowledgebase for drugs, drug actions and drug targets. *Nucleic Acids Res.* 36(Database Iss), D901-D906.

Xu, P., Drewes, J.E., Bellona, C., Amy, G., Kim, T.U., Adam, M. and Heberer, T. (2005). Rejection of emerging organic micropollutants in nanofiltration-reverse osmosis membrane applications. *Water Environ. Res.* 77(1), 40-48.

Yao, C.C.D. and Haag, W.R. (1991). Rate constants for direct reactions of ozone with several drinking water contaminants. *Water Res.* 25(7), 761-773.

Zuccato, E., Castiglioni, S. and Fanelli, R. (2005). Identification of the pharmaceuticals for human use contaminating the Italian aquatic environment. *J. Hazard. Mater.* 122(3), 205-209.

Vita

Lee Michael Blaney was born in Philadelphia, PA to James and Joann Blaney. After graduating from Father Judge High School for Boys (Philadelphia, PA) in 2001, Lee began his lengthy college career at Lehigh University in Bethlehem, PA. For the first two years of college, Lee studied Civil Engineering; however, after a presentation by Dr. Arup SenGupta, Lee switched majors to Environmental Engineering. Lee received his B.S. in Environmental Engineering (2005), and decided to stay at Lehigh and complete his M.S. (2007) with Dr. SenGupta. During the summer of 2007, Lee worked with Dr. Yongguan Zhu at the Research Centre for Eco-Environmental Sciences (Beijing, China) as a fellow in the National Science Foundation (NSF) East Asia and Pacific Summer Institute program. In Fall 2007, Lee commenced his Ph.D. studies with Drs. Desmond Lawler and Lynn Katz at the University of Texas at Austin. During his time at the University of Texas, Lee received funding from a NSF Graduate Research Fellowship and the University of Texas at Austin Thrust and University Fellowships. After graduating with his Ph.D. in Civil Engineering, Lee will start as an Assistant Professor at the University of Maryland, Baltimore County (UMBC) in the Department of Chemical, Biochemical and Environmental Engineering.

Permanent address: 2689 Winchester Avenue, Philadelphia, PA 19152

This dissertation was typed by the author.